The role of Strigolactone and KAI2 signalling in seedling development

Maxime Josse

Submitted in accordance with the requirements for the degree of Doctor of Philosophy

The University of Leeds

Faculty of Biological Sciences

School of Biology

March 2022

I confirm that the work submitted is my own and that appropriate credit has been given where reference has been made to the work of others.

Acknowledgements

First, I would like to thank Dr. Tom Bennett for supervising my work and providing me with valuable guidance, and helpful advice throughout my PhD study.

My sincere thanks to Prof. Dr. Stefan Kepinski, Dr. Laura Dixon, Dr. Antoine Larrieu and other members of the Centre for Plant Science department for their generous advice and very useful feedback.

I also would like to express my gratitude to Dr. Xander Jones, and his team for giving me the time, and (financial and emotional) support to write my thesis and work on my paper during my employment in Cambridge.

Much thanks go to all members of the Bennett lab for all the emotional support you provided during my presence in the lab. My gratitude goes to Pablo and Roza for their valuable scientific and emotional support.

I would also like to thank my friends (Viv, Antoine, Irene, Meryem, et al.), my relatives, and my climbing pals for supporting and encouraging me over the course of this journey.

Last but not the least I would like to express my gratitude to Tatiana for the unconditional support. Thank you for keeping me sane and motivated to write this thesis during a global pandemic, and for helping me on the proof-reading. Can't wait to feel more human and less grumpy again.

Finalement, cette thèse est dédiée à ma mère.

Abstract

Strigolactones (SL) and the endogenous KAI2-ligand (KL) are butenolide compounds acting as hormonal signals to regulate multiple aspects of plant development and architecture. Perception of these signals in *Arabidopsis thaliana* requires respectively DWARF14 (D14) and KARRIKIN INSENSITIVE 2 (KAI2) receptors and the shared F-box protein MAX2. The MAX2-mediated ubiquitination and subsequent degradation of SUPPRESSOR OF MAX2 1 (SMAX1), SMAX1-like 2 (SMXL2), or their homologues SMXL6, SMXL7, and SMXL8 triggers the downstream effects of KL or SL signalling. SL signalling is a potent regulator of shoot architecture and increase in SL biosynthesis is linked with the plant response to nutrients depletion. The regulation of root development by SL signalling has also been proposed, although it remains elusive given it is mainly based on the use of *max2* mutant and *rac*-GR24 treatments, both acting indiscriminately in SL and KL signalling. The exact functions of SMXL6, 7, and 8 are not yet fully understood, but it is clear that D14-mediated strigolactone signalling pathway regulates auxin distribution by re-modelling auxin transport in the shoot. Despite considerable interest in its function, the role of KAI2 and its proteolytic targets SMAX1/SMXL2 in seedling development remains poorly understood. KAI2 signalling is required for a normal photomorphogenetic development of the seedlings, such as hypocotyl growth and germination, but it is yet unknown if KAI2 also accounts for some aspects of the MAX2-mediated root development.

The close origins between SL and KAI2 signalling pathways prompted us to reassess the role of SL and KL signalling in root development by phenotyping mutants affected in both pathways. My results indicate a dual role of SL and KL in root development. SL signalling promotes primary root growth, and KAI2 signalling is a newly discovered important regulator of the lateral root and root hair development. I demonstrated that the strong phenotypes of *kai2* are correlated with altered auxin sensitivity in roots.

Given both pathways appear to regulate physiological processes in the root and seedlings, I investigated if either the functions of SL and/or KL signalling in seedling development were associated with environmental stress responses. I found that KL and SL signalling are required for the correct developmental adaption in response to low phosphorus availability; and KAI2 and SMAX1/SMXL2 modulate root hair and lateral root proliferation consequently. In addition, I showed that KAI2 signalling is required for the correct photomorphogenic remodelling of seedling growth, and that *kai2* and *smax1*

smxl2 mutants display a range of phenotypic traits and atypical adaptive responses associated with defect in auxin biosynthesis/response.

Following a detailed analysis of the KAI2-mediated photomorphogenic remodelling, I demonstrated that KAI2 control the light-induced remodelling of PIN-mediated auxin transport system. Although the exact mechanisms remain unclear, I showed that KAI2 is required for appropriate changes in PIN protein abundance at the plasma membrane in various tissues affected by light-remodelling.

Table of Contents

List of Figures

Abbreviations

(v/v) – (volume/volume)

µm – micrometer

µmol - micromolar

ABCB - ATP-BINDING CASSETTE sub-class B

ACS7 - ACC synthase 7

AMF - arbuscular mycorrhizal fungi

AR - adventitious root

ARF - AUXIN RESPONSE FACTOR

ARp - adventitious roots primordia

ATS - Arabidopsis thaliana salts

AUX1 - AUXIN RESISTANT1

AuxREs - auxin response elements

BBX20 - BOX DOMAIN PROTEIN 20

BRC1 - BRANCHED1

CCD7 - CAROTENOID CLEAVAGE DIOXYGENASE 7

CK – Cytokinin

CL – Carlactone

CLA - carlactonoic acid

Col-0 – Columbia

D14 - DWARF 14

D27 - DWARF27

D3 - DWARF3

D53 - DWARF 53

dd – day dark

dl – day light

DLK2 - DWARF14-LIKE2

DNA - Deoxyribonucleic acid

dpg - days post-germination

EAR - ETHYLENE-RESPONSE FACTOR Amphiphilic Repression

ER - endoplasmic reticulum

GFP – green fluorescent protein

GH3s - GRETCHEN HAGEN 3s

HCl – hypochlorite acid

HP - high phosphate

htl1 - HYPOSENSITIVE TO LIGHT1

HY5 - ELONGATED HYPOCOTYL5

IAA - indole-3-acetic acid

IPA1 - IDEAL PLANT ARCHITECTURE1

IPyA - indole-3-pyruvic acid

KAI2 - KARRIKIN INSENSITIVE 2

KAR – Karrikin

KL - KAI2-ligand

KUF1 - KARRIKIN UPREGULATED F-BOX1

LAX - LIKE-AUXIN RESISTANT1

LBO - LATERAL BRANCHING OXIDOREDUCTASE

Ler - Landsberg erecta

L-Kyn - L-kynurenine

LP - low phosphate

LR - lateral root

LRD - lateral root density

LRe - emerged LR

LRP - lateral root primordia

L-Tpr - L-tryptophan

MAX2 - MORE AXILLARY GROWTH 2

MAX3 - MORE AXILLARY GROWTH 3

MDZ – middle differentiated zone

MeCLA - methyl carlactonoate

ml – milliliter

mm – millimeter

mM - millimolar

MZ – meristem zone

nm – nanometer

no-Suc – no sucrose

NPA - 1-N-naphthylphthalamic acid

ODZ – older differentiated zone

oxIAA - 2-oxoindole-3-acetic acid

PAT - polar auxin transport

PCR - Polymerase chain reaction

Pi - inorganic phosphorus

PI - Propidium iodide

PIF - PHYTOCHROME INTERACTING FACTOR

PILs - PIN-like proteins

PIN - PIN-FORMED

pin347 - pin3-3 pin4-3 pin7-1

PM – plasma membrane

PR – Primary root

PRL - Primary root length

QC - quiescent center

qRT-PCR - Quantitative reverse transcription PCR

RAM – root apical meristem

RH – root hair

RHD - root hair density

RHL - root hair length

RNA - Ribonucleic acid

RSA – root system architecture

s1 s2 - smax1 smxl2

SL – Strigolactone

SMAX1 - SUPPRESSOR OF MAX2 1

SMXL - SMAX1-LIKE

SPL - SQUAMOSA PROMOTER BINDING PROTEIN-LIKE

SRJ – *shoot-root junction*

Suc+ - sucrose supplementation

TAA1 - TRYPTOPHAN AMINOTRANSFERASE OF ARABIDOPSIS 1

TAR1 - TAA1-RELATED 1

TIR1 - TRANSPORT INHIBITOR RESPONSE1

TPL - TPL

UBC10 - POLY*UBIQUITIN10*

UGTs - UDP GLUCOSYL TRANSFERASEs

WT – wild-type

YDZ – young differentiated zone

List of publications

Research Papers

- Villaécija-Aguilar, J.A.; **Hamon-Josse, M**.; Carbonnel, S.; Kretschmar, A.; Schmidt, C.; Dawid, C.; Bennett, T.; Gutjahr, C. SMAX1/SMXL2 regulate root and root hair development downstream of KAI2-mediated signalling in Arabidopsis. **PLoS Genet**. 2019, 15, e1008327.

- Wheeldon, CD, Walker, CH, **Hamon-Josse, M**, Bennett, T. Wheat plants sense substrate volume and root density to proactively modulate shoot growth. **Plant Cell Environ**. 2021; 44: 1202– 1214.

- Villaécija-Aguilar JA, Körösy C, Maisch L, **Hamon-Josse M**, Petrich A, Magosch S, Chapman P, Bennett T, Gutjahr C. KAI2 promotes Arabidopsis root hair elongation at low external phosphate by controlling local accumulation of AUX1 and PIN2. **Current Biology** (2021) doi: 10.1016/j.cub.2021.10.044.

- **Hamon-Josse M.**, Villaecija-Aguilar JA., Ljung K., Leyser O., Gutjahr C., Bennett T. KAI2 regulates seedling development by mediating light-induced remodelling of auxin transport. **New Phytol**, Accepted (05 March 2022)

Review paper

- Machin, D.C., **Hamon-Josse, M.** and Bennett, T. (2020), Fellowship of the rings: a saga of strigolactones and other small signals. **New Phytol**, 225: 621-636. https://doi.org/10.1111/nph.16135

List of contributions

In the following list are referenced the work presented in this thesis that have been carried at least in part by a person other than me, including experimental design, data collection or analysis.

Chapter3:

Some data from this chapter are published in (Villaécija-Aguilar et al., 2019).

- **Figure 3.3 A-B**. Panels were designed by José Antonio Villaécija-Aguilar as part of a joint-authored study (Villaécija-Aguilar et al., 2019)

- **Figure 3.3 E-F**. Experimental design, data collection and analysis, and graphs were performed by José Antonio Villaécija-Aguilar as part of a joint-authored study (Villaécija-Aguilar et al., 2019).

- **Figure 3.9**. Figure is adapted from an original figure designed by José Antonio Villaécija-Aguilar as part of a joint-authored study (Villaécija-Aguilar et al., 2019).

Chapter4:

Data from figure 4.7 are now published in Hamon-Josse et al., 2022

- **Figure 4.7 D-E**. Experimental design and data collection was performed by José Antonio Villaécija-Aguilar. Data analysis and graph were done by me.

Chapter5:

Some data used in this paper are now published in Hamon-Josse et al., 2022.

- **Figure 5.1 A-C**. Experimental design and data collection was performed by Tom Bennett. IAA measurements were performed by Karin Ljung. Data analysis and graphs were done by me.

- **Figure 5.3 F**. Experimental design and data collection was performed by José Antonio Villaécija-Aguilar. Data analysis and graph were done by me.

- **Figure 5.7 A**. Data collection and design of the panel with microscopy images was performed by Tom Bennett.

- **Figure 5.8**. Experimental design and data collection were performed by Tom Bennett. Graphs and analysis were performed by me.

Chapter 1 Introduction

1.1 Plant hormones

To ensure optimum development and growth, plants integrate information in the form of signals, of endogenous or environmental origins, which, in addition to the genetic program of the individual, will determine its morphology. In this context, phytohormones, or plant hormones, *"are a group of naturally occurring, organic substances which influence physiological processes at low concentrations"* (J.Davies, 2004). A molecule of phytohormone acts as an information vector recognised by a target cell, which will be sensitive to its action thanks to the presence of a receptor, that once activated induces downstream mechanisms leading to a biological response. Hormones, as it is defined from a mammalian sense, are mobile signals, acting at long distance from their synthesis site, however, phytohormones do not completely fit in this definition. As for mammalian systems, phytohormones biosynthesis can be local and occurs in specific cell types; or can happen in a wider range at the tissues or organs level. Some hormones such as auxin or cytokinin can be transported systemically and act at distances, while others such as ethylene can also act locally within the cell where it is synthesised. Thus, long-distance transport is not essential for all phytohormones, but because of the complex nature of plant development and the need for a plant to constantly adapt to varying environmental conditions, the transfer of hormonal signal across tissues is essential. The presence of specific transport networks having the capacity to be constantly modulated to deliver the best "decision-signal" according to the growth conditions is essential in the function of plant hormones.

1.1.1 Discovery of phytohormones

Mention of plant hormones can be found a far as Charles Darwin's book *The power of movement in Plants* (1880), where he described the coleoptile of *Phalaris canariensis* can adapt its curvature and growth in response to light direction. He observed that decapitation of the coleoptile tip or covering it to block light perception at the tip was enough to inhibit the bending and would likely be the results of an "*influence*" coming from the stimulus perception site and signalling to the below tissues to bend and adapt their growth in direction of the light.

This "*influence"* described by Darwin, later gained further insight with the work of Peter Boysen-Jensen (1911) who showed that grafting a coleoptile tip onto another decapitated coleoptile was enough to rescue the bending in response to

light perception. His experiments further demonstrated that inserting a piece of gelatine between the graft and the coleoptile would not interrupt the transmission of the bending signal to the bellow tissues, while a mica insert would prevent bending of the coleoptile. Therefore, it suggests that the "*influence"* described by Darwin is a mobile chemical substance and its flow toward the base of the plant is essential for the bending response. It is in 1928 that the substance responsible for coleoptile bending is independently characterised by Frits Warmolt-Went and Nicolai Cholodny, whom (using respectively grass roots and coleoptiles) showed the asymmetric accumulation of a signal occurs in response to a tropic stimulus, and that this asymmetric gradient of "*influence*" stimulates the differential growth between the inner and outer side of the tissue that results in tropic curvature (Holland et al., 2009). This substance, named auxin from the Greek *auxein* meaning "growth" is finally chemically identified as indole-3-acetic acid (IAA) in 1934 by Dutch chemists Kögl and Haagen-Smit (Hopkins, 2003, Heller et al., 2004, Holland et al., 2009).

Since the discovery of auxin, other groups of the plant hormones have been discovered. Phytohormones are present in plant tissues at low concentration and working locally or at long-distance across plant tissues to transmit developmental or adaptive decisions. The activities of plant hormones depend on cellular context and exhibit interactions that can be either synergistic or antagonistic. These hormones are classed into 9 different groups: Gibberelin, Brassinosteroid, Absisic acid, Ethylene, Jasmonate, Salicylic acid, Cytokinin, Auxin, and Strigolactones.

1.2 Auxin

Among those, auxin is considered as a general coordinator of growth and development used and re-used throughout the life cycle of plants to mediate communication between cells and tissues at short and long ranges. This master regulator of plant development and growth, regulates cell proliferation, cell elongation and cell differentiation during all stages of the plant life, from the development of the embryo (embryogenesis) to the development of fruits, and senescence. About auxin, Ottoline Leyser wrote in 2018:

> *"There is a clear consensus that auxin is extremely important, that it is involved in virtually every aspect of plant biology, and that this baffling array of functions makes the task of understanding auxin daunting to say the least". "The question of how auxin works is not the question of what happens when some*

auxin arrives at a cell. There is always auxin. The absolute and relative amount of auxin at any one location in the plant varies over time, and this tunes and retunes the balance within a set of interlocking feedback loops operating at subcellular, cellular, tissue, organ, and whole-plant scales" (Leyser, 2018).

1.2.1 Auxin Homeostasis

In this regard, the first step by which cells, tissues, or whole plants control the auxin gradients is by keeping a tight balance over its homeostasis.

Auxin is a class of small organic compounds among which Indole-3-acetic acid (IAA) appears to be the major naturally occurring one (Woodward and Bartel, 2005, Simon and Petrášek, 2011). In most plants, including the model species *Arabidopsis thaliana*, there are two main mechanisms of IAA synthesis, one relying on IAA synthesis from its precursor L-tryptophan (L-Trp), and a tryptophan-independent pathway which remain poorly characterised. During *de novo* synthesis of IAA, L-Trp can be converted into three IAA-intermediates, indole-3-pyruvic acid (IPyA), indole-3-acetamide (IAM) and indole-3-acetaldoximine (IAOx). Among those, the IPyA pathway (the best characterised) relies on the action of TRYPTOPHAN AMINOTRANSFERASE OF ARABIDOPSIS 1 (TAA1) and its two homologues TAA1-RELATED 1 (TAR1) and TAR2. Then the family of flavin monooxygenase–like enzymes called YUCCAs catalyse the conversion of IPyA into IAA (Mashiguchi et al., 2011, Stepanova et al., 2011, Won et al., 2011, Zhao, 2012, Ljung et al 2013) (figure 1.1 A). In opposition to *de novo* auxin synthesis, formation of auxin conjugates removes active IAA. Auxin conjugates can be formed when IAA is conjugated to amino acids (Ala, Asp, Phe, and Trp) via a class of adenylate-forming enzymes named GRETCHEN HAGEN 3s (GH3s) (Staswick et al., 2005), or conjugation to a sugar via UDP GLUCOSYL TRANSFERASEs (UGTs) (Jackson et al., 2001). IAA can also be oxidised into 2-oxoindole-3-acetic acid (oxIAA) (Ljung, 2013, Peer et al., 2013, Pencík et al., 2013). The formation of auxin conjugates and their degradation has been proposed to be a mechanism by which cells form a pool of inactive auxin, from which some conjugates can be reversibly cleaved to release active IAA, while other conjugates irreversibly remove active auxin from the cell, contributing in maintaining auxin homeostasis in the cell (Rampey et al., 2004).

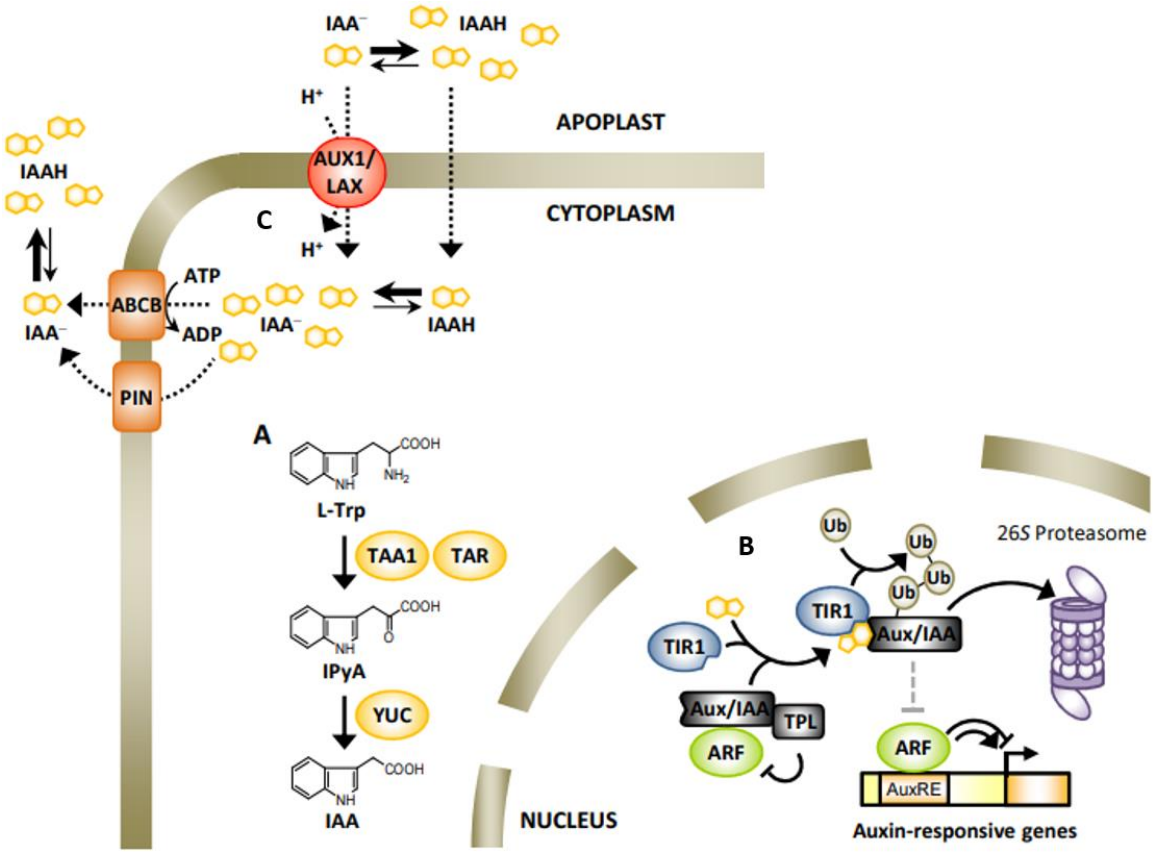

Figure 1-1 Overview of auxin biosynthesis, transport and signalling
(A) IAA is primarily synthesised from L-Trp by a pathway involving TAA1 and TAR tryptophan aminotransferases as well as flavin monooxygenases of the YUC family.
(B) Auxin signalling takes place in the nucleus, where Aux/IAA proteins and their co-repressor TPL inhibit the activity of ARFs in the absence of auxin. Auxin allows TIR1 and Aux/IAA proteins to interact, whereupon the Aux/IAA proteins are ubiquitinated by the SCFTIR1-E3 ubiquitin ligase and subsequently degraded in the 26S proteasome. Therefore, the ARFs are de-repressed and regulate auxin-responsive genes by binding to auxin response elements (AuxREs) in their promoter.
(C) Auxin is transported into the cell by a pH-driven ion-trap mechanism: uncharged IAA (IAAH) diffuses through the membrane and is converted to its anionic form (IAA) in the cytosol. In addition, auxin is imported via transporters of the AUX1/LAX family and exported via transporters of the PIN and ABCB families. Adapted with permission from Martin Balcerowicz, 2013 (personal communication).

1.2.2 Auxin Signalling

Auxin's main function is to regulate transcription via a signalling transduction pathway. In this pathway auxin mediates the binding of proteins member of the Aux/IAA transcriptional repressors family with a co-receptor F-box protein TRANSPORT INHIBITOR RESPONSE1/AUXIN SIGNALING F-BOX (TIR1/AFB). There is variety of TIR1/AFB pairs, due to the presence in Arabidopsis of 6 known AFB (Prigge et al., 2016), and the TIR1/AFB pairs are believed to have different degree of affinity with different types of auxins (Villalobos et al., 2012). The Aux/IAA – TIR1/AFB pair can be recruited in a SCF-type ubiquitin protein ligase E3 complex comprising three subunits (Skp1, Cullin, and TIR1/AFB) which activates polyubiquitination of Aux/IAAs which results in their degradation (Smalle and Viestra 2004, Kepinski and Leyser 2005, Tan et al., 2007) (figure 1.1 B). In cells where IAA concentration is low, Aux/IAA proteins can recruit corepressors of the TOPLESS (TPL) protein family in an ETHYLENE-RESPONSE FACTOR Amphiphilic Repression (EAR) motif-dependent manner, which in turn prevent transcription by recruiting remodelling proteins forming repressive chromatin structures. Aux/IAA-TPL complexes bind to transcription factors of the AUXIN RESPONSE FACTOR (ARF) family, which in turn represses ARFs ability to promote transcription (Guilfoyle and Hagen 2007, Szemenyei et al., 2008). In presence of high concentration of auxin, IAA acts as a glue mediating the binding of TIR1/AFB-SCF to Aux/IAAs, followed by poly-ubiquitination and subsequent degradation of Aux/IAAs by the 26S proteasome (Gray et al., 2001, Tan et al., 2007, Maraschin et al., 2009) (figure 1.1 B). This in turn alleviates the transcriptional repression on ARFs proteins and activates the expression of auxin-inducible genes via the binding of auxin response elements (AuxREs) into their promoter (Ulmasov et al., 1997, Tiwari et al., 2004, reviewed in Guilfoyle and Hagen 2007) (figure 1.1 B).

1.2.3 Auxin Transport network

In Arabidopsis, all parts of the young seedling have the potential to *de novo* synthesise the auxin needed for growth and development, not only young leaves, but also all other parts of the plant such as cotyledons, expanding leaves and root tissues (Ljung et al., 2001). However, during early seedling development, auxin main source is the cotyledons and young leaves while the root system is unable to synthesis significant amount of IAA (Bhalerao et al., 2022). The distribution of auxin in subcellular, and cellular compartment, and across tissues relies on active and passive transport of auxin by the auxin transport network, underlying formation of local auxin minima and maxima essential to plant development.

Because of its chemical properties, the weak acid IAA exists in protonated (IAA-H) or deprotonated forms (IAA^-). The protonated IAA-H can passively diffuse from the apoplast, where the pH is around 5.5, to the cytosol, where the pH is more basic (pH 7.0), through the plasma membranes (figure 1.1 C). After diffusion from apoplast to cytosol, IAA in the cytosol become more likely to be deprotonated as a result of the chemical equilibrium of the cell. IAA^- is unable to passively cross the biological membranes to the next cell. In addition to this mechanism of passive auxin diffusion into the cell, known as the chemiosmotic model of auxin transport (Raven, 1975; Rubery and Sheldrake, 1974), mechanisms of active auxin influx into cells have also been identified.

Four proteins from the AUXIN RESISTANT1 (AUX1) and LIKE-AUXIN RESISTANT1 (LAX) 1-3 family have been shown to be essential for the correct import of IAA from the apoplast to cytoplasm (Bennett et al., 1996, Swarup et al., 2001, Peret et al., 2012). AUX1 and LAX proteins are auxin influx carriers, located at the plasma membrane, mediating auxin uptake at the expense of a H+ influx (Yang et al, 2006) (figure 1.1 C). Since IAA- cannot cross membranes passively, passive diffusion and active influx of IAA-H via AUX1/LAXs traps the auxin in the cytosolic compartment into its deprotonated IAA^- form. This suggests that auxin molecules require the activity of efflux carriers at the plasma membrane to exit the cell. Auxin efflux from the cells is mediated by 2 protein families, the PIN-FORMED (PIN) family, the ATP-BINDING CASSETTE (ABC) transporters, sub-class B. In addition, a third protein family, the PIN-like (PIL) proteins family, is involved in auxin efflux within the cell.

ABCB is a subset of 21 plasma membrane auxin transporters functioning in cellular efflux. ABCBs localization at the PM is mainly non-polarized, facilitating non-directional (non-polar) auxin efflux, although localization can be polar (Geisler et al., 2005, Petrášek et al., 2006, Cho et al., 2013) (figure 1.1 C). Interestingly, in addition to a main function as auxin efflux carrier, ABCB4 can switch its directional auxin transport and increase non-polar auxin influx (Yang and Murphy, 2009). Similarly, nitrate transport NRT1.1 has been shown to participate in auxin influx under low nitrate conditions (Krouk et al., 2010), linking nutrient status of the plant with auxin homeostasis.

PILS protein are phylogenetically and topologically related to PIN proteins, although phylogenetic analysis reveals there are 7 PILS identified in Arabidopsis, and that PILS are also present in unicellular algae and chlorophyte clades, suggesting they are evolutionary older than PINs (Barbez et al., 2012, Feraru et al., 2012, Viaene et al., 2013). By opposition with the other auxin efflux transporters, PILS contribute to auxin transport and homeostasis by regulating

intracellular auxin accumulation between cell compartments. PILS are believed to sequester auxin in the endoplasmic reticulum lumen, thereby limiting auxin diffusion into the nucleus where signalling takes place (Barbez et al.,2012, Béziat et al., 2017).

The PIN protein family is of particular importance for long-distance auxin transport and consists in Arabidopsis of 8 members subdivided into 2 classes (reviewed in Bennett, 2015). First, “long” canonical PINs (PIN1, PIN2, PIN3, PIN4, and PIN7) are characterised by a long hydrophilic loop, they are mainly polar, and their PM localized distribution determines the direction of the auxin flow from cell-to-cell (Gälweiler et al., 1998, Luschnig et al., 1998, Friml et al., 2004; Petrášek et al., 2006, Wiśniewska et al., 2006, Bennett et al., 2014) (figure 1.1 C). The second class contain PIN5, PIN6, and PIN8, which are classed as “short” non-canonical PINs because of the presence of a less conserved and shorter hydrophilic loop. In opposition to the role of canonical PINs, these “short” PINs participate in intracellular auxin transport as they can localize on the ER (Mravec et al., 2009, Dal Bosco et al., 2012, Bennett et al., 2014).

1.2.4 Polar auxin transport and the making of a seedling

The presence of active auxin transporters localized at the plasma-membrane is an important feature for plant development, as it facilitates the transport of auxin from cell-to-cell and controls the directionality and rate of auxin efflux. By fine-tuning auxin distribution, the polar auxin transport (PAT) ensures the correct spatio-temporal development of the plant during various stages of life such as embryogenesis, photomorphogenesis, root and shoot organogenesis, phyllotaxis, and tropic growth responses (such as the light-tropism described by Charles Darwin 1880, or the root gravitropic response) (reviewed in Adamowski & Friml 2015, and Sauer & Kleine-Vehn 2019). Because they are polarly localized at the plasma membranes opposite to PINs, AUX1/LAX1-3 also participate in polar auxin influx (Kleine-Vehn et al., 2006). Most auxin transport-dependent developmental processes rely on the directional localization of the PIN proteins, and as such, basal, apical, or lateral polarization at the PM is essential for ensuring a flexible multi-directional developmental patterning of the plant.

Embryogenesis: PIN-driven PAT is a crucial process from as early as embryogenesis, during which the embryo of Arabidopsis expresses four *PIN* genes, namely PIN1, 3, 4, and 7 (Benková et al., 2003, Friml et al., 2003) (figure 1.2.A). During the first stages of the embryo development, PIN7 drives the preferential accumulation of auxin in the apical cells by adopting an apical polarization in the suspensor cell(s) while PIN1 maintains homogeneous

distribution of auxin between the apical cells by adopting a lateral polarity (figure 1.2.A). Then, at the globular stage, PIN1 adopts a more basal polarity at the PM, redirecting auxin to the suspensor cells (Kleine-Vehn et al., 2008). Simultaneously, PIN7, in addition to PIN4, changes polarization to drive the auxin flow downward and creating an auxin gradient with an auxin maxima in the hypophysis. Ultimately, the heart-stage embryo adopts a bilateral symmetry through auxin maxima at the initiating cotyledons (embryonic leaves), generated by apical PIN1-mediated auxin flux, associated to a basal rearrangement PIN1, 7, and 4, ensuring rootward auxin flow (reviewed in Petrášek & Friml 2009) (figure 1.2.A).

At post-embryonic stages, PIN-driven PAT ensures the correct patterning of shoot and roots apices, in addition to ensuring the development of lateral organs (lateral roots, adventitious roots, root hairs, future branches etc.). The formation of local auxin maxima along the shoot-root axis marks the site where new organs will be initiated and later will develop (Benková et al., 2003) (figure 1.2.B).

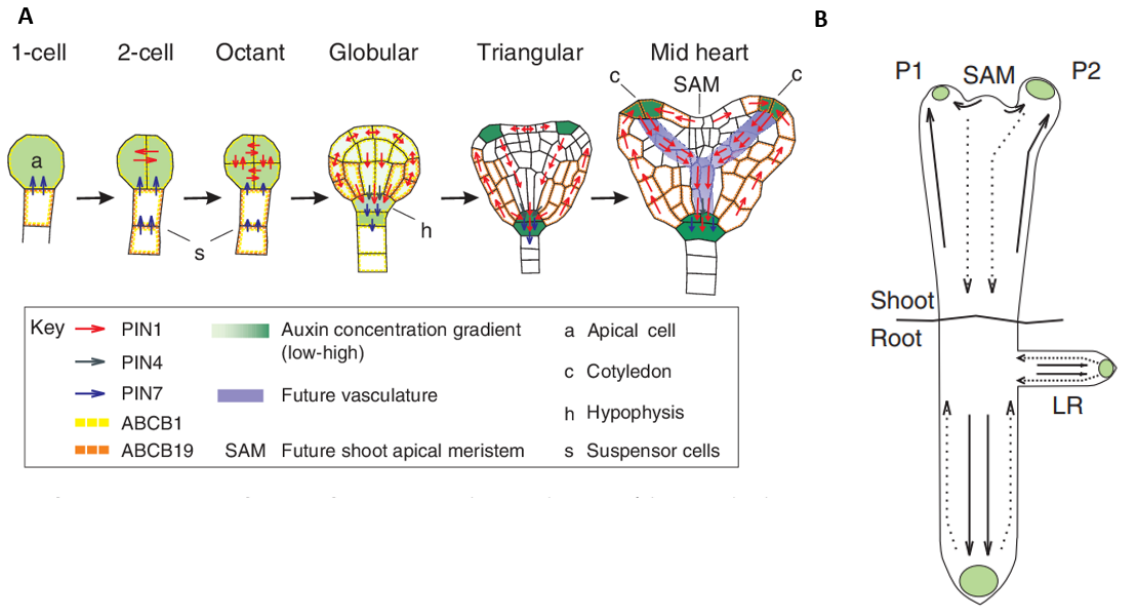

Figure 1-2 A model for the PIN-mediated formation of auxin gradient during embryo patterning

(A) Arabidopsis embryo follows a series of regular and directional cell divisions from the 1-cell stage to the mid heart shape stage. The PIN proteins polarity ensure the correct directional distribution of auxin in addition to ABCB transporters, to maintain the formation of an auxin gradient with local high and low auxin abundance within the cells. From 1-cell stage to octant stage, PIN7 drives auxin accumulation in the apical cells while lateral polarity of PIN1 maintain homogeny distribution of auxin between the apical cells. From the globular stage, the simultaneous action of PIN4 and 7 generate a downward auxin stream with a local auxin maxima in the hypophysis, while PIN1 proteins polarity changes to form an auxin flux from the sites of cotyledons initiation toward the hypophysis and a shootward reflux loop to maintain auxin maxima in the cotyledons.
(B) At post-embryogenic stages, once the seedlings have adopted a clear shoot/root conformation, PAT ensures the correct auxin distribution along the shoot-root axis from the source local auxin maxima in the cotyledons toward a sink auxin maxima in the root meristem. The PIN-mediated rootward auxin transport along the seedlings also ensure the formation of local auxin maxima marking the site lateral organogenesis (adventitious roots, lateral roots, and root hairs). Adapted from Petrášek and Friml, 2009.

Root meristem: In the seedling, PAT-mediated auxin flow to the root apical meristem is essential to maintain its organization and activity. First, auxin is transported from the shoot toward the root tip via the vasculature in a PIN- and AUX1-dependent manner (figure 1.2 B and figure 1.3). In the stele cells at the meristem zone (MZ) the basal localization of PIN1, but also PIN3 and PIN7, maintains the auxin flux toward the initial stele, endodermis, and cortical cells (Blilou et al., 2005) (figure 1.3). There, PIN4 has an inner-lateral and basal polarity directing auxin to the quiescent centre (QC) where an auxin maxima is maintained (Friml et al., 2002a). In the columella, PIN3 and PIN7 redirect auxin toward the lateral root cap and epidermis where apically polarized PIN2, and basally positioned AUX1 mediates the redistribution of auxin shootward toward the differentiation and elongation zones (Sieber et al., 2000, Abas et al., 2006, Swarup et al., 2001) (figure 1.3). The redirection of auxin toward the elongation and differentiation zones operated by PIN2 and AUX1 is determinant in the fate of epidermal cells initiating root hairs and root hair elongation (Jones et al., 2009, Ganguly et al., 2010, Retzer & Weckwerth, 2021). Upstream of the elongation zone, PIN1, PIN3, and PIN7 at the inner lateral PM of epidermis and cortex cell files creates an auxin reflux loop toward the stele (Blilou et al., 2005).

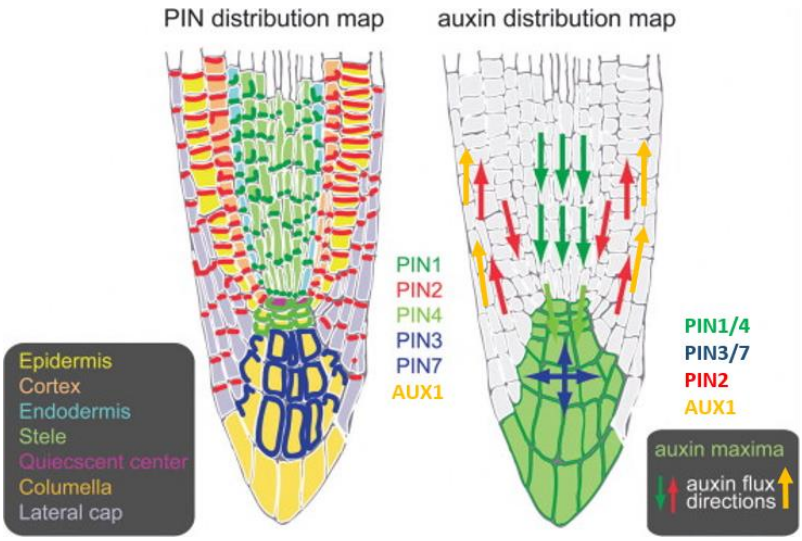

Figure 1-3 Formation and maintenance of root meristem identity and activity by PIN-mediated auxin transport
In the root meristem zone, the basal polarity of PIN1 in the vasculature upward the root tip maintains acropetal auxin flux toward the root apical meristem. The bottleneck action of PIN4 in the initial stele cells ensures the redirection of all auxin toward the QC where a local auxin maxima is formed. The joint action of PIN3 and PIN7 in the root tip and root cap cells then redirect auxin laterally and longitudinally toward the lateral root cap. In these tissues, the action of apically-polarized PIN2 and basally positioned AUX1 is essential for the basipetal redistribution of auxin in the elongation zone where it drives cell elongation and initiation of root hairs. Modified from Rosquete et al., 2012.

Lateral root: Formation of lateral roots (LR) from the embryonic primary root is a key determinant for the plant root system architecture (RSA) and contributes to its ability to uptake nutrients and water. These types of post-embryogenic roots originate deep into the main root tissues from pericycle founder cells, and their fate to initiate and emerge as lateral root relies heavily on the formation of auxin maximum by the PAT system (reviewed in Du and Scheres, 2018). LR formation is characterised by series of developmental stages from the stage I (LR initiation) to the stage VIII at which point the LR is formed and emerges from the primary root (reviewed in Péret et al., 2013) (figure 1.4). During the first step of LR formation, PIN3 stimulates auxin reflux toward the LR founder cells from the endodermal cells overlaying them. The formation of a PIN3-mediated local auxin maxima induces an anticlinal division leading to the formation of a layer of LR founder cells (Benková et al., 2003, Dubrovsky et al., 2008, Marhavý et al., 2013) and the entry of the lateral root primordia (LRp) into stage II of its development (figure 1.4). In addition, auxin, transported rootward via the vasculature, is also injected into the founder cells by the action of AUX1/LAX3 and participates in the initiation of LRp development (Péret et al., 2013). The periclinal polarization of PIN3 and PIN1 maintains a constant auxin reflux toward the primordium tip which facilitates the softening of the cell layers overlying the LRp. This promotes LRp development which can undergo a series of periclinal divisions leading to a dome shape and the deformation and crossing of the endodermis and Casparian strip (Péret et al., 2013, Marhavý et al., 2013, Vermeer et al., 2014, Omelyanchuk et al., 2015) (figure 1.4). At later stages of LRp development, the action of auxin transporters LAX3 and PIN3 redirects auxin into the cortical and epidermal cells in which auxin-mediated peptides and enzymes involved in cell wall remodelling drives mechanical processes allowing the LRp to cross-emerge through the layers of epidermal cells, leading to the formation of a freshly emerged lateral root (LRe) (Swarup et al., 2008, Péret et al., 2013, Kumpf et al., 2013) (figure 1.4).

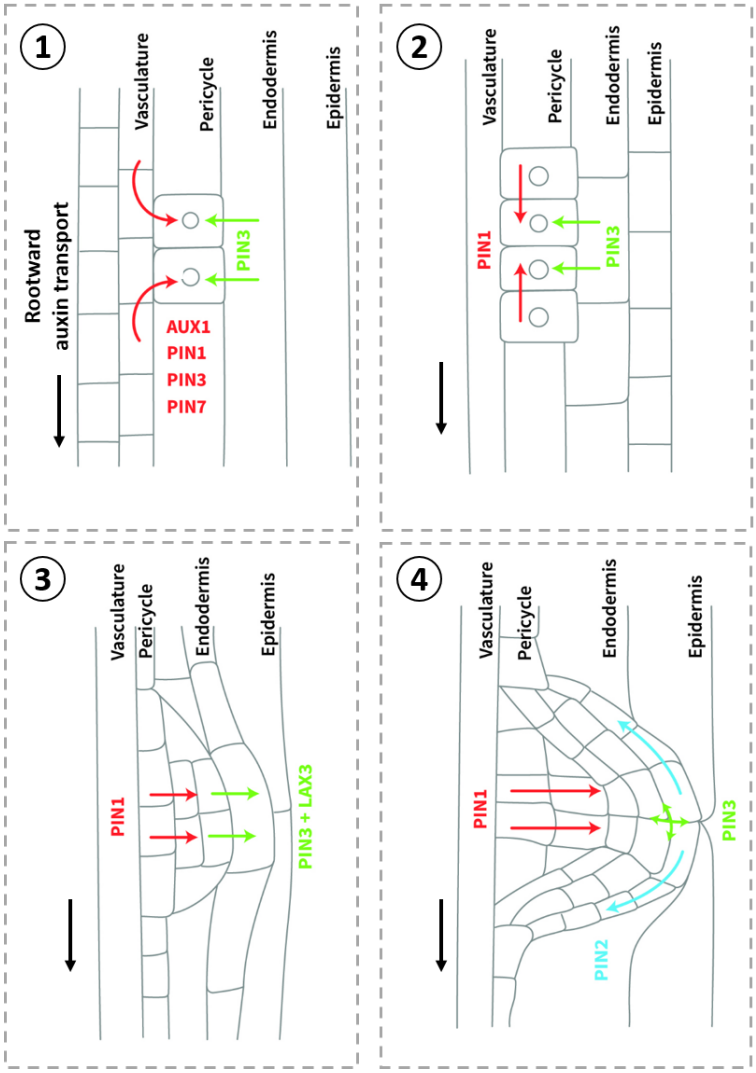

Figure 1-4 Model for the role of PIN proteins and auxin transport during lateral root development

All stages of lateral root development from initiation to emergence relies on the correct distribution of auxin, ensured by PIN proteins and AUX1/LAXs proteins. (1) During LR initiation (stage 1) inner-lateral polarization of PIN3 in endodermal cells stimulates auxin accumulation in the founder cells. At the same time, in the vasculature PIN1, 3 and 7, but also AUX1, “inject” some of the rootward auxin stream toward the LR initiation site. (2) The formation of a maxima in the LR founder cells in the pericycle induces a first anticlinal divisions leading to the formation of a layer of LR founder cells (now forming a stage 2 lateral root primordia). (3) The auxin maxima in the LRp cells in maintained by PIN3 and PIN1 periclinal localization, and it drives a series of periclinal divisions leading to the formation of a dome shaped LRp now deforming the endodermal and epidermal cell layers. At this stage, auxin is redirected by PIN3 toward the cortical and epidermal cells where auxin-mediated peptides activity drives mechanical processes, such as cell-wall loosening, allowing the LRp to cross through the layers. (4) This leads to the emergence of a new lateral root in which the meristem organization also depends upon the PIN1-mediated stream of auxin toward the tip, the action of PIN3 (but also PIN4 and 7 once the LR meristem has adopted its definitive patterning) redirects auxin laterally and longitudinally into the epidermal layers where PIN2 ensure a reflux essential for cell elongation. Adapted from Peret et al., 2012, Vilches-Barro and Maizel, 2015.

1.2.5 Practical case. Auxin role during seedling transition to photomorphogenesis

When seeds germinate in the darkness of the soil, or on agar plates wrapped up in foil in a laboratory, the seedling undergoes a physiological program of development called skotomorphogenesis, in which resources and growth decisions are directed toward the elongation of the hypocotyl (etiolation), to the detriment of the root tissues, to ensure rapid access to the light and transition to a photosynthetic state before the seed reserves are exhausted (reviewed in Halliday et al., 2009) (figure 1.5.A-B). Once it reaches the light, the seedling undergoes rapid photomorphogenic developmental changes, including cessation of hypocotyl elongation, opening of the apical hook, expansion of the cotyledons and development of a competent root system. This transition to photomorphogenesis is associated with the production of photosynthetic pigments, and the switch to a photosynthetic metabolism in the seedling shoot underlying an autotrophic growth (figure 1.5.A-B). More generally, photomorphogenesis involves a transition from a heterotrophic growth based on elongation of pre-existing cells already present in the embryo, to the growth and development of new cells and organs by the activity of shoot and root meristems (Sassi et al, 2012). A key regulator of seedling skoto- and photomorphogenesis is the hormone auxin (Jensen et al., 1998). Auxin status within the seedling is strongly influenced by light signalling, including its biosynthesis, perception, and distribution (Halliday et al., 2009). In low light, auxin synthesis is positively regulated by PHYTOCHROME INTERACTING FACTOR (PIF) transcription factors (Zhao & Bao, 2021), and drives hypocotyl elongation, at least in part by acidification-induced changes in cell wall stiffness (Li et al, 2021; Lin et al, 2021, Jonsson et al., 2021). Auxin, and its distribution/transport is also closely associated with formation, maintenance, and opening of the apical hook (Beziat & Kleine-Vehn, 2018), and with the phototropic bending of the hypocotyl in either skoto- or photomorphogenic seedlings (Fankhauser & Christie, 2015). Formation of the apical hook in darkness depends on differential growth of the cells located on the external and internal sides of hypocotyl caused by asymmetrical distribution of auxin by PIN, AUX1/LAX, and PILS proteins (reviewed in Beziat & Kleine-Vehn, 2018) (figure 1.5.A, C). When the seedling finally perceives light, the auxin gradient dissipates in a PIN/AUX1/PILs-mediated manner causing the dissipation of the auxin-maxima at the inner-side of the hook, and thus leading to cell elongation and hook opening (figure 1.5.B). In addition, transfer of seedlings from light to dark induces a strong remodelling of the PAT system and a reduction of auxin delivery to the root system (Sassi et al, 2012), suggesting that changes in auxin distribution might also account for photomorphogenic changes in root

growth. The dark-light transition is followed by an increase auxin delivery to the root meristem, promoted by a remodelling of the PAT, which awakes the root meristem activity, ensuring for the growth and development of a competent root system. The flourishing of the root system, sustained by carbohydrates sourced from the photosynthetic activity of the shoot, and its multidirectional expansion is essential for the seedling to sustain with uptake of nutrients and water, and ensuring its anchorage in soil (figure 1.5.A, D). Overall, because of its all-pervading influence on plant development auxin is an excellent candidate to mediate coherent photomorphogenic changes within the seedling.

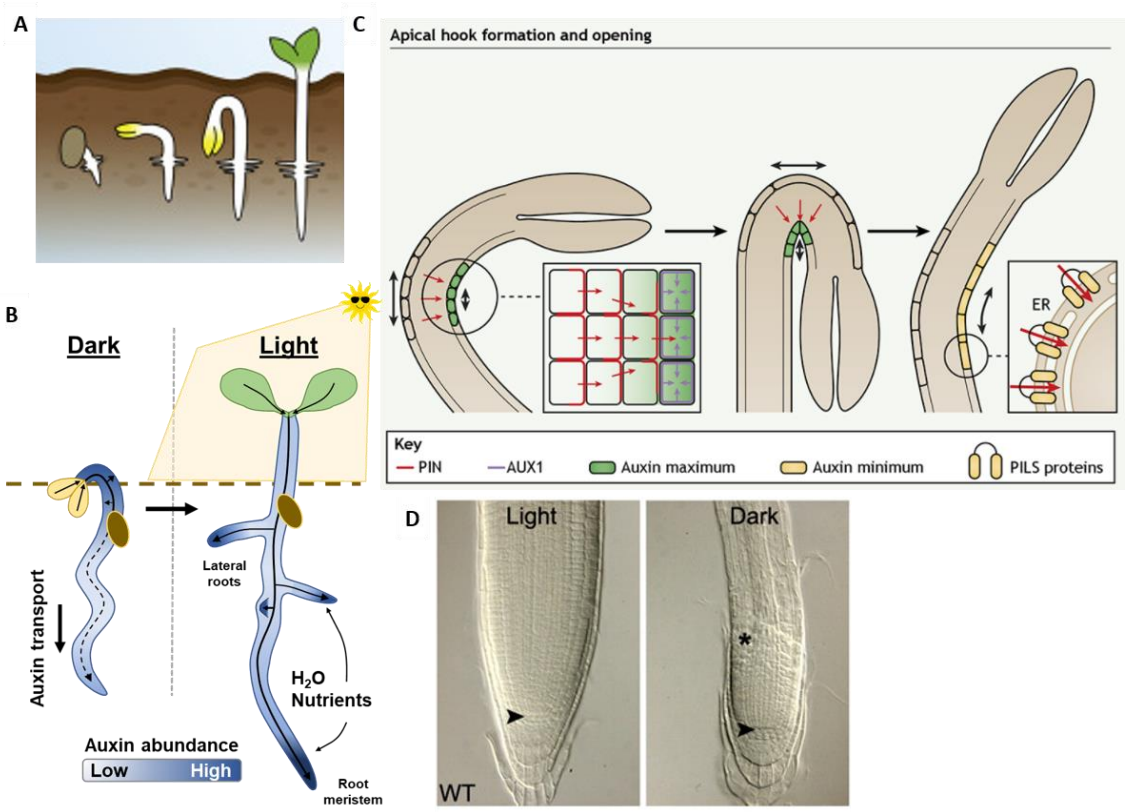

Figure 1-5 Auxin role during seedling transition to photomorphogenesis in Arabidopsis

(A) After germination in the soil, the seedling undergoes a skotomorphogenic phase until the cotyledons finally reach the light where the seedlings transitioned to photomorphogenic development. (B) Auxin distribution (arrows) plays an important role in this remodelling of the seedling. In the dark, auxin is predominantly abundant (dark blue) in the hypocotyl where it maintains hypocotyl etiolation and formation and maintenance of a closed apical hook. While the reduced rootward auxin stream creates an auxin minima (light blue) which inhibits root development. At the transition to photomorphogenesis, the auxin distribution is remodelled and is mainly transported to the root meristem (D) to ensure correct development of the root system. The auxin-driven development of the root meristem, in addition to the formation of lateral root, is essential for nutrients and water uptake.

(C) PIN proteins activity is key in the remodelling of the seedlings development. In the case of the apical hook, its formation in the dark is the result of asymmetrical accumulation of auxin in the cells of the inner side through the action of laterally polarized PIN and AUX1 protein. The auxin maxima inhibits cell elongation on the inner side of the forming hook while auxin minima on the outer cell layers promotes there elongation and the closure of the hook. The hook is maintained close in the darkness by the constant PIN-mediated auxin efflux toward the inner side. After light perception, the auxin distribution network is remodelled: the PIN driven stream to the inner side is stopped. Meanwhile, PILs proteins redirect cytosolic and nuclear localized free auxin into the endoplasmic reticulum, which ensures the dissipation of the auxin maxima in the inner cells. Finally, PIN protein redirect auxin flux in the elongating cells at the outer side, thus increasing auxin abundance and stopping the outer side elongation. Adapted from Sassi et al., 2012, Sauer and Kleine-Vehn, 2019, Jonsson et al., 2021.

1.3 Strigolactone and KAI2 signalling pathways

Two of the most recently discovered classes of signalling molecules modulating plant growth and development are Karrikin (KAR) and Strigolactone (SL).

1.3.1 Biosynthesis and structure

1.3.1.1 Karrikins

Karrikins were originally discovered in the 1990's when de Lange and Boucher reported a water-soluble chemical compound, found in smoke from plant-derived material burning, triggering the seeds germination of the local South-African fire-following specie *Audouinia capitata* (de Lange & Boucher, 1990). The stimulatory effect of this "smoke water" on germination was further reported to work at very low concentration and in numerous other plant species and it was found that it also stimulates the response to environmental cues, such as light and temperature, but also other signalling molecules operating during seed germination (reviewed in Brown & Van Staden. 1997). This active compound was finally identified as a new family of butenolide-derived compounds, named Karrikin in reference to the Nyungar aboriginal world *karrik* meaning "smoke" (Flematti et al., 2004, Dixon et al., 2009). The Karrikin group is composed of 50 different analogues which can be synthesized, among which 6 KARs (KAR1-KAR6) differing in their methyl substitutions have been identified from plant-derived smoke (Flematti et al., 2004, Flematti et al., 2007, Sun et al., 2008, Flematti et al., 2009) (figure 1.6). Structurally, KARs have similarities with the plant hormones Strigolactone (SLs), the second group of recently discovered signalling molecules (figure 1.6).

1.3.1.2 SL

Strigolactones (SLs) are a class of carotenoid-derived hormones characterized for their role in the control of plant development and rhizosphere signalling. The first SL to be described was strigol, an exudated compound that stimulates germination of the parasitic-plant *Striga lutea* in a dose-dependent manner (Cook et al., 1966). Much later, strigol-like compounds in *Lotus japonicus* exudates along with a synthetic SL analogue (GR24) were identified as inducers of hyphal branching in arbuscular mycorrhizal fungi (Akiyama et al., 2005). More recently SLs were classified as plant hormone after demonstration of their role in the inhibition of shoot branching in plants (Umehara et al., 2008). The SL biosynthesis pathway begins in the plastid with the action of DWARF27 (D27) on a carotenoid precursor. Afterward, the sequential action of CAROTENOID CLEAVAGE DIOXYGENASE7 (CCD7) and CCD8 (encoded respectively by *MORE AXILLARY GROWTH 3* and *4* (*MAX3*, *MAX4*) in Arabidopsis) (Schwartz et al., 2004) on the D27 product yields the formation of Carlactone (CL) (Alder et al., 2012) (figure 1.6). CL is the endogenous SL precursor and its oxidation catalysed by MAX1 in the cytosol results in the formation of carlactonoic acid (CLA) and subsequently in methyl carlactonoate (MeCLA) by the action of an unidentified enzyme (Abe et al., 2014, Seto et al., 2014) LATERAL BRANCHING OXIDOREDUCTASE (LBO) protein then catalyses the hydroxylation of MeCLA into diverse SL-like compounds likely to be the active forms of SL in plant (Brewer et al., 2016).

SL and SL-like compounds have a characteristic try-cyclic lactone moiety “ABC rings” assembling via an enol-ester bridge to a butenolide moiety “D-ring” (figure 1.6). SLs are further sub-classified as canonical SL if the molecule contains a full ABC-rings, or non-canonical SL if it has a non-ABC ring system linked to the D-ring (reviewed in Machin, Hamon-Josse, and Bennett, 2020). To date, 23 different canonical SLs and 6 non-canonical SLs (including Carlactone) have been identified (Yoneyama et al., 2018). In addition to naturally occurring SLs, the SL synthetic analogue *rac*-GR24 is - if not specially purified - a racemic mixtures of enantiomers $GR24^{5DS}$ and $GR24^{ent\text{-}5DS}$ (figure 1.6). Treatment with *rac*-GR24 causes a dual effect in plants as it induces SL signalling responses by the action of $GR24^{5DS}$, whereas the $GR24^{ent\text{-}5DS}$ enantiomer triggers KAR-like responses (Scaffidi et al., 2014, Conn et al., 2015), thus indiscriminately activating two signalling cascades.

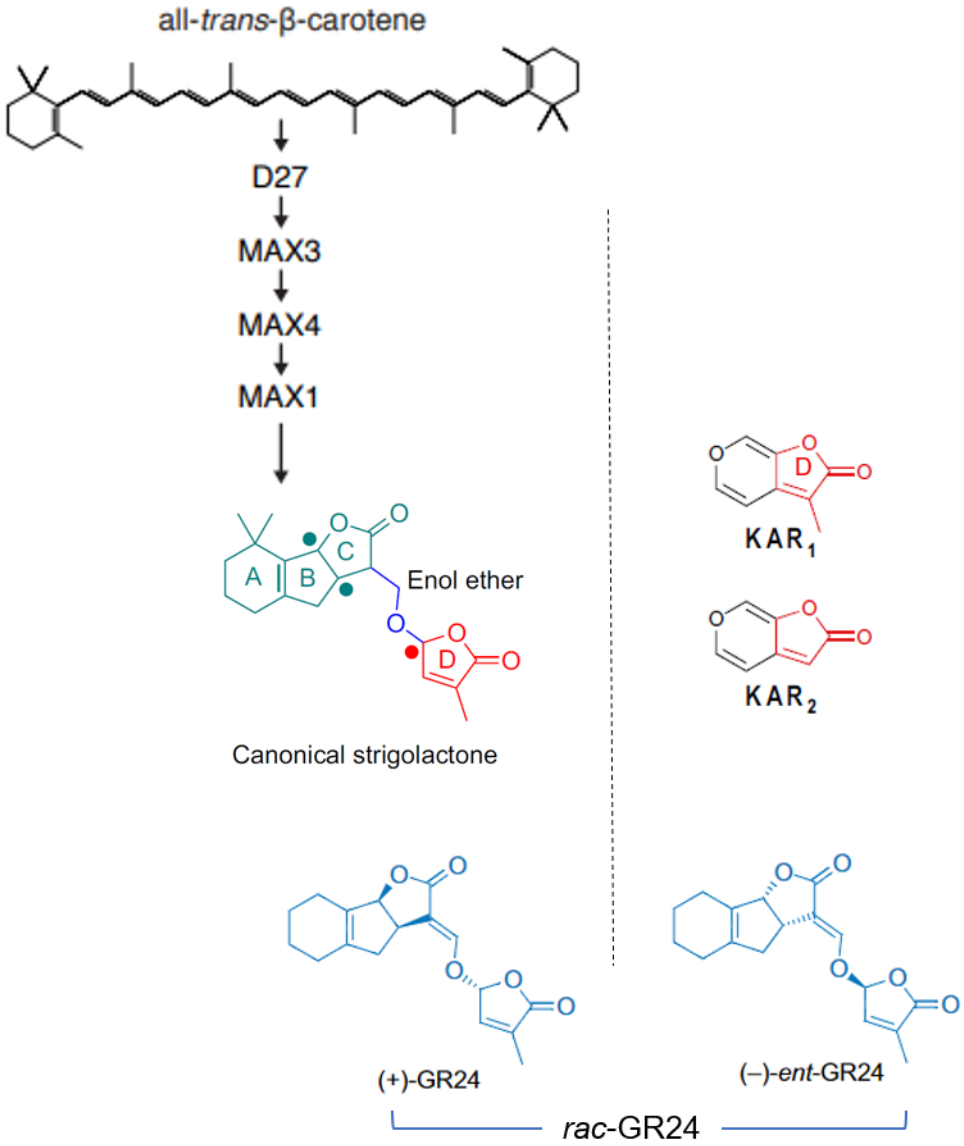

Figure 1-6 Structure and synthesis of SL and Karrikin compounds
The synthesis of Strigolactone (SL) is ensured by the transformation of a carotenoid-derived precursor into a molecule of SL by the action of D27, MAX3, MAX4, andMAX1 (in order of pathway). SL molecules can be classed into two groups, canonical SL is formed from complete ABC rings and D-ring, or non-canonical if containing only partial ABC rings in addition to the D-ring which is essential for SL perception and signalling. The D-ring can also be found in smoke-derived compounds Karrikins (KARs), among which KAR1 and KAR2 are the two usually used in laboratory to study Karrikin signalling pathway has it mimic KAI2-ligand (KL). SL and Karrikin action in Arabidopsis can also be mimicked by rac-GR24 which is a synthetic compound formed of two enantiomers: (+)-GR24 also referred as $GR24^{5DS}$ which mimics SL action, and (-)-ent-GR24 also referred as $GR24^{ent\text{-}5DS}$ which is an analogue of KAR/KL. Adapted from Machin et al., 2020.

1.3.2 Signalling

1.3.2.1 The D14/KAI2 receptor family

In land plants, KAR and SL are perceived by KARRIKIN INSENSITIVE 2 (KAI2) and DWARF 14 (D14) proteins respectively, which are two very closely related enzymatically active *α/β*-hydrolase receptors (Arite et al., 2009, Waters et al., 2012, Hamiaux et al., 2012, Guo et al. 2013) (figure 1.7). Phylogenetic analysis reveal that D14 has evolved by neo-functionalization after gene duplication in an ancestral KAI2 lineage. D14 can only be found in Gymnosperm and Angiosperms while KAI2-like proteins are present in all plant clades including non-vascular plants (mosses, liverworts, hornworts), which evolved from an ancient KAI2-like lineage present in algae (Delaux et al. 2012, Waters et al., 2015b, Bythell-Douglas et al. 2017, reviewed in Machin et al., 2020) (figure 1.7.A). Interestingly, *D27*, *CCD7*, and *CCD8* are present in liverworts, mosses and bryophyte, and moss *Physcomitrella patens* produces SLs and possesses KAI2 receptor, while *D14* is not present, suggesting perception of SL could be an ancestral function of KAI2 in basal plants (Delaux et al. 2012). This hypothesis is further supported by the presence in parasitic plants of a receptor derived from early KAI2 receptors that senses SL in the rhizosphere, allowing them to sense their host's presence and germinate at the correct time and in the correct place (Conn et al., 2015, Toh et al. 2015). However, promoter swap between *D14* and *KAI2* does not rescue the known functions of *D14* and *KAI2* respectively, indicating distinct functionalities in Arabidopsis (Waters et al., 2015a); thus, contradicting this hypothesis. In addition, the careful analysis of the evolutionary history of SLs across green lineages revealed that there is no true CCD7 or CCD8 enzymes in charophyte algae (Walker et al., 2019), consistent with the idea that canonical SL biosynthesis is solely the hallmark of land plants, and their perception does not require KAI2. Intriguingly, defects in KAI2 lead to developmental abnormalities including defects in germination, leaf expansion and hypocotyl elongation in non-fire-following plants including our model species *Arabidopsis thaliana* (Nelson et al., 2009, Nelson et al., 2010, reviewed in Machin, Hamon-Josse, and Bennett, 2020). These observations, in addition to the lack of evidence for KAR synthesis by plants, suggest that KAR mimics an endogenous signal perceived by KAI2 and named KAI2-ligand (KL) (Conn and Nelson, 2016).

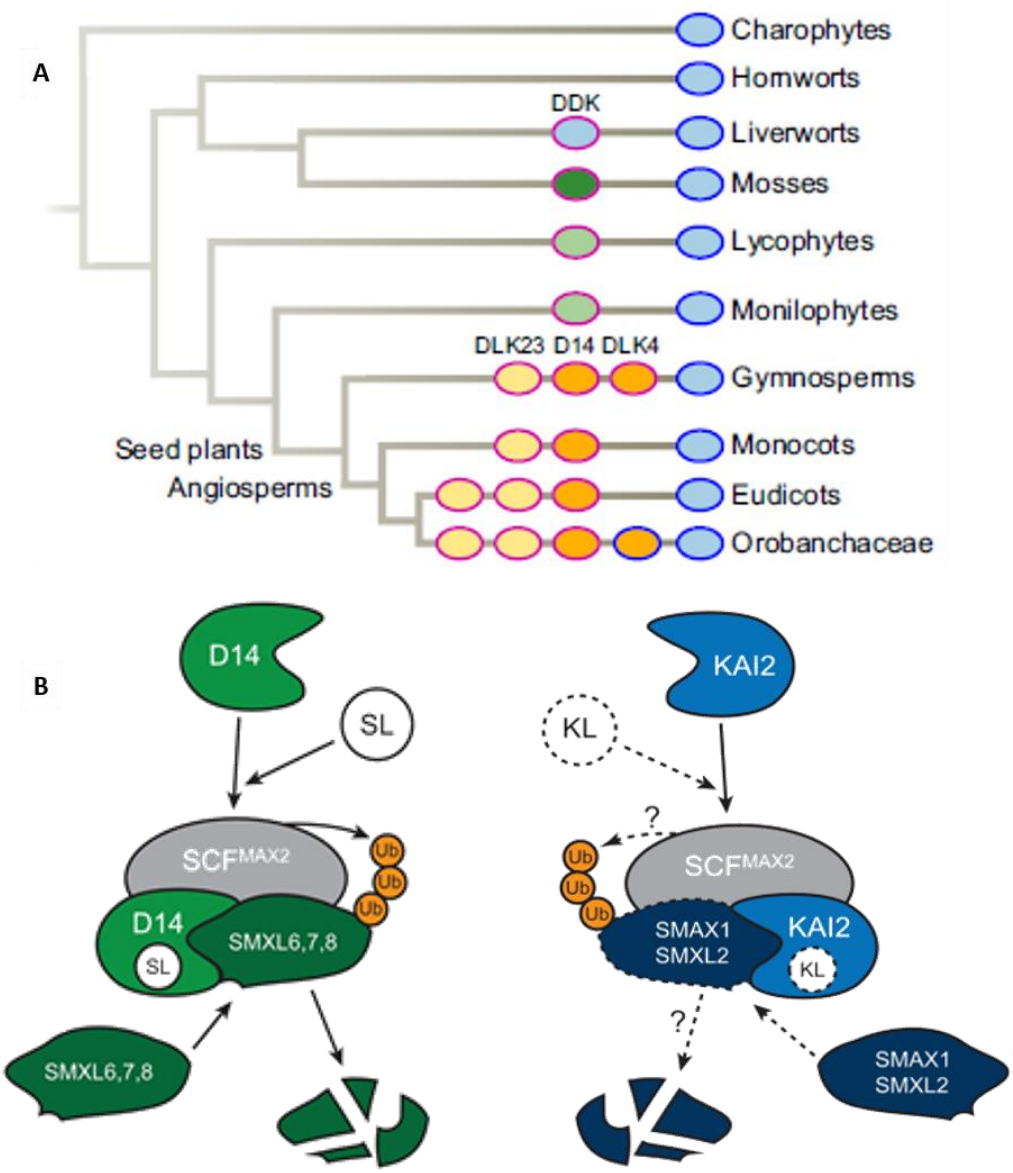

Figure 1-7 Phylogeny of D14/KAI2 proteins family, and model of SL and KL signalling pathways

(A) Gene duplication events are indicated as D1, before the emergence of tracheophytes, and D2 after the split of angiosperms and gymnosperms. From Waters et al., 2015.

(B) (Left) SL and GR24^{5DS} bind to D14 allowing the conformational change of D14 required to form the D14-SCF^{MAX2} complex. D14-MAX2 complex then recruits SMXL6, 7, 8 proteins. After formation of the complex SMXL6, 7, 8 are poly-ubiquitinated and degraded by the 26S proteasome. Recruitment of SMXL proteins 6, 7 and 8 in a SL-dependent manner induces responses such as regulation of the shoot and leaf development, and regulation of the root development. (Right) KAR1, GR24ent-5DS, and the yet unidentified KAI2-ligand (KL) compound can bind to KAI2 which then form a KAI2-SCFMAX2 complex to recruit the downstream targets of KL signalling pathway. SMAX1 and SMXL2 are the two targets of KAI2 signalling, and their recruitment and ubiquitination/degradation in a MAX2-dependent manner allow the regulation of seed germination, photomorphogenesis and hypothetically a control of RSA in a KL/KAI2 dependent manner. Adapted from Villaécija-Aguilar et al., 2019.

1.3.2.2 The receptor complex with MAX2

From a structural aspect, both D14 and KAI2 contain a ligand-binding pocket with a catalytic triad consisting of a serine (Ser/S) at position 147, histidine (His/H) at position 297, and aspartic acid (Asp/D) at position 268 (Kagiyama et al. 2013, Zhao et al. 2015). The docking of SL, or the synthetic GR24^{5DS} to the binding pocket of D14 allows the hydrolysis of the SL and the liberation of its tricyclic ABC-rings and the generation of a 'covalently linked intermediate molecule' (CLIM) from the D-ring (Kagiyama et al., 2013, Zhao et al., 2013, Yao et al., 2016). The hydrolysis of SL induces an irreversible open-to-close switch of the D14 pocket (Zhao et al. 2015, Nakamura et al. 2013), which stabilizes the interaction between D14 and the SL-signalling component DWARF3 (D3) (rice), or MAX2 (Arabidopsis) (figure 1.7.B). MAX2 is a F-box leucine-rich repeat protein, functioning in complex with an SCF (Skp1, Cullin, F-box) E3 ubiquitin ligase complex (SCF^{MAX2}), to poly-ubiquitinate specific proteins, targeting them for proteolysis (Stirnberg et al., 2007).

The formation of D14-SCF^{MAX2} complex leads to the MAX2-dependent ubiquitination and degradation of SL signalling proteolytic targets by the 26S proteasome driving downstream signalling responses (Zhao et al. 2015, Yao et al. 2018, reviewed in Machin et al., 2020) (figure 1.7.B). Similarly, it was shown that the catalytic triad is essential for the docking of KAR and GR24$^{ent-5DS}$ into KAI2 pocket, and the formation of a KAI2-MAX2 complex. Genetically, the *max2* mutant reflects a beautiful combination of *d14* and *kai2* phenotypes: increased shoot branching from *d14*, increase seed germination and decreased photomorphogenesis due to *kai2* (Nelson et al., 2011, Waters et al., 2012b, Stanga et al., 2013).

1.3.3 The proteolytic target SMXL proteins

In the search to identify proteolytic targets of SL and KL signalling, screening for mutation suppressing *max2* phenotypes led to the characterization of the SUPPRESSOR OF MAX2 1 (SMAX1) / SMAX1-LIKE (SMXL) family of proteins, which is composed of 8 members in Arabidopsis, and which were hypothesised to be SL and KAI2 downstream targets (Stanga et al., 2016) (figure 1.7 B and figure 1.8.A). Among those 8 members, *smax1* and *smxl2* mutations were shown to completely suppress (with some degree of redundancy) all phenotypes associated to seed germination, cotyledon development, and hypocotyl elongation in *max2* (Stanga et al., 2013, Stanga et al., 2016); SMAX1/SMXL2 were later shown to also mediate *kai2* related root phenotypes, including defects in root hair development, abnormal root skewing, and adventitious root

proliferation (Swarbreck et al. 2019, Carbonnel et al., 2020, Swarbreck et al. 2020). However, *smax1 smxl2* does not suppress the dwarf and branchy shoot phenotype of *max2*, which led to the conclusion that other members of the SMXL family would be implicated in these SL-related phenotypes (Stanga et al. 2013, Soundappan et al. 2015). The SMXL proteins sub-group associated to SL signalling was first identified in rice, where *dwarf 53* (*d53*) has been reported as a mutant with increased tillering (i.e. basal shoot branching) (Jiang et al., 2013). Examination of *D53* expression revealed its expression is up-regulated in WT plants treated with exogenous *rac*-GR24. By contrast, SL-deficient and SL-insensitive plants exhibit a down-regulation of *D53* or equivalent *SMXL6*/*7*/*8* in *Arabidopsis thaliana*, suggesting a negative feedback control of SL signalling by these proteolytic targets (Jiang et al., 2013, Zhou et al., 2013). Later three co-orthologues of D53 in Arabidopsis (SMXL6, SMXL7, SMXL8) were identified as proteolytic targets of D14-MAX2 complex downstream of SL perception (Wang et al., 2015, Soundappan et al., 2015) (figure 1.8.A).

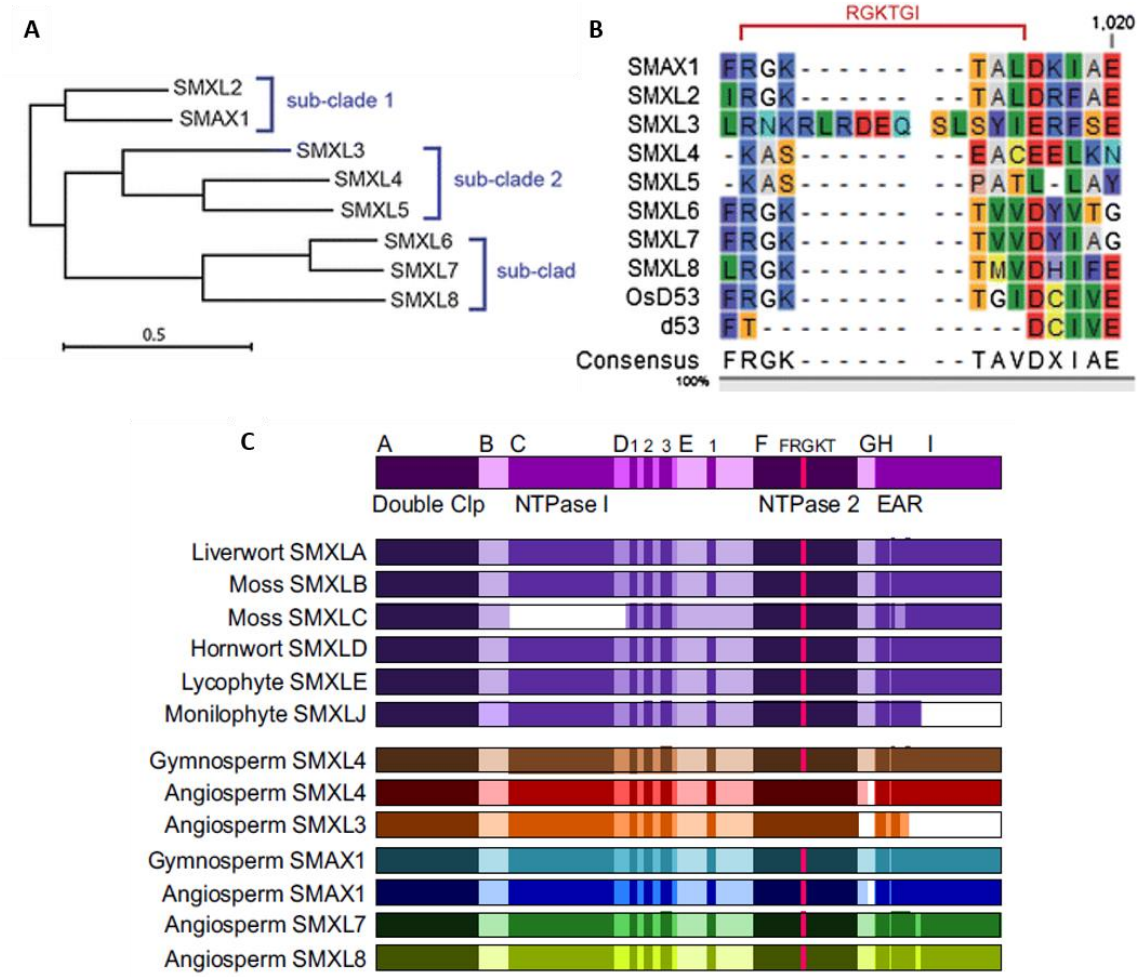

Figure 1-8 Phylogeny and diversity of structure among SMXL proteins family

(A) SMXL proteins family is composed of three sub-groups in Arabidopsis: the sub-clade one contains SMAX1 and SMXL2 and is involved in KL signalling. The second sub-clade contains three proteins, SMXL3, 4 and 5, acting independently of SL and KL signalling. The third sub-clades contain the downstream effectors of SL signalling (SMXL6, 7 and 8). Adapted from Wallner et al., 2016.
(B, C) General structure of SMXL proteins across land plants (C - top). SMXL proteins have a highly conserved, multidomain structure (domains A–I) (C - bottom). The degree of sequence conservation across the family is indicated by shading; darker colours indicate more conserved domains. The FRGKT motif indicated in pink is present in all SMXL proteins apart from SMXL3, 4 and 5 in Arabidopsis (B), and is essential for recruitment/degradation of SMXL proteins through SL and/or KL signalling. The position of the EAR motifs is also indicated. Adapted from Wallner et al., 2016, Machin et al., 2020.

1.3.4 Receptor-SMXL complex

SMXL proteins structure is characterized by the presence of a large and highly conserved multidomain (figure 1.8 B-C). Some of these domains have been well characterised and their function is understood, alike the exceptionally well conserved ‘double Clp’ domain containing a nuclear localised signal; Although the function of others is yet unclear (figure 1.8 C). The domains F-I represent one of the two NTPase present in SMXL proteins. The exact the function of these domains is a subject of contradiction and discussion in the literature (Zhou et al., 2013; Shabek et al., 2018, reviewed in Machin et al., 2020); However, there is a consensus that the conserved RGKTGI motif present in the domain F of most SMXLs is required for the SL-induced ubiquitination and degradation of the SMXL proteins (Jiang et al., 2013, Zhou et al., 2013, Soundappan et al., 2015) (figure 1.8.B-C). To this regard, rice mutant *d53* is characterized by an eight amino acid deletion of the conserved RGKTGI motif which prevents its Strigolactone-mediated degradation. The interaction of SMXL7/D53 with D14-D3 pair (or its orthologue MAX2) was demonstrated *in vitro* and *in planta*, and SMXL6/7/8 degradation requires D14 and D3 as well as the presence of SL or the SL analogue *rac*-GR24, although there is no direct binding of SMXL7 to MAX2 (Jiang et al., 2013, Zhao et al., 2014, Wang et al., 2015, Soundappan et al., 2015, Liang et al., 2016). Similarly, the KAI2-SCF^{MAX2} complex was shown to target SMAX1 and SMXL2 for degradation (Khosla et al., 2020; Wang et al., 2020b), although a D14-mediated SMXL2 targeting and degradation is possible (Wang et al., 2020b).

Analysis of the structural and amino acid sequence of the SMXL proteins shows that SMXL3, SMXL4, and SMXL5 proteins (from the third sub-clade of SMXL proteins in flowering plants) lack the RGKTGI motif, suggesting that these three SMXLs might not be degraded by SCF^{MAX2} (Soundappan et al., 2015, Wallner et al., 2016) (figure 1.8.B-C). Indeed, Wallner et al., (2017) showed that SMXL3,

SMXL4, and SMXL5 act independently of MAX2-mediated SL and KL signalling in the control of the phloem formation in Arabidopsis, consistent with the conclusions of Soundappan et al. (2015). Their stability is not disrupted by the addition of *rac*-GR24 contrary to SMXL6, SMXL7 and SMXL8, which are rapidly degraded after treatment. However, expression of SMAX1 under the SMXL5 promoter in the *smxl4 smxl5* double mutant can partially restore the phenotype, but the application of GR24 triggers a MAX2-dependent degradation of SMAX1 and abolished this rescue. In contrast, SMXL5:SMXL5-YFP in the same experiment can rescue the *smxl4 smxl5* double mutant phenotype even in the presence of exogenous rac-GR24 application. These results indicate that some proteins of the SMXL family act independently of SL- or KL- signalling in the regulation of plant development. The ability of SMAX1 to rescue the phenotype of *smx4 smxl5* also suggests that SMXL proteins may be largely interchangeable at a molecular level, but are regulated differently (Wallner et al., 2017).

1.3.4.1 Function of SMXL proteins

Transcriptional regulators

SMXL proteins, as well as the components of SL and KL receptor complexes, all have a nuclear localization (Liang et al. 2016, Soundappan et al. 2015, Jiang et al. 2013, Zhou et al. 2013, Khosla et al., 2020, Wang et al., 2020b) (figure 1.8.C). The function of SMXL proteins downstream of SL and KL signalling can be seen to some extent as an analogy to auxin signalling, in which the transcriptional repression on ARFs proteins mediated by Aux/IAA-TPL can be alleviated by TIR1-induced degradation. Indeed, SMXL proteins, as for Aux/IAA, do not have DNA-binding motif themselves but contain EAR motifs allowing protein-protein interaction with the TPL/TPR transcriptional co-repressor family (Causier et al., 2012, Martin-Arevalillo et al., 2017, Jiang et al., 2013, Soundappan et al., 2015, Wang et al., 2015, Moturu et al., 2018, Liang et al., 2017, Ma et al., 2017) (figure 1.8.C). It was demonstrated *in vivo* that SMXL7 and SMAX1 proteins lacking EAR motif were unable to interact with TPR2 (Soundappan et al., 2015, Liu et al., 2017) (figure 1.9), however, the relevance of these interactions *in planta* remains to be validated. At the functional level, it was shown in Arabidopsis that most phenotypic effects of SMXL7 were unaffected in variants lacking the EAR motif (SMXL7mEAR), although mediation of shoot branching partially relies on the presence of the motif (Liang et al., 2016). To the question, do SMXL proteins mediate transcriptional repression, the answer is yes, as there is an increasing number of evidence pointing toward it. For instance, the BRANCHED1 (BRC1) class of TCP-domain transcription factors, have an important role in shoot branching in several plant species, and appear to be directly targeted

downstream of SL signalling (figure 1.9). In Arabidopsis, there is a rapid transcriptional down-regulation of *BRC1* to GR24 treatment, and its expression is reduced in *smxl6 smxl7 sxml8* triple mutants. By opposition, its transcription is up-regulated in SL deficient and SL insensitive mutants (Braun et al., 2012; Dun et al., 2012; Soundappan et al., 2015; Seale et al., 2017). In addition, two independent studies on rice and wheat demonstrated an interaction between SL signalling and SQUAMOSA PROMOTER BINDING PROTEIN-LIKE (SPL) proteins in the control of plant architecture (Song et al., 2017, Liu et al., 2017) (figure 1.9). SL signalling component D53/SMXLs binds to the transcriptional factor SPL14 (Song et al., 2017), encoded by *IDEAL PLANT ARCHITECTURE1* (*IPA1*) and involved in the negative regulation of the tillering in rice. D53 interaction with SPL14 promotes SPL14 binding to the promoter of *OsTB1* (the homolog of *BRC1*) via its SBP-box and represses its expression (Miura et al., 2010) (figure 1.9). Similarly, SL signalling repressor D53/SMXL678 is functionally associated to TaSPL3 and TaSPL17 transcription factors in wheat to regulate the transcription of *TaTB1* (Liu et al., 2017).

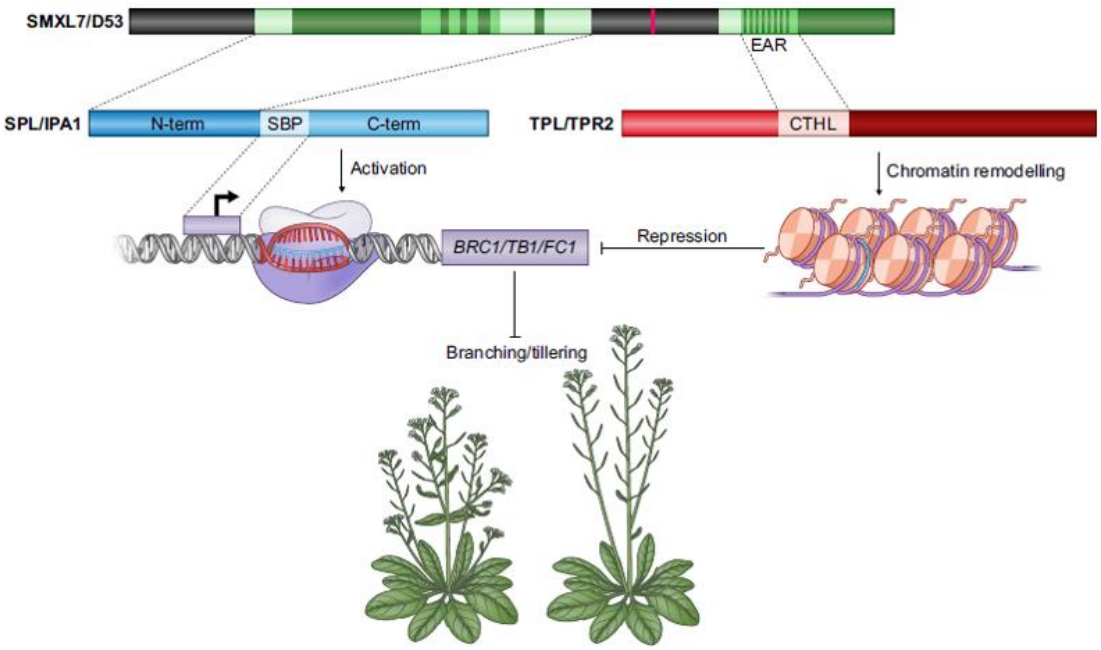

Figure 1-9 Model for the function of SMXL proteins downstream of SL signalling

SMXLs exert transcriptional inhibition of target genes BRC1, involved in shoot branching. First, SMXL proteins EAR motifs allow for interaction with TPL/TPR transcriptional co-repressors resulting in assembly of repressive chromatin structures that turn off BRC1 transcription and thereby promoting branching. Secondly, SMXLs can interact with SPL proteins which in turn repress the transcription of the target genes. From Machin et al., 2020.

In contrast to SL signalling, the transcriptional activity downstream of KL signalling is poorly understood, although SMAX1 and SMXL2 are nuclear-localized and carry an EAR motif (figure 1.8.B-C), suggesting they could act in a similar fashion to SMXL6/7/8 and have direct transcriptional targets that remain to be identified (Soundappan et al., 2015). Evidence toward a transcriptional activity come from the differential expression of some genes in a KAR/KL signalling dependent manner. For instance, KAR treatment strongly induces *DWARF14-LIKE2 (DLK2), KARRIKIN UPREGULATED F-BOX1 (KUF1), and B-BOX DOMAIN PROTEIN 20 (BBX20)* expression (Nelson et al., 2010, Waters et al., 2012, Bursch et al., 2021, Sepulveda et al., 2022). This transcriptional effect is confirmed by a downregulation of their transcription in *kai2* and *max2* mutants, while being upregulated in *smax1 smxl2*. Although *DLK2* (a paralogue of KAI2) expression is mediated by KL signalling and is considered as a hallmark of KAI2 signalling (Nelson et al., 2011, Waters et al., 2012, Stanga et al., 2016, Bursch et al., 2021), DLK2 function in plants is not yet understood as *dlk2* mutant is aphenotypic in Arabidopsis (Vegh et al., 2017). The transcriptional induction of *BBX20* in a KL signalling-dependent manner was recently shown to be a component of the hypocotyl growth responses to KAR/KL, paving the road for a better understanding of the downstream mechanisms of KAI2 signalling (Bursch et al., 2021).

Regulation of auxin transport

Although the functions of SMXL proteins remain largely enigmatic, the work achieved in the past two decades to understand how SL signalling modulates shoot branching has led to a series of evidence connecting SL signalling and auxin transport in the branches (Shinohara et al., 2013, Crawford et al., 2010, Van Rongen et al., 2019). First, SL-deficient mutants display an increased auxin transport capacity correlating with an increased shoot branching (Bennett al., 2006). Second, SL signalling represses the main polar auxin transport stream in stems via a rapid removal of the PIN1 auxin efflux proteins from the basal membrane of xylem parenchymal cells (Shinohara et al., 2013, Bennett et al., 2016b). Moreover, stabilization of SMXL7 is sufficient to increase both basal PIN1 accumulation and auxin transport through the stem, and to alter shoot branching (Liang et al., 2016). Consistent with these results, SMXL6, SMXL7 and SMXL8 are proposed to act as positive regulators of auxin transport, and their degradation through SL signalling triggers a decrease of PIN accumulation and auxin transport to the buds, repressing their initiation and outgrowth. Although the role of SL in the root remains obscure (see paragraph 1.3.4), PIN2 expression in the epidermal cells of the elongation zone is up-regulated and PIN2 polarization

in the PM is enhanced in response to *rac*-GR24 treatment (Pandya-Kumar et al., 2014).

Concerning a role of KL signalling on auxin transport, less is known. Bursch et al., (2021) recently reported a list of auxin-responsive genes regulated downstream of KAI2 signalling. In addition, it was suggested that enhanced auxin transport contributes in part to the hypocotyl elongation of *max2* seedlings grown in the light (Shen et al., 2012). Indeed, *max2* is disproportionally sensitive to inhibition of polar auxin transport by *N*-1-naphthylphthalamic acid (NPA) (Shen et al., 2012), known to specifically block PIN activity (Abas et al., 2021). Finally, a recent study demonstrates that KAI2 signalling is required for the correct modulation of auxin transport associated to phosphorus depletion responses in Arabidopsis (Villaécija-Aguilar et al., 2021). In this study, Villaécija-Aguilar et al., (2021) report that KAI2 and MAX2 promote shootward auxin transport in the meristematic zone, and KL signalling is required for tissue-specific accumulation of AUX1 and PIN2 ensuring correct root hair elongation. Intriguingly, all SMXL proteins are localized in the nucleus while PIN proteins are PM localized; making it difficult to understand the mechanism(s) by which changes in SMXLs level could affect PINs abundance and/or polarization. Recent data show that MAX2 and *rac*-GR24 signalling inhibits the inhibitory effect of auxin on PIN endocytosis in roots (Zhang et al, 2020), suggesting a mechanism by which SL signalling and SMXL6/7/8 directly target PIN recycling from the plasma membrane. Although Zhang et al. suggested these effects reflected the output of strigolactone signalling, they might equally reflect outputs of KAI2 signalling, given the use of *max2* mutants and *rac*-GR24 in these experiments. Additionally, given the strong structural and amino acid sequence similarities between SMXL7 and SMAX1 sub-clades, and the fact that SMAX1 is evolutionary ancestral to SMXL7, it would be interesting to test whether the targeting of the PIN-mediated auxin transport is a specificity to SMXL7 group or instead an ancestral function of KAI2-targeted SMXL proteins (SMAX1 and SMXL2) in seed plants.

1.3.5 SL and KL functions in plant development

The first SL to be described was strigol, an exuded compound that stimulates germination of the parasitic-plant *Striga lutea* in a dose-dependent manner (Cook et al., 1966). Much later, strigol-like compounds in *Lotus japonicus* exudates along with a synthetic SL analogue (GR24) were identified as inducer of hyphal branching in arbuscular mycorrhiza fungi (AMF) (Akiyama et al., 2005). SLs were classified as plant hormone when it became clear they acted long distance as an endogenous signal controlling the plant architecture in a large cohort of species. Firstly, SLs were shown to repress shoot branching (Umehara et al., 2008) (figure

1.10). Since then, the identification of D14 and MAX2 receptor complex and the characterization of SMXL7 have led to a better understanding of the mechanisms by which SL inhibits branching (reviewed in Rameau et al., 2019). In short, it involves the synergistic effects of SMXL6, SMXL7, and SMXL8 on both the transcriptional regulation of BRC1 and the modulation of PIN-mediated auxin transport to the buds (see 1.3.3.2). While shoot branching is the flagship phenotype of SL mutants, SL signalling regulates other aspects of flowering plant development, including stem and internode elongation (de Saint Germain et al., 2013) and leaf shape (Stirnberg et al., 2002, Scaffidi et al., 2013, Soundappan et al., 2015) (figure 1.10).

Meanwhile, KL signalling does not participate in shoot branching and stem elongation, but KAI2 acts in parallel of D14 to control leaf and petiole development (Waters et al., 2012, Soundappan et al., 2015, Bennett et al., 2016a). In addition, while the mechanisms remain unknown, KAI2 is required for establishing arbuscular-mycorrhizal symbiosis, while its proteolytic target SMAX1 facilitates the fungal colonization by mediating SL production in rice (Gutjahr et al., 2015, Choi et al., 2020) (figure 1.10). Among the other roles of KL signalling in plant development, *kai2* mutant was shown to have strong hypocotyl elongation, short cotyledon and hyponastic petioles and a defect in germination, along *max2*, in Arabidopsis (Sun and Ni, 2011; Waters et al., 2012) (figure 1.10). It was reported that SMAX1 and SMXL2 act with a certain degree of redundancy downstream of the KAI2-MAX2 complex to regulate these early developmental traits of the seedlings (figure 1.10). While regulation of the hypocotyl elongation requires the joint action of both SMAX1 and SMXL2, it appears leaf shape, germination, and petiole orientation are traits predominantly controlled by SMAX1 only (Stanga et al., 2013, Stanga et al., 2016). Importantly, both KARs and $GR24^{ent\text{-}5DS}$ can mimic the endogenous KAI2-ligand (KL) to promote seed germination and enhance the photomorphogenic growth of Arabidopsis seedlings by inducing KAI2-SCF^{MAX2}-dependent targeting of SMAX1 and SMXL2 for proteolysis (Nelson et al., 2010, Khosla et al., 2020, Wang et al., 2020b). Notably, a recent study demonstrated that not only $GR24^{ent\text{-}5DS}$ but also $GR24^{4DO}$ (analogue of SL) can trigger the poly-ubiquitination and degradation of SMXL2 in either a KAI2- or D14-dependent manner to modulate hypocotyl elongation (Wang et al., 2020b). These new data suggest SMXL2 as a proteolytic target of not only KAI2 but also SL signalling, and thus raises interrogations on whether there is a degree of convergence in the roles of SL and KL pathway in modulating certain aspects of seedling development. Hypocotyl elongation is a very easily observed phenotype and is the hallmark of KAI2 signalling in seedlings, however, the mechanisms by which KL signalling operates downstream of SMAX1/SMXL2

remain mostly unidentified. The convergent roles of D14 and KAI2 in regard to the regulation of hypocotyl elongation opens new perspectives to understand the mechanisms of action of KAI2; indeed, more is known about SL downstream targets (e.g. SL-dependent modulation of polar auxin transport) and given the close similarities between SL and KL pathways it is possible/likely that they share a same mechanism downstream of SMXL2 to modulate hypocotyl elongation.

1.3.5.1 SL and KL signalling functions in roots

- Primary root

The wide use of *max2* mutants and *rac*-GR24*,* before full understanding of the D14-KAI2 dichotomy, have led to a cohort of studies attributing changes in root growth caused by *max2* and *rac-GR24* to SL signalling (reviewed in Machin et al., 2020). However, the use of GR24 and *max2* precludes clear understating of roles for each pathway.

SL mutants often display a reduced primary root length (PRL) in Arabidopsis, rice, and barley (Ruyter-Spira et al., 2011, Arite et al., 2012, Marzec et al., 2016) (figure 1.10), while *rac*-GR24 treatment in wild-type induces primary root growth resulting from an increased cell number in meristem and transition zone (Ruyter-Spira et al., 2011). Thus, Strigolactones have long been proposed to regulate the primary root growth in several species, while it appears it has a lesser/no impact on other species (Koltai et al., 2010, de Cuyper et al., 2015), and that in some species such as rice the effect is conditional on the growth conditions (phosphorus and nitrate availability in the growth media) (Mayzlish-Gati et al., 2012, Sun et al., 2014). SL-deficient mutants (*max3*, *max4*, *max1*) display a shorter PRL than wild-type in several species including Arabidopsis. The primary root phenotype of *max2* is more subtle, it varies between slightly shorter PRL to no differences compared to wild-type depending the species, growth conditions, and experimental designs used (reviewed in Marzec et al., 2018). Moreover, the PRL phenotype of the SL-insensitive mutant *d14* remains poorly characterized, adding a level of uncertainties on understanding the exact role of SL in the primary root development.

Characterizing the role of SMXL on primary root development, downstream of D14/KAI2, has received little attention from the strigolactone community. For instance, it appears *smxl678* mutations do not affect the PRL in 10 days-post-germination Arabidopsis seedlings, while *smax1 smxl2* results in a subtle but consistent reduction of primary root growth in the same experiments (Wallner et al., 2017) (figure 1.10). This last observation is further supported by a recent study showing that *smax1* mutation results in reduced PRL in young *Lotus japonicus* seedlings and demonstrated that SMAX1 fine-tunes the primary root

development by regulating the synthesis of ethylene in a KAI2-MAX2-dependent manner (Carbonnel et al., 2020). This report on SMAX1 is consistent with the observation of *SMAX1* promoter activity in the root cap of primary roots in Arabidopsis (Soundappan et al., 2015, Wallner et al., 2017). Excitingly, the role of SMXL3, SMXL4, and SMXL5, was also recently uncovered, with a role in phloem formation and therefore primary root development, in a SL- and KL-independent manner (Wallner et al., 2017). These recent discoveries raise important questions as it seems SL biosynthesis and D14-MAX2 complex are required for the correct development of the primary root, meanwhile SMXL678 do not seem to be important, and no *SMXL6*, *SMXL7*, or *SMXL8* promoter activity can be observed in the meristem zone of the primary root (Soundappan et al., 2015). On the other hand, SMAX1 appears to regulate PRL despite not being a commonly agreed target of SL signalling, and the root phenotype of *kai2* remains globally uncharacterized.

- Lateral roots

SLs have also been proposed to affect the development of lateral roots (LR). On one hand, in Arabidopsis SL deficient mutants *max3* and *max4* shows an unclear lateral root density (LRD) phenotype, while SL deficient mutants in rice have a strong increased LRD compared to a wild-type but inconsistent between experiments (Kapulnik et al., 2011, Ruyter-Spira et al., 2011, Arite et al., 2012, Sun et al., 2014) (figure 1.10). On the other hand, *max2* seedlings exhibit a clear and consistent increased LRD, stronger than the SL biosynthesis mutants. Furthermore, *rac*-GR24 treatment inhibits LR formation in a MAX2-dependent manner (Kapulnik et al., 2011, Ruyter-Spira et al., 2011). It was further suggested that MAX2 and *rac*-GR24 may regulate LR during the outgrowth of new emerged LR (LRe), and that affecting polar auxin stream at the initiation sites could be an underlying mechanism (Jiang et al., 2016). The inhibitory effect of *rac*-GR24 on LRD is proposed to result from an alteration of the LR outgrowth in the mature root tissues rather than on the formation of new prebranching sites (Jiang et al., 2016). However, the effects of *rac*-GR24 on LRD might well reflect a cohesive action on inhibition of primary root growth and induction of lateral root proliferation, given that LRD is the ratio between number of LR and length of the primary root. Interestingly, *smxl6 smxl7 smxl8* mutation appears to supress the LRD phenotype of *max2* (Soundappan et al., 2016) consistent with a role of SL signalling in LR development. But *smax1* mutation alone could not supress the enhanced LR phenotype of *max2* (Soundappan et al., 2015), however, the role of SMXL2 has not been addressed to this regard. To date, the role of D14 and KAI2 in the MAX2-dependent regulation of lateral root development has not been characterized. Over the last 10 years, we have seen a rising number of reviews

mentioning SL as an essential regulator of LR development, but so far there is no clear answers on what falls under D14-MAX2 or KAI2-MAX2 dependency. The current knowledge on the topic is at best in a grey area, and a great care should therefore be taken when drawing conclusions and disseminating them in the literature.

- Adventitious roots

The development of adventitious roots (AR) from non-root tissues is another root trait SL signalling has been associated with. In Arabidopsis and pea, SL deficient mutants (*max1*, *max3*, and *max4*) exhibit up to a 3-fold increase in AR number, but in an inconsistent fashion between mutants from the same biosynthesis pathway. On the other hand, *max2* mutants develop 5-fold more AR than wild-type when seedlings are etiolated for 4-days in the dark before transfer to light, and *rac*-GR24 treatment shows an inhibitory effect on AR formation, suggesting a negative role of SL on AR development (Rasmussen et al., 2012) (figure 1.10). By opposition, rice *d10, d17, d14* and *d3* mutants (respectively orthologues of *max4, max3, d14,* and *max2* in Arabidopsis) have fewer crown roots (a type of adventitious roots in monocots) than wild-type plants, while addition of GR24 induces a strong AR proliferation in SL biosynthesis mutants, suggesting a positive role of SL in AR formation (Sun et al., 2015, Arite et al., 2012). Thus, the evidence of a role of SL signalling on AR development appears inconsistent between experiments and species. On the other hand, a recent study investigating the role of SL and KL on adventitious root development showed that while Arabidopsis *d14* mutant exhibits only a small increase in the number of AR compared to wild-type, *kai2* mutants display a significant AR proliferation to a same degree of magnitude as *max2, or kai2 max2* double mutant (Swarbreck et al., 2020). In addition, in these experiments, *smxl6 smxl7 smxl8* and *smax1* single mutant had no AR phenotype, but both *smxl678* and *smax1* mutants could suppress *max2* phenotype. This new insight supports the idea that KL rather than SL would be involved in AR development in Arabidopsis. These data also raise questions regarding a potential role of SMXL6/7/8 downstream of KAI2-MAX2 in regulating AR development (Swarbreck et al., 2020).

- Root hair

Root hair (RH) proliferation is a root developmental process highly regulated by plant hormones, among which SLs have been proposed to act on both root hair density (RHD) and root hair length (RHL). Most assumptions on the role of SL in root hair are based on the early observations that *rac*-GR24 treatment induces a strong elongation of the RHL in tomato and Arabidopsis (Koltai et al., 2010, Kapulnik et al., 2011). There is no difference in RHL between wild-type and a SL

biosynthesis mutant (*max4*) which displays a same response to GR24 than wild-type; but *max2* seedlings consistently display shorter RH and are insensitive to *rac*-GR24 (Kapulnik et al., 2011). The MAX2-dependent regulation of RHs was further shown to be important in the root hair proliferation in response to low phosphorus availability (Mayzlish-Gati et al., 2012). Interestingly, the effects of *rac*-GR24 and MAX2 on root hair elongation were shown to not only require ethylene synthesis, but also to be convergent with the effects of auxin signalling on root hair responses, hence suggesting a crosstalk where ethylene pathway forms a link between SL and auxin to mediate root hair elongation (Kapulnik et al., 2010). On the other side of the spectrum, KARs treatment was also recently shown to enhance the ethylene biosynthesis gene *ACC SYNTHASE 7* (*ACS7*) expression, and the Karrikin regulator SMAX1 to mediate RH elongation by suppressing ethylene biosynthesis in *Lotus japonicus* (Carbonnel et al., 2020), consistent with previous observations (Kapulnik et al., 2010). However, these data also raise interesting questions in regard to the previous conclusion on the role of SL in RH development. Indeed, given the lack of RH phenotypes in SL biosynthesis mutants, the uncharacterized RH phenotype in *d14* or *smxl678* mutants, and the newly reported role of KARs/SMAX1, it appears the previously reported MAX2-dependent mediation of RH growth is linked to KL rather than SL signalling (figure 1.10).

- Root skewing

Lastly, KAI2-MAX2 complex and SMXL proteins have recently been suggested to regulate root skewing, which refers to the deviation of the primary root from the gravity vector (Swarbreck et al., 2019, Roy and Bassham, 2014). Mutants *kai2* and *max2* display an exaggerated rightward deviation compared to wild-type when grown vertically on the surface of agar plates. By opposition, SL biosynthesis mutants shows a reduced rightward skewing, while *d14* mutant is comparable to wild-type. The authors of this study therefore concluded that KAI2 but not SL is required for root skewing. In addition, this study shows that both *smax1 smxl2* and *smxl678* mutants can restore *max2* skewing phenotype, suggesting both SMAX1/SMXL2 and SMXL6/7/8 are required for KAI2-MAX2 mediated root skewing (Swarbreck et al., 2019). These new data challenge the current model of a dichotomy between KAI2-SMAX1/SMXL2 and D14-SMXL6/7/8 pairs (Soundappan et al., 2015) and rather support the concept of non-canonical signalling. It also call into question a possible interchangeability between SMXL proteins, a point already suggested by the observation of a rescue of *smxl4 smxl5* root phenotype by SMAX1 protein expressed under SMXL5 promoter (Wallner et al., 2017), and the recent report of a D14-MAX2-SMXL2 dependent modulation of hypocotyl elongation (Wang et al., 2020b). It

also supports the concept of partial redundancy between SMXL proteins and KL/SL pathways as already reported for other development processes:

- SMAX1 and SMXL2 in regard to hypocotyl growth and leaf shape (Soundappan et al., 2015, Stanga et al., 2016),

- SMXL2 and KAI2/D14 in regard to hypocotyl elongation (Wang et al 2020b)

- SMXL6/7/8 in regard to all knows strigolactone-related phenotypes (including shoot branching) (Soundappan et al., 2015, Wang et al., 2015),

- SMXL3/4/5 regarding phloem formation (Wallner et al., 2017),

- SMAX1, KAI2, and D14/SL biosynthesis regarding primary root growth (Marzec et al., 2018, Carbonnel et al., 2020),

- SL biosynthesis, MAX2, SMAX1 and SMXL6/7/8 regarding MAX2-mediated AR development (Swarbreck et al., 2020).

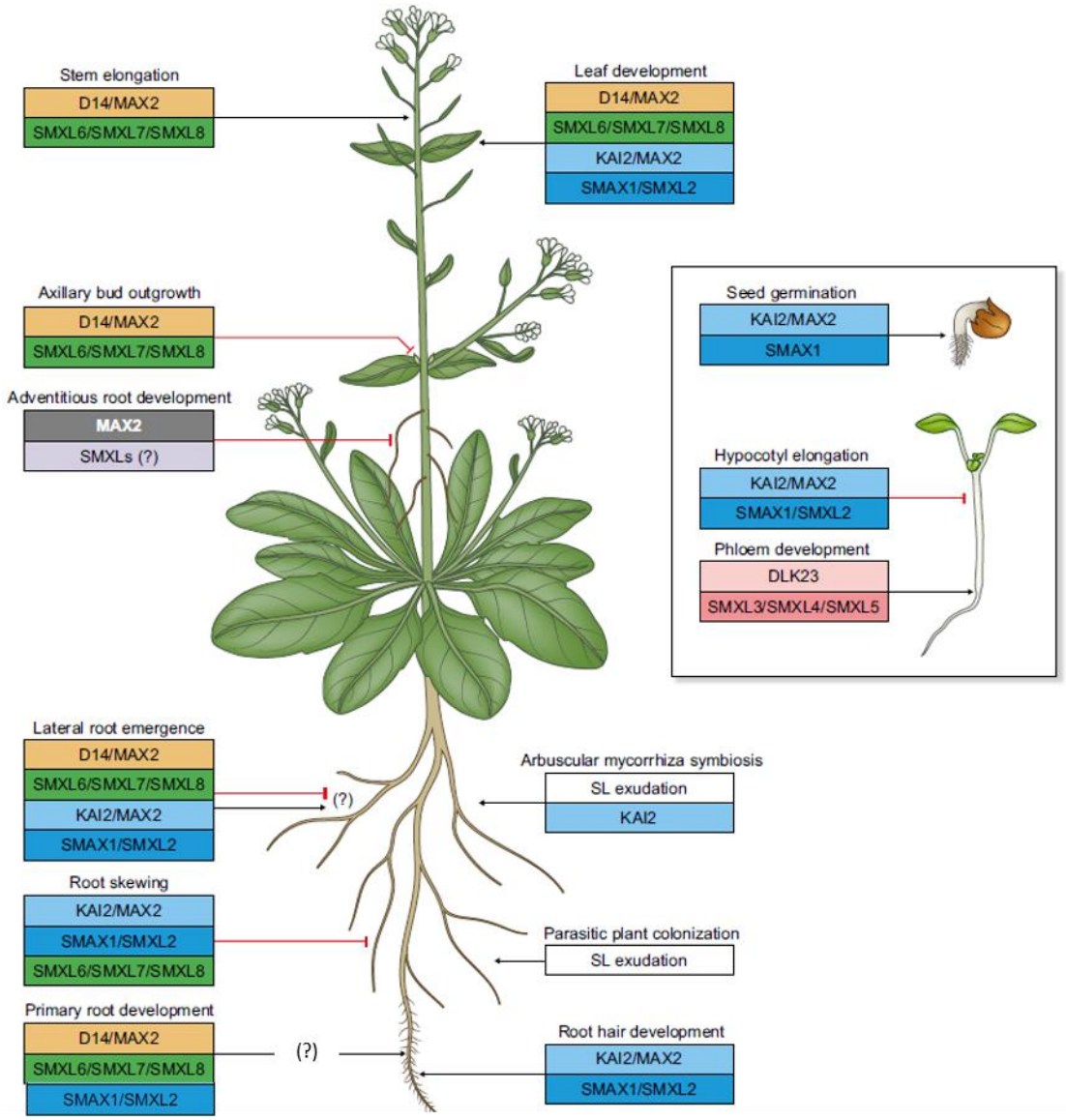

Figure 1-10 Function of SL and KL signalling in plant development
D14/KAI2 and SMXL protein roles in flowering plant development. Summary of known functions of Strigolactones and D14/KAI2 and SMXL protein family members at different stages of flowering plant development. Arrows indicate a positive effect and plain lines indicate an inhibitory effect. Question mark indicates the conclusion regarding the exact role of the indicated proteins remains unclear. Nomenclature is based on Arabidopsis. From Machin et al., 2020.

1.4 Aims of the thesis

First, both KAI2 and D14 act through the same MAX2 proteins, and *max2* mutants are insensitive to both SLs and KARs. Most studies aiming at characterizing the roles of SL signalling in Arabidopsis roots have been based on the use of *max2* mutants because this mutant was available before *d14* and *kai2.* Conclusions based on *max2* root phenotypes therefore give us an incomplete picture as it indiscriminately reflects a combination of impairment in SL and KL signalling without comparing the specific roles of D14 or KAI2 receptors in these phenotypes (Machin et al., 2020). In addition, *rac*-GR24 has been largely used to draw conclusion regarding SL roles, but as for the characterization of *max2* phenotypes, it is now known that while one stereoisomer ($GR24^{5DS}$) is a potent activator of D14 signalling, another stereoisomer ($GR24^{ent\text{-}5DS}$) appears to stimulate KAI2 signalling instead. As such, while it is clear that MAX2 and SMXL proteins are regulating several aspects of root system architecture (PRL, RH, LRD, AR, skewing), it remains unclear whether the observed functions are associated with SL signalling, KL signalling, or both. The first aim of my thesis is to re-assess the roles of D14 and KAI2 pathways with respect to root development in young Arabidopsis seedlings, as well has characterizing the roles of SMXL proteins downstream of SL and KL.

Secondly, SL and KL actions on root and seedling development have been largely associated with environmental conditions; from modulation of LRD and RH proliferation by SL signalling in response to phosphorus and sugar availability, to regulation of hypocotyl elongation by KAI2 in response to light signals. However, the current knowledge remains sketchy and the links between SL and KL pathway and abiotic stress/developmental response has to be further investigated. The second aim of this thesis is therefore to address the relation between SL/KL-mediated seedling development and adaptive responses to the environment, with a focus on resource availability (nutrients, light).

The third aim of this thesis is to investigate the molecular mechanisms downstream of KL signalling. To date, no specific targets of KAI2 have been identified, while the paralogue SL pathway has been shown to act through transcriptional repression and direct modulation of polar auxin transport. While the link between KL signalling and auxin remains puzzling, there is growing suit of evidence pointing toward a crosstalk between the two pathways. I will therefore investigate whether KAI2 signalling mediates seedlings development by regulating auxin homeostasis.

Chapter 2 Materials and Methods

2.1 Plant material

Arabidopsis thaliana genotypes were in *Columbia* (Col-0) or *Landsberg erecta* (Ler) parental backgrounds. The following mutants were used:

SL biosynthesis mutant:
d27-1, max3-9, max4-5, max1-1 (in pathway order)

SL signalling mutant:
d14-1, d14-1 kai2-2,

KL signalling mutant:
kai2-1, kai2-2, htl3, kai2-4, kai2-1 (Ler), kai2-2 (Ler), max2-1, max2-8 (Ler)

SMXL mutants:
smax1-2, smax1-2 smxl2-1 (s1s2), smxl6-4, smxl7-3, smxl8-1, smxl6-4 smxl7-3 smxl8-1 (smxl678), smxl6-4 smxl7-3, smax1-2 max2-1, smxl678 max2-1

Genotypes previously described can be found in the following: Ler: *max2-8* [Nelson 2011], *kai2-1*, *kai2-2* [Nelson 2011]

Col-0: *kai2-2* [Bennett 2016a], *max3*-9 [Booker 2005], *max4*-5, *d14*-1 *kai2*-2 [Bennett 2016a], *d14*-1 [Waters 2012], *d27*-1, *max1*-1, *max2*-1, *max2*-2 [Strirnberg 2002], *smax1*-2, *max2*-1 *smax1*-2 [Stanga 2013], *smax1*-2 *smxl2*-1, *max2-1 smax1-2 smxl2-1* [Stanga 2016], *smxl6-4 smxl7-3 smxl8-1, max2-1 smxl6-4 smxl7-3 smxl8-1* [Soundappan 2015].

DR5v2:GFP (Liao et al, 2015), pin3-3 pin4-3 pin7-1 (Bennett et al, 2016b), *PIN1:PIN1-GFP* (Benkova et al, 2003), *PIN3:PIN3-GFP*, *PIN4:PIN4-GFP, PIN7:PIN7-GFP* (Blilou et al, 2005), *PIN2:PIN2-GFP* (Xu & Scheres, 2005), lines have all been previously described.

New genotypes were assembled by crossing relevant existing genotypes and required homozygous lines were identified using visible, fluorescent, or selectable markers or using PCR genotyping. The *kai2-1 PIN1:PIN1-GFP* and *kai2-1 PIN2:PIN2-GFP* lines were constructed using a *kai2-1* allele backcrossed 4 times into Col-0, rather than the original *kai2-1* allele in L*er.*

2.2 Plant growth conditions

For analysis of root growth, *Arabidopsis thaliana* seeds were grown in axenic conditions on 12x12cm square plates containing 60 ml agar-solidified medium. Seeds were surface sterilized either by gas sterilization, or by washing with 1 ml of 70% (v/v) ethanol and 0.05% (v/v) Triton X-100 with gentle mixing by inversion

for 6 minutes at room temperature, followed by 1 wash with 96% ethanol and 5 washes with sterile distilled water. Seedlings were grown on plates containing *Arabidopsis thaliana* salts (ATS) medium (Wilson et al, 1990) supplemented with 1% sucrose (w/v) and solidified with 0.8% ATS at pH5.6. Plates were stratified at 4°C for 2–3 days in the dark, and then transferred to a growth cabinet under controlled conditions at 22°C, 16-h/8-h light/dark cycle (intensity ~120 µmol m^{-2} s^{-1}) for 6 to 10 days.

Seedlings for dissections, pharmacological treatments, auxin quantification, qPCR and confocal imaging were grown in axenic culture. Seeds were surface sterilized using 2 hours vapour sterilization method (3 ml of HCl 37% in 100 ml bleach), then sown onto 0.8% agar-solidified ATS media (pH 5.6) with 1% (w/v) sucrose, in square petri dishes (12 x 12cm, 60 ml media per plate), and stratified in the dark at 4°C for 2-3 days.

2.2.1 Hydroponics

For figure 3.1 D, plants were grown in hydroponic system for 3 weeks following the methods previously described in Conn et al., 2013. Growth media used was changed to standard ATS instead of the media described in Conn et al., 2013.

2.2.2 Low Phosphate

For analysis of root growth under phosphate depletion, seedlings were prepared as described in 2.2, but ATS growth media was modified with low Phosphorus (10 µM), or high Phosphorus (1 mM) Pi with KH_2PO_4, and potassium concentrations were adjusted with KCl.

2.2.3 Low Sucrose

For analysis of root growth under sucrose supplementation, seedlings were prepared as described in 2.2, but ATS growth media was modified with no sucrose supplementation (no suc), or with standard sucrose supplemented ATS (suc+ 1%).

2.2.4 Light intensity assays

For analysis of seedling development growth under two light-intensity regimes, seedlings were prepared as described in 2.2, but plates were placed in growth cabinets (Grobotic Systems - https://www.groboticsystems.com/) under controlled conditions at 22°C, 16-h/8-h light/dark cycle with two different light-intensity regimes: high intensity ~150 µmol.m^{-2}.s^{-1} or low intensity ~50 µmol.m^{-2}.s^{-1} 10 days.

2.2.5 Dark/light shift experiments

For plants grown in normal light conditions, plates were oriented vertically, and seedlings grown for 6-10 days in growth chamber under a 16-h/8-h light/dark cycle (20°C/18°C) with light provided by fluorescent tubes (120 $\mu molm^{-2}s^{-1}$), both root and shoot tissues were equally exposed to the light. In experiments with transfer from dark to light conditions, after stratification, plates were placed for 8 hours at 120 $\mu molm^{-2}s^{-1}$ light / 20°C to promote germination and then placed in complete darkness for 4 days at 20°C in a black plastic box in a growth chamber. After 4 days in darkness plates were transferred in normal light conditions described above (16h/8h light/dark cycle (20°C/18°C) / 120 $\mu molm^{-2}s^{-1}$), for an additional 1 to 6 days of growth and both root and shoot tissues were equally exposed to the light.

2.3 Phenotypic analysis

Measurements of seedlings were made at various time points described in the text.

2.3.1 Primary root length and lateral root density

A dissecting microscope was used to score the lateral roots number on each root system. Plants were then imaged using a flatbed scanner and primary root was measured from the resulting images using Fiji (https://imagej.net/Fiji/Downloads). Lateral root density was quantified as the number of lateral roots per mm of primary root. Lateral root primordia (LRp) numbers in figure 2.10 (E) was scored by observing DR5v2:GFP as a primordia marker in Col-0 and *kai2*-2 with a Laser-scanning confocal microscope LSM880 upright (see laser microscopy section below).

For the root apical meristem size, roots were mounted on glass slides and stained with Propidium iodide (PI). PI excitation was performed using a 561 nm laser, and fluorescence was detected between above 610nm. RAM size was measured using Fiji straight segment tool as the length from the first non-dividing cortical cell near the elongation zone and the cells forming the quiescent centre.

2.3.2 Root skewing and waving

These parameters were measure from plates previously scanned (see section above) following parameters as illustrated in figure 3.4 A: root skewing angle (α)

and root straightness (Lc/L) (with root length (L), ratio of the straight line between the hypocotyl-root junction and the root tip (Lc), and vertical axis (Ly)).

2.3.3 Root hair

Images of the root tip were taken with a Keyence VHX-7000 microscope (Osaka, Japan). The density of root hairs (RHD) was determined by counting the root hairs between 2 and 3 mm from the root tip on each root, and root hair length (RHL) was measured for 10 root hairs per root in a minimum of 8 roots per genotype and condition using Fiji (https://imagej.net/Fiji/Downloads) according to Villaécija-Aguilar et al (2021). KAR_2 treatment realised in Figure 2.11 (E-F) was performed by Dr. Jose Villaécija-Aguilar can be found in Villaécija-Aguilar et al., 2019.

2.3.4 Hypocotyl length

For measure of hypocotyl length, Plants were grown on vertical plates, as described in 2.2, and then imaged using a flatbed scanner and hypocotyl length was measured from the resulting images using Fiji.

2.3.5 Apical hook angle and hypocotyl bending

For measure of apical hook angle and hypocotyl bending, plants were grown on vertical plates, as described in 2.2 and etiolated for 4 days in darkness and then imaged using a flatbed scanner. The angle of apical hook closure was measured from the resulting images as shown in figure 4.4 C, and the hypocotyl bending was measure as shown on figure 4.4 A, using Fiji.

2.3.6 Adventitious root number

For the measure of the adventitious root number, plants were grown as described in 2.2, and a dissecting microscope was used to score the adventitious roots number in each root system. We considered as adventitious roots any root strictly growing from the hypocotyl or from the shoot root junction (junction roots).

2.4 Seedling dissections

Four-day old etiolated seedlings were dissected in-situ on agar plates using a very sharp scalpel. Decapitation assays were performed by removing the seedling meristem and cotyledons at the junction of the cotyledons and hypocotyl.

2.5 Gravitropic-response assay

Gravitropic assay was performed as described in Schöller et al., 2018, with modification on the preparation of the seedlings to match the methods used in the rest of the experiments (see 2.2 Plant growth conditions). Seedlings were also grown for 5 days under standard growth regime, rather than 4 as described in Schöller et al., 2018, before doing the 90° rotation of the plates.

2.6 Pharmacological Experiments

For pharmacological experiments, 1000X stock solutions 1-N-naphthylphthalamic acid (NPA) (Duchefa), and L- kynurenine (Sigma-Aldrich), by dissolving the appropriate mass of the compound in a 2% DMSO, 70% ethanol solution. From these stocks 60µl/plate was added to hand-warm ATS-agar media prior to pouring plates. Control plates contained 60µl/plate of 2% DMSO, 70% ethanol solvent control solution. Seed were either germinated directly on plates containing to the pharmacological treatments, or were transferred after initial growth on plain plates, as indicated in the figure legends. For KAR treatment, KAR2 from Olchemim (Olomouc, Czech Republic) was dissolved in 70% methanol for the preparation of 1 mM stock. The volume required to reach the final concentration of these different stock solutions was added to molten media prior to pouring Petri dishes. In each experiment, an equivalent volume of solvent was added to Petri dishes for untreated controls.

2.7 Free IAA Determination

For (Figure 5.1 A), seedlings were grown for 4 days on ATS-agar medium with sucrose in the dark. Seedlings were quickly flash frozen on the bench to minimize the light exposition. There were 4 biological samples for each genotype and time point, each containing pooled tissue from 60 seedlings. From these samples (10-20 mg fresh weight) IAA was purified and analysed by gas chromatography-tandem mass spectrometry (GC-MS/MS) as described in Andersen et al (2008) with minor modifications. To each sample, 500 pg $^{13}C_6$-IAA was added as an internal standard before extraction.

For (Figure 5.1 B), seedlings were grown for 4 days on ATS-agar medium with sucrose in the dark, and then transferred to the light. Some seedlings were dissected immediately, with the cotyledons separated from the hypocotyl + roots, and flash frozen in liquid nitrogen. The other seedlings were dissected after 1 further day of growth in the light, and then dissected in the same way. There were

4 biological samples for each genotype and time point, each containing pooled tissue from 60 seedlings.

For (Figure 5.1 C), seedlings were grown for 6 days on ATS-agar medium with sucrose in the light, at which point the roots were dissected from the seedlings, and flash frozen. The analysis was proceeded as explained for figure 5.1 A.

2.8 Auxin transport assay

For the auxin transport assay, *Arabidopsis thaliana* seed sterilization and seedling growth were performed as described for root hair measurements in light conditions. An agar droplet containing 100 nM ^{3}H-IAA (Hartmann analytic) and solvent (DMSO) or 10 µM NPA (Olchemim) in DMSO was applied below the aligned root-shoot junctions of 5 days post germination Arabidopsis seedlings. 18 hours after the treatment, the amount of radioactivity was quantified in a 5 mm apical segment as previously described in Lewis and Muday (2009).

2.9 RNA extraction and gene expression analysis

For expression analysis of PIN genes, Col-0 and *kai2-2* seedlings were grown for 4 days on ATS-agar medium with sucrose in the dark, and then transferred to the light for 0, 1 or 3 additional days of growth. For each time point and genotype, 3 biological samples were collected by pooling ~16 seedlings, which were then flash-frozen in liquid nitrogen. Total RNA was extracted using RNeasy Plant Mini kits (Qiagen), and then DNase treated using Turbo DNA-free kit (Ambion), both as per manufacturer's instructions. RNA was quantified using a Nanodrop 1000. For cDNA synthesis, Superscript (Invitrogen) II was used to reverse transcribe 500 ng of total RNA according to manufacturer's instructions. Quantification of transcript levels was carried out using SYBR Green reactions with 5 ng cDNA in a 20 µl volume on a Light Cycler 480 II (Roche) relative to the reference gene *UBC10* (*POLYUBIQUITIN10, At4g05320*). Three technical replicates were run for each biological replicate and averaged. Calculation of the expression levels was done using the ΔΔCt method (Czechowski et al, 2005). Primers used were:

PIN1-F: 5′-CAGTCTTGGGTTGTTCATGGC-3′;
PIN1-R: 5′-ATCTCATAGCCGCCGCAAAA-3′.

PIN3-F: 5′-CCATGGCGGTTAGGTTCCTT-3′;

PIN3-R: 5′-ATGCGGCCTGAACTATAGCG-3′.

PIN4-F: 5′-AATGCTAGAGGTGGTGGTGATG-3′;

PIN4-R: 5′-TAGCTCCGCCGTGGAATTAG-3′.

PIN7-F: 5′-GGTGAAAACAAAGCTGGTCCG-3′;

PIN7-R: 5′-CCGAAGCTTGTGTAGTCCGT-3′

UBQ10-F: 5’-GGTTTGTGTTTTGGGGCCTTG-3’;

UBQ10-R: 5’-CGAAGCGATGATAAAGAAGAAGTTCG-3

2.10 Laser Scanning Confocal Microscopy

To visualize fluorescent reporter lines Laser-scanning confocal microscopy was performed on either Zeiss LSM700 or LSM880 imaging system with a 20X lens. Tissues were stained with propidium iodide (10ug/ml) and mounted on glass slides. GFP excitation was performed using a 488 nm laser, and fluorescence was detected between 488 and 555nm. Propidium iodide excitation was performed using a 561 nm laser, and fluorescence was detected between above 610nm. The same detection settings were used for all images captured in a single experiment. GFP quantification was performed on non-saturated images, using Zeiss ‘ZEN’ software.

For the different GFP lines (DR5v2:GFP, PIN1-GFP, PIN2-GFP, PIN3-GFP, PIN4-GFP, and PIN7-GFP) fluorescence was quantified in regions of interest (Supplemental Figure 3E-F) either in the hypocotyl, the shoot-root junction, the older differentiated zone (ODZ, between the first two emerged lateral roots), the middle differentiated zone (MDZ) between the last emerged LR and the first LR primordia), the young differentiated zone (YDZ, in the root hair elongation zone), or in the meristem zone (MZ) including columella and quiescent centre nuclei as appropriate. For *DR5v2:GFP*, the fluorescence intensity is plotted as the mean GFP intensity measured in 5-10 nuclei/seedling in the region of interest. For PIN1, fluorescence intensity is plotted as the mean GFP intensity measured in 5-10 basal plasma membranes/seedling in the region of interest (stele cells above the RAM). For PIN2, fluorescence intensity is plotted as the mean GFP intensity measured in 5-10 apical plasma membranes/seedling in the epidermal cells of the meristem zone. For PIN1-GFP and PIN2-GFP, the PM were selected using

ImageJ segmented line tool with a “line width of 5”. For PIN3-GFP and PIN7-GFP, fluorescence intensity is plotted as the mean GFP intensity measured in a rectangle of 40 µm x 80 µm (width x height) covering the region of interest. For PIN3-GFP and PIN7-GFP in the MZ, fluorescence intensity is plotted as the mean GFP intensity measured at the plasma membrane of columella cells (selected using ImageJ segmented line tool with a “line width of 5”).

2.11 Statistical Analyses

Data generally show independent biological replicates, although in a small number of cases we pooled data from two replicates, where the distributions of data between the replicates were sufficiently similar. Statistical analyses were performed in R-studio and GraphPad Prism (9.3.1). If comparing two groups, we used t-test with *Welch’s* correction (unequal variances t-test) with (*,**,***,****) p-value ≤ (0.05, 0.01, 0.001, 0.0001) indicating differences between genotype and/or conditions, as appropriate. If the comparison contained more than two groups, we used one-way Analysis of Variance (ANOVA), followed by Tukey HSD post hoc test (CI 95%). Different letters indicates statistical differences between groups. The test(s) performed for each graph is indicated in the legends.

Chapter 3 Deciphering the roles of KL and SL signalling in root development

3.1 Aims

The first aim of this chapter is to reassess the role of SL and KL signalling in root development, from SL biosynthesis to the signal transduction to the downstream targets. The unclear dichotomy between SL and KL signalling, due to their close origins and their shared synthetic ligand (*rac*-GR24) and signalling component (MAX2), raises questions about the roles of each pathway in root development. In the literature, the regulation of many root parameters (primary root growth, lateral root development, root hair development etc.) are attributed to SL signalling, but these conclusions are mainly based on the use of *max2* mutant and *rac*-GR24 treatments, which we now know to be acting in SL and KL signalling (reviewed in Machin et al., 2020). On the other hand, the role of KAI2 belowground remains poorly characterised, apart for a recent report suggesting KAI2 regulates root skewing in Arabidopsis seedlings (Swarbreck et al, 2019). A key aspect of SL and KL signalling is the inactivation and ubiquitination of target proteins upon perception of SLs, KARs, GR24, and KL by D14/KAI2. These key regulators of plant development, from the SMXL family, are divided into 3 major clades in Arabidopsis:

(1) SMAX1 and SMXL2 that act downstream of KARs/KL signalling (Stanga et al., 2013 and 2016, Khosla et al., 2020; Wang et al., 2020).
(2) SMXL6, SMXL7, and SMXL8 that function downstream of SL signalling (Wang et al., 2015, Soundappan et al., 2015).
(3) SMXL3, SMXL4, and SMXL5 that have been showed to act independently of KL or SL-signalling to regulate phloem development (Wallner et al., 2017).

In the shoot, the strigolactone-induced turnover of SMXL678 proteins is key to correctly shaping shoot architecture (Jiang et al., 2013, Soundappan et al., 2015). In the root, the role of SMXL proteins remain elusive, although SMXL678 have been suggested to be important for regulation of lateral root density (LRD) (Soundappan et al., 2015) and root skewing in concert with SMAX1-SMXL2 (Swarbreck et al., 2019). Given the aforementioned points and the unclear dichotomy between SL and KL signalling in respect to root development, I hypothesised that not only SL but also KAI2 signalling regulate root development in Arabidopsis. I evaluate this hypothesis in more detail by using mutants specific to each signalling pathways, as well as the combinations of higher order mutants with *max2*.

The second aim of the chapter is to address the specificity of SMXL proteins in regard to SL and KL signalling, and to better understand their function/structure. Recent reports have raised new question in regard to the specificity of KAI2 and D14 in their SMXL targets and their putative role in the regulation of root development. First, Wallner et al. (2017) showed that some SMXL proteins are a major regulator of the root development independently of the MAX2-dependent SL and KL signalling pathways. This study also suggested a functional interchangeability between SMXL proteins. On the other hand, Swarbreck et al. (2019) demonstrated a probable role of KAI2, but not D14, in the regulation of root skewing through MAX2. Results of this study also suggest the regulation of root skewing by KAI2-SCF^{MAX2} operates through SMXL6/7/8 rather than SMAX1 and SMXL2. Taken together these data suggest a certain interchangeability in SMXL protein function to control root development These new reports also challenge the commonly accepted model of specific degradation of SMXL6/7/8 in response to D14-mediated SL signalling and SMAX/SMXL2 by KAI2-mediated KL/KAR (KAI2) signalling. While it is commonly agreed the two SMXL proteins sub-family (SMAX1-SMXL2 and SMXL6/7/8) are essential downstream of KL and SL signalling to shape plant development, the specific mechanisms of action of SMXL proteins remain elusive (reviewed in Machin et al., 2020). Most of the attention is focused on the presence of an EAR-motif, hallmark of an interaction with proteins of the TPL/TPR transcriptional co-repressor family, suggesting SMXL proteins act through the transcriptional regulation of genes involved in plant development. However, Liang et al, 2016 addressed this point and showed that different aspects of SMXL7 are EAR-dependent and EAR-independent, suggesting that this is not the only mechanism for SMXL7 function. Therefore, little is understood about how the structure of SMXL proteins participate in their functional outputs in shaping the root architecture.

3.2 Results

To investigate the roles of SL and KL signalling in root development, I used a reverse genetic approach and characterised the root development of loss-of-function mutants carrying T-DNA insertion into the coding region of SL or KL related genes.

SL biosynthesis mutant:
d27-1, max3-9, max4-5, max1-1 (in pathway order)

SL signalling mutant:
d14-1, d14-1 kai2-2,

KL signalling mutant:
kai2-1, kai2-2, htl3, kai2-4, kai2-1 (Ler), kai2-2 (Ler), max2-1, max2-8 (Ler)

SMXL mutants:
smax1-2, smax1-2 smxl2-1 (s1s2), smxl6-4, smxl7-3, smxl8-1, smxl6-4 smxl7-3 smxl8-1 (smxl678), smxl6-4 smxl7-3, smax1-2 max2-1, smxl678 max2-1

3.2.1 SL but not KL regulates primary root length

The analysis of the root architecture of SL synthesis mutants (here arranged in pathway order) reveals they all exhibit a statistically significantly shorter primary root (PR) at 10 days post-germination (dpg) compared to the corresponding wild-type control (Col-0) (figure 3.1 A). This reduction of PR length (PRL) observed in SL deficient mutants appears as early as 6 dpg and remains consistent in the following early stages of the seedling development (8 and 10 dpg) (figure 3.1 B). Similarly, SL-insensitive mutant *d14-1*, lacking the ability to respond to SL, exhibits the same statistically significantly shorter PRL observed in SL synthesis mutant *max4-5* (figure 3.1 C). On the other hand, the KL-insensitive mutant *kai2-2*, lacking the ability to respond to KL and karrikin, displays a PRL of same length as wild-type (WT), and the double mutant *d14-1 kai2-2* exhibits the same PRL phenotype as *d14-1* (figure 3.1 C). Interestingly, in addition to a reduced PRL, I also observe a reduction of root biomass in plants impaired in SL signalling (d14-1 and *d14 kai2*) grown for 3 weeks in hydroponics, whereas KL insensitive plants have a normal root biomass (figure 3.1 D).

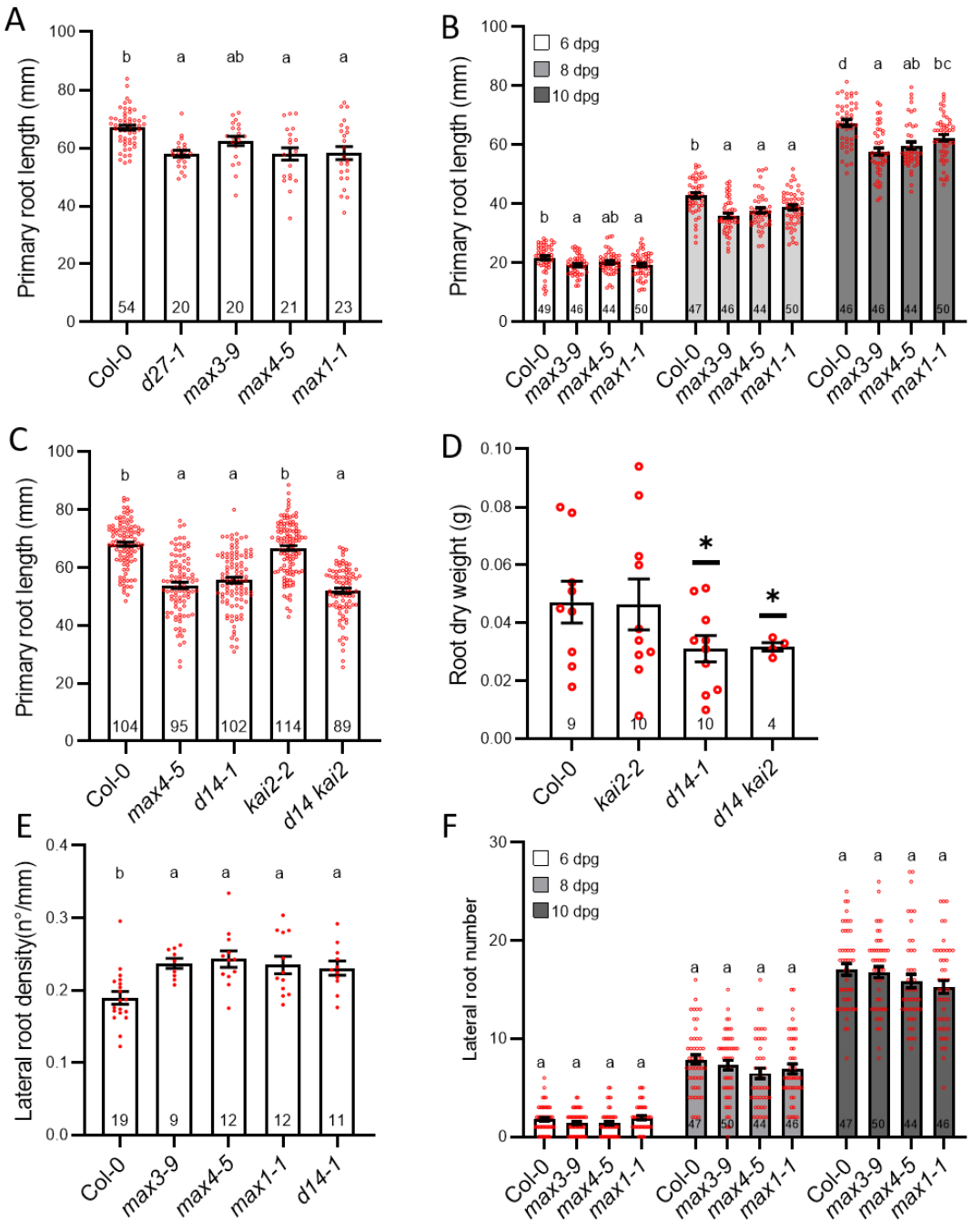

Figure 3-1 Strigolactone signalling regulate primary root growth but not lateral root growth

(A) Primary root length of *d27*, *max3*, *max4*, max1 SL-deficient (arranged in order of pathway) and *d14-1* SL-insensitive mutants at 10 days post germination. (B) Kinetic of Primary root growth in SL-deficient mutants at 6, 8, and 10 days post germination. (C) Primary root length in Col-0 wild-type, SL biosynthesis mutant *max4-5*, and the *d14-1 kai2-2* double mutant and the respective single mutants. (D) Root dry weight of *d14-1 kai2-2* double mutant and the respective single mutants were grown for 3 weeks in hydroponics. (E) Lateral root density of *max3*, *max4*, *max1* SL-deficient and *d14-1* SL-insensitive mutants at 10 days post germination. (F) Number of lateral roots in SL-deficient mutants at 6-, 8-, and 10-days post germination.

(A-F) Sample size is indicated with numbers in bars. All graphs represent data from one experimental replicate, and all experiments were repeated at least two times with similar results, except (D) which represents one experimental replicate. Data represent mean ± SE, red dots represent individual data. Different letters indicate different statistical groups (ANOVA, posthoc Tukey, p≤ 0.001). For (D), * (p-value ≤ 0.05) indicates difference compared to wild-type (Welch's t-test).

3.2.2 KL promotes lateral root development

The decreased primary root length (PRL) in SL biosynthesis and signalling mutants is associated with a statistically significant increase in lateral root density (LRD) (figure 3.1 E). However, a careful examination of the number of LR (LRN) at 6, 8, and 10dpg shows the increased LRD in SL mutants is not due to an increased LRN compared to WT, but rather the result of the reduction of PRL induced by SL mutations (and hence an increase in the LRN/PRL ratio) (figure 3.1 F).

Conversely, despite a normal PRL and overall root biomass, I observed a significantly increased LRD in three allelic *kai2* mutants (*kai2-1*, *kai2-2*, and *htl3*), of the same magnitude as seen *d14-1* and *max2-1* mutants (figure 3.2 A-B). Consistent with this observation, I found a similarly increased LRD in *kai2* mutants in the Landsberg *erecta* (L*er*) background compared to the corresponding WT (figure 3.2 C). The increased LRD observed in *kai2* seedlings is stable throughout the first days of seedling development (6, 8 and 10 days old seedling) (figure 3.2 D). However, in 3 weeks old plants grown in hydroponics I could not observe differences in total root biomass in *kai2* compared to WT (figure 3.2 D). These data would suggest KAI2 regulates root development at the early stages of the seedling growth. To test whether the increased LRD induce by *kai2* mutation was the result of a failure to regulate LR initiation or increased LR emergence, I scored the lateral root primordia (LRp) and emerged LR (LRe) in Col-0 and *kai2-2* using DR5v2:GFP auxin response marker as a marker of the founder cells of LR primordia. I observed a significant increase in the number of LRp and LRe in *kai2-2* in 8-day old seedlings (figure 3.2 E), indicating KAI2 signalling regulates both priming and emergence of new lateral roots during the early stages of the seedling development.

Overall my data indicate that both SL and KL signalling regulate LRD in Arabidopsis. Consistent with previous report (Ruyter-Spira et al., 2011), I found SL signalling is involved in the development of the primary root in Arabidopsis, but I couldn't observe any direct effect of SLs on the lateral root development. In contrast, I found KAI2 signalling does not affect PR growth, but is required for the formation of lateral root primordia and their emergence. In the double mutant

(*d14-1 kai2-2*), both SL- and KL-insensitive, I observe a greater LRD increased compared to the respective single mutants and WT (figure 3.2 A). This observation is consistent with a co-regulation of LRD by SL and KL signalling, acting in a synergic manner to modulate both the PRL through SL signalling, and LR proliferation via KAI2 signalling.

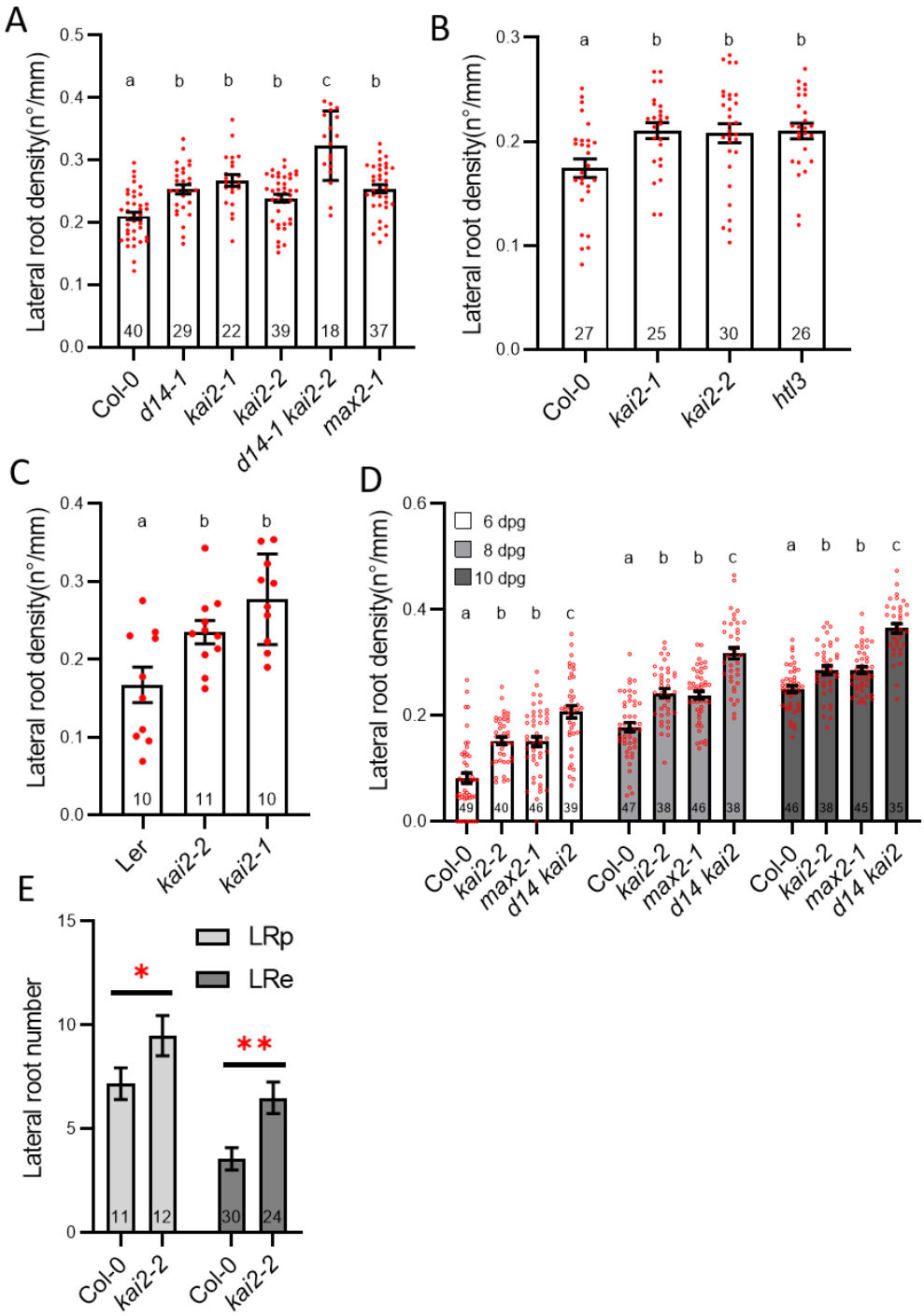

Figure 3-2 KAI2-MAX2 complex is required for normal lateral root development

(A) Lateral root density in the *d14-1 kai2-2* double mutant and the respective single mutants, and *max2-1* at 10 days post germination. (B-C) Lateral root density in different allelic *kai2* mutants in Col-0 and Ler background at 10 days post germination.
(D) Change in lateral root density in the *d14-1 kai2-2* double mutant and the respective single mutants at 6, 8, and 10 days post germination. (E) Number of primordia (LRp) and emerged (LRe) lateral roots in *kai2* mutant and wild-type at 10 days post germination. (A-E) Sample size is indicated with numbers in bars. All graphs represent data from one experimental replicate, and all experiments were repeated at least two times with similar results. Data represent mean ± SE, red dots represent individual data. Different letters indicate different statistical groups (ANOVA, posthoc Tukey, p≤ 0.001). For (E), *, ** (p-value ≤ 0.05, 0.01) indicates difference compared to wild-type (Welch's t-test).

3.2.3 Root hair development requires KAI2 but not SL

In addition to a role in PRL, SLs have been repeatedly reported as regulators of RH development in Arabidopsis (Kapulnik et al., 2011, Koltai et al., 2010). In contrast with these previous assumptions, I found by measuring the root hair development (figure 3.3 A) in SL mutants that neither root hair length (RHL) or root hair density (RHD) are altered in SL-deficient *max4-5* and SL-insensitive *d14-1* mutants (figure 3.2 B-D). Consequently, the previously reported root hair phenotype of *max2* mutants must be the result of a defect in another MAX2-dependent signalling pathway, such as KL signalling. Measurements of the root hair formation (RHD and RHL) in two allelic *kai2* mutants in Col-0 (*kai2-1* and *kai2-2*) corroborate this idea. The RHL and RHD of both mutants phenocopied the reduced root hair development observed in *max2* mutant (figure 3.2 B-D). Thus, the previously reported RH phenotype of *max2*, attributed to a defect in SL signalling, must actually result from a lack of KL signalling. To further confirm this hypothesis, our collaborators (J.A. Villaécija-Aguilar and C. Gutjahr, joint-authored publication Villaécija-Aguilar et al., 2019) tested if the development of root hair could be influenced by the application of exogenous karrikin (KAR2) in a KAI2-dependent manner. Treatment with 1 µM KAR2 was sufficient to increase both RHD and RHL in wild-type (Ler) seedlings relative to a control treatment with a solvent, in a KAI2-dependent manner (figure 3.2 E-F). These data confirm the role of KAI2 in promoting the development of root hairs.

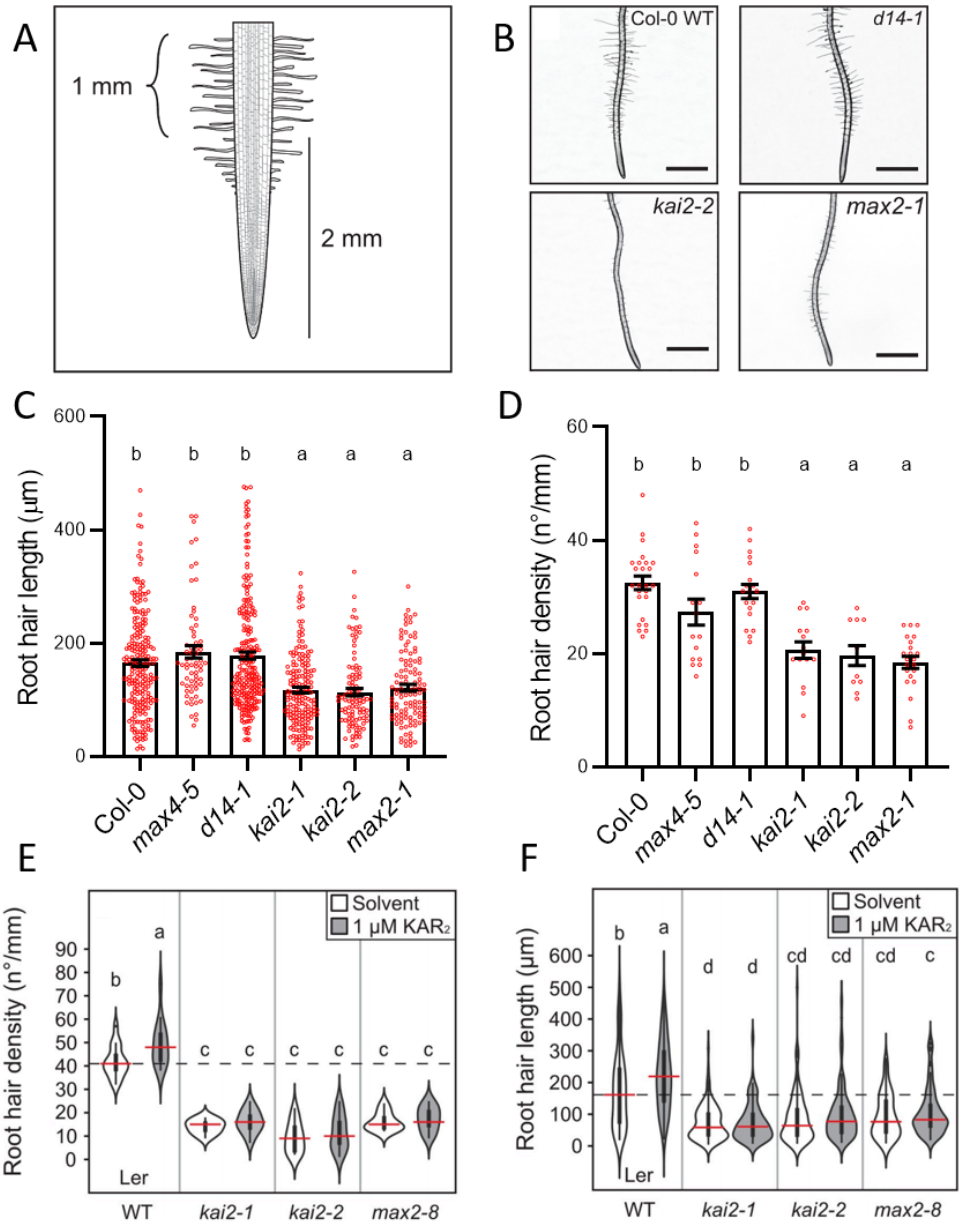

Figure 3-3 KL perception mutants are impaired in root hair development
(A) Diagram showing the primary root zone used for root hair phenotyping (curly bracket). Root hair density and length were quantified in 1 mm primary root length between 2 and 3 mm from the root tip. (B) Representative images of root hair phenotypes of the indicated genotypes. Scale bar, 1 mm. (C-D) Root hair length (C) and root hair density (D) in wild-type Col-0, SL-deficient *max4-1*, in the *d14-1 kai2-2* double mutant and the respective single mutants, and *max2-1* mutant. (E-F) Effect of 1 µM KAR2 treatment or mock treatment with solvent (70% Methanol) on the root hair density (E) and root hair length (F) in two allelic *kai2* mutants, and *max2-8* mutant in Ler background. (C-F) All graphs represent data from one experimental replicate, and all experiments were repeated at least two times with similar results. Data represent mean ± SE, red dots represent individual data. (C, F) n=10 root hairs from 10 seedlings. (D-E) n=8 seedlings. Different letters indicate different statistical groups (ANOVA, posthoc Tukey, p≤ 0.001). (E-F) Data collection, analyse and plots were realized by Dr. José Antonio Villaécija-Aguilar as part of a co-authored publication Villaécija-Aguilar et al., 2019.

3.2.4 KAI2-MAX2 regulates skewing and waving

In addition to the lateral root and root hair phenotypes, I found that *kai2* and *max2* mutants exhibit an increased right-handed root skewing phenotype when grown vertically on the surface of agar plates (figure 3.4 A-C). These observations were consistent in four different allelic *kai2* mutants in Col-0 background, as well as in two allelic *kai2* mutants in Landsberg ecotype (figure 3.4 D). Although I did not observe abnormal skewing in SL mutants *max4-5* and *d14-1* compared to WT, the double mutation *d14-1 kai2-2* leads to a greater increase of the skewing phenotype compared to the single mutant *kai2-2* (figure 3.4 C). This observation could reflect a yet uncharacterised requirement for both SL and KL signalling to maintain not only the correct development of the primary root by strigolactone, but also a normal directional growth of the root system via a redundant action of D14 and KAI2.

The skewing phenotype observed in *kai2* mutants is accompanied by an increased waving of the root, corresponding to a decrease of the primary root straightness, compared to WT and SL mutants *max4-5* and *d14-1* (figure 3.4 E). The analysis of the double mutant *d14-1 kai2-2*, exhibiting a straightness of same magnitude as *kai2-2*, confirms the function of KAI2 but not SL signalling in regulating root growth straightness.

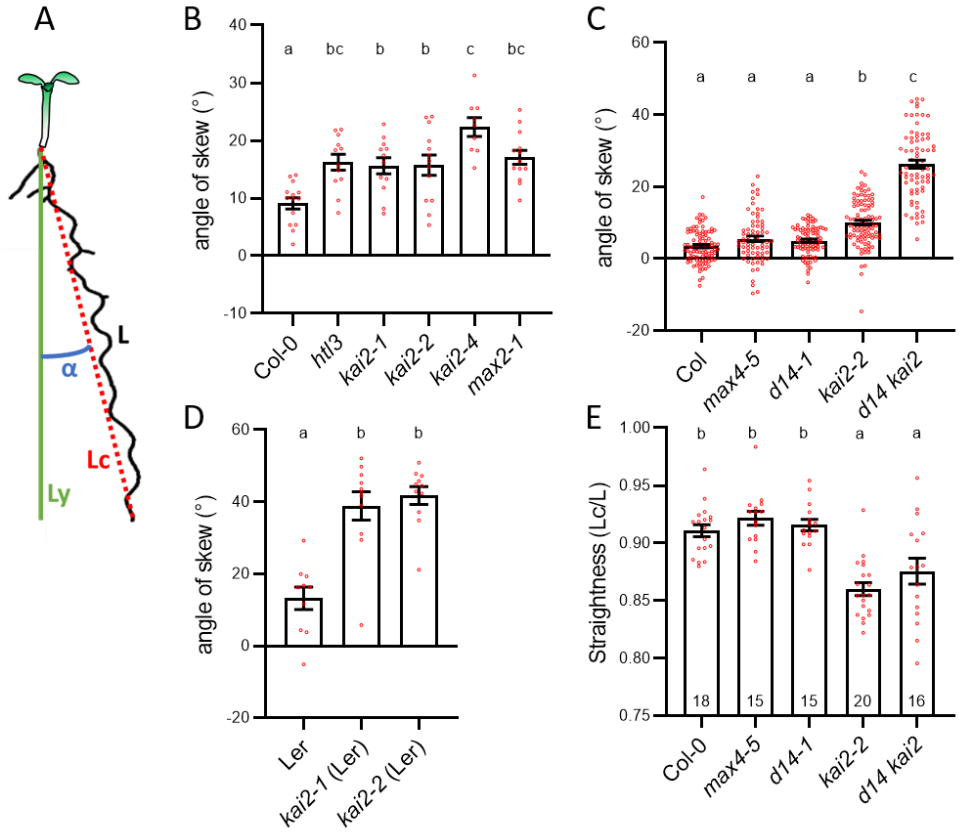

Figure 3-4 KL perception mutants display an exaggerated root skewing and waving

(A) Diagram showing how the primary root rightward skewing and straightness (waving) was determined (see Material and Methods 2.3.2 for more details). (B, D) Angle of skew of the primary root in different allelic *kai2* mutants, *max2-1* single mutant in Col-0 background (B) and in two allelic *kai2* mutants and wild-type control in Ler background (D) at 10 days post germination. (C, E) Primary root skewing (C) and straightness (E) in SL biosynthesis mutant *max4-5*, and in the *d14-1 kai2-2* double mutant and the respective single mutants in Col-0 background at 10 days post germination. (B-E) All graphs represent data from one experimental replicate, and all experiments were repeated at least two times with similar results. Data represent mean ± SE, red dots represent individual data. (B, D) n=10 seedlings per genotype. (C, E) sample is the same and is indicated in bars in (E). Different letters indicate different statistical groups (ANOVA, posthoc Tukey, $p \leq 0.001$).

3.2.5 SMAX1-SMXL2 and SMXL678 regulate lateral root density

To better understand the roles of SMXL proteins pairs in root development, and their potential function through canonical or non-canonical signalling downstream of D14 and KAI2, I monitored the root development of seedlings mutated in either SMXL678 or SMAX1/SMXL2 function, and/or impaired in MAX2 function. I found both *smax1 smxl2* double and *smxl678* triple mutants exhibit a reduced PRL, LRN, and LRD compared to Col-0 WT and *max2-1* at 6, 8, and 10 dpg (figure 3.5 A-C). Moreover, despite *smax1 smxl2* and *s678* mutations attenuating the effect of *max2* mutation on LR development, none of the two sets of SMXL mutation is fully epistatic to *max2* (figure 3.5 B). The most parsimonious explanation for these results is that both SMAX1/SMXL2-MAX2 and SMXL678-MAX2 pairs regulate root development, and that KAI2 signalling canonically regulates SMAX1-SMXL2 accumulation, and SL signalling canonically promotes SMXL678 turnover, with no need to invoke non-canonical signalling to explain these effects.

Interestingly, despite the normal PR development in *kai2* and *max2* mutants, the absence of functional SMAX1 and SMXL2 proteins inhibits the primary root growth (figure 3.5 A). My data (figure 3.1) show SL signalling promotes PR growth, allegedly by regulating SMXL678 accumulation and function in the root apical meristem; therefore one might expect *smxl678* mutant to exhibit a PR phenotypes opposite to *max4* or *d14*. Instead, our time course data shows *smxl678* has a slightly reduced PRL compared to WT (figure 3.5 A). Similarly, our results shows the PR development is independent of KAI2 and MAX2 (figure 3.1 C-D) as both mutants exhibit a WT phenotype for this trait, however, I observed in *smax1 smxl2* double mutant a strong and consistent reduction of the primary root development over time.

As for the PRL, the LRN observed in *smxl678* and *smax1 smxl2* mutants also raises ambiguity toward the exact role of each SMXL protein sub-family. In one

hand, *smax1 smxl2* double mutation inhibits LRN, consistent with the increased LR phenotype observed in *max2* and *kai2*. On the other hand (despite our data suggesting SL signalling does not affect LR development, but only the primary root), I observed in *smxl678* a reduction of LRN around the same magnitude as *smax1 smxl2*, and in both case not completely epistatic to *max2* (figure 3.5 B).

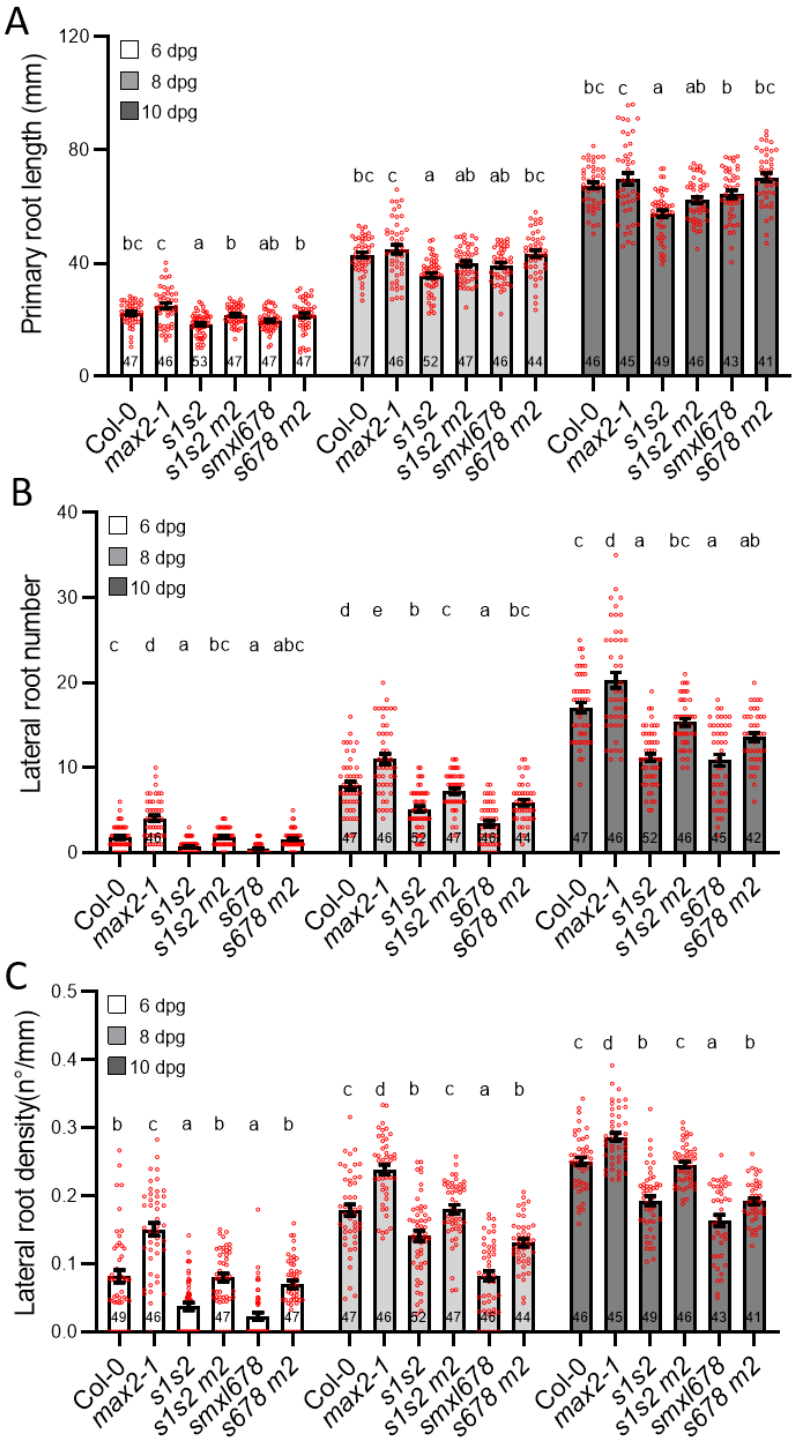

Figure 3-5 SL- and KL-associated SMXL proteins regulate lateral root density
(A-C) Primary root length (A), lateral root number (B), and lateral root density (C) in Col-0 and the indicated genotypes at 6, 8, and 10 days post germination (the mutant alleles are *max2-1 (m2), smax1-2 smxl2-1 (s1 s2), smxl6-4 smxl7-3 smxl8-1 (s678/smxl678)*). Sample size is indicated in bars. All graphs represent data from one experimental replicate, and all experiments were repeated at least two times with similar results. Data represent mean ± SE, red dots represent individual data. Different letters indicate different statistical groups (ANOVA, posthoc Tukey, p≤ 0.001).

3.2.6 SMAX1 and SMXL2 regulates skewing and waving downstream of KAI2-MAX2

Another recent report proposed the skewing phenotype in *kai2* and *max2* was associated with the non-canonical degradation of SMXL678 in addition to the canonical degradation of SMAX1 and SMAX2 through KAI2-MAX2 complex (Swarbreck 2019). Under our growth conditions, I found *smax1-2 smxl2-1* double mutation results in a decreased skewing compared to Col-0, in an opposite fashion to *kai2*/*max2* phenotype, and is sufficient to rescue *max2* phenotype, whereas *smxl678* triple mutant has a phenotype of same magnitude as WT and cannot rescue the skewing observed in *max2* (figure 3.6 A).

Moreover, I observed the loss-of-function *smax1 smxl2* was sufficient to rescue the decreased waving of *max2*, whereas *smxl678* triple mutant had a WT waving phenotypes and could not suppress the waving phenotype of *max2* (figure 3.6 B). Our results contradict the findings of Swarbreck et al. 2019, as under our growth conditions the KAI2-dependent promotion of SMAX1-SMXL2 turnover, but not of SMXL678, is required for the correct waving and growth direction of the roots. These new data are consistent with the generally accepted idea SMAX1 and SMXL2 act canonically via KAI2 signalling to regulate root development.

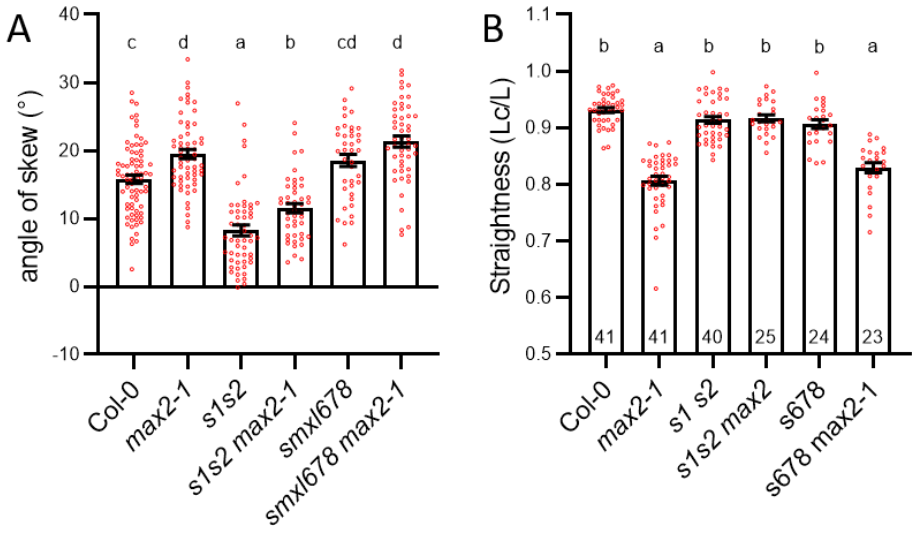

Figure 3-6 SMAX1 and SMXL2 regulates root skewing and waving downstream of KL perception

(A-B) Primary root skewing (A) and straightness (B) in SMXL protein mutants and *max2* mutants at 10 days post germination. The mutant alleles are *max2-1, smax1-2 smxl2-1 (s1 s2), smxl6-4 smxl7-3 smxl8-1 (smxl678*). All graphs represent data from one experimental replicate, and all experiments were repeated at least two times with similar results. Data represent mean ± SE, red dots represent individual data. Sample is same in both panels and is indicated in bars in (B). Different letters indicate different statistical groups (ANOVA, posthoc Tukey, p≤ 0.001).

3.2.7 KL signalling is a key regulator of RH development

Given the root hair phenotypes observed in *kai2* and *max2* but not in SL biosynthesis or *d14* mutants, I hypothesised the regulation of RH development by KL signalling occurs through its canonical SMAX1-SMXL2 effectors. Consistent with my hypothesis, I found that *smax1 smxl2* exhibit a strong increase in RHL and RHD, opposite to *kai2* and *max2* RH phenotype, and the double mutation is completely epistatic to *max2* (figure 3.7 A-B). Additionally, a jointly-authored report (Villaécija-Aguilar et al., 2019) shows that *smxl678* seedlings display a RH development similar to WT and did not suppress the RH phenotypes of *max2* mutants. These data are in line with the idea that KL signalling is a newly discovered and important regulator of root hair development. In addition to RHL and RHD phenotypes, I found *smax1* single and *smax1 smxl2* double mutants exhibits a shorter distance between the RAM and the 1st formed root hair (figure 3.7 C), consistent with the observation of a reduced primary root length in the mutant (figure 3.5 A).

3.2.8 Functional redundancy in the SMAX1/SMXL2 pair

SMAX1 and SMXL2 proteins appear to be important for root development, but given the distinct expression patterns of the genes (personal communication), I hypothesised that they might play distinct roles in these processes. I therefore investigated if SMAX1 and SMXL2 have redundant or non-redundant functions downstream of KAI2 signalling to regulate root development.

I found that *smax1-2* does not display the RHD and RHL phenotypes observed in *smax1 smxl2* double mutant and cannot rescue the RH phenotypes of *max2-1* (figure 3.7 A-B). However, *smax1-2* alone is sufficient to reduce the distance between the root tip and first root hair, and is fully epistatic to *smxl2* and *max2* in this respect (figure 3.7 C). These data suggest that on one hand SMAX1 alone is sufficient to control the distance from the root tip to the first root hair (presumably by modulating the size of the elongation and division zones in the root tip). This idea is consistent with the expression of SMAX1 promoter in the primary root cap (Soundappan et al., 2015, Wallner et al., 2017). On the other hand SMXL2 might be equally or more important than SMAX1 for the control of root hair density and length (figure 3.7 A-B), as proposed in a recent jointly-authored report showing that *smxl2* single mutants display an increased RHL with respect to WT and *smax1*, suggesting that *smax1* mutation alone was not sufficient to induce the increase in length and density observed in *smax1 smxl2* (Villaécija-Aguilar et al., 2019).

The primary root length of *smax1 smxl2* double mutant but also *smax1-2* single mutant is significantly shorter than wild-type (figure 3.7 D). In addition, PRL in *smax1 smxl2* is completely epistatic to *max2*. These findings are in line with the idea that SMAX1 is required to regulate the growth of the root tip, and therefore the size of the elongation and division zone (figure 3.7 C). These data also suggest that SMXL2 might not be involved in this process, however, the characterization of *smxl2* single mutant (which I did not have at the moment of this study) would be necessary to confirm this hypothesis.

Overall these data demonstrate SMAX1 and SMXL2 genetically act downstream of KAI2 signalling to ensure the tight control of root development. The partial redundancy between SMAX1 and SMXL2 has been reported for other aspect of the seedling development such as seed germination, hypocotyl growth, and leaf shape (Soundappan et al., 2015, Stanga et al., 2016). Here, we shows that SMAX1 and SMXL2 also likely regulate root development with a certain degree of redundancy, depending the tissues. The most parsimonious explanation for these observations is a tissues specific expression pattern of *SMAX1* and *SMXL2* genes: in tissues where only one of the two proteins is expressed, removing this one is sufficient to suppress the phenotype.

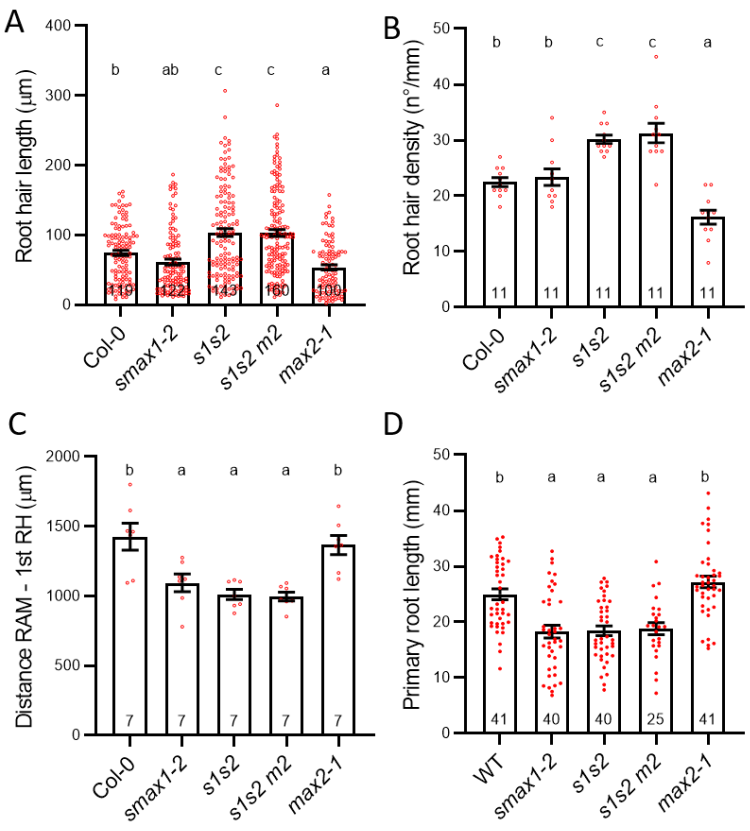

Figure 3-7 SMAX1 and SMXL2 display a partial redundancy essential to shape root architecture downstream of KL perception

(A-D) Root hair length (A), root hair density (B), distance from the root tip to the first root hair (C), and primary root length (D) in Col-0 wild-type and indicated genotypes. The mutant alleles are *smax1-2, smax1-2 smxl2-1 (s1s2), max2-1, and smax1-2 smxl2-1 max2-1 (s1s2 m2)*. All graphs represent data from one experimental replicate, and all experiments were repeated at least two times with similar results. Data represent mean ± SE, red dots represent individual data. Sample is indicated in bars. For (A), sample size represent the pool of at least 10 root hair per seedlings from 10 seedlings. Different letters indicate different statistical groups (ANOVA, posthoc Tukey, p≤ 0.001).

3.2.9 Functional redundancy of SMXL678

Given SL signalling is required to regulate certain aspects of root development such as primary root growth, and the loss-of-function of its downstream effectors *smxl678* induces a defect in lateral root development, I investigated the functional redundancy of SMXL678 protein as well as the relationship between the structure of SMXL7 protein and its functions in roots.

I found no difference in PRL between *smxl678* triple mutant and wild-type, but the single mutation *smxl6*-4 and *smxl8*-1, but not *smxl7*-3, induces an abnormal development of the primary root (figure 3.8 A). Loss-of-function *smxl6* alone is associated with a shorter PRL with regards to WT, but double mutants *smxl6 smxl7* display a normal WT phenotype, while *smxl8* mutation results in an increase of the PR growth. These ambiguous data suggest that SL-dependent primary root development may be very sensitive to the stoichiometry of SMXL6, SMXL7, and SMXL8 proteins or that SMXL6 and SMXL8 act in different cells or on different mechanisms of the root tip growth (e.g. cell division or cell elongation).

Similarly, *smxl678* triple mutant exhibits a strong decrease in LRD that is only partially matched by single mutant *smxl6* and double mutant *smxl6 smxl7*, while *smxl7* and *smxl8* mutations alone have a LRD of same magnitude as WT (figure 3.8 B). The fact that *smxl6* and *smxl6 smxl7* mutants only partially phenocopied *smxl678* triple mutant suggests that the lateral root density is a parameter highly sensitive to the stoichiometry of SMXL6, SMXL7, and SMXL8 proteins. It also support the idea of a strong interchangeability between the three SL signalling proteolytic targets.

3.2.10 Structure/Function of SMXL7

The structure/function relation of SMXL7 protein was recently addressed with respect to shoot branching (Liang et al., 2016). This study shows the tissues specific sensitivity to SMXL7 activity and dose, the EAR motif of SMXL7 contribute but is not essential to all the functions of the protein downstream of SL signalling. Given our data on the role of SMXL678 for lateral root development, I investigated whether the EAR motif is involved in the function of SMXL7 in root development, by measuring the lateral root density of SMXL7 variants expressed in the *smxl678* background.

I found the expression of *SMXL7pro:SMXL7-VENUS* (*SMXL7-VS*) can partially rescue the LRD phenotype of *smxl678*, but doesn't not influence LRD development when expressed in Col-0 (figure 3.8 C). The rescued LRD phenotype of *smxl678* by ectopic SMXL7 support the idea of a strong

interchangeability or redundancy between SMXL6, SMXL7, and SMXL8, and the presence of one protein of the triad is sufficient to partially fulfil the function of the others. Interestingly, these data also show the expression of the stabilised SMXL7 variant SMXL7^{d53} (in which the protein has been stabilized by replacing amino acids 812-RGKTVV-817 with T, and cannot undergo SL-dependent ubiquitination-degradation) does not affect LR development when expressed in a wild-type background. This contrasts strongly with the shoot, where the same transgenic line has a strong, *d14*-like phenotype (Liang et al., 2016).

Interestingly, I found that *smxl678* seedlings in which the SMXL7^{dEAR} variant (lacking the EAR motif required for SMXL7 to interact with TPR/TPL proteins) is expressed still rescues the *smxl678* phenotype to the same degree as the non-truncated SMXL7 protein (figure 3.8 C), indicating the EAR motif is not essential to SMXL7 function in the context of LRD, consistent with what has been reported in shoot branching (Liang et al., 2016). Overall, these observations imply the accumulation of SMXL7 proteins over a certain threshold does not influence LRD nor SMXL7 function, but rather the SMXL7-dependent regulation of LRD is achieved by a precise control of SMXL6/7/8 abundance by SL signalling. Consistent with Liang et al., 2016, it appears the SL-mediated regulation of lateral root development by SMXL7 is an EAR-independent mechanism, which remains to be identified.

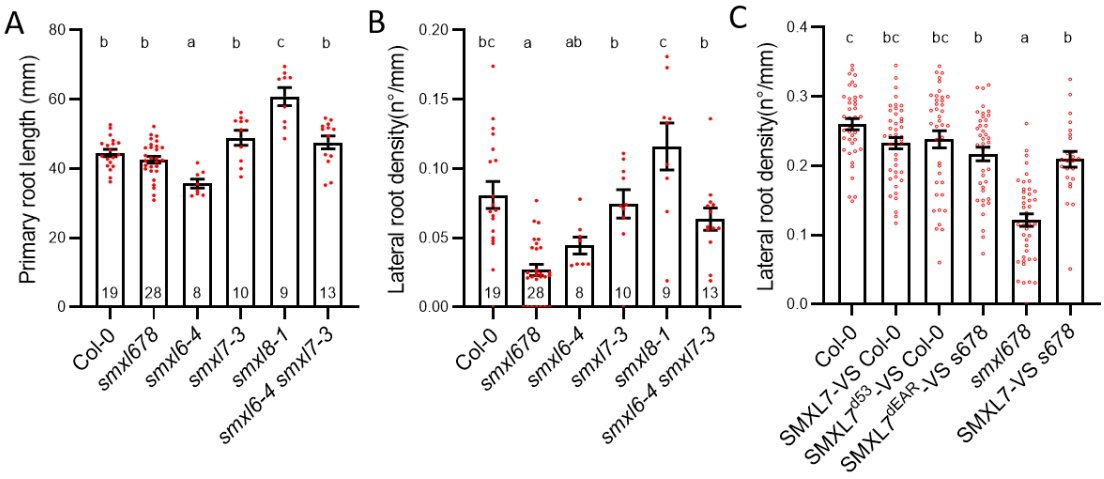

Figure 3-8 SMXL678 display partial functional redundancy in roots
(A-B) Primary root length (A) and lateral root density (B) in Col-0 wild-type and *smxl6-4 smxl7-3 smxl8-1* triple mutant and respective single mutants at 10 days post germination. (C) Lateral root density in Col-0 untransformed or transformed with *SMXL7pro:SMXL7-VENUS* or *SMXL7pro:SMXL7^{d53}-VENUS* and in *smxl6-4 smxl7-3 smxl8-1* triple mutant untransformed, or transformed with *SMXL7pro:SMXL7-VENUS* or *SMXL7pro:SMXL7$^{\Delta EAR}$-VENUS* at 10 days post germination. (All lines were previously described in Liang et al., 2016).
All graphs represent data from one experimental replicate, and all experiments were repeated at least two times with similar results. Data represent mean ± SE, red dots represent individual data. Sample is indicated in bars. For (C), sample size is n=20-40 seedlings per genotype. Different letters indicate different statistical groups (ANOVA, posthoc Tukey, p≤ 0.001).

3.3 Results summary

I demonstrate in this study that under controlled conditions, correct patterning of the root architecture in Arabidopsis seedlings relies on the action of both SL and KL signalling. We propose a new model in which SL signalling regulates primary root development (and by extension lateral root density), but for which most phenotypic outputs of *max2* mutation previously attributed to D14 signalling, are rather the mark of KAI2 signalling which appears to be a key regulator of root development (root hair and lateral root proliferation, and skewing and waving of the primary root) (figure 3.9).

3.3.1 Regulation of RSA through KAI2 and D14 signalling

Overall, my results indicate that KAI2-MAX2 complex and its proteolytic targets SMAX1/SMXL2 are controlling several aspect of the root architecture. Importantly, while some aspects of the RSA such as the root hair proliferation appears to be solely regulated by KL signalling, other parameters such as the lateral root density seems to also rely on the function of SL signalling (figure 3.9). While it is clear that KAI2 is required for the formation of lateral root, D14 on the other side seems to ensure the correct development of the primary root meristem, which surprisingly also seems to require the action of SMXL6/7/8 and SMAX1, despite *kai2* and *max2* mutants being aphenotypic in regard to primary root length. Similarly, the phenotypic outputs of SMXL proteins on root skewing downstream of KAI2-MAX2 remains disputed in the literature (Swarbeck et al., 2018, Machin et al., 2020, Villaécija-Aguilar et al., 2019), although my data suggest a solely canonical KAI2-SMAX1/SMXL2 action. Understanding the function of SMXL proteins in root architecture appears to be a key challenge for future studies.

Similarly, the mechanism of action of SL and KL in root remain unknown. It has previously been proposed that SL actions in root are the reflection of a change on the auxin landscape (Ruyter-Spira et al., 2011), I hypothesised that it might as well be the case of KAI2 signalling. The hypothesis that D14-SMXL678 and KAI2-SMAX1/SMXL2 pairs would modulate auxin landscape, for example by regulating auxin distribution or abundance in a given root tissues, is likely possible and would therefore explain variability of the phenotypic outputs of the pathways observed in this study and in previous reports. In addition, change in auxin landscape have been largely linked with change in environmental conditions such as nutrient availability, temperature or light regimen (Ljung et al., 2013). SL biosynthesis in the roots is linked with the nutrient status of the plant, and a MAX2-dependent regulation of root hair development in response to phosphorus

scarcity and auxin transport has previously been suggested (Yoneyama et al., 2008, Lopez-Raez et al., 2008, Sun et al., 2014). However, links between growth conditions and KL signalling are yet mainly elusive, although a link with light perception seems likely; thus understanding how KAI2 affect seedlings growth in response to environmental changes will provide important clues and tools in this regard. Indeed, it is likely that both pathways are affected by environmental conditions and fine-tune the root development accordingly.

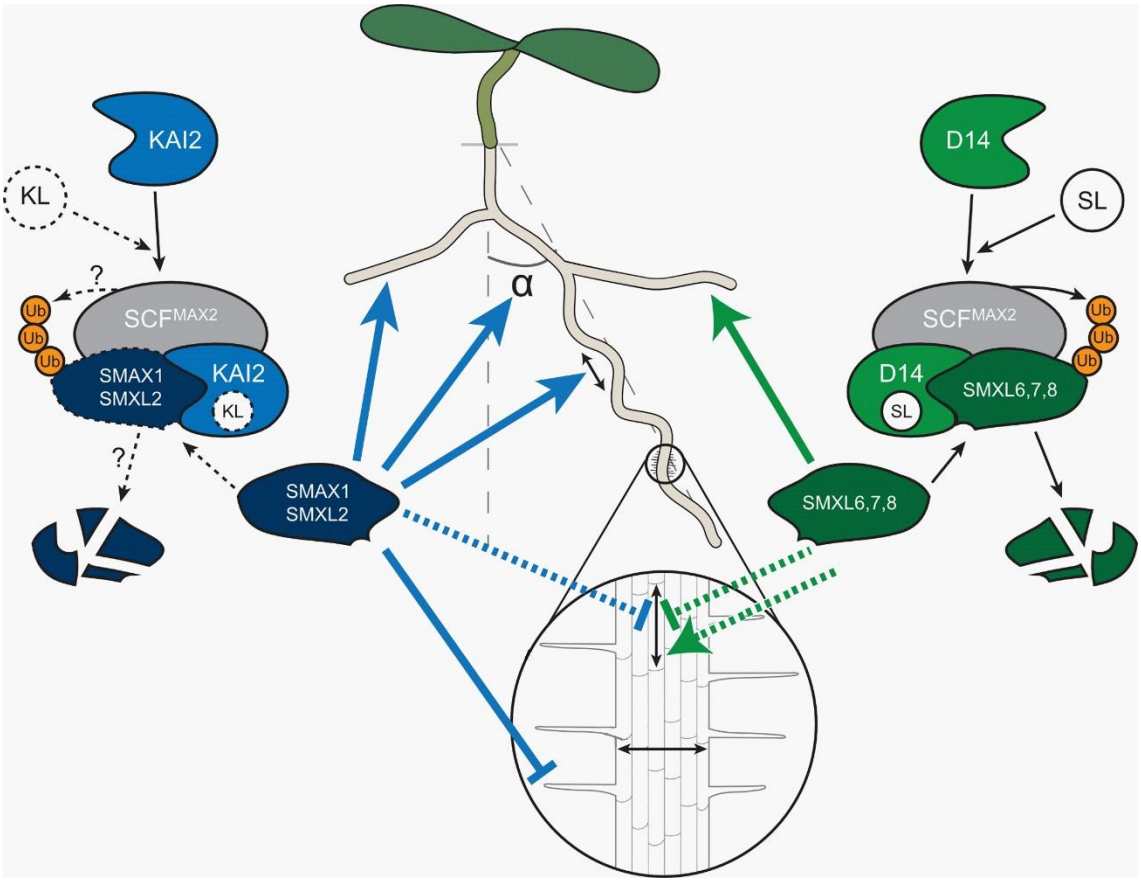

Figure 3-9 Model for KL and SL signalling regulation of root development in Arabidopsis seedling

SL and KL signalling act in the root system of *Arabidopsis thaliana* through the same MAX2-dependent proteolytic mechanism directing the degradation of repressors from the SMXL protein family. SL biosynthesis and signalling via D14 promote the primary root growth and participate to the lateral root development. This mechanism is ensured by D14-MAX2-dependent degradation of SMXL6, 7 and SMXL8, although the role of SMXL6, 7, 8 in primary root growth remains unclear (represented by dashed arrows). On the other hand, SMAX1 and SMXL2 repress root hair development and growth, promote rightward skewing of the primary root, and promote lateral root proliferation downstream of KAI2-MAX2. As for SMXL678, the role of SMAX1 and SMXL2 in mediating the primary root development remains unclear (represented by dashed arrows). Adapted from Villaécija-Aguilar et al., 2019.

Chapter 4 SL and KL signalling are essential for the seedling to integrate developmental responses to its surrounding

4.1 Aims

The first aim of this chapter is to address the roles of SL and KL signalling in the adaptive responses of the seedlings to environmental stresses, given that both SL and KL are involved in regulating the early stages of plant root development (figure 3.10). In the literature, strigolactone biosynthesis has been largely associated with response to low nutrient availability (phosphorus and nitrogen) in the soil (reviewed in Yoneyama, 2016). However, the link between the functions of SL in shaping the root system architecture and the developmental responses the seedlings undergo to address a nutrient depletion remains unclear. In addition, the results reported in this thesis (Chapter 3) show that SL signalling accounts for a minor contribution in shaping the RSA, and that KL signalling is of a major importance given it regulates lateral root development, root hair proliferation, and maintenance of a correct gravitropic index of the primary root. It is as a consequence important to investigate the link between abiotic stress/stimuli responses and KL and SL signalling functions.

The second aim of this chapter is to address the function of KL signalling in the seedling at the skotomorphogenesis to morphogenesis transition. Loss-of-function *kai2* and *max2* mutants were first identified as hyposensitive to light, and the seedlings display abnormal phenotypes only as a response to certain light stimuli (Shen et al., 2007, Sun & Ni, 2011). Although recent studies have shed light on a link between components of the light signalling hub and the role of KL signalling during early stages of the seedlings development (Bursch et al., 2021), how the functions of KAI2 and the downstream degradation of SMAX1 and SMXL2 is translated into morphogenetic responses is yet largely undescribed.

4.2 SL and KL shapes RSA in response to low external phosphate

Phosphorus deprivation in Arabidopsis is associated with local developmental changes in the root system architecture (RSA) such as a strong inhibition of the primary root development, formation and elongation of lateral roots, and increased root hair proliferation (reviewed in Péret et al., 2011). We examined whether SL and KL signalling mediate the RSA in response to varying external inorganic phosphorus (Pi) level by growing SL biosynthesis and SL and KL

insensitive mutants under two different Pi levels: high phosphate (HP, 1mM Pi) corresponding to standard growth media or low phosphate (LP, 10µM Pi).

Consistent with previous reports (reviewed in Péret et al., 2011), we found a limited Pi availability (LP) inhibits the growth of the primary root in the wild-type seedlings but also in *kai2-2* mutants, suggesting KAI2 is not required for this response (figure 4.1 A). In contrast, the PRL of SL deficient *max4-5* and SL-insensitive *d14-1* mutants is insensitive to Pi limitation. Consistent with these results, the double mutant *d14 kai2* displays a *d14-1* phenotype and is also irresponsive to phosphorus depletion. These data suggest SL signalling, but not KL signalling, is required for the correct inhibition of the primary root growth in response to phosphate availability.

By opposition to the effect on the primary root, we found under our growth condition that low Pi availability triggers a significant increased LRD in the wild-type Col-0 (figure 4.1 B), consistent with previous reports (reviewed in Peret et al., 2011). Interestingly, all the mutants analysed were unresponsive to low Pi and fail to increase LRD under this condition. As shown in Chapter 3, SL signalling is involved in regulating LRD mainly through modulation of the PRL but with negligible effect on LR initiation, and KL signalling acts on LRD solely by regulating LR initiation and emergence but not PRL. Under low Pi, our data show the two signalling pathways operate accordingly: SL signalling mutants develop LR in a similar fashion to wild-type while failing to inhibit the PRL, leading to no change in LRD (figure 4.1 A-B); on the other hand, *kai2* correctly reduces its PRL but fails to increase its LRD in response to low Pi, leading to either no change or a slight decrease in LRD (PRL/LRN ratio) (figure 4.1 A-C). The second observation is supported by the fact the double mutant *smax1 smxl2* also fails to promote LR proliferation in response to LP compared to Col-0. These data indicate that SL and KL signalling act as a duo to regulate the RSA in response to low Pi availability by mediating respectively the primary root growth and the initiation and development of lateral roots.

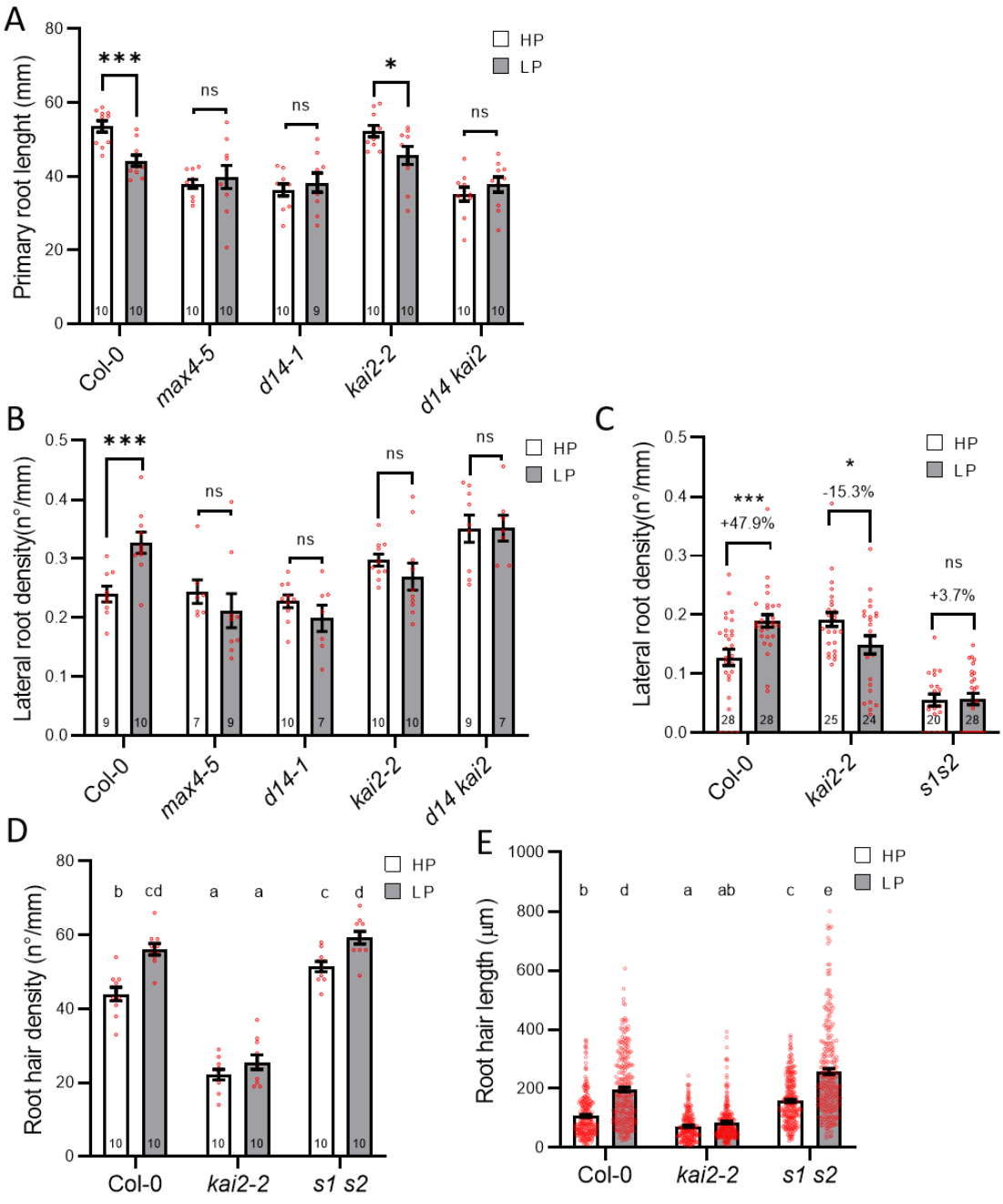

Figure 4-1 SL and KL signalling regulate primary root and lateral root development in response to phosphorus availability

(A-B) Primary root length (A) and lateral root density (B) in Col-0 wild-type, SL biosynthesis mutant *max4-5*, and in the *d14-1 kai2-2* double mutant and the respective single mutants at 10 days post germination in seedlings grown under standard phosphate (HP, 1mM Pi) or low phosphate (LP, 10µM Pi) treatment. (C) Lateral root density in Col-0 wild-type, *kai2*-2, and *smax1*-2 *smxl2*-1 (*s1s2*) mutants grown 10 days under standard phosphate (HP, 1mM Pi) or low phosphate (LP, 10µM Pi) treatment. (D-E) Root hair length (D) and root hair density (E) in Col-0 wild-type, *kai2*-2, and *smax1*-2 *smxl2*-1 (*s1s2*) mutants grown 10 days under standard phosphate (HP, 1mM Pi) or low phosphate (LP, 10µM Pi) treatment.

(A-E) Sample size is indicated by numbers in bars. For (E), sample size is the pool of at least 10 root hairs from 10 seedlings for each genotype. All graphs represent data from one experimental replicate, and all experiments were repeated at least two times with similar results Data represent mean ± SE, red dots represent individual data. (A-C) *, **, *** (p-value ≤ 0.05, 0.01, 0.001) indicates difference compared to control treatment (Welch's t-test). (D-E) Different letters indicate different statistical groups (ANOVA, posthoc Tukey, p≤ 0.001).

An increase of root hair density (RHD) and length (RHL) is another crucial aspect of the adaptive response of plants to low phosphate availability in soils, and this response relies on the modulation of the crosstalk between various plant hormones such as auxin and ethylene (Bates et al., 1996, Bhosale et al., 2018, Jones et al., 2009). We showed KAI2 signalling is an important regulator of RH development (figure 3.3), and SMAX1 and SMXL2 were recently suggested to act on RH elongation by repressing ethylene biosynthesis (Carbonel et al., 2020, Villaecija-Aguilar et al., 2021). I examined if the KAI2 and SMAX1/SMXL2-mediated regulation of the root hair development and elongation was part of the plants tool-box to mitigate phosphorus scarcity (figure 4.1 D-E). I found low Pi induces a significant increase of RHD and RHL in wild-type, but not in *kai2* mutant which is unresponsive. On the other hand, LP induces in *smax1 smxl2 (s1s2)* an increase of RHD of same magnitude as Col-0, but the RHL baseline observed in *smax1 smxl2* when grown under standard Pi level is already significantly stronger than what is observed in Col-0. These data indicate KL signalling promotes root hair elongation, and to some extent RHD, and KAI2 and SMAX1/SMXL2 are required for the correct RH elongation in response to low external Pi level. These data are consistent with similar findings we recently reported in a co-authored study (Villaecija-Aguilar et al., 2021).

Taken together these results suggest SL and KL signalling are essential for the remodelling of the RSA in response to low external Pi level; SL signalling is required for correct inhibition of the primary root, and KL signalling is necessary to regulate LR proliferation and RH elongation. In addition to the RSA remodelling, the formation of symbiotic associations between plant and fungi (arbuscular mycorrhizae) is an essential part of the plant strategy to facilitate nutrients acquisition, for example to overcome the deleterious effects of low Pi availability in the soil (reviewed in Chiu and Paszkowski, 2019). Several studies have demonstrated that SL exudation, but also functional KAI2 and SMAX1 proteins are essential for the formation of such symbiotic partnership (Akiyama et al., 2005, Choi et al., 2020, Gutjahr 2015, Yoshida et al 2012), supporting the idea that SL and KL signalling are two important elements of the developmental responses to low Pi.

4.3 Sucrose supplementation perturbs KAI2 and D14 function in roots

In addition to the properties of the soil where the roots forage for nutrients, plant root plasticity depends greatly on the carbohydrate availability. There is a growing suit of evidence that, in addition to its role as source of energy, sucrose may also serve as a distinct long-distance signal involve in several physiological processes, including root development (MacGregor et al., 2008; Kircher et al., 2012; Roycewicz and Malamy 2012). Supplementation of the growth media with a source of carbohydrates strongly affect seedling development, although the magnitude of the developmental changes varies depending on the nature of the carbohydrate. For instance, sucrose supplementation promotes hypocotyl elongation and primary root growth to a stronger degree than glucose supplementation (Garcia-Gonzalez et al., 2021). Addition of glucose or sucrose in the media alter several aspects of the RSA, including increased root hair proliferation (density and length), increased lateral root development, and perturbation of the primary root gravitropic index (Mishra et al., 2009, Mugdil et al., 2016, Dimitrov and Tax 2018, Garcia-Gonzalez et al., 2021). These changes in the RSA in response to exogenous sugar supplementation are associated with an increase meristem activity and enhanced indole-3 acetic acid (IAA) biosynthesis in the root tip and shoot tissues (Mishra et al., 2009, Kircher et al., 2012, Sairamen et al., 2013). In recent years, studies have led to a better understanding of the interplay between sucrose and auxin signalling, and the essential role of the sugar-auxin interaction in regulating the growth, development, and morphology of the plant (reviewed in Mishra et al., 2021).

Given the potent effect of sugar signalling on root traits also regulated by SL and/or KL signalling, we investigated a possible sugar-SL/KL crosstalk. To do so, I measured the root development in SL and KL signalling mutants after 8 days of growth in a media with 1% sucrose supplementation (Suc+) or with no sucrose added (no Suc) (figure 4.2). As described in Garcia-Gonzalez et al., 2021, we found sucrose supplementation significantly promotes primary root growth in wild-type and *kai2-2* mutant (figure 4.2 A). Contrastingly, SL insensitive mutants *d14-1* and *d14-1 kai2-2* display a significant reduction of PRL in response to the addition of sucrose (suc+) compared to seedling growing without sucrose in the media (figure 4.2 A). The absence of phenotype in *kai2*, in addition to a same magnitude of response in *d14* single and *d14 kai2* double mutant suggests that sucrose supplementation interferes with the SL dependent regulation of the primary root development. Given the key role of auxin in the regulation of the PRL, and the fact sucrose addition has been shows to interfere with auxin

biosynthesis, transport and signalling, we speculate that SL and auxin signalling work in concert to regulate the development of the primary root, and addition of exogenous sucrose in the growth media affects the synergy of the SL-auxin crosstalk.

Sucrose supplementation induces a 23% increase of lateral root density in Col-0 compared to the non-supplemented condition (no Suc), although the difference is statistically non-significant (figure 4.2 B). Conversely, addition of sucrose had no effects on the lateral root density in SL and KL insensitive mutants *d14* and *kai2* (1% increase, and 5% decrease of LRD respectively), but strongly reduces LRD in *d14 kai2* seedlings (figure 4.2 B). Given that SL and KL pathways co-regulates LRD by affecting the primary root development and the lateral root proliferation under standard growth condition (figure 3.1 and 3.2), we can speculate that sucrose supplementation interferes with the mechanisms of action of SL and KL signalling to this regards, leading to aberrant lateral root development in *d14 kai2* mutant.

It has previously been demonstrated that carbohydrate availability influences the gravitropic index of the primary root (also referred as “root deviation from the gravity axis” and referred in this thesis as “skewing”) (Mishra et al., 2009, Garcia-Gonzalez et al., 2021). Consistent with these reports, my data show that skewing is significantly increased in wild-type seedlings grown with 1% sucrose supplementation (figure 4.2 C). The addition of sucrose does not affect *d14-1* and *kai2-2* seedlings, despite *kai2* mutants exhibiting an angle of skewing significantly greater than wild-type and *d14* in both conditions (as seen in figure 3.4). By opposition, sucrose supplementation induces a significant increase of skewing in *d14 kai2* compared to non-supplemented seedlings (figure 4.2 C). Interestingly, *d14 kai2* double mutant displays the same phenotype as *kai2* when non-supplemented, but the addition of sucrose exacerbates the double mutant phenotype beyond what we observe in the single mutants. These data are consistent with my previous observations (figure 3.4 C) in which the analysis was carried on sucrose-supplemented seedlings. A possible explanation for the strong defect observed in *d14 kai2* double mutants in Suc+ compared to *kai2* and *d14* single mutants could be that the two proteins work with a certain degree of redundancy, and despite not being the endogenous function of D14, the protein could partially overcome for the lack of functional KAI2 in *kai2* mutant. The most parsimonious explanation would be that sucrose supplementation disrupts the D14-dependent regulation of primary root meristem activity and the KAI2-dependent regulation of primary root gravitropic index; thus leading to an aberrant directional growth in *d14 kai2*. I hypothesise that this mechanism relies on

sucrose affecting a common target of SL and KL signalling, known to act in regulation these two root parameters.

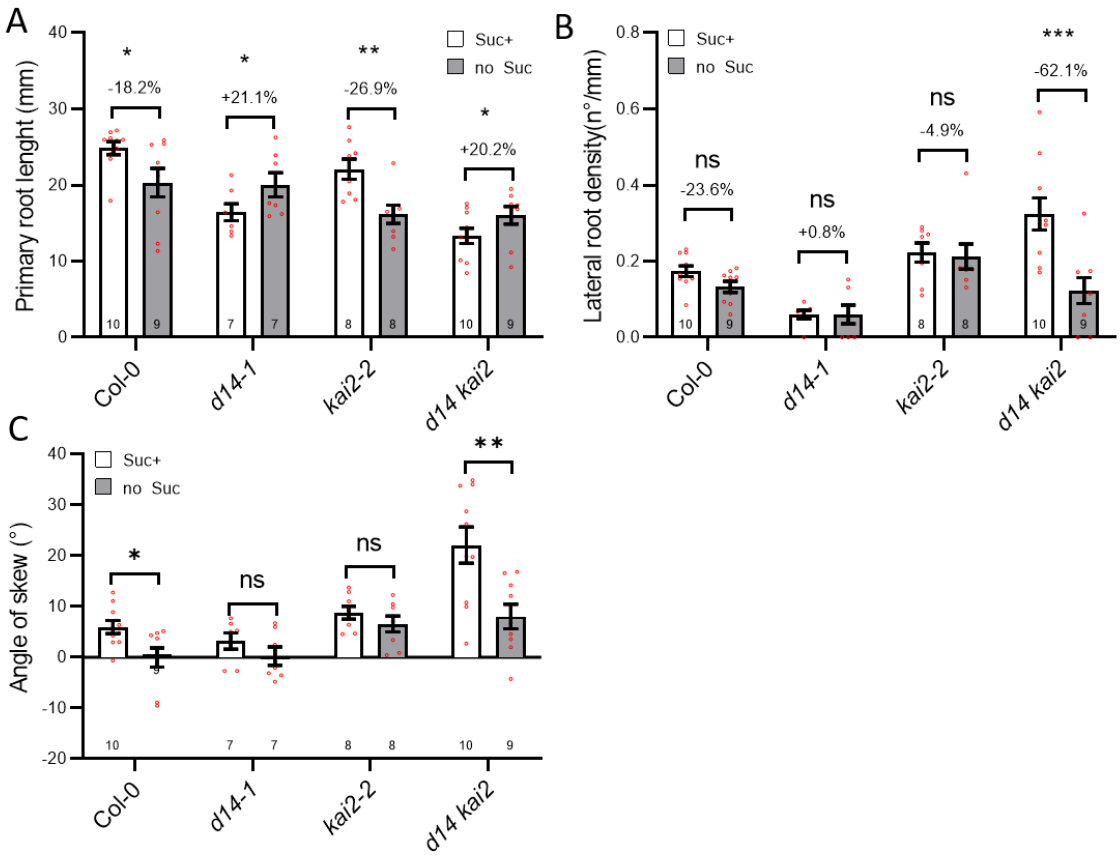

Figure 4-2 KL and SL signalling regulation of root development is perturbed by sucrose supplementation

(A-C) Primary root length (A), lateral root density (B), and primary root skewing (C) in Col-0 wild-type and in the *d14-1 kai2-2* double mutant and the respective single mutants at 10 days post germination in seedlings grown in agar media with sucrose supplementation (Suc+, 1% sucrose) or in non-supplemented agar media (no suc). Sample size is same for each panel and is indicated by numbers in bars. All graphs represent data from one experimental replicate, and all experiments were repeated at least two times with similar results Data represent mean ± SE, red dots represent individual data. *, **, *** (p-value ≤ 0.05, 0.01, 0.001) indicates difference compared to control treatment (Welch's t-test).

Interestingly, primary root growth and primary root gravitropic index both emerge from a tight control of the RAM and elongation zone activity by auxin signalling (reviewed by Roychoudhry & Kepinski 2021), while lateral root initiation, emergence, and growth also depend upon auxin transport and signalling (Casimiro et al., 2001). Moreover, Mishra et al. 2009 and Garcia-Gonzalez et al. 2021 showed the change in PRL and gravitropic index after sugar supplementation results from a modulation of the auxin homeostasis and shootward auxin transport to the elongation zone by the regulation of PM

localized auxin efflux carrier abundance (e.g. PIN2). KL signalling has recently been shown to control the PIN2/AUX1-dependent shootward auxin transport from the root tip to the elongation zone to ensure correct RH development in response to phosphorus depletion (Villaecija-Aguilar et al, 2021). One would therefore speculate/hypothesise that sucrose signalling and KL signalling (but also SL signalling for PRL) induce similar developmental changes to the RSA, such as lateral root proliferation and maintenance of the correct gravitropic index, by targeting the same downstream components, namely auxin homeostasis/transport.

4.4 Gravitropic-response is defective in *kai2* mutant

Given the gravitropic index (angle of skew) of the primary root is abnormal in *kai2* mutants, I investigated if KAI2 was involved in the root gravitropic response. Gravitropism assays based on time-lapse imaging were conducted to investigate the response of the root tip to reorientation. Seedlings were grown in normal light conditions on vertical agar plate such that the primary root grows toward the vector of gravity, then the plate was placed in the dark and rotated 90° to induce gravitropism (figure 4.3 A). Still in darkness, images were collected every 10-minutes for 6-hours by computer-controlled cameras using infrared backlight. The angle of the root apex toward gravity (bend rate) was measured from the images in *kai2-2* mutants and its Col-0 wild-type control (figure 4.3 A). Our measurements of the angle toward gravity indicates the *kai2-2* mutant redirects its root tip to the direction of the gravity vector faster than the wild-type control (Col-0) over the course of the experiment (figure 4.3 B), suggesting a difference in gravitropic behaviour. However, the careful analysis of the root growth over the same period shows *kai2-2* seedlings exhibit a significantly increased growth rate (mm/min) compared to Col-0 when gravity-stimulated by rotating at 90° the root tip (figure 4.3 C). As previously described in Schöller et al., 2018, the gravitropic response of the root depends on its growth rate, and differences on the growth rate between two roots results in variation of the bending kinetic of the organ. Consequently, I normalised the early gravitropic response (gravitropic curvature normalised by the root growth) of *kai2* and Col-0 to discriminate if either their differences of gravitropic behaviour were the results of a gravitropic defect or root growth defect. Normalization to growth rate diminishes the observable differences of angle toward gravity over time between the two genotypes, but, the normalized gravitropic growth analysis of *kai2* seedlings still shows a statistically significant reduction in gravitropic bending compared to wild-type (figure 4.3 D-E).

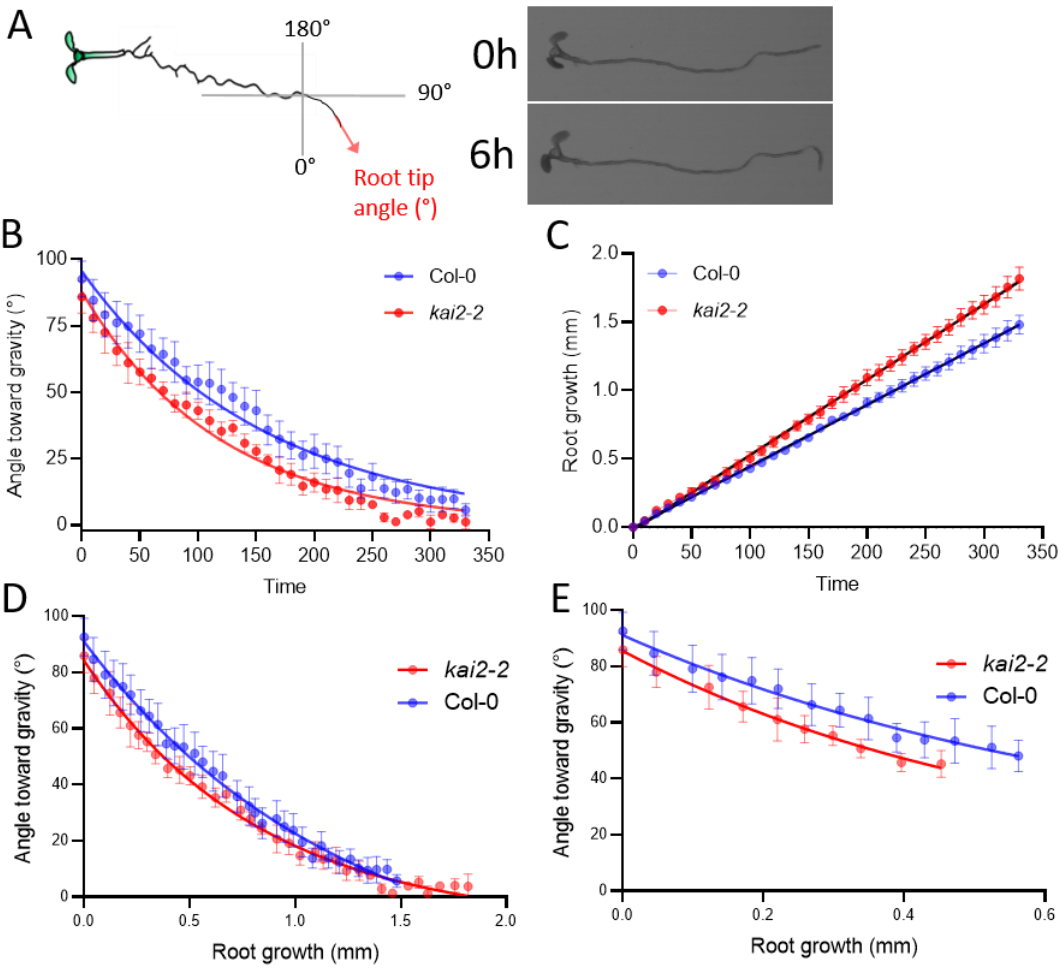

Figure 4-3 Gravitropic response is altered in *kai2* mutant
(A) Diagram showing Arabidopsis primary root tip gravistimulation, when reoriented with a 90° angle and tracked for 6 hours. (B-D) Kinetics of full gravitropic response of Col-0 wild-type and *kai2-2* seedlings; Before (B), and after normalization (D) to growth rate (C). (E) Kinetics of early gravitropic response (angle toward gravity < 45°) of Col-0 wild-type and *kai2*-2 seedlings normalized to the speed of growth (C). (B, D, E) Non-Linear regression Exponential One-phase decay extra sum-of-square F test (95%). For (B) p.values <0.0001, (D) p.values <0.001, (E) p.values <0.05, correspond to the comparison of fitted nonlinear regression with extra sum-of-squares F test; (C) p.values <0.0001 correspond to the comparison of slope (95% confidence) of linear regressions.
All graphs represent data from one seedling, the experiment was repeated with four other seedlings showing similar results. Data represent mean ± SE,

Finally, auxin was shown to regulate organ growth direction in response to gravity stimulation by forming a lateral gradient with a auxin maxima on the lower side of the organ regarding the vector of gravity. The formation of the gradient requires rapid redistribution of auxin after gravity perception (Friml et al., 2002, Kleine-Vehn et al., 2010) (in this case after a 90° rotation of the seedlings); and it was shown the asymmetric auxin distribution was then gradually lost when the root tip reaches an angle of 45° towards gravity, before returning to a symmetric

distribution on both sides of the root (Band et al., 2012, reviewed in Zhang et al., 2019). Considering these facts, I analysed the gravitropic growth of *kai2* and Col-0 during the first phase of the gravitropic response, hereafter the period comprised between the initial 90° redirection of the root tip until the root tip reaches an angle of 45° toward gravity (figure 4.3 E). Notably, the difference of normalised half-gravitropic response between *kai2* and Col-0 appears distinctive with *kai2* gravitropic response being more pronounced than wild-type (figure 4.3 E). This observation suggest that *kai2* is somehow able to hastily remodel its directional growth in response to gravity stimulation during the “auxin-dependent phase” following the perception of a gravity-stimulation.

4.5 KL signalling modulates the seedling development at the dark-light transition

4.5.1 KAI2 is required for correct skotomorphogenic development

In addition to the defect in the gravitropic response in the roots (figure 4.3), *kai2* shows a significant alteration of the negative gravitropic index of its hypocotyl when compared to Col-0. I measured the angle of the hypocotyl in seedlings etiolated for 4-days in the dark, and then plotted the data as the frequency of angle obtained using a polygonal x-axis frequency graph (figure 4.4 A-B). The data show the hypocotyl gravitropic angle in etiolated *kai2-2* seedlings is around 90° (negative gravitropism) with slight variation (only 28% of the seedlings have a hypocotyl angle bending more than 15° leftward or rightward). In contrast, etiolated Col-0 seedlings show a broader distribution of hypocotyl gravitropic index with nearly 50% of the seedlings bending leftward or rightward.

Observations of the apical hook in etiolated seedlings also suggest an abnormal skotomorphogenic development in KL signalling mutants. Measures of the apical hook angle (figure 4.4 C) in 4-days etiolated seedlings show *kai2* mutant displays a narrower (closed) apical hook than wild-type (figure 4.4 D-E). Strikingly, we found that *smax1 smxl2*, by opposition to *kai2* mutant and the wild-type, fails to form an apical hook to protect their cotyledons during skotomorphogenesis (figure 4.4 D-E), but display a normal hypocotyl gravitropic angle when etiolated (figure 4.3 A-B). The experiment was repeated twice, and was performed with a single end-point measurement at 4 days after germination; another explanation for the opened apical hook in *smax1 smxl2* could be that the mutant opens its apical hook at earlier stages than wild-type and *kai2*, therefore after 4 days of etiolation the hook would appear inexistent because already fully opened. These

data would also be consistent with the fully closed hooked in *kai2*, which in this hypothesis would be due to sluggishness to open the hook due to SMAX1 and SMXL2 accumulation. As for the gravitropic response, the formation, maintenance, and opening of the apical hook strongly relies on the action of auxin and the formation of auxin gradients in the hook by auxin transporters (PINs, AUX1/LAX, PILs) (reviewed in Beziat & Kleine-Vehn, 2018). Although there is no direct evidence that KL signalling mediates the apical hook development by modulating the auxin transporters, it would be logical to investigate this hypothesis.

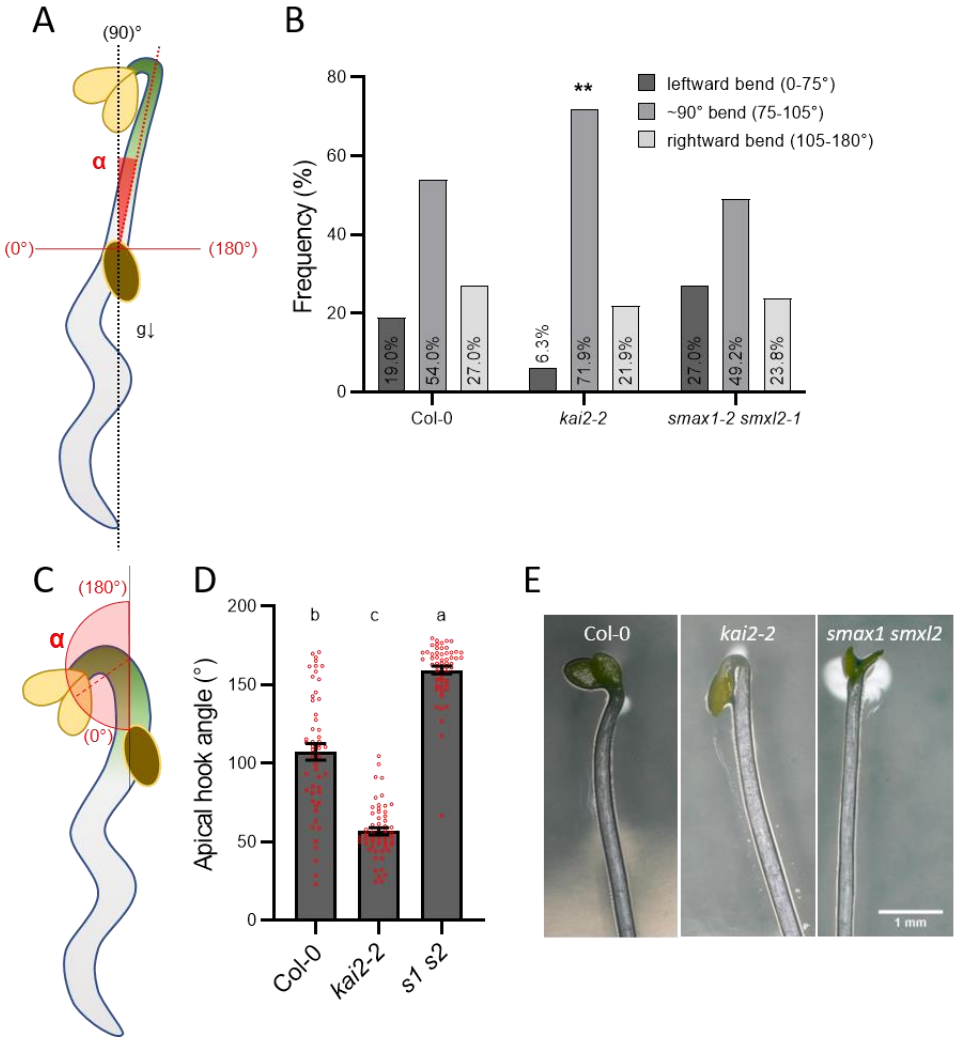

Figure 4-4 KL signalling is required for correct skotomorphogenic development of the hypocotyl

(A) Diagram showing how the gravitropic angle (α) of Arabidopsis hypocotyl etiolated for 4 days in the dark is measured. (B) Frequency of hypocotyl bending leftward (0-75°), rightward (105-180°), or keeping a neutral anti-gravitropic orientation (75-105°) in Col-0 wild-type, *kai2*, and *smax1-2 smxl2-1* mutants. (C) Diagram showing how the angle of the apical hook (α) is measured in Arabidopsis seedlings etiolated for 4 days.

(D-E) Average angle of the apical hook (D) and representative images (E) in Col-0 wild-type, *kai2*, and *smax1-2 smxl2-1* mutants etiolated for 4 days in the dark.

(B) and (D) n= 50-53 seedlings pooled together from three independent experimental replicates showing similar results. Data represent mean ± SE, (D) red dots represent individual data. For (B) ** (p-value ≤ 0.01) indicates difference compared to wild-type (Welch's t-test). For (D), different letters indicate different statistical groups (ANOVA, posthoc Tukey, p≤ 0.001).

4.5.2 Light intensity

The KL-insensitive *max2* and *kai2* mutants (also referred as *htl1* *HYPOSENSITIVE TO LIGHT1*) were initially identified as hyposensitive to light and it was reported that both MAX2 and KAI2 transcription and their physiological effects on hypocotyl elongation were modulated by light intensity (Shen et al., 2007, Sun and Ni, 2011). Given the major role of KAI2 signalling in root development I reported in this manuscript, and given the important adaptive changes Arabidopsis seedlings undergo in response to light (Maloof et al., 2001), I hypothesised the overall altered seedling development of *kai2* mutant is the result of the mutant hyposensitivity to light in both hypocotyl and root tissues. To test this hypothesis I grew *kai2*, *smax1 smxl2* and wild-type control (Col-0) in petri dish plates with direct light illumination at two different white light intensities: 50 $\mu mol.m^{-2}.s^{-1}$ (low light intensity) or 150 $\mu mol.m^{-2}.s^{-1}$ (high light intensity), and in a control condition of 0 $\mu mol.m^{-2}.s^{-1}$ (darkness) and assessed their development at 4 days post-germination for the hypocotyl and 8 days post-germination for the root parameters (figure 4.6). (*NB*: I did not measure the root phenotypes of dark grown roots given that 8 days in darkness resulted in sickly/dead seedlings, likely due to exhaustion of the seeds reserve).

First, consistent with Shen et al., 2007 and Sun & Ni, 2011 I did not observe difference in hypocotyl length between *kai2-2* and wild-type seedlings when grown in the dark, but interestingly *smax1 smxl2* seedlings show a markedly reduced hypocotyl elongation during etiolation (figure 4.5 A). A possible explanation for this phenotype of *smax1 smxl2* in the dark would be that the seedlings starved due to using all energy resource contained in the seeds. However, the media was supplemented with sucrose and all necessary nutrients, thus ruling-out this hypothesis. Under white-light illumination, *kai2-2* exhibits a light-hyposensitivity resulting in a greater elongation of its hypocotyl compared to Col-0 (figure 4.5 A). On the other side of the spectrum, perception of low light intensity is sufficient to totally inhibit hypocotyl elongation in *smax1 smxl2* double mutant, and the mutant does not exhibit the light intensity-dependent inhibition observed in wild-type and *kai2* hypocotyl (figure 4.5 A). Thus it appears clear that regulation of SMAX1 and SMXL2 abundance by KAI2 is required for the correct hypocotyl de-etiolation, as previously suggested (Stanga et al., 2013, Stanga et al., 2016).

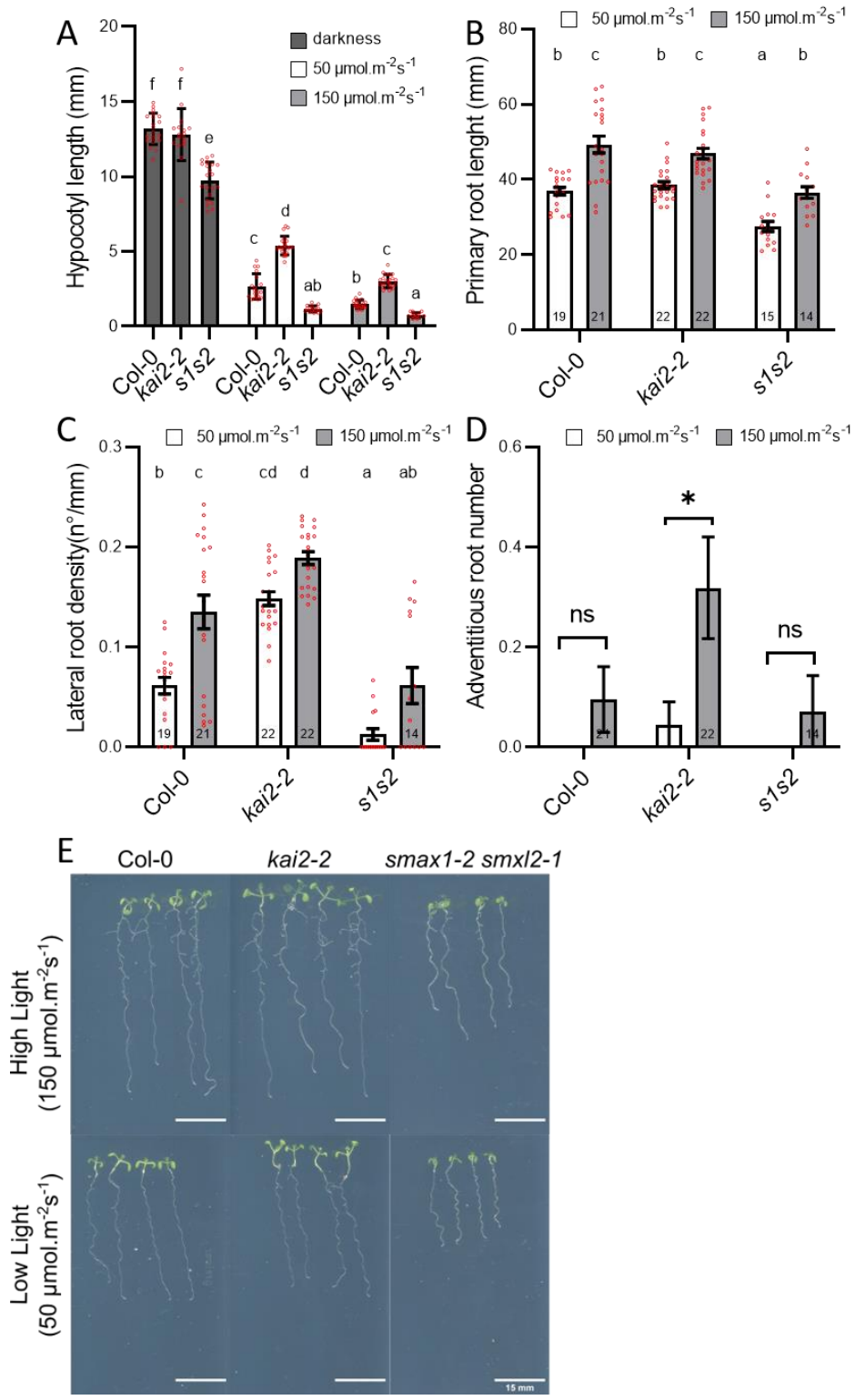

Figure 4-5 Effect of light intensity of the function of KAI2 signalling in seedling development

(A-D) Hypocotyl length (A), primary root length (B), lateral root density (C), and adventitious root number (D) in Col-0 wild-type, *kai2*, and *smax1-2 smxl2-1* seedlings. For (A), seedlings were grown in darkness (black), under low light intensity (white, 50 µmol. $m^{-2}.s^{-1}$), or in high light intensity (grey, 150 µmol.$m^{-2}.s^{-1}$) for 4 days. For (B-D), seedlings were grown under low light intensity (white, 50 µmol. $m^{-2}.s^{-1}$), or high light intensity (grey, 150 µmol. $m^{-2}.s^{-1}$) for 10 days. (E) is a representative image of (B-D). Scale bar represents 15 mm.

(A-D) Sample size is indicated by numbers in bars. All graphs represent data from one experimental replicate, and all experiments were repeated at least two times with similar results Data represent mean ± SE, red dots represent individual data. (A-C) Different letters indicate different statistical groups (ANOVA, posthoc Tukey, p≤ 0.001). (D) * (p-value ≤ 0.05) indicates difference compared to control treatment (Welch's t-test).

Comparing the primary root growth (figure 4.5 B, E), I did not observe differences between *kai2* and wild-type under the two light-intensity treatments, consistent with the general observation I made that KAI2 is unlikely to affect primary root development in Arabidopsis. However, under low or high white-light fluence, *s1s2* double mutants exhibit a consistent reduction of PRL compared to *kai2* and WT. These results are consistent with the observations reported in Chapter3 that *smax1 smxl2* double mutation impairs the correct development of the primary root independently of KAI2. Moreover, this mechanism does not seem to depend upon light intensity given that *smax1 smxl2* exhibits a light intensity-dependent inhibition of PRL of same magnitude as wild-type and *kai2* (figure 4.5 B, E).

In the dark, we could not observe any lateral or adventitious root development regardless of the genetic background (figure 4.5 C, E). The illumination of the root system promotes LR development in an intensity-dependent manner in wild-type seedlings with a significant (two-fold) increase LRD under high light- intensity compared to low intensity. As previously described in chapter 3, *kai2* and *smax1 smxl2* mutants exhibit opposing LRD phenotype when grown under standard light condition (~120 µmol.m^{-2}.s^{-1}). Interestingly, in both *s1s2* and *kai2* mutants, growth under low and high light-intensity does not significantly change the LRD (figure 4.5 C, E). The latest finding is rather surprising, given that under standard growth condition it appears clear that KAI2 acts as a negative regulator of LR development. The most parsimonious explanation for the absence of differences in *kai2* LRD between low and high light intensities is that in *kai2* mutants the accumulation of SMAX1 and SMXL2 reaches a threshold which promotes the development of new LR even at low light intensity, and increasing the light intensity above this threshold does not influence further the abundance of SMAX1/SMXL2 and therefore does not induce further LR proliferation. This idea is further supported by *smax1 smxl2* mutant which is unresponsive to light intensity (figure 4.5 C, E), likely because the absence of SMAX1 and SMXL2 prevents the initiation of the mechanism mentioned above. The most parsimonious explanation, would be that *kai2* mutation leads to accumulation of SMAX1/SMXL2, and the regulatory events downstream of SMAX1/SMXL2 are in *kai2* at a threshold that can't be pushed further by increasing light intensity. By opposition, wild-type seedlings are able to work within the limits of this threshold

and as a consequence can modulate the LR proliferation as a response to light intensity.

Finally, we found *kai2* mutant, but not wild-type or *smax1 smlx2* double mutant, shows an abnormal adventitious root proliferation when grown under high light intensity (figure 4.5 D-E).

Taken together, these data indicate KL signalling components are required for the correct patterning of at least some aspects of the young seedling development in response to light signalling. The differential elongation of *kai2* hypocotyl in response to different light intensity but not darkness supports the idea of *kai2* being hyposensitive in the shoot. However, the same mutants display exaggerated adventitious root outburst when grown under high light intensity, and exhibit an abnormal apical hook formation during etiolation (figure 4.4); in addition, *smax1 smxl2* double mutants display a phenotype on the other side of the spectrum and fails to correctly etiolate and de-etiolate its hypocotyl, to produce new LR in light condition (figure 4.5 C), but also to form or maintain an apical hook in darkness (figure 4.4 C-D). These observations do not refute that *kai2* mutant has a hyposensitivity to light in the shoot, but rather indicate that KL signalling components (KAI2, SMAX1/SMXL2) are more likely to be critical for the correct skotomorphogenic development of the seedling. This idea is further supported by Mizuno et al., 2019 reporting a KAI2-dependent suppression of gemma in dark-grown but not light grown *Marchantia polymorpha*.

4.5.3 Defect in KAI2 signalling leads to an abnormal adventitious root development in young seedlings

Etiolated growth can promote development of adventitious roots (AR) which are *de novo* formed roots emerging from any above-ground part of the plant or from callus in tissue culture, except root tissues. Several hormones are involved in the control of AR formation, among which auxin has a key role (Sorin et al., 2005, da Costa et al., 2013, Lakehall et al., 2019). During AR formation the tight regulation of rootward auxin transport from the cotyledons to the hypocotyl plays a crucial role in the different steps leading to the formation of new AR (da Costa et al., 2020). Among the other hormones involved in the regulation of AR proliferation, strigolactone have been suggested to play a role, based on the significant increase of AR number observed in *max2* mutant, and to a lesser degree in SL biosynthesis mutants, when compared to wild-type seedlings; in addition to the inhibitory effect of *rac*-GR24 on AR proliferation (Rasmussen et al., 2012). As demonstrated in Chapter 3, contrary to previously accepted conclusions, the MAX2- and rac-GR24-mediated control of root branching in Arabidopsis results

on the synergistic effects of both SL and KL signalling rather than solely to SL pathway. More recently, Swarbeck et al., 2020 showed in Arabidopsis that loss-of-function *kai2* and/or *max2* results in an increased AR number compared to a wild-type when grown in standard conditions. The findings of this study partially dispute the conclusions of Rasmussen et al., 2012, and rather suggest that KAI2 overlaps with the effect of MAX2/rac-GR24 in the formation of junction roots. The junction roots are a specific type of AR developing at the junction between the shoot and the root system in eudicots such as bean and Arabidopsis (reviewed in Steffens and Rasmussen, 2016). When grown in absence of stress, Arabidopsis seedlings rarely display neither junctions root nor adventitious root on the hypocotyl, unless grown in addition of exogenous auxin. However, AR proliferation arises as a stress-response on the hypocotyl upon light perception during de-etiolation after a period of etiolation of the seedling in the darkness (Sorin et al., 2005; da Costa et al., 2018). Given the new insights brought by Swarbeck et al., 2020, and based on the reported hyposensitivity to light of *kai2* and *max2* mutants and resulting abnormal etiolation of their hypocotyl (Shen et al., 2010, Sun and Ni, 2011), I hypothesised that KAI2 rather than SL signalling was involved in regulating AR proliferation in de-etiolating seedlings. To test my hypothesis, I re-examined the propensity of various mutants affected in SL or KL signalling to form AR (figure 4.6). For more clarity, the results presented below as “AR number” are the sum of junction roots and adventitious roots growing on the hypocotyl.

First, I scored the number of emerged AR in 8-days old non-etiolated (absence of AR stress-response) seedlings. As previously reported (Sorin et al., 2005), non-etiolated wild-type seedlings produce no (Col-0) or few (Ler) AR depending on the genetic background (figure 4.6 A-B). By opposition with previous report (Rasmussen et al., 2012), I found SL mutants *max4-5*, *d14-1,* but also the triple mutant *smxl678* do not exhibit changes of AR number compared to Col-0 when grown under normal conditions. Consistent with Swarbeck et al., 2020, I also observed that different allelic *kai2* mutations as well as *max2* mutation result in a significant increase of AR number in both *Col-0* and *Ler* backgrounds (figure 4.6 A-C). These data suggest that rather than a function of SL pathway, as previously thought (Rasmussen et al., 2012), AR development is a hallmark of KAI2 signalling. Notably, the double mutation *d14 kai2* induces a burst of AR of same magnitude as single mutants *kai2* and *max2* (figure 4.6 A), as previously discussed by Swarbeck et al., 2020, supporting the idea that D14 and the SL pathway are not required for AR emergence.

Because seedling etiolation is a well characterized AR-stress response inducer, and given the significant increase of emerged ARs I observed in *kai2* and *max2*

mutants, I repeated the measures on seedlings etiolated for 4 days in the dark, to promote AR formation, and then transferred for a subsequent 6 days in standard light conditions. I used the auxin response marker *DR5v2:GFP* expressed in Col-0 and *kai2-2* background as a marker of the founder cells of priming AR to examined if the increased AR number in *kai2* was the result of increased AR initiation and formation of AR primordia, or solely the result of an increased emergence (figure 4.6 D). I observed in *kai2-2* a larger amount of AR primordia than Col-0 after de-etiolation, but also found that de-etiolation exacerbates the emergence of AR in *kai2-2* compared to the wild-type (figure 4.6 D), consistent with the idea that a defect in KAI2 causes increased AR proliferation (initiation and emergence).

To test further the implication of these findings, I investigated if SMAX1 and SMXL2 were involved in AR development downstream of KAI2-MAX2. The double mutant *s1 s2* exhibits a wild-type AR phenotype when grown under standard conditions (figure 4.6 A, C), but is completely epistatic to *max2* and can rescue *max2* AR phenotype to a wild-type level (figure 4.6 A, C). The major implication of these findings is that KAI2-MAX2 complex is involved in inhibiting the AR development, likely by regulating the abundance of SMAX1 and SMXL2 in the hypocotyl.

Finally, AR proliferation has been largely described as a wound-induced stress-response, where a wound such as de-rooting causes formation of an local auxin maximum where auxin accumulates at the wound and induces *de novo* adventitious rooting (Steffens and Rasmussen, 2016). Wound-induced (de-rooting) AR proliferation is the basis of cutting propagation and has been previously used as a model to study AR development in Arabidopsis (reviewed in da Costa et al., 2013). After etiolating Col-0, *kai2-2*, and *s1s2* seedlings for 4 days in the dark (4dd) and subsequently transferred them in standard light condition for 3 days (3dl), I de-rooted them by carefully dissecting their cotyledons and assessed their AR at 4dd 7dl. As expected this treatment induced AR development in wild-type. Interestingly, de-rooting treatment resulted in a significant proliferation of AR in *kai2* compared to wild-type, while *s1s2* seedlings seemingly failed to develop AR (figure 4.6 E-F). These data are thus consistent with the idea that a wound-induced increased auxin accumulation in the hypocotyl would cause an exaggerated initiation of new adventitious roots of *kai2*.

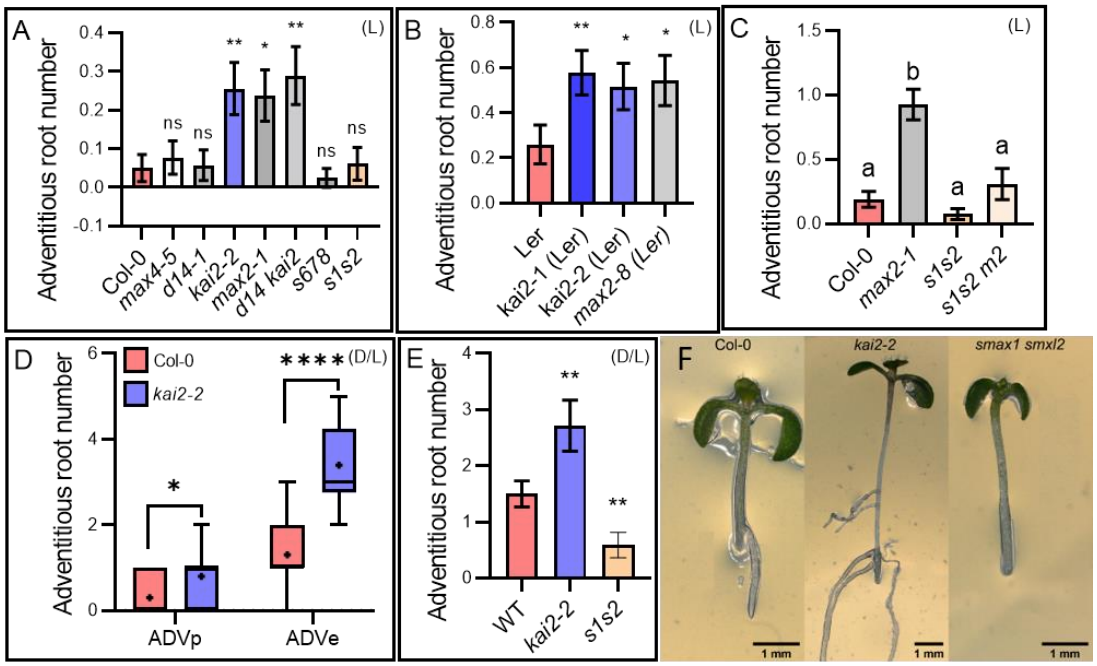

Figure 4-6 SMAX1 and SMXL2 promotes adventitious root development downstream of KAI2

(A) Adventitious and junction root number in 10-day old light-grown seedlings impaired in SL biosynthesis, signalling, downstream targets (respectively, *max4*-5, *d14-1*, *smxl6 smxl7 smxl8* (*smxl678*)), KL signalling and downstream target (*kai2-2, smax1 smxl2* (*s1s2*), *smax2 smxl2 max2*) or SL and KL signalling (*d14 kai2*, *max2*-1). Data correspond to one experimental replicate (n=43-91 seedlings per genotype), three other independent experimental replicates gave comparable results. *,** (p-value ≤ 0.05, 0.01) indicates differences compared to wild-type (Welch's t-test). ns = no significant difference. Error bars represent ± s.e.m.

(B-C) Adventitious and junction root number in 10-day old light-grown seedlings of KL signalling mutants in Lansberg erecta (Ler) ecotype (B), and KL signalling mutants in Columbia ecotype (C). Data correspond to two independent experimental replicates pooled together (n=19-44 seedlings per genotype). In (B), *,** (p-value ≤ 0.05, 0.01) indicates differences compared to wild-type (Welch's t-test). In (C), letters represent statistical groups determined by one-way ANOVA with post hoc Tukey HSD (CI 95%). Error bars represent ± s.e.m.

(D) Number of primordia and emerged adventitious roots in 11-day old de-rooted and etiolated Col-0 or *kai2*-2 seedlings. Data correspond to one experimental replicate (n=10 seedlings per genotype); two other independent experimental replicates gave comparable results.

(E-F) Adventitious root number (E) and representative images (F) in 11 days old de-rooted Col-0 wild-type, *kai2*, and *smax1*-2 *smxl2*-1 seedlings. Data are pooled from three independent experimental replicates with comparable results (n = 17-21 per experiment). ** (p-value ≤ 0.01) indicates differences compared to wild-type (Welch's t-test). Error bars represent ± s.e.m. (F) Scale bar represents 1 mm. For (A-C), (L) indicates that Arabidopsis seedlings were grown under a standard light regime (16 hours light, 8 hours dark). For (D-F), (D/L) indicates that seedlings were pre-etiolated for 4 days in the dark, then transferred under a standard light regime. For (E-F), 3 days after transfer to light condition, seedlings were de-rooted and grown for another 4 days before measuring adventitious root number.

4.5.4 KL signalling regulates the photomorphogenic remodelling of the seedling

Since *kai2* mutants display stronger phenotypes in younger seedlings, particularly in the roots (Chapter 3 and Villaecija-Aguilar et al, 2019), we hypothesized that *kai2* phenotypes arise from sluggish adaption to the light, rather than a long-term inability to grow correctly in the light. To test this idea, we grew wild-type (Col-0), *kai2-2,* and *smax1 smxl2* seedlings in the dark for 4 days (4dd), before tracking their development 2 days (4dd/2dl) and 4 days (4dd/4dl) after the transition to the light (figure 4.7). In wild-type, we observe an etiolation of the hypocotyl in the darkness and a rapid cessation of elongation after transfer to light at 4dd 2dl, followed by a slight hypocotyl growth as well as the development of adventitious and lateral roots by 4dd 4dl (figure 4.7 A-C). Consistent with previous reports, we found *kai2* has a wild-type hypocotyl etiolation and no adventitious or lateral root proliferation when grown in darkness. However, after transfer to the light, *kai2* fails to correctly de-etiolate and instead maintains a noticeable hypocotyl growth until 4dd 4dl. In addition, the rapid and sustained proliferation of adventitious and lateral root in *kai2* at 2 and 4 days after transfer to the light is more pronounced than in wild-type. We also monitored *smax1 smxl2* development during this dark-light transition, and found that not only *s1s2* exhibit a reduced hypocotyl growth in the dark, but *s1s2* hypocotyls also over-respond to light exposure, in addition to failing to induce a correct adventitious and lateral root proliferation at 2 and 4dl (figure 4.7 A-C).

We showed KL signalling is a new important regulator of root hair development, and that *kai2* mutants fail to develop root hair (reduced RHD) and to maintain growth of pre-existing ones (reduced RHL) (figure 3.3 C-D). Interestingly, in a context of transition from skoto- to photomorphogenesis, we found the RH phenotypes of *kai2* can already be observed during the dark phase; and while transition from dark-to-light induces a strong RH proliferation in wild-type, *kai2* seedlings are unable to promote further RH development and growth in response to light perception (figure 4.7 D-E).

Furthermore, we have previously shown that SMAX1 and SMXL2 act in the regulation of the primary root development, although it is unlikely that KAI2-MAX2 complex is involved in the process given *kai2* and *max2* exhibit a wild-type PRL under standard and low phosphorus condition (Chapter 3 and Villaecija-Aguilar et al, 2019). As expected, when monitoring seedlings development during the dark-light transition, we found that *kai2* exhibits normal PRL during both skoto- (4dd) and photo-morphogenesis (4dl). This observation is further confirmed by the similar size of the root apical meristems of *kai2-2* and Col-0 seedlings before

(4dd) and after light-transition (3dl). By opposition, the shorter primary root of *smax1 smxl2* seedlings described in Chapter 3 and Villaecija-Aguilar et al, 2019 appears to result from a defect to correctly adapt after transition to light growth conditions (figure 4.7 F-G).

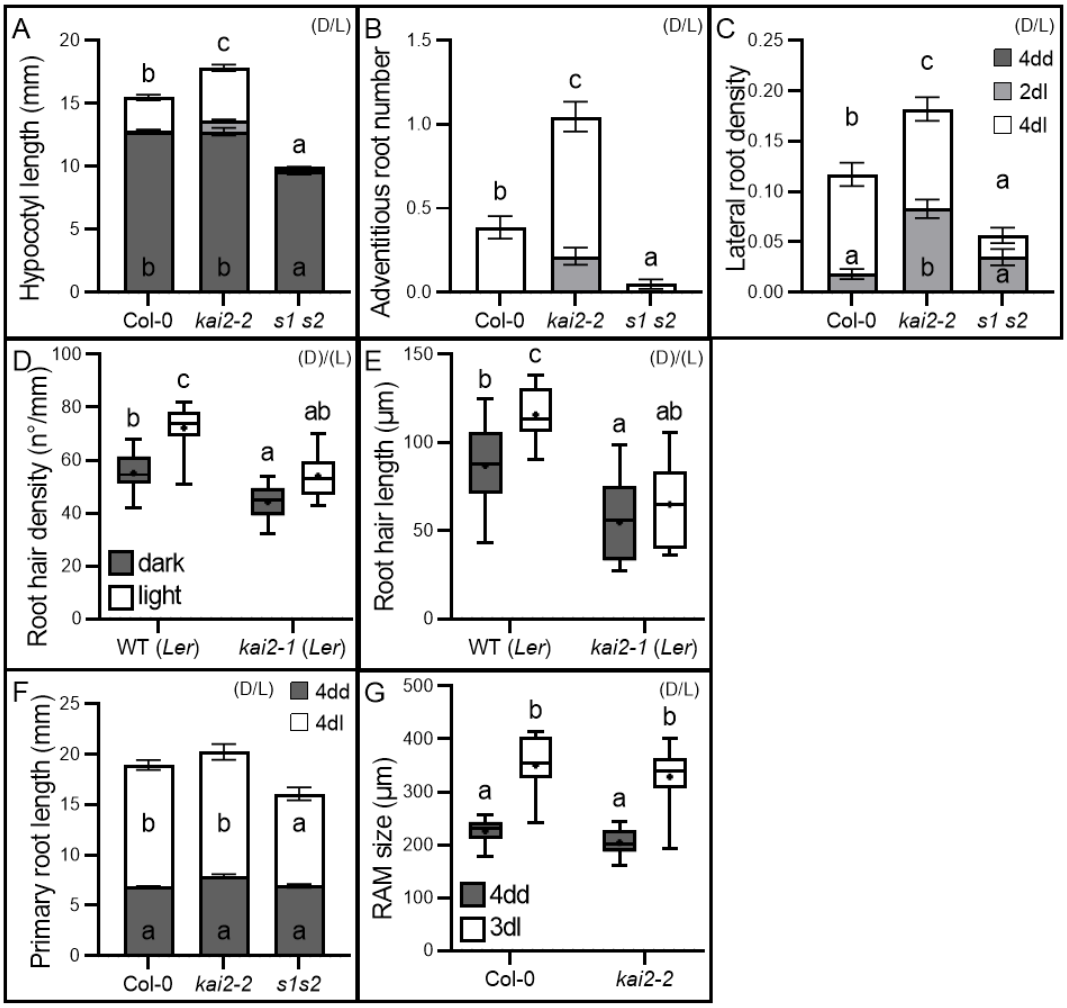

Figure 4-7 KAI2 mediates light induced remodelling of seedling development

(A-C) Hypocotyl length (A), adventitious root number (B), and lateral root density (C) in wild-type (Col-0), *kai2-2*, and *smax1-2 smxl2-1* (*s1s2*) seedlings at 4 days growth in the dark (4dd), and after subsequent transfer to normal light conditions for 2 and 4 days (2dl and 4dl). Data are from two independent replicates pooled together (n=43-91 seedlings per genotype and condition); a third independent replicate gave comparable results.

(D,E) Root hair density (C) and length (D) in 5-day old seedlings grown in the dark (dark), or in normal light conditions (light). Data correspond to one experimental replicate (n =8-10 seedlings per genotype and condition); a second independent experimental replicate gave comparable results. Experimental design and data collection were carried by José Antonio Villaécija-Aguilar as part of a collaborative work.

(F,G) Primary root length (F), and root apical meristem size (G) in wild-type (Col-0), *kai2-2*, and *smax1-2 smxl2-1* (*s1s2*) seedlings at 4 days growth in the dark (4dd), and after subsequent transfer to normal light conditions for 3 or 4 days (3dl and 4dl). (F) Data correspond to two independent experimental replicates pooled together (n =43-91 seedlings per genotype and condition); a third independent experimental replicate gave comparable results. (G) One experiment was performed (n=8-10 seedlings per genotype and time-point).
(D,E,G) The boxes in the box plot show the lower and upper quartiles and median values, mean is represented as (●), whiskers show minimal and maximal data values.
(A-G) Statistical groups indicated by letters were determined by one-way ANOVA with post hoc Tukey HSD (CI 95%), different letters indicate statistical differences between groups.
For all figure panels (D) indicates Arabidopsis plants were grown in continuous darkness, (L) indicates that plants were grown under a standard light regime (16 hours light, 8 hours dark), and (D/L) indicates that plants were grown in continuous darkness for a number of days before transfer to standard light conditions.

4.6 Results summary

- KL and Strigolactone signalling are required for the correct developmental adaption in response to low phosphorus availability. KL modulates root hair and lateral root proliferation, while D14 mainly acts on controlling the adaptive response of the primary root.
- Mutants affected in KL signalling (*kai2*, *smax1 smxl2*) share a range of phenotypic traits and atypical adaptive responses associated with defect in auxin biosynthesis/response, including abnormal response to sugar supplementation, defective gravitropic response, incorrect hypocotyl etiolation and apical hook formation, but also abnormal root hair, adventitious, and lateral roots proliferation.
- KAI2 is required for the correct photomorphogenic remodelling of seedling growth.

Chapter 5 KAI2 regulates remodelling of auxin transport at the dark-light transition

5.1 Aims

The recent advances in “strigolactone-like” signalling led to increased amount of evidence pointing to a link between auxin signalling and not only SL signalling, but also KL signalling.

First, seedlings treated with exogenous IAA exhibit elongated hypocotyl, epinastic cotyledons, altered hook formation, exfoliation of the hypocotyl, adventitious root formation from the hypocotyl, secondary root hair and lateral root proliferation; similar phenotypes are hereby presented in *kai2* and *max2* mutants, and have previously been reported to be phenocopied in mutants with high auxin level such as *superroot* (Boerjan et al., 1995, Bak et al., 2001) or in lines overexpressing YUCCA/TAA enzymes (Mashiguchi et al., 2011)

Second, *max2* mutants show several auxin-related defects such as increased adventitious rooting (Rasmussen et al., 2012), altered root hair development and increased lateral root density (Kapulnik et al., 2011). The hypocotyl of *max2* mutants are disproportionately sensitive to the auxin transport inhibitor NPA (Shen et al., 2012), and the shoot branching phenotype of *max2* is related to increased stem auxin transport (Bennett et al., 2006). In this thesis, I reported that most of the phenotypic defects of *max2* mutants (excluding the shoot branching defect strictly SL-dependent) are shared by *kai2* mutants (chapter 3).

Third, strigolactone and auxins are intricately linked in feedback loops that underpin the regulation of shoot branching. Auxin up-regulates the expression of strigolactone biosynthetic genes in Arabidopsis, pea, and rice (Foo et al., 2005; Arite et al., 2007; Hayward et al., 2009). And indeed the regulation of shoot branching by D14-MAX2-SMXL678 module relies at least partially on the SL-dependent repression of the main polar auxin transport stream from axillary buds via a rapid removal of the PIN1 auxin efflux proteins from the basal membrane of xylem parenchymal cells (Crawford et al, 2010; Shinohara et al, 2013; Soundappan et al, 2015; Bennett et al, 2016a, Seale et al, 2017).

Fourth, both *kai2* and *max2* mutants show elevated levels of IAA1 expression (Hayward et al., 2009; Nelson et al., 2011; Waters et al., 2012), consistent with increased auxin levels and/or signalling (Park et al., 2002; Yang et al., 2004), and, Bursch et al., 2021 recently reported a list of high-confidence KAR response genes containing a number of auxin-responsive genes that are downregulated in *smax1 smxl2* but upregulated in *kai2* and *max2* mutants.

Finally, the KL pathway is very similar to, and indeed overlapping with the strigolactone signalling pathway, although the KAI2 signalling pathway appears to be more ancient, with strigolactone signalling only arising in seed plants (Bythell-Douglas et al, 2017, Walker et al, 2019). Both D14 and KAI2 act through the SCF^{MAX2} ubiquitin ligase complex to recruit and induce ubiquitination and proteolysis of SUPPRESSOR OF MAX2-LIKE (SMXL) proteins; D14 primarily promotes degradation of SMXL6, SMXL7 and SMXL8, although SMXL2 can also be targeted (Soundappan et al, 2015, Liang et al, 2016, Wang et al, 2020b), while KAI2 primarily promotes degradation of SMAX1 and SMXL2 (Khosla et al, 2020, Wang et al, 2020b). Given the close relation between the two pathways, it is generally agreed that they must have some shared generic downstream functions and highly likely to operate through similar downstream mechanisms - although they certainly seem to influence transcriptional responses, SMXL proteins are not transcription factors themselves, and they may influence different responses through different adapter proteins (Soundappan et al, 2015, Wang et al, 2015, Song et al, 2017, Machin et al, 2020, Wang et al, 2020a).

Given the aforementioned points, the converging and central role of auxin and KL signalling in seedling photomorphogenesis, and the ability of the closely related D14-mediated strigolactone signalling pathway to regulate auxin distribution by re-modelling auxin transport in the shoot, I hypothesised that KAI2 signalling regulates seedling development by modulating auxin transport. In this study, I took advantage of the inability of *kai2* mutant to correctly pattern its photomorphogenic development, and the possibility to induce rapid developmental changes relying on the remodelling of the auxin homoeostasis at the transition from skoto- to photomorphogenesis to address this hypothesis.

4.7 KAI2 modulates auxin distribution in the seedling

Given the prominent role of auxin in hypocotyl elongation and root growth (Jensen et al, 1998, Lavenus et al, 2013), and its known roles downstream of light perception (Casal et al, 2013, Fankhauser & Christie, 2015), I hypothesized that the *kai2* phenotype might arise due to perturbations in auxin homeostasis. To test this idea, we first investigated whether the *kai2* phenotypes might be caused by increased auxin content in *kai2* mutants, by directly measuring auxin levels (carried by our collaborator Karin Ljung from Umeå Plant Science, Sweden) (figure 5.1). In seedlings dark-grown for 4 days, auxin levels in *kai2* and wild-type are identical (figure 5.1 A), but in 4dd/1dl seedlings, auxin levels in *kai2* seedlings were reproducibly higher than in wild-type (figure 5.1 B). These data could consequently be consistent with increased auxin abundance causing the *kai2* phenotype. Interestingly, however, this increase was larger in the hypocotyl/root compartment compared to the shoot apex (figure 5.1 B). It is also notable that in the roots of 5-day old light-grown (5dl) seedlings, auxin levels were similarly increased in *kai2* mutants relative to wild-type, but so were levels in the *d14-1* SL receptor mutant, which does not have the same hypocotyl and root phenotypes as *kai2-2* (figure 5.1 C) (Villaecija-Aguilar et al, 2019). Conversely, the *s1s2 (smax1-2 smxl2-1)* and *smxl6-4 smxl7-3 smxl8-1* (*s678*) triple mutant (which lacks the proteolytic targets of D14 activity) have the same auxin levels as wild-type, but have dramatic root phenotypes not present in wild-type (Villaecija-Aguilar et al, 2019). Thus, changes in auxin abundance alone are unable to explain the specific phenotypes observed in *kai2* and *smax1 smxl2* mutants.

Following the hypothesis of an abnormal partitioning of auxin in de-etiolated and light grown *kai2* seedlings, I examined the expression of the *DR5v2pro:GFP* auxin reporter in various tissues along the seedlings axis (figure 5.2 I). I found that auxin response is increased in the hypocotyl (figure 5.2 A-B), adventitious root primordia (figure 5.2 C-D) and proliferating lateral roots in *kai2* compared to wild-type (figure 5.2 E-F), consistent with the idea that auxin response is perturbed in *kai2* mutant. Surprisingly, however, I observed a greatly reduced auxin response in the root apical meristem (RAM) region of *kai2* seedlings grown under standard conditions (figure 5.2 G-H). Overall, these data show a perturbation of the auxin response along the *kai2* seedling axis, with increased auxin response in the hypocotyl and older root tissues, and strongly reduced auxin response in the RAM, thus consistent with my hypothesis of an abnormal partitioning of auxin distribution.

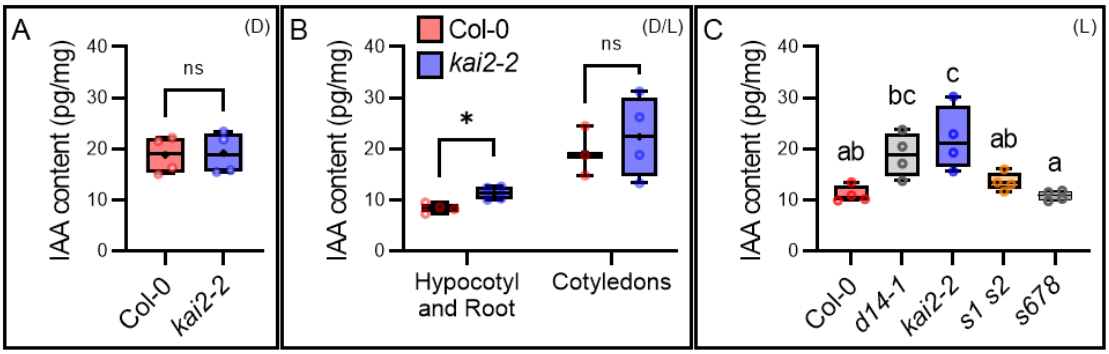

Figure 5-1 Auxin is abnormally partitioned in kai2 seedlings
(A-C) IAA quantification (pg IAA per mg of tissue, pg/mg) in whole seedlings grown for 4 days in the dark (A), or roots grown 5 days under normal light conditions (B), or in cotyledons and hypocotyl/root sections of seedlings grown for 4 days in the dark and subsequently transferred to normal light conditions for 1 day. (C). (n=3-4 pools of 30 seedlings). (A-B) * (p-value ≤ 0.05) indicates differences compared to wild-type (Welch's t-test). ns = no significant difference. (C) Statistical groups indicated by letters were determined by one-way ANOVA with post hoc Tukey HSD (CI 95%).
For figure panels (D) indicates Arabidopsis plants were grown in continuous darkness, (L) indicates that plants were grown under a standard light regime (16 hours light, 8 hours dark), and (D/L) indicates that plants were grown in continuous darkness for a number of days before transfer to standard light conditions.

Figure 5-2 KAI2 modulates auxin response patterning in the seedling
(A-G) Auxin response (average DR5v2:GFP fluorescence intensity) in various Col-0 and kai2 seedlings seedling tissues.
(A, C, E, G) show GFP quantification in the hypocotyl (A) the adventitious root primordia (C), the lateral roots (E), and the root meristem zone (G). (B, D, F, H) show the show representative microscopy images of the tissues (in same order a above mentioned) with bright field (grey) and GFP signals represented in false colour with dark blue as low signal intensity and bright white as high signal intensity. Scale bars represent 50 µm.
For (A) Data correspond to the average GFP intensity of 10 seedlings per genotype, where each sample was the average of 10 nuclei per hypocotyl, from one experimental replicate; a second independent experimental replicate gave comparable results. (C) Data correspond to the average GFP intensity of 7-8 adventitious root primordia of similar stage (from 4-5 seedlings per genotype), and each sample was the average of 10 nuclei, from one experimental replicate; a second independent experimental replicate gave comparable results. (E) Data correspond to the average GFP intensity in 8-10 lateral root primordia of similar stage, and 8-10 emerged lateral roots of similar stage, taken from 5 seedlings per genotype, where each sample is the average of 5 nuclei, from one experimental replicate; two other independent experimental replicates gave comparable results. (G) Data correspond to three independent experimental replicates pooled together (n = 37-44 seedlings per genotype). *, ***, **** (p-value ≤ 0.05, 0.001, 0.0001) indicates differences compared to wild-type (Welch's t-test). The boxes in the box plot show the lower and upper quartiles and median values, mean is represented as (●), whiskers show minimal and maximal data values. For figure panels (A, C), (D/L) indicates that plants were grown in continuous darkness for 4 days before transfer to standard light conditions for another 4 days. For panels (E-G), (L) indicates that plants were grown for 6 days under a standard light regime (16 hours light, 8 hours dark).
(I) Representative image of location of the different tissues analysed.

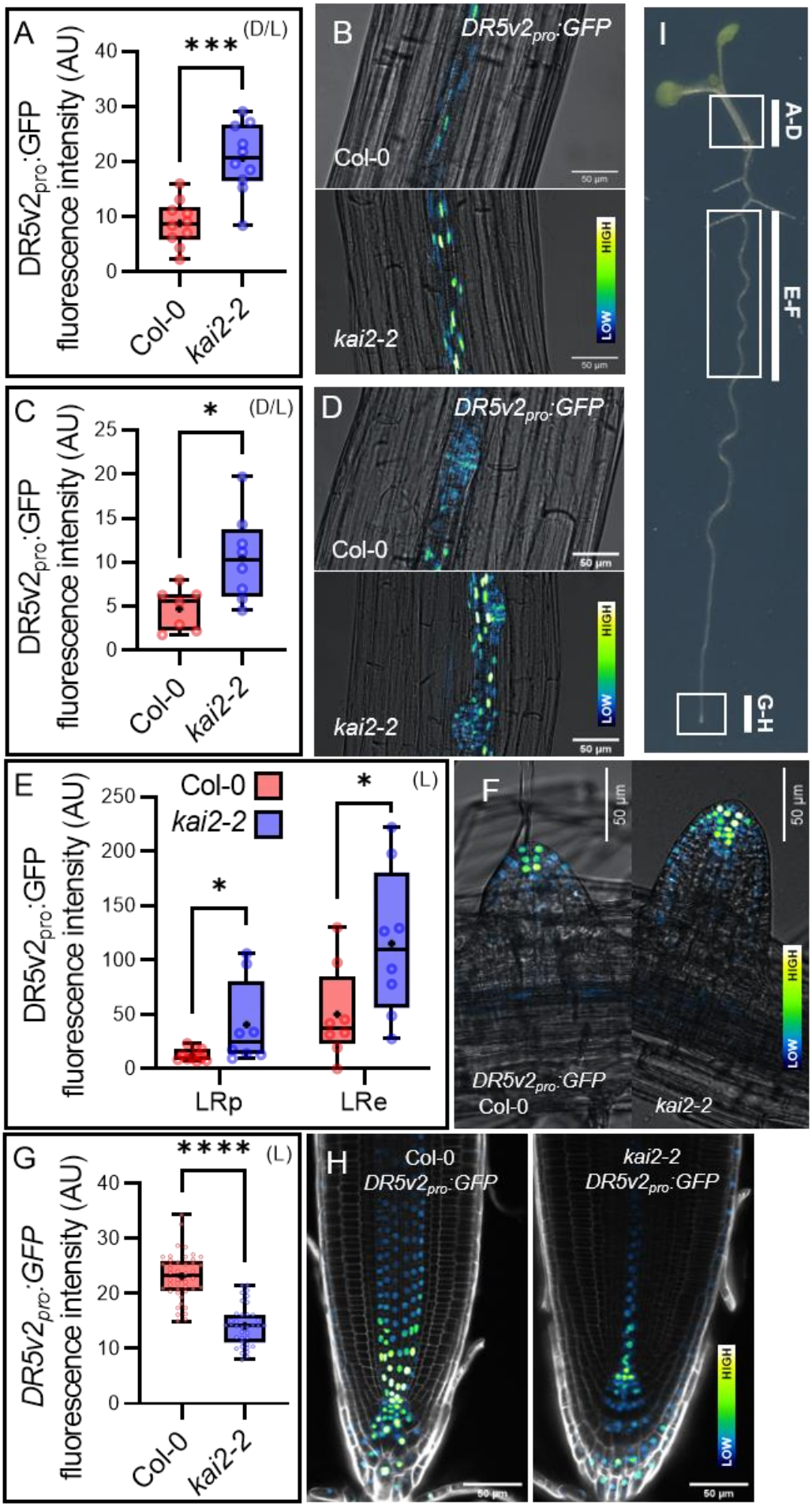
A
DR5v2pro:GFP fluorescence intensity (AU)
***
(D/L)
Col-0
kai2-2
B
DR5v2pro:GFP
Col-0
kai2-2
HIGH
LOW
50 µm
C
DR5v2pro:GFP fluorescence intensity (AU)
*
(D/L)
Col-0
kai2-2
D
DR5v2pro:GFP
Col-0
kai2-2
HIGH
LOW
50 µm
I
A-D
E-F
G-H
E
DR5v2pro:GFP fluorescence intensity (AU)
Col-0
kai2-2
*
*
(L)
LRp
LRe
F
50 µm
DR5v2pro:GFP
Col-0
kai2-2
HIGH
LOW
G
DR5v2pro:GFP fluorescence intensity (AU)
****
(L)
Col-0
kai2-2
H
Col-0
DR5v2pro:GFP
kai2-2
DR5v2pro:GFP
HIGH
LOW
50 µm

4.8 KAI2 regulates rootward auxin flux

Given the global increased auxin content in the root tissues of *kai2*, but the contrasted partitioning of the auxin response (increase DR5v2 signal in the older root tissues and strongly decreased DR5v2 signal in the RAM) I reasoned that the effects of KAI2 on seedling development might relate more to altered auxin distribution rather than increased auxin levels *per se*. Specifically, I hypothesized that failure to downregulate auxin transport from the cotyledons towards the root might account for all *kai2* seedling phenotypes described above (Chapter 3 and Chapter 4). To test this idea, I used microsurgical approaches to de-capitate wild-type and *kai2-2* seedlings at 4dd by removing the seedling apex, and then assessed their phenotype at 4dd/3dl. Removal of the cotyledons was sufficient to restore the *kai2* hypocotyl, adventitious root, and lateral root phenotypes to wild-type level (figure 5.3.3 A-E), consistent with apically-derived auxin driving these effects. These observations are further supported by the de-rooting assay which strongly amplified the *kai2* adventitious root phenotype but had no effect on *smax1 smxl2* seedlings and induced little AR proliferation in Col-0 (figure 4.6 E-F).

To further test whether *kai2* may be affected in rootward auxin transport, IAA transport was examined directly in wild type, *kai2* and *max2* mutants using radiolabelled [3H]IAA (figure 5.3 F). Consistent with a role of KAI2 signalling in promoting rootward auxin transport, [3H]IAA transport is greatly reduced in *kai2* and *max2* mutant roots compared to wild-type. Interestingly, inhibiting polar auxin transport with 1-N-naphthylphthalamic acid (NPA) strongly blocked rootward IAA transport toward the root meristem of Col-0, while *kai2* and *max2* mutants displays a hyposensitivity to this treatment (figure 5.3 F). These observations confirm that KAI2 signalling is required for correct rootward auxin flux in the seedling, and suggest that KAI2 signalling might modulate this mechanism through an action on PIN proteins auxin efflux transporters.

Taken together, our data are thus consistent with increased auxin transport and accumulation in the hypocotyls of *kai2*. As a consequence, the phenotype of *kai2* appears to be associated with increased auxin abundance, increased rootward auxin flux, and disruption of the PIN-dependent polar auxin transport system, similar to the mechanisms causing shoot branching phenotypes of strigolactone mutants (Bennett et al, 2006, Shinohara at el, 2013, Bennett et al, 2016a).

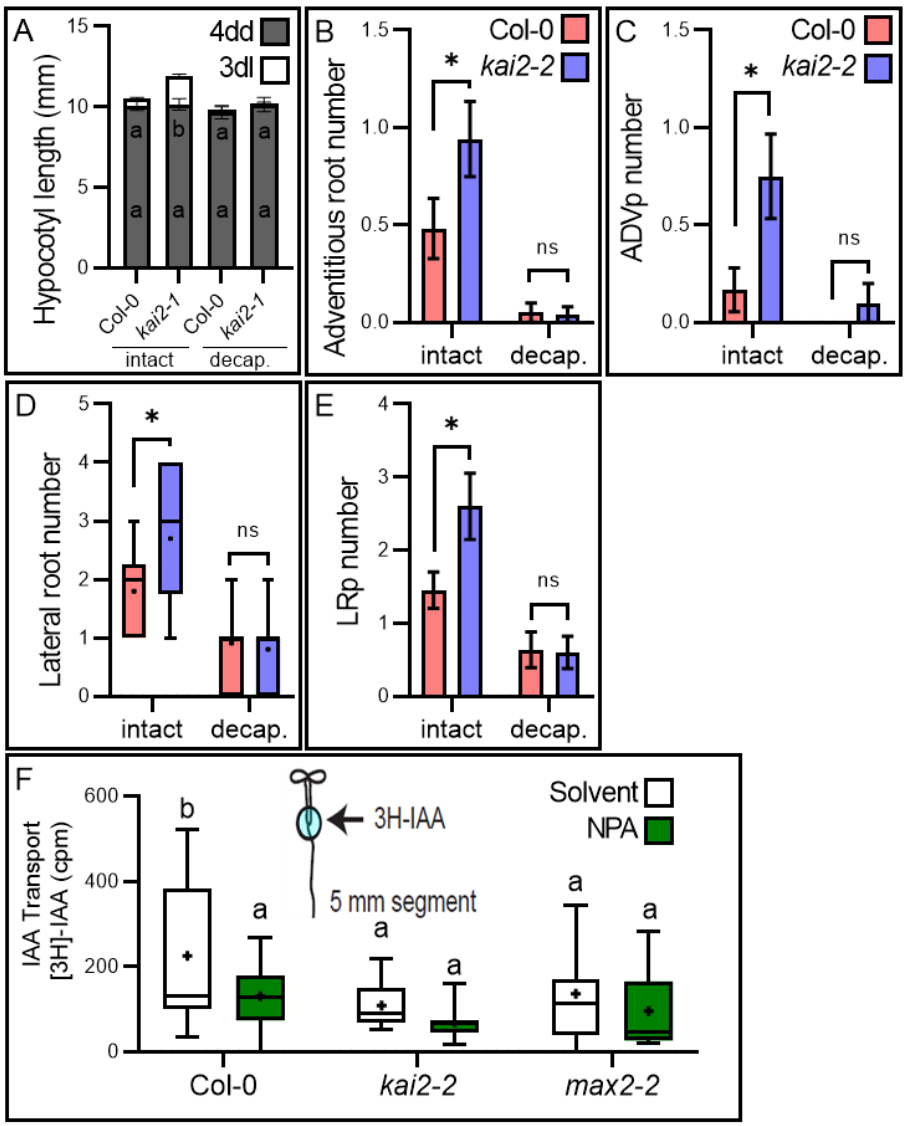

Figure 5-3 KAI2 regulates rootward auxin transport

(A) Measurement of hypocotyl length in Col-0 and *kai2-1* seedlings grown for 4 days in the dark (4dd) before subsequently undergoing apex decapitation or left intact prior to transfer to normal light conditions for 3 days (3dl). Stacked bars indicate length before treatment after 4dd (grey) and additional growth in the light after treatment (3dl, white). Data correspond to one experimental replicate (n=12-14 seedlings per genotype); a second independent experimental replicate gave comparable results. Statistical groups indicated by letters were determined by one-way ANOVA with post hoc Tukey HSD (CI 95%).

(B-E) Measurement adventitious root number (B), lateral root number (C), Adventitious root primordia (D) and lateral root primordia (E) of seedlings grown for 4 days in the dark and subsequently undergoing apex decapitation or left intact prior to transfer to normal light conditions for 3 days. Data correspond to one experimental replicate (for (B) n=20-32 seedlings per genotype, for (C) n=10-11 seedlings per genotype), a second independent experimental replicate gave comparable results. For (D-E), data correspond to one experimental replicate (n = 10-12 seedlings per genotype and treatment); a second independent experimental replicate gave comparable results. * (p-value ≤ 0.05) indicates differences compared to wild-type (Welch's t-test). ns = no significant difference. Error bars represent ± s.e.m.

(F) Basipetal [3H]IAA auxin transport in 5-day old seedlings. Arrow indicates the site of [3H]IAA or solvent application at the shoot-root junction, radioactivity was measured in a 5 mm segment at the primary root meristem. Data correspond to one experimental replicate (n = 10-13 seedlings per genotype and treatment), a second independent experimental replicate gave comparable results. Statistical groups indicated by letters were determined by one-way ANOVA with post hoc Tukey HSD (CI 95%).
(A, B, C, E) Error bars represent ± s.e.m. (D, F). The boxes in the box plot show the lower and upper quartiles and median values, mean is represented as (●), whiskers show minimal and maximal data values

4.9 PIN-mediated auxin transport system is altered in kai2

Given the apparent failure of *kai2* seedlings to correctly distribute auxin along the seedling axis, and the hyposensitivity to NPA observed in *kai2* and *max2* roots, we postulated that the reduced auxin transport of *kai2* might be caused by decreased abundance of members of the PIN family of auxin efflux carriers in the roots, which play major roles in mediating directional auxin transport (Adamowski & Friml, 2015), and have been implicated in the phenotypic effects of strigolactone signalling (Bennett et al, 2006; Shinohara et al, 2013, Bennett et al, 2016a, Zhang et al, 2020). To test this hypothesis I examined the abundance of PIN proteins in wild-type and *kai2* along the root system (figure 5.4 and 5.5). I found in young *kai2-2* seedlings grown under standard conditions a significant increase of PIN7 in older root tissues, including the shoot-root junction (SRJ) and the old differentiation zone (ODZ), but also in “young” tissues such as the meristematic zone (MZ) when compared to wild-type (figure 5.4 A-B and figure 5.4 H). This observation suggests KAI2 could be involved in promoting the rootward auxin transport toward the root tip, although the increased abundance of PIN7 is mainly observed in the older root tissues surrounding the area of lateral root initiation and emergence (figure 5.4 A, B, H). However, this hypothesis is contradicted by the decreased rootward auxin transport we observed (figure 5.3 F), and by the fact that *kai2* seedlings do not exhibit a shorter primary root and/or increased root hair proliferation, as it would be expected from seedlings with increased auxin content at the MZ. On the contrary *kai2* has normal PRL and much reduced RH proliferation (Chapter 3). Secondly, our observations rather show a decreased DR5v2 response in the meristem of *kai2* compared to Col-0 (figure 5.3.2 G-H), indicating a decrease in auxin transport toward the meristem rather than an increase. This second observation is corroborated by the analysis of PIN1-GFP and PIN2-GFP abundance in the meristem zone (figure 5.4 C-G) where I observed strong reduction of overall PIN1-GFP abundance in the vasculature directly neighbouring the quiescent centre and the root apical meristem (RAM) of *kai2* seedlings (figure 5.4 C-D, G), consistent with the reduced

auxin transport to the root tip (figure 5.3 F). In addition *kai2* has a remarkable decrease of PIN2-GFP abundance at the apical plasma membrane (PM) of epidermal cell of the meristem/differentiation zone in *kai2* (figure 5.4 E-F, G). Thus, it appears the auxin transport system is differentially regulated along the root axis in a PIN- and tissues specific manner, with increased PIN7 in older root tissues and RAM, and reduced PIN1 and PIN2 abundance in the meristem zone.

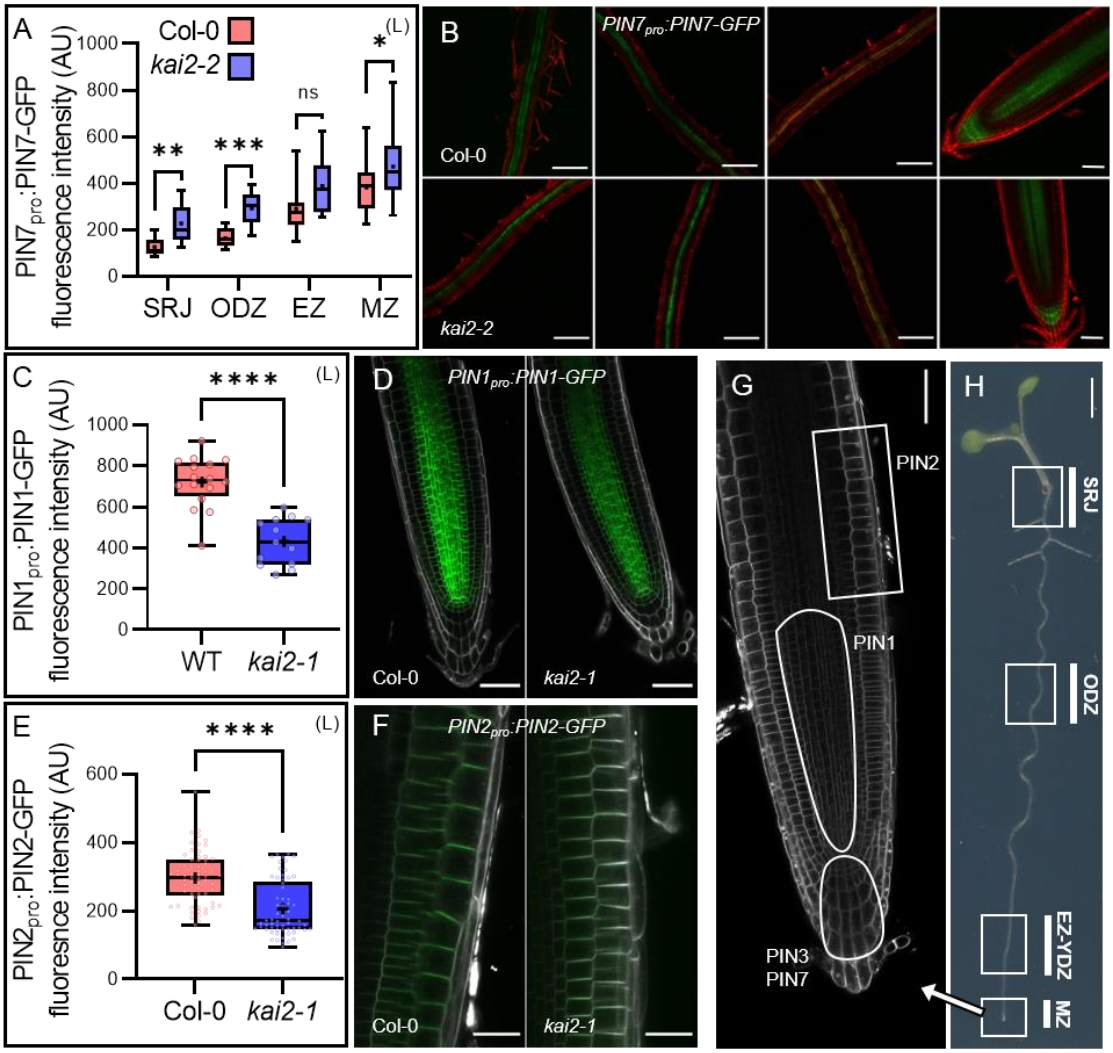

Figure 5-4 PIN-mediated auxin transport system is altered in *kai2*
For all figure panels (L) indicates that Arabidopsis plants were grown under a standard light regime (16 hours light, 8 hours dark).
(A-B) Quantification (A) and representative microscopy images (B) of PIN7-GFP signal in the shoot-root junction (SRJ), older differentiation zone (ODZ), junction of the elongation and young differentiation zone (EZ-YDZ), and meristem zone (MZ) of 6-day old wild-type and *kai2-2* seedlings grown under normal light conditions. Data correspond to one experimental replicate (n=8-18 seedlings per genotype); a second independent experimental replicate gave comparable results. *,**,*** (p-value ≤ 0.05, 0.01, 0.001) indicates differences compared to wild-type (Welch's t-test). ns = no significant difference. (B) Microscopy images overlay propidium iodide staining (red) and GFP-derived signal represented in green. Scale bars represent 50 µm.

(C-D) PIN1-GFP quantification (C) and representative microscopy images (C) in the meristem zone of 6-day old wild-type and *kai2-1* seedlings grown under normal light conditions. PIN1-GFP signal is measured in the stele from 70 µm to 150 µm from the root tip. PIN3-GFP, PIN7-GFP, and DR5v2:GFP signals are measured in the apical root meristem Data correspond to one experimental replicate (n=13-16 seedlings per genotype); two other independent experimental replicates gave comparable results. **** (p-value ≤ 0.0001) indicates differences compared to wild-type (Welch's t-test).
(E-F) PIN2-GFP quantification (E) and representative microscopy images (F) in the apical plasma membrane of epidermal cells in the meristematic zone of 4-day old wild-type and *kai2-1* seedlings grown under normal light conditions. PIN2-GFP signal is measured in the epidermis from 210 µm to 250 µm from the root tip. Data correspond to one experimental replicate (n = 61-65 plasma membranes from 5-6 seedlings of each genotype. **** (p-value ≤ 0.05, 0.01, 0.001, 0.0001) indicates differences compared to wild-type (Welch's t-test).
(G-H) Root tip regions (G) and seedling tissues (H) used for measurements in Figure 5.2, 5.3, 5.4, 5.5, 5.6, 5.8, 5.9, 5.10. Scale bar represents 50 µm. (H) Seedling tissues, shoot-root junction (SRJ), older differentiation zone (ODZ), junction of the elongation and young differentiation zone (EZ-YDZ), and meristem zone (MZ). Scale bar represents 10 mm.
(A,C,E) The boxes in the box plots show the lower and upper quartiles and median values, mean is represented as (●), whiskers show minimal and maximal data values. (D-F) Microscopy images overlay propidium iodide staining (grey) and GFP-derived signal represented in green. Scale bars represent 50 and 20 µm respectively.

Given the nature of the PAT which relies heavily on the polarity of the PIN proteins to ensure appropriate directional stream of auxin, I investigated further these findings by testing either the local difference of PIN proteins abundance between *kai2* and Col-0 was due to a global change of PIN abundance at the cell and tissue levels, or if there were changes at the sub-cellular level. To test this I measured PIN1-GFP abundance either at the basal PM or internalized in the rest of the cellular compartments in the stele cells (figure 5.5 A-C, figure 5.4 G). Interestingly, I found the strong decrease of PIN1 observed in *kai2* MZ (figure 5.4 C-D) is the result of a local decreased PIN1 polarization at the basal plasma membrane rather than a change in the global abundance in the cell (figure 5.5 A-C). Thus, indicating that the mediation of PIN1 abundance by KAI2 could be the result of local PM-localised increase of PIN rather than a global change in the protein abundance in the cell, consistent with the idea that KL signalling mediates PIN polarization. This idea is further confirmed by the measure of plasma membrane localised PIN3 and PIN7 abundance in the root apical meristem. For PIN3, I found no difference in abundance between *kai2* and wild-type seedlings (figure 5.5 D-E), consistent with no global change in PIN3 abundance in the root meristem (data not shown). Whereas for PIN7, I found that the difference reported

in (figure 5.4 A-B) is likely due to increased PIN7 at the plasma membrane in *kai2* seedlings (figure 5.5 F-G).

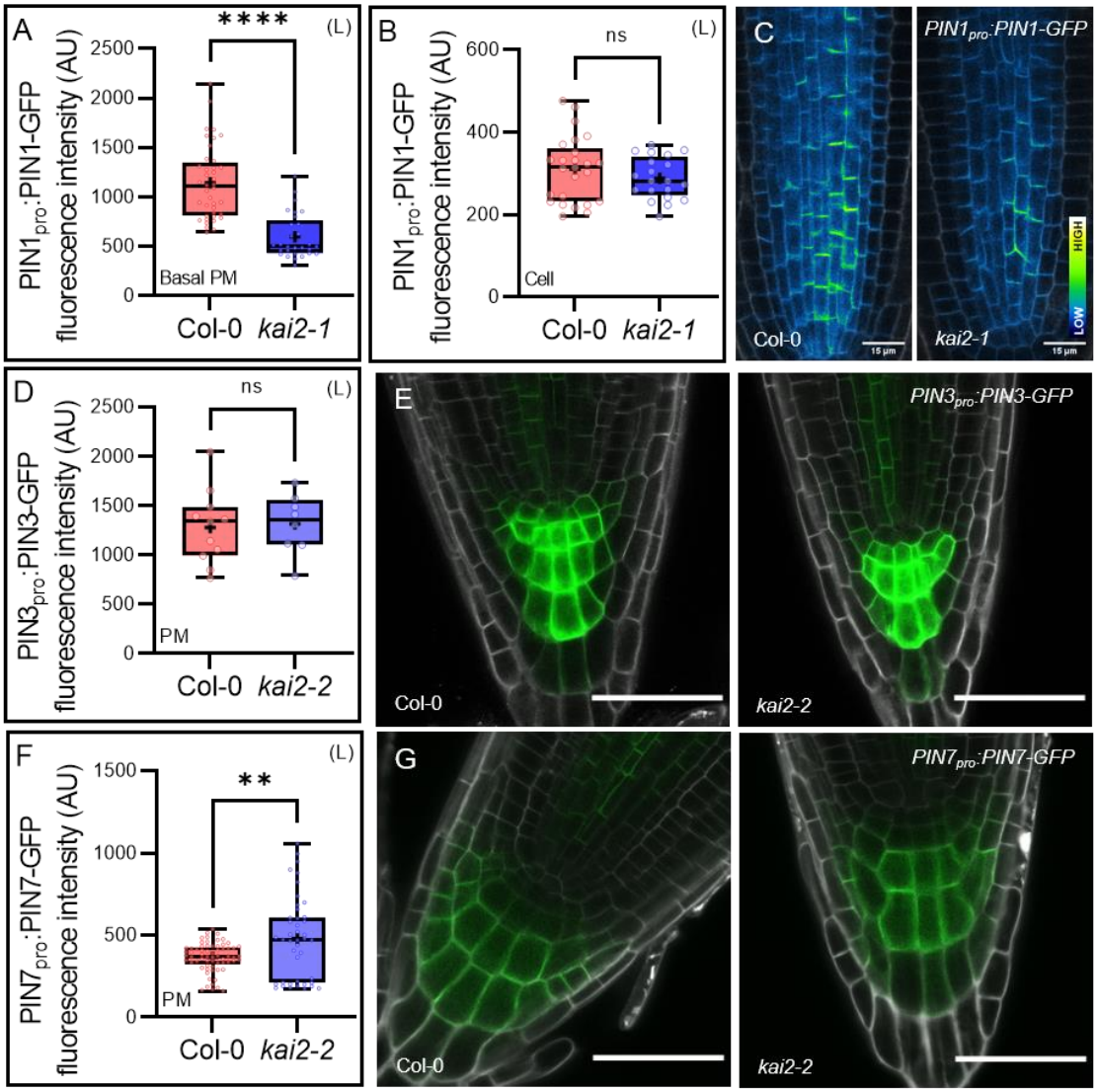

Figure 5-5 KAI2 regulates the PM localization of certain PIN proteins
For all figure panels (L) indicates that Arabidopsis plants were grown under a standard light regime (16 hours light, 8 hours dark).
(A-C) Quantification of PIN1-GFP signal at the basal plasma membrane (A) and in the rest of the cell (B) in the meristem zone of 6-day old wild-type and *kai2-1* seedlings grown under normal light conditions. Data correspond to one experimental replicate. (n = 20-40 PM/cell from 5-6 seedlings of each genotype; a second independent experimental replicate gave comparable results. *,**,**** (p-value ≤ 0.0001) indicates differences compared to wild-type (Welch's t-test). ns = no significant difference. (C) Representative microscopy images of (A-B) overlay propidium iodide staining (red) and GFP-derived signal represented in false colour with dark blue as low signal intensity and bright white as high signal intensity. Scale bars represent 15 µm.

(D-E) PIN3-GFP quantification at the plasma membrane (D) and representative microscopy images (E) in the meristem zone of 6-day old wild-type and *kai2-2* seedlings grown under normal light conditions. Data correspond to one experimental replicate (n=7-10 seedlings per genotype); a second independent experimental replicates gave comparable results. ns = no significant difference. (Welch's t-test). (E) Microscopy images overlay propidium iodide staining (grey) and GFP-derived signal represented in green. Scale bars represent 50 µm.
(F-G) PIN7-GFP quantification at the plasma membrane (F) and representative microscopy images (G) in meristematic zone of 4-day old wild-type and *kai2-2* seedlings grown under normal light conditions. Data correspond to one experimental replicate. n = 43-65 plasma membranes from 5-6 seedlings of each genotype. ** (p-value ≤ 0.01) indicates differences compared to wild-type (Welch's t-test). (G) Microscopy images overlay propidium iodide staining (grey) and GFP-derived signal represented in green. Scale bars represent 50 µm.
(A,B,D,F) The boxes in the box plots show the lower and upper quartiles and median values, mean is represented as (●), whiskers show minimal and maximal data values.

Given KAI2 acts as a negative regulator of lateral and adventitious roots development, I also investigated if either of these phenotypes of *kai2* could result from differences in PIN proteins abundance in the LR and AR primordia initiation sites. To test this I measured plasma membrane localised PIN3 and/or PIN1 abundance in lateral root and adventitious root primordia (figure 5.6) (PIN2, PIN4, and PIN7 being not easily detectable in these tissues during the early developmental stages). Interestingly, in the LRp I found no difference for PIN1 between *kai2* and wild-type (figure 5.6 A-B), however the abundance of PIN3 protein laterally localized to the inner plasma membrane in the pericycle cells was significantly greater in *kai2* lateral root primordia compared to Col-0 (figure 5.6 C-D). By opposition, no PIN3-GFP could be detected in the adventitious root primordia, while PIN1 was detectable and significantly more abundant at the plasma membrane in *kai2* primordia compared to wild-type (figure 5.6 E-F). Together, these data indicate a role of KAI2 in ensuring the correct PIN protein patterning and accumulation at the plasma membrane in various tissues along the root axis. Therefore, the abnormal control of the PIN proteins abundance observed in *kai2* mutant likely accounts for some of the phenotypes observed in its roots.

For instance, PIN3 abundance at the lateral PM of pericycle cells has previously been reported to be critical to allow formation of local auxin maxima in the pericycle and endodermis and induces the initiation of new lateral root primordia (Péret et al., 2013, Marhavy et al., 2013). It is therefore likely that in *kai2* mutant the increased abundance of laterally localized PIN3 at the plasma membrane

promotes the formation of auxin maxima, driving the initiation and/or development of new lateral root primordia.

Similarly, PIN1 is observed at very early stages on AR primordia and remained in the primordia and emerged tissues afterwards, while PIN3 is observed at a later stage of primordia development and emerged adventitious root, and PIN7-GFP is hardly detectable in adventitious root primordia tissues (Omelyanchuk et al., 2016, da Costa et al., 2018). In addition, PIN1 is critical for the auxin-dependent AR emergence in rice, and Arabidopsis *pin1* mutant exhibits a significant reductions in AR formation (Xu et al., 2005), indicating that PIN1 proteins mediate AR formation by ensuring auxin efflux toward the site of initiation and development of new adventitious roots. It is therefore likely that in *kai2* mutant the high abundance of PIN1 increases auxin transport and IAA accumulation, driving the increased initiation and/or development of ARs in the hypocotyl (figure 5.6 E-F).

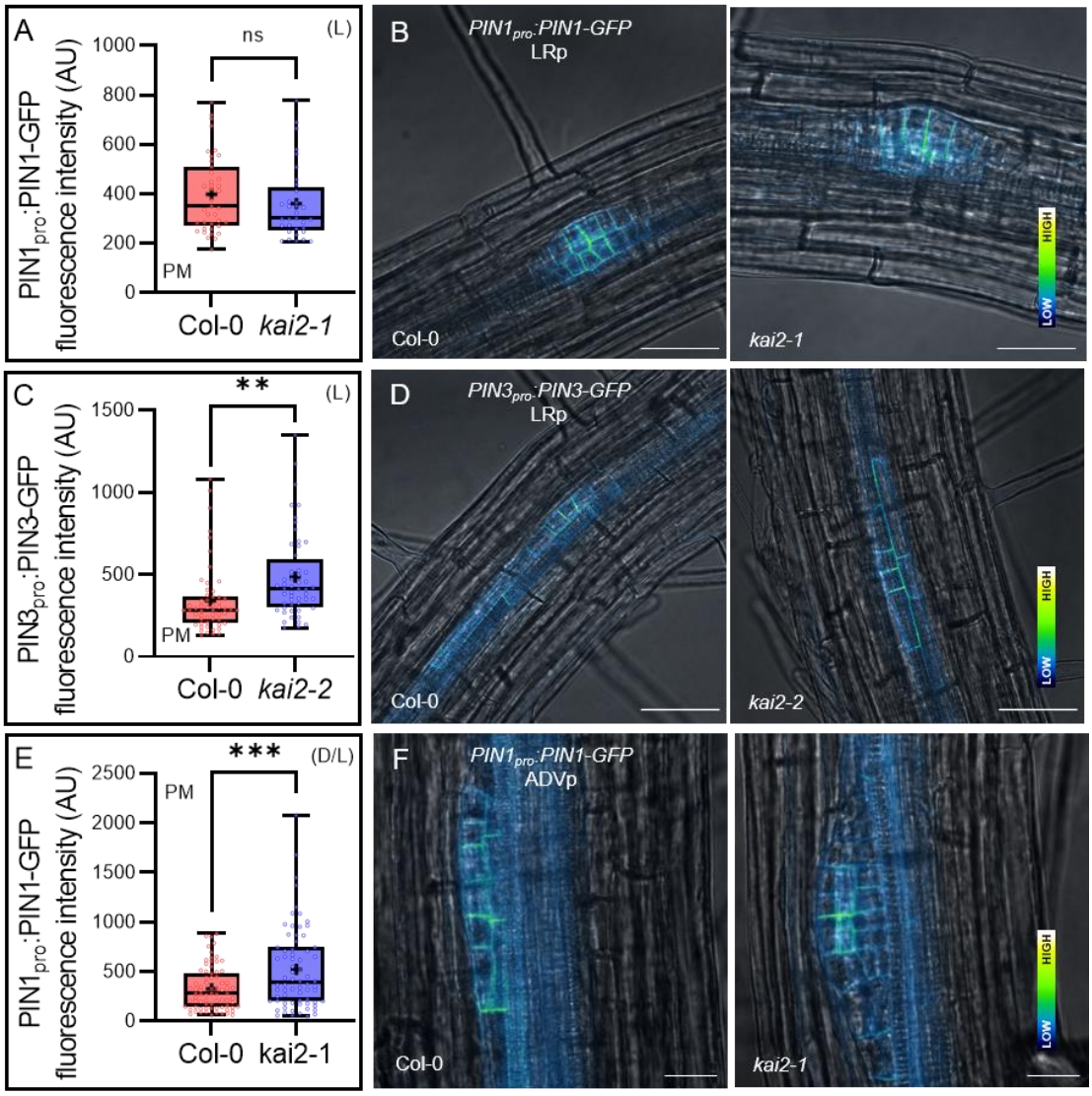

Figure 5-6 KAI2 regulates the PM localization of certain PIN proteins

For all figure panels (L) indicates that Arabidopsis plants were grown under a standard light regime (16 hours light, 8 hours dark).
(A-C) Quantification of PIN1-GFP signal at the plasma membrane (A) and in the rest of the cell (B) in the meristem zone of 6-day old wild-type and *kai2-1* seedlings grown under normal light conditions. Data correspond to one experimental replicate. (n = 20-40 PM from 5-6 seedlings of each genotype; a second independent experimental replicate gave comparable results. *,**,**** (p-value ≤ 0.0001) indicates differences compared to wild-type (Welch's t-test). ns = no significant difference. (C) Representative microscopy images of (A-B) overlay propidium iodide staining (red) and GFP-derived signal represented in false colour with dark blue as low signal intensity and bright white as high signal intensity. Scale bars represent 15 µm.
(D-E) PIN3-GFP quantification at the plasma membrane (D) and representative microscopy images (E) in the meristem zone of 6-day old wild-type and *kai2-2* seedlings grown under normal light conditions. Data correspond to one experimental replicate (n=7-10 seedlings per genotype); a second independent experimental replicates gave comparable results. ns = no significant difference. (Welch's t-test). (E) Microscopy images overlay propidium iodide staining (grey) and GFP-derived signal represented in green. Scale bars represent 50 µm.
(F-G) PIN7-GFP quantification at the plasma membrane (F) and representative microscopy images (G) in meristematic zone of 4-day old wild-type and *kai2-2* seedlings grown under normal light conditions. Data correspond to one experimental replicate. n = 43-65 plasma membranes from 5-6 seedlings of each genotype. ** (p-value ≤ 0.01) indicates differences compared to wild-type (Welch's t-test). (G) Microscopy images overlay propidium iodide staining (grey) and GFP-derived signal represented in green. Scale bars represent 50 µm.
(A,B,D,F) The boxes in the box plots show the lower and upper quartiles and median values, mean is represented as (●), whiskers show minimal and maximal data values.

4.10 Auxin transport system in the seedling is remodelled at the dark-light transition

The phenotypes of *kai2* mutants are more pronounced in seedlings exposed to light after dark acclimation (figure 4.7), and in the roots of young seedlings (Chapter 3 and Villaecija-Aguilar et al, 2019). That being the case, I hypothesised these phenotypes are the result of a differential organisation of the PIN protein system, as can be observed in light-grown *kai2* seedlings. More precisely, because the transition from skoto- to photomorphogenesis is characterized by a rapid remodelling of the seedling developmental program (figure 4.7), we hypothesised that *kai2* phenotypes arise because the seedlings are enable to undergo a rapid switch to this developmental program because of a delayed remodelling of the PIN system. These would lead to an impaired inhibition of hypocotyl elongation, stagnant PIN in the old root tissues and delay in the activation of the auxin redirection toward the root tip in *kai2*. To test this hypothesis, I designed experiments where all seedlings undergo a

skotomorphogenic, etiolated state for four days in the dark (4dd), followed by a dark-to-light transition to a photomorphogenic stage during which they de-etiolate for another one to three days (1dl/3dl) under normal long-day light conditions.

First, I assessed if the dark-light transition resulted in changes in PIN abundance along the seedlings of WT, consistent with previous report that transfer of seedlings from light to dark induces rapid change in PIN1 and PIN2 abundance in the meristem zone (Laxmi et al., 2008). We found that in the dark PIN3 was very abundant in the hypocotyl, and that transfer to light induces a turnover by 3dl (figure 5.7 A). Consistent with observation from Friml et al. of high PIN3::GUS signal in 3-day-old etiolated hypocotyl, and observations from Ding et al., of a gradual decrease in PM localized PIN3-GFP in hypocotyl of 4-day-old etiolated seedlings undergoing illumination from all sides with white light (10 $\mu mol.m^{-2}.s^{-1}$) for 4 to 12 hours (Friml et al., 2002b, Ding et al., 2011). PIN4 and PIN7 were also observable in the hypocotyl in dark etiolated seedlings (4dd), and their abundance greatly decreased after transfer to light (4dd/3dl) (figure 5.7 A).

I also investigated these changes in the roots of wild-type seedlings (figure 5.7 B-I). I measured a sustained increase of PIN1 abundance in the vasculature tissues above the root tip between 4dd and 3dl (figure 5.7 B-C), consistent with the findings from Laxmi et al., 2008. Similarly, PIN2 accumulation at the PM of the epidermal cells in the elongation zone is induced by exposure to light (figure 5.7 D-E), consistent with previous report from Sassi et al., 2012. By opposition, PIN3 and PIN7 are abundant along the whole root length at 4dd (figure 5.7 F-I). However, in the older root tissues (SRJ, ODZ) their abundance decreased after dark-light transition (4dd/1dl), while in the elongation and meristem zone their abundance is maintained or slightly increases (figure 5.7 F-I).Thus, exposure to light after a period of etiolation in the dark causes a major re-organization of the seedling auxin transport network. Expression of the PIN genes, as assessed by qRT-PCR, reflects these changes in PIN abundance, with PIN3, PIN4 and PIN7 all downregulated and PIN1 upregulated at 4dd/1dl and 4dd/3dl relative to 4dd (figure 5.8). Our observation of a rapid upregulation of PIN1 after 1 day of light exposure is consistent with previous observation of an increased PIN1 expression 24h after transfer from dark to light (Sassi et al., 2012).

I then questioned whether these changes in PIN protein expression at the dark-light transition also resulted in observable changes in auxin distribution and/or response, as visualized by the DR5v2:GFP reporter. In hypocotyls, I observed a dramatic down-regulation of DR5 signal between dark grown (4dd) seedlings and those transferred to the light (4dd1dl) (figure 5.9 A-B), while in the root apical

meristem of wild-type I observed a gradual increase of DR5 signal between 4dd and 4dd1dl and 4dd3dl seedlings (figure 5.9 C-D).

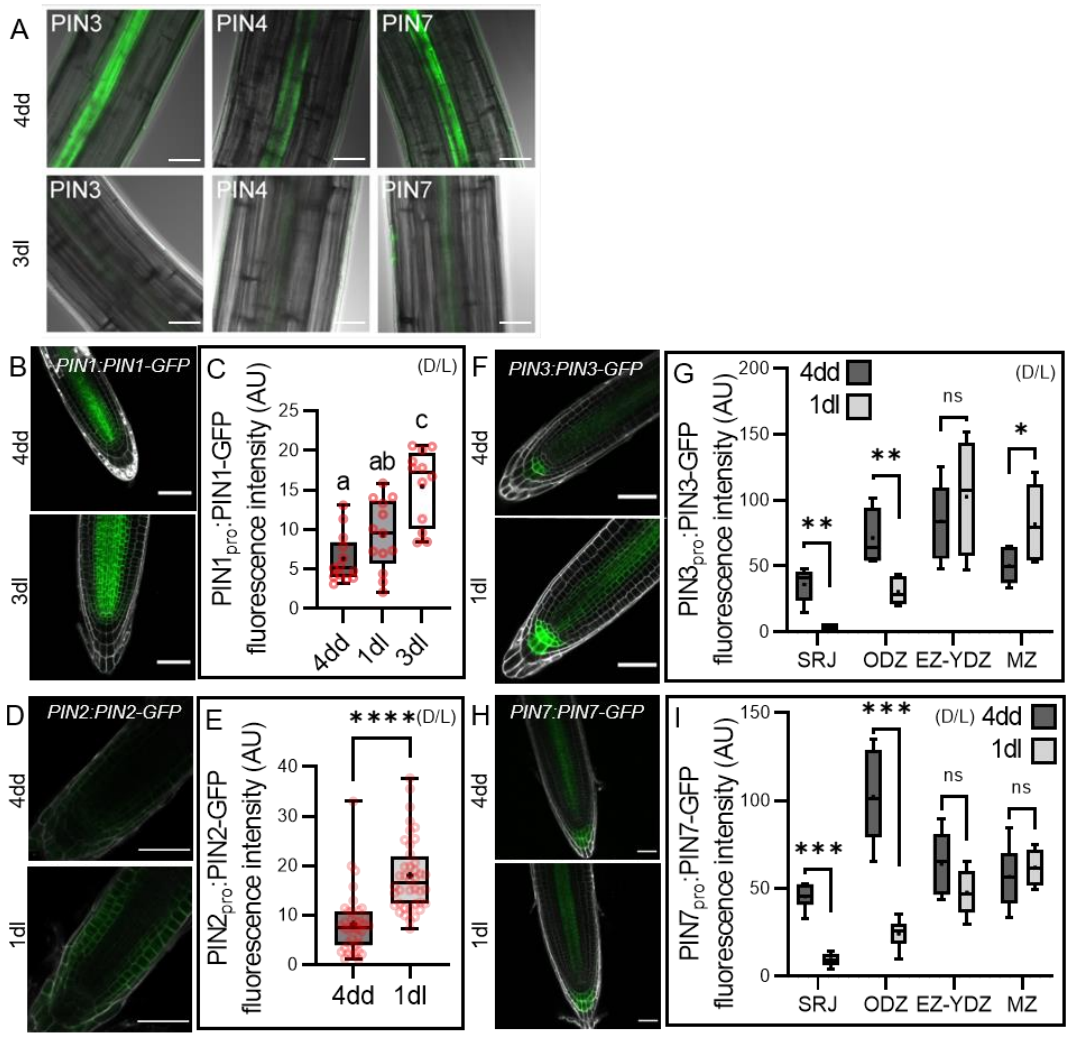

Figure 5-7 Re-modelling of auxin transport at the dark-light transition
For all figure panels (D/L) indicates that plants were grown in continuous darkness for a number of days before transfer to standard light conditions (16 hours light, 8 hours dark).
(A) PIN3-GFP, PIN4-GFP, and PIN7-GFP abundance at the very basal end of hypocotyls of wild-type seedlings after 4 days growth in the dark (4dd, top row), and subsequent transfer to normal light conditions for 3 days (3dl, bottom row). Images overlay bright field (grey) and GFP signals (green). Scale bars represent 30 µm.
(B,D,F,H) PIN1-GFP, PIN2-GFP, PIN3-GFP, and PIN7-GFP abundance in meristem zone (MZ) of wild-type seedlings after 4 days growth in the dark (4dd, top row), and subsequent transfer to normal light conditions for 1 or 3 days (1dl, 3dl). Microscopy images overlay propidium iodide (grey) and GFP signals (Green). Scale bars represent 50 µm.

(C,E) Quantification of PIN1pro:PIN1-GFP (C) and PIN2pro:PIN2-GFP (E) signals in meristem zone (MZ) of wild-type seedlings after 4 days growth in the dark (4dd), and subsequent transfer to normal light conditions for 1 or 3 days (1dl, 3dl). For (C) data correspond to the averaged PIN1-GFP intensity in the MZ from one experimental replicate (n=12-13 seedlings per genotype and time-point); two other independent experimental replicates gave comparable results.
For (E) data correspond to the averaged PIN2-GFP intensity in the apical plasma membrane of MZ epidermal cells from one experimental replicate (n=39-40 plasma membranes from 4 seedlings for each genotype and time-point). Statistical groups indicated by letters were determined by one-way ANOVA with post hoc Tukey HSD (CI 95%). **** (p-value ≤ 0.0001) indicates differences compared to wild-type (Welch's t-test).
(G,I) Quantification of PIN3-GFP (G) and PIN7-GFP (I) signals in the shoot-root junction (SRJ), older differentiation zone (ODZ), junction of the elongation and young differentiation zone (EZ-YDZ), and meristem zone (MZ) of wild-type seedlings after 4 days growth in the dark (4dd), and subsequent transfer to normal light conditions for 1 day (1dl). Data correspond to one experimental replicate (n=4-7 seedlings per genotype and time-point); for (G) a second independent experimental replicate gave comparable results. *,**,*** (p-value ≤ 0.05, 0.01, 0.001) indicates differences compared to wild-type (Welch's t-test). ns = no significant difference.
(C,G,E,I) The boxes in the box plot show the lower and upper quartiles and median values, mean is represented as (●), whiskers show minimal and maximal data values.

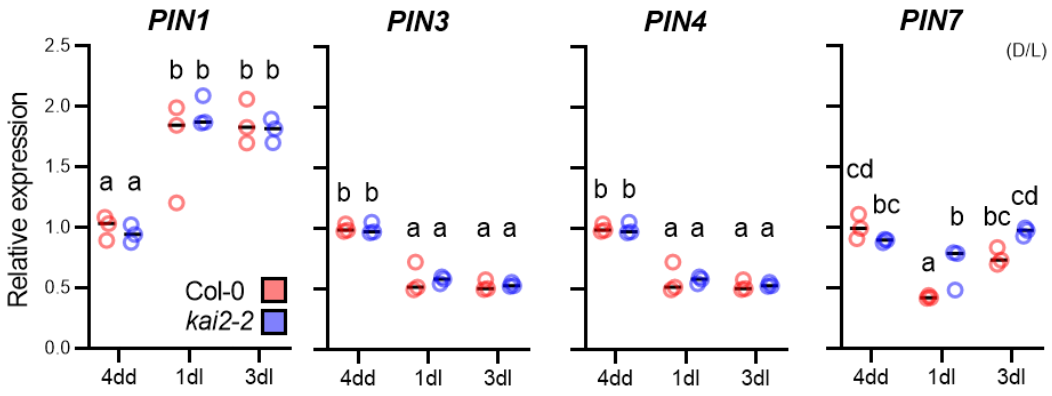

Figure 5-8 Transcriptional re-modelling of auxin transport at the dark-light transition

Expression of *Arabidopsis thaliana PIN1/3/4/7* genes relative to the reference gene *UBC10* in wild-type and *kai2-2* seedlings after 4 days growth in the dark (4dd), and subsequent transfer to normal light conditions (D/L) for 1 and 3 days (1dl, 3dl). For each gene, expression is normalised to the expression in wild type at 4dd). (n=3 biological samples collected by pooling ~16 seedlings per genotype and time-point. Statistical groups indicated by letters were determined by one-way ANOVA with post hoc Tukey HSD (CI 95%). Black lines represent mean.

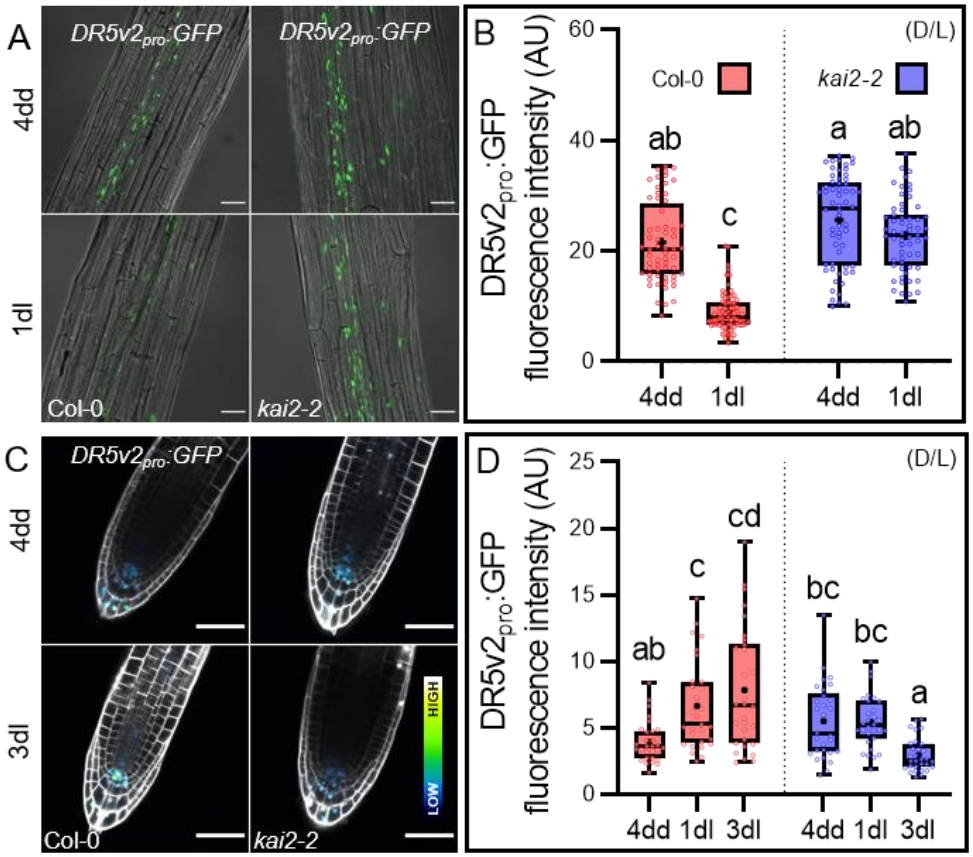

Figure 5-9 Re-modelling of auxin distribution/response at the dark-light transition is altered in kai2

For all figure panels (D/L) indicates that Arabidopsis plants were grown in continuous darkness for a number of days before transfer to standard light conditions.

(A-D) Auxin response (DR5v2:GFP fluorescence intensity) in the hypocotyl (A, B) and root apical meristem (C, D) of seedlings of wild-type or *kai2-2* mutants grown 4 days in the dark and then transferred in light condition for 1 day (top row) or 3 days (bottom row) (1dl, 3dl). (A) and (C) show representative microscopy images with overlay of either bright field or propidium iodide staining (grey) and GFP signals represented in green (A) or with false colour with dark blue as low signal intensity and bright white as high signal intensity (C). Scale bars represent 50 µm.

(B) GFP quantification in the hypocotyl; Data correspond to one experimental replicate (n=60-70 nuclei measured out of 6-7 seedlings of each genotype); a second independent experimental replicate gave comparable results.

(D) GFP quantification in the RAM; Data correspond to one experimental replicate (n=29-30 nuclei measured out of 3-5 seedlings of each genotype.

(B,D) Statistical groups indicated by letters were determined by one-way ANOVA with post hoc Tukey HSD (CI 95%). The boxes in the box plot show the lower and upper quartiles and median values, mean is represented as (●), whiskers show minimal and maximal data values.

4.11 KAI2 regulates light-induced remodelling of PIN-mediated auxin transport

I next tested whether this re-organization of the seedlings auxin transport network is delayed in *kai2* mutants, consistent with the changes in auxin distribution/response we observed (figure 5.2). The rapid physiologic changes in hypocotyl after exposure to light (anthocyanin and photosynthetic pigments accumulation) made the imaging of this tissue difficult and inconsistent across experimental replicates, maybe in part due to the increase in autofluorescence (Donaldson, 2020). I therefore focused on PIN abundance in the root (figure 5.10). I observed no difference in PIN7 abundance in mature root tissues between wild-type and *kai2-2* at 4dd, but there was a clear failure to decrease PIN7 abundance in *kai2-2* after transfer to the light, relative to wild-type (figure 5.10 A-B). Conversely, for PIN1 abundance in the meristem zone, I observed the opposite; there was no difference between wild-type and *kai2-1* at 4dd, but there was delay in the increase of PIN1 abundance at 4dd/1dl and 4dd/3dl in *kai2* seedlings (figure 5.10 C-D). Likely, these differences are long-lasting, explaining why light-grown *kai2* seedlings show increased PIN7 abundance along the root axis, decreased PIN1 in the RAM, and reduced PIN2 abundance in the elongation zone relative to wild-type seedlings (figure 5.4). Thus, *kai2* mutants show a general reduction in the rate that the auxin transport system is re-modelled after transition to the light.

We then measured PIN gene expression in *kai2* mutant after transfer to light to examine if the KAI2-mediated remodelling of the PIN-mediated auxin transport system at the dark-light transition was to the results of differential regulation of PIN genes. There were no clear differences in PIN gene expression in *kai2* relative to Col-0 at 4dd, 4dd/1dl or 4dd/3dl (figure 5.8). One possibility would be that we missed subtle localized differences in the expression levels between wild-type and *kai2*. Indeed the measurements of PIN genes expression by qPCR were performed on whole-seedling RNA and therefore account for global changes in their expression across tissues. However, the observation we made are of a large-scale KAI2-mediated remodelling and changes in PIN abundance across various tissues. We therefore reasoned that these data (figure 5.8) reflect the same light-mediated changes in transcription between Col-0 and *kai2*, and a parsimonious explanation would be that the response to these transcriptional changes is tardy in the *kai2* mutants.

Consistent with this delay in remodelling auxin transport after exposure to light, I also observed a delay in changes to *DR5v2:GFP* expression in *kai2* seedlings (figure 5.9). While wild-type seedlings grown for 4 days in the dark show a strong

reduction of *DR5v2* activity in hypocotyls after 1 day of light exposure, and a gradual increase in *DR5v2* signal in the RAM over 3 days of light exposure, these changes did not occur in *kai2* mutants (figure 5.9 A-D). Indeed, if anything *DR5v2* expression declines in the RAM after transfer to the light. Thus, the observed reduction in auxin transport remodelling in *kai2* mutants after transfer to light delays changes in auxin response in seedling tissues, and I hypothesize this leads to the observed phenotypes in *kai2* mutants.

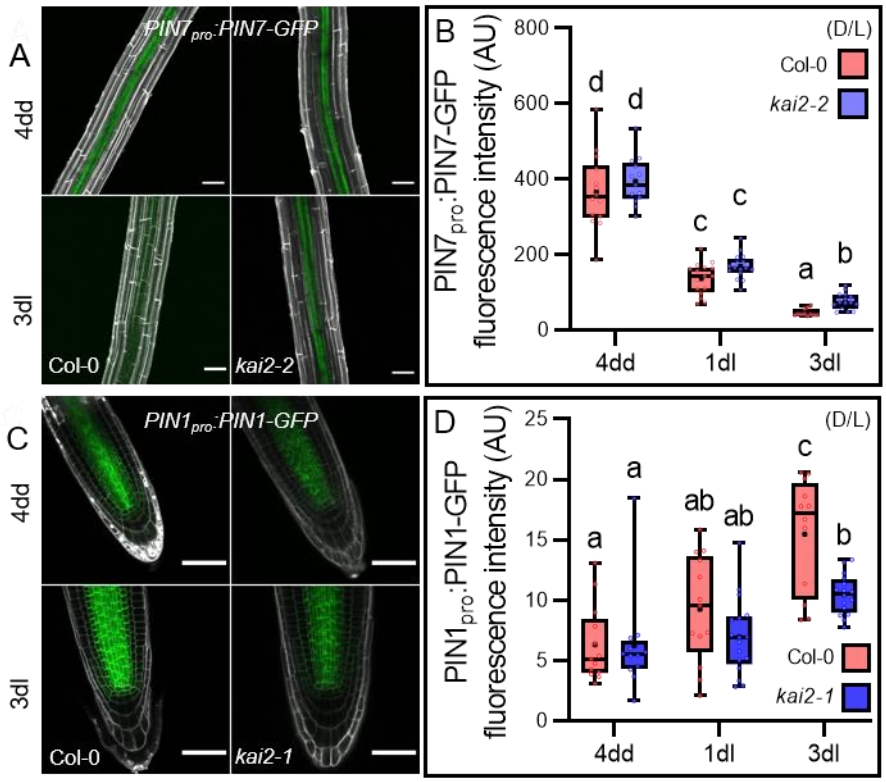

Figure 5-10 KAI2 mediates re-modelling of auxin transport at the dark-light transition

For all figure panels (D/L) indicates that plants were grown in continuous darkness for a number of days before transfer to standard light conditions (16 hours light, 8 hours dark).

(A,B) PIN7-GFP abundance quantification (B) and representative images (A) in the old differentiation zone (ODZ) of wild-type or *kai2-2* roots after 4 days growth in the dark (4dd), and subsequent transfer to normal light conditions for 1 and 3 days (1dl, 3dl). Data correspond to two independent experimental replicates pooled together (n=11-16 seedlings per genotype and time-point).

(C,D) PIN1:GFP abundance quantification (D) and representative images (C) in root meristem zone of wild-type or *kai2-1* seedlings after 4 days growth in the dark (4dd), and subsequent transfer to normal light conditions for 1 and 3 days (1dl, 3dl). Data correspond to two independent experimental replicates pooled together (n=12-17 seedlings per genotype and time-point.

(A,C) Microscopy images overlay propidium iodide (grey) and GFP signals (green). Scale bars represent 50 µm.

(B,D) Statistical groups indicated by letters were determined by one-way ANOVA with post hoc Tukey HSD (CI 95%). The boxes in the box plot show the lower and upper quartiles and median values, mean is represented as (●), whiskers show minimal and maximal data values.

4.12 The phenotypic effects of KAI2 signalling are mediated by PIN-mediated auxin transport

Our data show an incorrect distribution of the auxin response (figure 5.2 and figure 5.9) due to a failure to remodel the PIN-mediated auxin transport system in *kai2* seedlings after dark-to-light transition (figure 5.10). These observations strongly support a model in which failure to remodel the PIN-mediated auxin distribution causes the abnormal pattering of the root system and the delayed developmental changes accompanying dark-to-light transition in *kai2*. To test this model, I grew *kai2* and wild-type seedlings in presence of auxin transport inhibitor 1-N-naphthylphthalamic acid (NPA) (Abas et al, 2021) to try and rescue the *kai2* phenotype. Consistent with our model, treatments in the range of 0.1-1 µM NPA were sufficient to reduce the light grown hypocotyl, adventitious root, and lateral root phenotypes of *kai2* to a wild-type level (figure 5.11 A-C). The use of the auxin synthesis inhibitor L-kynurenine (He et al, 2011) gave similar effects, and treatment with 10 nM L-Kyn resulted in a significant reduction of lateral and adventitious root proliferation in *kai2* to a wild-type level (figure 5.11 D-E). To provide independent verification of these results, we crossed *kai2-2* to the *pin3-3 pin4-3 pin7-1* triple mutant (Bennett et al, 2016b, van Rongen et al, 2019), and assessed the mutants development after growth in the dark (4dd) followed by de-etiolation in standard light conditions (3dl). The verified quadruple mutant (*k2 pin347*) restored the hypocotyl phenotype to a wild-type level (figure 5.11 F). Similarly, the adventitious and lateral root phenotypes of *kai2* are also rescued in the quadruple mutant (figure 5.11 G-H). Although this data indicates that the loss-of-function *pin347* rescues the phenotypes of *kai2*, these phenotypes must be analysed with care since *pin3 pin4 pin7* significantly impairs seedling development in wild-type background, as seen with decreased hypocotyl elongation, AR number, and LRD in *pin347* (figure 5.11 F-H).

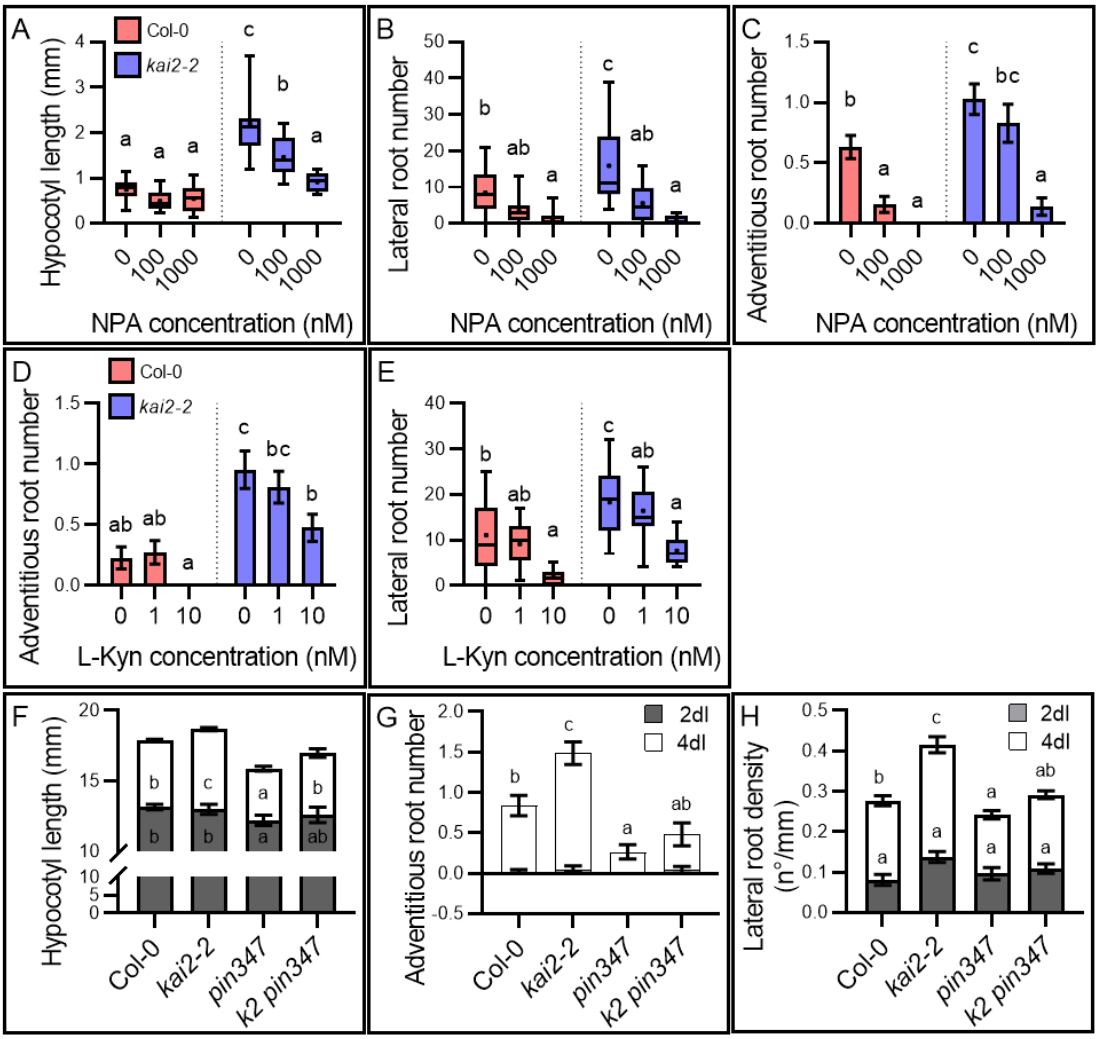

Figure 5-11 The phenotypic effects of KAI2 signalling are mediated by PIN-mediated auxin transport

(A-C) Effect of auxin transport inhibitor 1-N-naphthylphthalamic acid (NPA) on hypocotyl length (A) lateral root number (B) and adventitious root number (C) in 10-day old wild-type and kai2-2 seedlings. For (A) data correspond to one experimental replicate (n=11-13 seedlings per genotype and treatment); two other independent experimental replicates gave comparable results; for (B) data correspond to one experimental replicate (n=18-22 seedlings per genotype and treatment); a second independent experimental replicate gave comparable results; for (C) data correspond to one experimental replicate (n=38-42 seedlings per genotype and treatment); a second independent experimental replicate gave comparable results. Statistical groups indicated by letters were determined by one-way ANOVA with post hoc Tukey HSD (CI 95%). (C) Error bars represent ± s.e.m.

(D, E) Effect of auxin biosynthesis inhibitor L-kynurenine (L-KYN) on adventitious (D) and lateral root (E) number in 10-day old wild-type and *kai2-2* seedlings. Data correspond to one experimental replicate (n=21-22 seedlings per genotype and treatment); a second independent experimental replicate gave comparable results. Statistical groups indicated by letters were determined by one-way ANOVA with post hoc Tukey HSD (CI 95%).

(F-H) Hypocotyl length (F), adventitious root number (G), and lateral root density (G) in wild-type, *kai2-2, pin3-3 pin4-3 pin7-1 (pin347)* and *kai2-2 pin3-3 pin4-3 pin7-1 (k2 p347*) seedlings grown for 4 days in the dark, and after subsequent transfer to normal light conditions for 2 and 4 days (2dl and 4dl). Data correspond to two experimental replicates pooled together (n=23-42 seedlings per genotype). Statistical groups indicated by letters were determined by one-way ANOVA with post hoc Tukey HSD (CI 95%).
(A,B,E,F) The boxes in the box plot show the lower and upper quartiles and median values, mean is represented as (●), whiskers show minimal and maximal data values. (C,D,F,G,H) Error bars represent ± s.e.m.

4.13 Results summary

- Here, using a combination of physiological, pharmacological, genetic and imaging approaches, I show that *kai2* phenotypes arise because of a failure to downregulate auxin transport from the seedling shoot apex towards the root system, rather than a failure to respond to light *per se*.
- I demonstrate that KAI2 controls the light-induced remodelling of the PIN-mediated auxin transport system in seedlings, promoting a reduction in PIN7 abundance in older tissues, and an increase of PIN1/PIN2 abundance in the root meristem. I show that removing PIN3, PIN4 and PIN7 from *kai2* mutants, or pharmacological inhibition of auxin transport and synthesis, is sufficient to suppress most *kai2* seedling phenotypes.
- I conclude that KAI2 regulates seedling morphogenesis by its effects on the auxin transport system. I propose that KAI2 is not required for the light-mediated changes in PIN gene expression but is required for the appropriate changes in PIN protein abundance at the plasma membrane.

Chapter 5 General discussion

5.1 KL and SL are regulators of root development

Roots play a crucial role in all aspects of a plant life, from early developmental phases to vegetative and flowering stages. The architecture of the root system is shaped by various signals to ensure the best survival chances in response to ever changing environmental conditions. In this regard, SL signalling has long been proposed as a regulator of RSA because *max2* mutant and *rac*-GR24 were commonly used to study SL signalling function before SL and KL specific receptors were identified, and before *d14* and *kai2* were made available. Here, I produced a comprehensive analyse of the role of SL and KL by dissecting both pathways' function in the control of various traits of root system (primary root, lateral root, root hair, skewing, and adventitious root development). I demonstrate that under standard growth conditions, KL signalling is a major regulator of root development and plays a more important role than SL signalling in shaping root system architecture (figure 3.9). This new insight into the role of SL and KL demonstrates that most root phenotypes associated to *max2* had been wrongly attributed to a function of SL signalling (reviewed in Machin et al., 2020).

5.1.1 KL signalling regulates LR development together with SL signalling

Previous reports have shown MAX2 negatively regulates lateral root development, while SMXL6/7/8 likely act downstream of MAX2 to promote LRD (Kapulnik et al., 2011, Ruyter-Spira et al., 2011, Soundappan et al., 2015). Consistent with the idea of a regulation of LRD by SL signalling, I found a consistently increased LRD in SL biosynthesis mutants *max3*, *max4*, *and max1* and in SL signalling mutants *max2* and *d14*. Although, the careful observation of this phenotype in SL biosynthesis and *d14* mutants points toward an increased LRD resulting from a shorter primary root (decreased PRL) with as many lateral roots as wild-type seedlings (figure 3.1). By opposition, *max2* mutants display normal PRL, but increased LR number and as a result an increased LRD. We found *kai2* mutant phenocopied *max2* phenotypes as per PRL and LRD (figure 3.2). Thus, in contradiction with the literature, the modulation of LR development by MAX2 depends upon KAI2 activity rather than SL signalling. Similarly, Ruyter-Spira et al., 2011 observed an increased LRp number in *max2* mutant and suggested SL regulates LR formation by inducing LRp formation; we found that *kai2* mutants display a similar increased LRp formation observed in *max2* by Ruyter-Spira et al., 2011, indicating that KAI2-MAX2 complex is required for normal lateral root primordia proliferation and emergence (figure 3.2 E). This

function of KAI2 appears to be conserved across plant species as *kai2* mutant in *Brachypodium distachyon* also exhibits an increase lateral root phenotype (Meng et al., 2021).

In addition, our data are consistent with Soundappan et al., 2015 regarding a role of SMXL6/7/8 in regulating LRD; but the incomplete epistasis of *smxl678* toward *max2* suggests that another yet uncharacterized mechanism/downstream target of MAX2 is at play (figure 3.5). Furthermore, we also report for the first time a decreased LRD in *smax1 smxl2* with a partial epistasis to *max2*, indicating the action of both SMXL6/7/8 and SMAX1/SMXL2 are required downstream of MAX2 to maintain a correct LR development, consistent with our model in which both D14 and KAI2 affect LRD (figure 3.5).

5.1.2 KL but not SL regulate RH proliferation

It has previously been proposed that SL signalling regulates root hair density and elongation, based on the observations of decreased RHL and RHD in *max2* mutants, and the ability of *rac*-GR24 to induce RH elongation in Arabidopsis seedlings (Koltai et al., 2010, Kapulnik et al., 2011). It was however unclear whether regulation of RH development relies upon SL, KL signalling, or a synergic action of both pathways. In collaboration with the team of Caroline Gutjahr, we re-assessed the role of each pathway (figure 3.3, figure 3.7 A-B, and Villaecija-Aguilar et al, 2019). While SL biosynthesis and *d14* mutants have a wild-type RH phenotype, we found *kai2* phenocopied the decreased RHD and reduced RHL of *max2* mutant (figure 3.11 A-D). In addition, treatment with KARs induced root hair development in wild-type (figure 3.11 E-F), similar to the previously reported effects of *rac*-GR24 treatment (Kapulnik et al., 2011). These data dispute previous conclusions, and rather point towards a solely role of KAI2-MAX2 complex in the control of root hair growth. Regulation of root hair development by KL signalling rather than SL makes sense from an evolutionary point of view. First, regulation of root hair development in Arabidopsis relies on genes with conserved function across land plants and operating in early land plants such as *Marchantia polymorpha* where the rhizoid of the gametophytes appears to be homologous to root hairs (Honkanen et al., 2016). Secondly, *KAI2* is ancestral to *D14* and is present in most land plant lineages and in algae, while *D14* occurs only in genomes of seed plants (Waters et al., 2012, Delaux et al., 2012, Bythell-Douglas et al., 2017). Thirdly, it appears to be a conserved features in other plant species, given that *kai2* mutants in *Brachypodium distachyon* also show a reduction in root hair growth (Meng et al., 2021), while *smax1* mutants in *Lotus japonicus* display an increased RHL (Carbonnel et al., 2020). As a consequence,

it is possible that KAI2-SMAX1 module is part of an ancient and conserved pathway regulating tip growth of epidermal cells.

Conversely, we did not observe differences between *smxl678* mutant and wild-type, but we found that SMAX1 and SMXL2 act as an important negative regulator of root hair initiation and elongation (Figure 3.15 and Villaécija-Aguilar et al., 2019), thus indicating KL signalling is a newly discovered key regulator of RH development.

In addition, KL signalling has been suggested as a critical regulator of plant survival in a post-fire environment and promotes drought resistance in Arabidopsis plants (Nelson et al., 2010, Li et al., 2017, Wang et al., 2018). Soil properties are severely altered post-fire and thus the development of root hairs and growth of the primary root appears as a relevant strategy for the young seedlings to mitigate adverse environmental conditions such as drought and ensuring correct anchoring in the soil. It is therefore possible that KARs, perceived by KL signalling, act as a signal carrying information regarding changes in the soil properties such as water availability. And the integration of this environmental information triggers a KL-mediated root hair proliferation as an adaptive-response. This hypothesis would further link the functions of KL signalling with the integration of environmental conditions, and remains to be investigated.

5.2 KL is required for correct developmental responses to the environment

5.2.1 KL and SL shape RSA in response to phosphorus availability

Phosphorus is frequently a limiting factor for plant growth and development and its depletion from soil triggers a set of plant adaptive responses (growth, developmental, and metabolic responses) with the aim of reducing Pi usage and increasing Pi uptake and recycling. A common strategy is the adaptation of the root system architecture which allows the plant to explore the soil in search for available inorganic phosphorus (Rouached et al., 2010, Desnos 2008, Peret et al., 2011). Among the physiological changes observed in the model plant *Arabidopsis thaliana* in response to low phosphate level, we observe reduced PRL, enhanced LRD, and increased root hair proliferation (figure 4.1) (reviewed in Péret et al., 2011). The action of long-distance signals (phytohormones) among which auxin, ethylene, cytokinin, and others is essential during this process. In connection with the Pi-deficiency response, SL signalling has also been suggested to be involved in the remodelling of the RSA. Indeed, SL biosynthesis

is induced upon Pi depletion (Yoneyama et al., 2007, Yoneyama et al., 2013), while induction of phosphate-response genes and root hair proliferation is impaired in *max2* in response to low phosphorus (Mayzlish-Gati et al., 2012). Consistent with the newly reported role of KL signalling on RSA, I found that *kai2* mutation attenuates lateral root and root hair proliferation in response to low Pi while *smax1 smxl2* mutant is unable to induce LR development and has constitutively more and longer RH even in presence of high phosphate availability (figure 4.1 B-E). These observations are further supported by a recent jointly authored report showing that KL signalling is required for a major portion of the RH elongation in response to low external Pi availability (Villaécija-Aguilar et al., 2021).

It was previously reported that *max2* has a similar primary root shortening than wild-type in response to Pi depletion (1 µM) (Mayzlish-Gati et al., 2012), suggesting low Pi-mediated inhibition of root growth occurs independently of strigolactone signalling. By opposition, I found SL mutants *max4* and *d14* were unresponsive to low P treatment (10 µM) (figure 4.1 A), consistent with the idea that remodelling of the RSA in response to Pi-scarcity is dependent on SL biosynthesis and signalling. An explanation for these contrasting results could come from the severity of the Pi depletion applied to the plants. In Mayzlish-Gati et al., 2012, 1 µM Pi is used as a low phosphate condition whereas in my experiment 10 µM was used. The lower the Pi availability is, the less meristematic activity and general growth an organism can undertakes, and it is generally known that very low Pi treatment in Arabidopsis grown on agar plate leads to the complete arrest of the meristematic activity in the root rip due to starvation-response. That being the case, I hypothesise that the normal Pi-response reported by Mayzlish-Gati et al., 2012 in *max2* mutants is a result of a death of the root meristem due to Pi starvation rather than clear evidence that SL signalling doesn't regulate low Pi-responses.

The remodelling of auxin biosynthesis and distribution by the action of the PIN proteins is essential for the adaptive response of the RSA to low external Pi. This remodelling of auxin homeostasis accounts for RH proliferation and LR proliferation (reviewed in Peret et al., 2011), but low phosphorous levels have also been shown to induce more vertical gravitropic set point angles in Arabidopsis lateral roots (Roychoudhry et al., 2017). Given that *kai2* mutation is associated with defect in RH, LR, and gravitropic index of the primary root (figures 3.2, 3.3, and 3.4), the presence of a crosstalk between KL and auxin in the context of low phosphorus-responses in the root is likely. To this regard, the recent finding from Villaécija-Aguilar et al. provides important clues for a mechanistic framework including KL signalling, ethylene and auxin signalling pathways in the regulation

of root hair formation in a context of phosphate stress-response (Villaécija-Aguilar et al., 2021).

5.2.2 KL signalling ensure correct photomorphogenic development of the seedling

The mechanisms by which seedlings use light information across their whole body (including those parts that remain in the dark such as the roots) to produce coherent developmental changes remain poorly characterized, although a range of recent work has advanced this area considerably (reviewed in Fankhauser & Christie, 2015, van Gelderen 2017). For instance, it has been shown that sugars arising from newly established photosynthesis serve as essential long-distance signals promoting root development (Kircher & Schopfer, 2012). Light perception in the cotyledons also triggers translocation of ELONGATED HYPOCOTYL5 (HY5) signalling protein from the shoot to the root through phloem where it acts to regulate root development (Chen et al, 2016, Zhang et al, 2017). Light perception mechanisms also trigger downstream regulation of hormonal signals that act as further developmental regulators (Symons & Reid, 2003, Gommers & Monte, 2018). Overall, the data we present here support the idea that KL signalling function is to ensure the correct spatial patterning of growth responses both in the root and shoot tissues, rather than the response to light *per se* (figure 4.7). The ability of KAR to promote light-dependent responses, and the defect of KL signalling mutants (*kai2*, *max2*, *smax1 smxl2*) in their ability to correctly germinate, inhibit hypocotyl elongation, modulate cotyledon expansion, and accumulate anthocyanin and chlorophyll (Nelson et al., 2009, 2010, Thussagunpanit et al., 2017) clearly showed that the KL signalling pathway is linked with light-mediated development. KAI2 signalling is certainly not needed for light perception *per se* but is required for a normal photomorphogenic development of the seedlings (Sun & Ni, 2011, Water et al, 2012, Lee et al, 2019, Bursch et al., 2021). A cross-regulation between KAI2 and a sub-set of light-responsive genes such as HY5 has previously been suggested to account for these effects (Sun & Ni, 2011). However, the evidence is not conclusive and light perception and HY5 functions are not essential for KAR perception and KAI2-dependent responses (Nelson et al., 2010, Waters & Smith, 2013, Bursch et al., 2021). Our data bring a new insight in a function of KAI2 signalling and links the pathway with the correct remodelling of the entire seedling development after transition from dark-to-light.

5.3 A model for the function of KAI2 in seedling development

All things considered; our data are consistent with a model that KAI2 mediates light-induced remodelling of the auxin transport system to regulate seedling development. During the skotomorphogenic phase, auxin, which is transported from the cotyledons, is mainly directed towards the shoot apex, the hypocotyl, and the shoot-root axis, where it ensures the correct patterning of the seedling growth, including formation and maintenance of a close apical hook and elongation of the hypocotyl (figure 6.1). Seedlings grown in the dark are characterised by a high abundance of PIN3, PIN4 and PIN7 along the shoot axis in the hypocotyl, and toward the shoot-root junction, while the abundance of PIN1 and PIN2 in the root tissues and the root meristem remains low (figure 6.1). To this regard, the exact role of the auxin transport network during this dark-grown phase is intriguing given *pin3 pin4 pin7* etiolates normally (figure 5.11 F), and that chemical inhibition of the polar auxin transport with NPA does not affect hypocotyl etiolation, but disrupts the gravitropic response, and the development of the apical hook (Jensen et al., 1998, Žádníková et al., 2010). The most parsimonious explanation would be that its function might relate more to the delivery of auxin to the root system for future development sustained by the photosynthetic metabolism (figure 6.1). Although in some tissues the PIN-mediated auxin transport is a key regulator of the skotomorphogenic development (e.g. apical hook).

After the transition to light, the PAT system is rapidly remodelled, with turnover of PIN3, PIN4 and PIN7 in the hypocotyl and older root tissues, and upregulation of PIN1, PIN2, and PIN3 in the root meristem (figure 5.12). These changes might account for the rapid and dramatic physiological changes the seedlings undergo following light perception. For instance, in the root tip *PIN1* upregulation and the increased abundance of basally polarized PIN1 at the plasma membrane of stele cells might drive the “auxin delivery” activating the meristematic activity of the root apex. Meanwhile PIN2, PIN3, PIN4 and PIN7 upregulation, in concert with AUX1 (Villaécija-Aguilar et al. 2021), promotes the ‘reflux’ of auxin from the root cap to the epidermis which drives elongation zone activity and root hair development (figure 5.12). This would account for the remarkable increase in root meristem size that occurs after transfer to light (figure 4.7 F-G) (Sassi et al., 2012).

However, in, *kai2* seedlings there is an apparent failure to re-model the PIN-mediated auxin transport system after transition to light (figure 6.1). Likely, it causes a continuous auxin efflux from the cotyledon into the hypocotyl leading to delayed apical hook opening and cotyledons expansion, delayed inhibition of the hypocotyl elongation, but also promotion of adventitious root proliferation (figure

6.1). Interestingly, while auxin reporter activity is stronger at the base of the hypocotyl in *kai2* compared to wild-type, the mutant displays a reduced auxin transport between the shoot-root junction and the root tip (figure 5.3 F). An explanation for this would be that the increased PIN7 abundance along the root axis in *kai2* promotes the initiation and emergence of new lateral roots, consistent with *kai2* LRD phenotype. In addition to these observations, DR5 activity is reduced in the primary root meristem of *kai2* (figure 5.2 E-F) but increased in the lateral roots (figure 5.2 G-H), and the abundance of laterally polarized PIN3 in the plasma membrane in initiating lateral roots is also strongly increased in *kai2* (figure 5.6 C). This is consistent with the idea of an excess of auxin is diverted into the lateral roots in *kai2*. Finally, the reduced amount of auxin reaching the primary root meristem likely accounts for some of the phenotypes observed in the root apex in *kai2* and *smax1 smxl2* (Chapter 3 and Villaecija-Aguilar et al, 2019).

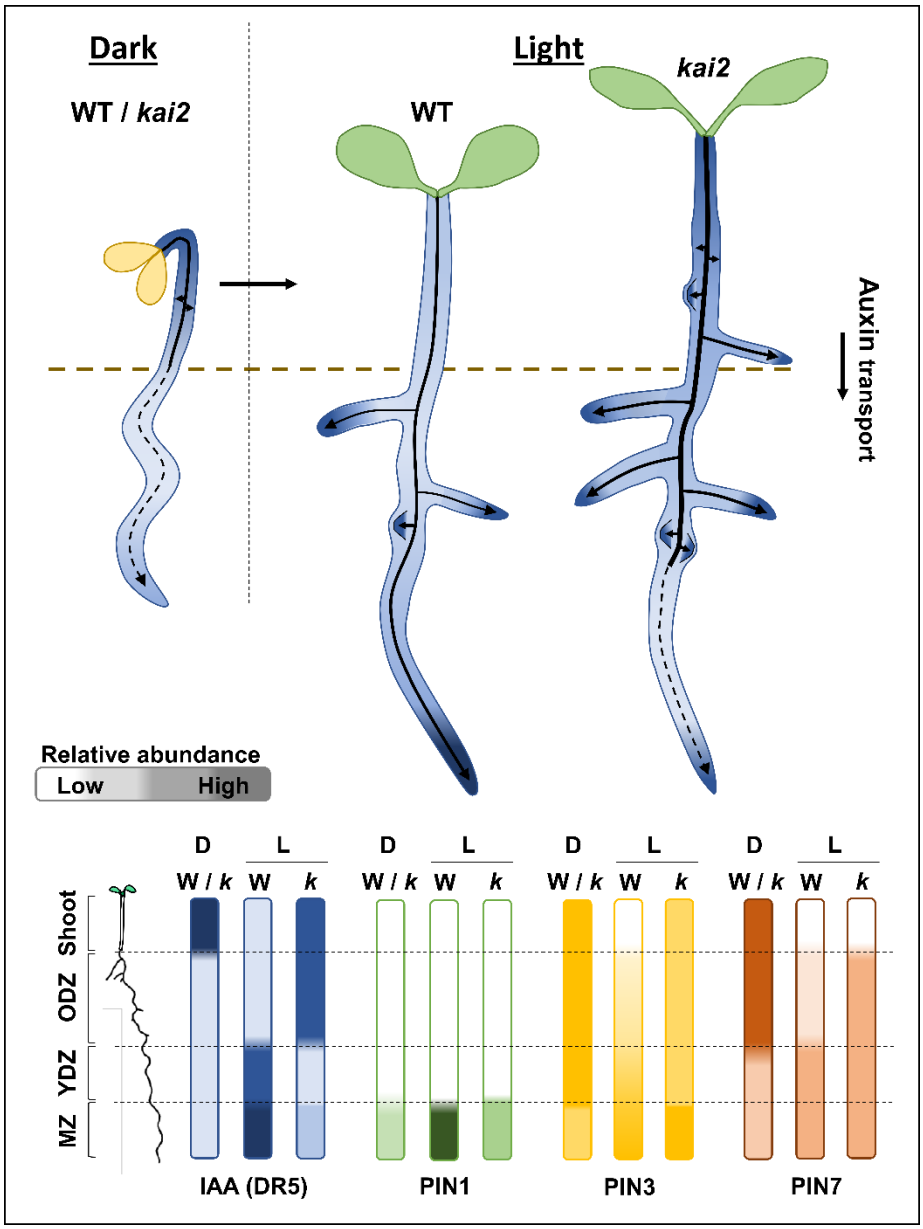

Figure 5-1 A model for KAI2 function in photomorphogenesis
Proposed model for light-induced remodelling of the auxin transport system to regulate Arabidopsis seedling development. During skotomorphogenesis, seedlings have a strong rootward auxin transport from the shoot apex, mediated by high PIN3 and PIN7 abundance, which drives the elongation growth of the hypocotyl and primary root in the dark (D). At the transition to photomorphogenic development, KAI2 promotes the rapid remodelling of the PIN-mediated auxin transport system, with a reduction of PIN3 and PIN7 abundance in older tissues, and increased PIN1, PIN3 and PIN7 abundance in the root meristem, to promote a meristematically-mediated growth in the light (L). In *kai2* mutants, the failure to remodel the auxin transport system transition leads to excess auxin in the shoot and older root tissues promoting continued hypocotyl elongation and increased adventitious and lateral roots growth in the shootward part of the root, with reduced auxin delivery to the primary root meristem zone. Plain arrows represent main auxin transport stream, dashed arrows represent reduced auxin transport; for the purpose of the model, the seedlings root tissues are compartmented as old-differentiation zone (ODZ), young-differentiation zone (YDZ), root meristem zone (MZ).

5.4 New perspectives on KAI2 signalling

The quest to a better understanding the function of KL signalling has received increased interest over the last few years. The ability of *smax1* and *smxl2* mutants to suppress the seedling phenotypes of *max2* have led to a speculative targeting and degradation of SMAX1 and SMXL2 mediated by KAI2-MAX2 (Stanga et al., 2013, Stanga et al., 2016), echoing the like of D14-MAX2-SMXL7 interaction (Machin et al., 2020). This hypothesis was recently confirmed by direct evidences of proteolysis and interaction of SMAX1 and SMXL2 mediated by KAI2 following KAR perception (Khosla et al, 2020, Wang et al, 2020b). Although the dynamic surrounding the interaction between the different actors of KL signalling appears now clearer, the signalling events downstream of KAI2-mediated proteolysis of SMAX1/SMXL2 remain nebulous. There is evidence leading toward a transcriptional activity of KAI2 signalling pathway on a set of genes including DWARF14-LIKE2 (DLK2), KARRIKIN UPREGULATED F-BOX1 (KUF1), and B-BOX DOMAIN PROTEIN 20 (BBX20) (Nelson et al., 2010, Waters et al., 2012, Bursch et al., 2021, Sepulveda et al., 2022), but the outputs of the transcriptional activation of these genes is not yet fully understood. One possibility would be a link between light and KL signalling with regards to hypocotyl elongation (Bursch et al., 2021), consistent with a role of KAI2 in photomorphogenetic development. An increase in ethylene biosynthesis has also been recently reported, and could account at least in part for the effect of KL signalling on seed germination, and on root hair and primary root development (Sami et al, 2019, Carbonnel et al, 2020). KAI2 has also long been speculated to interact at some level with auxin and light signalling to regulate growth and development. (Waters & Smith 2015). In this thesis, I provide clues for a mechanistic framework by linking the modulation of root/seedlings development by KAI2, and remodelling of the PIN-mediated auxin transport system. During the phase following exposure to light, seedlings undergo rapid physiological changes driven by a large-scale remodelling of the auxin transport system. This process relies on the ability of KAI2 to induce a re-modelling of the PIN-driven auxin transport at the cellular level. These findings are supported by another report showing that KL signalling coordinates the root hair response to low phosphate by regulating the tissue-specific accumulation of PIN2 and AUX1 in root tips (Villaécija-Aguilar et al. 2021). However, the mechanisms by which KAI2 regulates PIN auxin transporters to the plasma membrane in roots, and AUX1 abundance in the root apex, are not yet understood. One possibility would be that the action of KAI2 is alike of the analogous effect of D14 on PIN proteins in the context of shoot branching (Shinohara et al, 2013, Crawford et al, 2010).

The regulation of PIN protein accumulation downstream of SL signalling has more recently been proposed to be through modulation of PIN polarity and trafficking, given that *max2* and *rac*-GR24 repress the inhibitory effect of auxin on PIN endocytosis in roots (Zhang et al, 2020). Although, the conclusion of this study points toward the effects of strigolactone signalling, this might as well reflect outputs of KL signalling, given that *max2* indiscriminately mirrors a combination of impairments in SL and KL signalling, and that *rac*-GR24 equally activates both signalling cascades (Waters et al, 2012, Machin et al, 2020).

Another possibility would be that KAI2 transcriptionally regulates the auxin transport system. However, this hypothesis poses an ambiguity. Indeed, KAI2-SMAX1/SMXL2 pair is nuclear localized which is where their signalling events happen (Wang et al., 2020b), while changes in PIN abundance depend upon allocation/removal from the plasma membrane. One possibility for the KAI2-mediated changes in PM localized PIN would be a transcriptional regulation, but our data showed that PIN transcription is not mediated through KL signalling (figure 5.8). Similarly, in the shoot, the outputs of D14-mediated signalling on PIN proteins do not involve changes in *PIN* expression, and GR24-induced depletion of PM PIN1 level is unaffected by cycloheximide treatment (Shinohara et al, 2013). Nonetheless, there is increasing evidence for the role of SMXL6/7/8 as transcriptional regulators. First, SMXL7 is a demonstrated activator of BRC1 expression, and SMXL6 was recently shown to act as transcriptional co-repressor to regulate shoot branching (Wang et al, 2020a). Similarly, there is a number of auxin-responsive genes that are transcriptionally regulated in a KAI2-SMAX1/SMXL2 manner (Bursch et al., 2021). It is therefore possible that despite the absence of direct regulation of PIN genes, KAI2 signalling regulates the transcription of intermediates which in turns adjust PIN allocation at the plasma membrane.

The ability to use the seedling-based system described here will greatly simplify future investigations of downstream SMXL function, both transcriptional and non-transcriptional.

List of References/ Bibliography

Abas, L., Benjamins, R., Malenica, N., Paciorek, T., Wišniewska, J., Moulinier–Anzola, J.C., Sieberer, T., Friml, J. and Luschnig, C., 2006. Intracellular trafficking and proteolysis of the Arabidopsis auxin-efflux facilitator PIN2 are involved in root gravitropism. *Nature Cell Biology*, *8*(3), pp.249-256.

Abas, L., Kolb, M., Stadlmann, J., Janacek, D.P., Lukic, K., Schwechheimer, C., Sazanov, L.A., Mach, L., Friml, J. and Hammes, U.Z., 2021. Naphthylphthalamic acid associates with and inhibits PIN auxin transporters. *Proceedings of the National Academy of Sciences*, *118*(1), p.e2020857118.

Abe, S., Sado, A., Tanaka, K., Kisugi, T., Asami, K., Ota, S., Kim, H.I., Yoneyama, K., Xie, X., Ohnishi, T. and Seto, Y., 2014. Carlactone is converted to carlactonoic acid by MAX1 in Arabidopsis and its methyl ester can directly interact with AtD14 in vitro. *Proceedings of the National Academy of Sciences*, *111*(50), pp.18084-18089.

Adamowski, M. and Friml, J., 2015. PIN-dependent auxin transport: action, regulation, and evolution. *The Plant Cell*, *27*(1), pp.20-32.

Akiyama, K., Matsuzaki, K.I. and Hayashi, H., 2005. Plant sesquiterpenes induce hyphal branching in arbuscular mycorrhizal fungi. *Nature*, *435*(7043), pp.824-827.

Alder, A., Jamil, M., Marzorati, M., Bruno, M., Vermathen, M., Bigler, P., Ghisla, S., Bouwmeester, H., Beyer, P. and Al-Babili, S., 2012. The path from β-carotene to carlactone, a strigolactone-like plant hormone. *Science*, *335*(6074), pp.1348-1351.

Andersen SU, Buechel S, Zhao Z, Ljung K, Novák O, Busch W, Schuster C, Lohmann JU. (2008). Requirement of B2-type cyclin-dependent kinases for meristem integrity in Arabidopsis thaliana. *Plant Cell* 20, 88-100

Arite, T., Kameoka, H. and Kyozuka, J., 2012. Strigolactone positively controls crown root elongation in rice. *Journal of Plant Growth Regulation*, *31*(2), pp.165-172.

Arite, T., Umehara, M., Ishikawa, S., Hanada, A., Maekawa, M., Yamaguchi, S. and Kyozuka, J., 2009. d14, a strigolactone-insensitive mutant of rice, shows an accelerated outgrowth of tillers. *Plant and Cell Physiology*, *50*(8), pp.1416-1424.

Bak, S., Tax, F.E., Feldmann, K.A., Galbraith, D.W. and Feyereisen, R., 2001. CYP83B1, a cytochrome P450 at the metabolic branch point in auxin and indole glucosinolate biosynthesis in Arabidopsis. *The Plant Cell*, *13*(1), pp.101-111.

Bhalerao, R.P., Eklöf, J., Ljung, K., Marchant, A., Bennett, M. and Sandberg, G., 2002. Shoot-derived auxin is essential for early lateral root emergence in Arabidopsis seedlings. *The Plant Journal*, 29(3), pp.325-332.

Band LR, Wells DM, Larrieu A et al (2012) Root gravitropism is regulated by a transient lateral auxin gradient controlled by a tipping-point mechanism. Proc Natl Acad Sci U S A 109(12):4668–4673

Barbez, E., Kubeš, M., Rolčík, J., Béziat, C., Pěnčík, A., Wang, B., Rosquete, M.R., Zhu, J., Dobrev, P.I., Lee, Y. and Zažímalovà, E., 2012. A novel putative auxin carrier family regulates intracellular auxin homeostasis in plants. *Nature*, *485*(7396), pp.119-122.

Bates, T.R. and Lynch, J.P., 1996. Stimulation of root hair elongation in Arabidopsis thaliana by low phosphorus availability. *Plant, Cell & Environment*, *19*(5), pp.529-538.

Benková, E., Michniewicz, M., Sauer, M., Teichmann, T., Seifertová, D., Jürgens, G. and Friml, J., 2003. Local, efflux-dependent auxin gradients as a common module for plant organ formation. *Cell*, *115*(5), pp.591-602.

Bennett, M.J., Marchant, A., Green, H.G., May, S.T., Ward, S.P., Millner, P.A., Walker, A.R., Schulz, B. and Feldmann, K.A., 1996. Arabidopsis AUX1 gene: a permease-like regulator of root gravitropism. *Science*, *273*(5277), pp.948-950.

Bennett T, Liang Y, Seale M, Ward S, Müller D, Leyser O. (2016a). Strigolactone regulates shoot development through a core signalling pathway. *Biology Open* 5, 1806-1820.

Bennett, T., 2015. PIN proteins and the evolution of plant development. *Trends in Plant Science*, *20*(8), pp.498-507.

Bennett, T., Brockington, S.F., Rothfels, C., Graham, S.W., Stevenson, D., Kutchan, T., Rolf, M., Thomas, P., Wong, G.K.S., Leyser, O. and Glover, B.J., 2014b. Paralogous radiations of PIN proteins with multiple origins of noncanonical PIN structure. *Molecular Biology and Evolution*, *31*(8), pp.2042-2060.

Bennett, T., Hines, G., van Rongen, M., Waldie, T., Sawchuk, M.G., Scarpella, E., Ljung, K. and Leyser, O., 2016b. Connective auxin transport in the shoot facilitates communication between shoot apices. *PLoS Biology*, *14*(4), p.e1002446.

Bennett, T., Sieberer, T., Willett, B., Booker, J., Luschnig, C. and Leyser, O., 2006. The Arabidopsis MAX pathway controls shoot branching by regulating auxin transport. *Current Biology*, *16*(6), pp.553-563.

Beveridge, C.A., Murfet, I.C., Kerhoas, L., Sotta, B., Miginiac, E. and Rameau, C., 1997. The shoot controls zeatin riboside export from pea roots. Evidence from the branching mutant rms4. *The Plant Journal*, *11*(2), pp.339-345.

Béziat, C. and Kleine-Vehn, J., 2018. The road to auxin-dependent growth repression and promotion in apical hooks. *Current Biology*, *28*(8), pp.R519-R525.

Béziat, C., Barbez, E., Feraru, M.I., Lucyshyn, D. and Kleine-Vehn, J., 2017. Light triggers PILS-dependent reduction in nuclear auxin signalling for growth transition. *Nature Plants*, *3*(8), pp.1-9.

Bhosale, R., Giri, J., Pandey, B.K., Giehl, R.F., Hartmann, A., Traini, R., Truskina, J., Leftley, N., Hanlon, M., Swarup, K. and Rashed, A., 2018. A mechanistic

framework for auxin dependent Arabidopsis root hair elongation to low external phosphate. *Nature Communications*, *9*(1), pp.1-9.

Blilou, I., Xu, J., Wildwater, M., Willemsen, V., Paponov, I., Friml, J., Heidstra, R., Aida, M., Palme, K. and Scheres, B., 2005. The PIN auxin efflux facilitator network controls growth and patterning in Arabidopsis roots. *Nature*, *433*(7021), pp.39-44.

Boerjan, W., Cervera, M.T., Delarue, M., Beeckman, T., Dewitte, W., Bellini, C., Caboche, M., Van Onckelen, H., Van Montagu, M. and Inzé, D., 1995. Superroot, a recessive mutation in Arabidopsis, confers auxin overproduction. *The Plant Cell*, *7*(9), pp.1405-1419.

Booker, J., Auldridge, M., Wills, S., McCarty, D., Klee, H. and Leyser, O., 2004. MAX3/CCD7 is a carotenoid cleavage dioxygenase required for the synthesis of a novel plant signaling molecule. *Current Biology*, *14*(14), pp.1232-1238.

Bosco, C.D., Dovzhenko, A., Liu, X., Woerner, N., Rensch, T., Eismann, M., Eimer, S., Hegermann, J., Paponov, I.A., Ruperti, B. and Heberle-Bors, E., 2012. The endoplasmic reticulum localized PIN8 is a pollen-specific auxin carrier involved in intracellular auxin homeostasis. *The Plant Journal*, *71*(5), pp.860-870.

Boysen-Jensen P. La transmission de l'irritation phototropique dans l'avena, 1911. *Bulletin Academie des Sciences et Lettres de Montpellier*, vol. 3 (pg. 1-24)

Braun, N., de Saint Germain, A., Pillot, J.P., Boutet-Mercey, S., Dalmais, M., Antoniadi, I., Li, X., Maia-Grondard, A., Le Signor, C., Bouteiller, N. and Luo, D., 2012. The pea TCP transcription factor PsBRC1 acts downstream of strigolactones to control shoot branching. *Plant Physiology*, *158*(1), pp.225-238.

Brewer, P.B., Yoneyama, K., Filardo, F., Meyers, E., Scaffidi, A., Frickey, T., Akiyama, K., Seto, Y., Dun, E.A., Cremer, J.E. and Kerr, S.C., 2016. LATERAL BRANCHING OXIDOREDUCTASE acts in the final stages of strigolactone biosynthesis in Arabidopsis. *Proceedings of the National Academy of Sciences*, *113*(22), pp.6301-6306.

Brown, N.A.C. and Van Staden, J., 1997. Smoke as a germination cue: a review. *Plant Growth Regulation*, *22*(2), pp.115-124.

Bursch, K., Niemann, E.T., Nelson, D.C. and Johansson, H., 2021. Karrikins control seedling photomorphogenesis and anthocyanin biosynthesis through a HY5-BBX transcriptional module. *The Plant Journal*, *107*, pp.1346-1362.

Bythell-Douglas, R., Rothfels, C.J., Stevenson, D.W., Graham, S.W., Wong, G.K.S., Nelson, D.C. and Bennett, T., 2017. Evolution of strigolactone receptors by gradual neo-functionalization of KAI2 paralogues. *BMC biology*, *15*(1), pp.1-21.

Carbonnel, S., Das, D., Varshney, K., Kolodziej, M.C., Villaécija-Aguilar, J.A. and Gutjahr, C., 2020. The karrikin signaling regulator SMAX1 controls Lotus japonicus root and root hair development by suppressing ethylene biosynthesis. *Proceedings of the National Academy of Sciences*, *117*(35), pp.21757-21765.

Casal, J.J., 2013. Photoreceptor signaling networks in plant responses to shade. *Annual Review of Plant Biology*, *64*, pp.403-427.

Causier, B., Ashworth, M., Guo, W. and Davies, B., 2012. The TOPLESS interactome: a framework for gene repression in Arabidopsis. *Plant Physiology*, *158*(1), pp.423-438.

Chen X, Yao Q, Gao X, Jiang C, Harberd NP, Fu X. (2016). Shoot-to-Root Mobile Transcription Factor HY5 Coordinates Plant Carbon and Nitrogen Acquisition. *Current Biology* 26, 640-646.

Chiu, C.H. and Paszkowski, U., 2019. Mechanisms and impact of symbiotic phosphate acquisition. *Cold Spring Harbor Perspectives in Biology*, *11*(6), p.a034603.

Cho, M. and Cho, H., 2013. The function of ABCB transporters in auxin transport. *Plant Signaling & Behavior*, *8*(2), pp.642-54.

Choi, J., Lee, T., Cho, J., Servante, E.K., Pucker, B., Summers, W., Bowden, S., Rahimi, M., An, K., An, G. and Bouwmeester, H.J., 2020. The negative regulator SMAX1 controls mycorrhizal symbiosis and strigolactone biosynthesis in rice. *Nature Communications*, *11*(1), pp.1-13.

Cholodny N., 1928. Beiträge zur hormonalen Theorie von Tropismen, *Planta,* vol. 6 (pg. 118-134)

Conn, C.E. and Nelson, D.C., 2016. Evidence that KARRIKIN-INSENSITIVE2 (KAI2) receptors may perceive an unknown signal that is not karrikin or strigolactone. *Frontiers in Plant Science*, *6*, p.1219.

Conn, C.E., Bythell-Douglas, R., Neumann, D., Yoshida, S., Whittington, B., Westwood, J.H., Shirasu, K., Bond, C.S., Dyer, K.A. and Nelson, D.C., 2015. Convergent evolution of strigolactone perception enabled host detection in parasitic plants. *Science*, *349*(6247), pp.540-543.

Conn, S.J., Hocking, B., Dayod, M., Xu, B., Athman, A., Henderson, S., Aukett, L., Conn, V., Shearer, M.K., Fuentes, S. and Tyerman, S.D., 2013. Protocol: optimising hydroponic growth systems for nutritional and physiological analysis of Arabidopsis thaliana and other plants. *Plant Methods*, *9*(1), pp.1-11.

Cook, C.E., Whichard, L.P., Wall, M., Egley, G.H., Coggon, P., Luhan, P.A., and McPhail, A.T. (1972). Germination stimulants. II. Structure of strigol, a potent seed germination stimulant for witchweed (Striga lutea). Journal of the American Chemical Society 94: 6198-6199.

Crawford, S., Shinohara, N., Sieberer, T., Williamson, L., George, G., Hepworth, J., Müller, D., Domagalska, M.A. and Leyser, O., 2010. Strigolactones enhance competition between shoot branches by dampening auxin transport. *Development*, *137*(17), pp.2905-2913.

Czechowski T, Stitt M, Altmann T, Udvardi MK, Scheible WR. (2005). Genome-wide identification and testing of superior reference genes for transcript normalization in Arabidopsis. *Plant Physiology* 139, 5–17.

Da Costa, C.T., De Almeida, M.R., Ruedell, C.M., Schwambach, J., Maraschin, F.D.S. and Fett-Neto, A.G., 2013. When stress and development go hand in hand: main hormonal controls of adventitious rooting in cuttings. *Frontiers in Plant Science*, *4*, p.133.

Da Costa, C.T., Gaeta, M.L., de Araujo Mariath, J.E., Offringa, R. and Fett-Neto, A.G., 2018. Comparative adventitious root development in pre-etiolated and flooded Arabidopsis hypocotyls exposed to different auxins. *Plant Physiology and Biochemistry*, *127*, pp.161-168.

Darwin, C. and Darwin, F.E., 1888. The 'Power of movement in plants.'--1880.

Davies, P.J., 2004. Introduction. In Plant Hormones: Biosynthesis, Signal Transduction, Action! *P.J. Davies, ed (Dordrecht, The Netherlands: Kluwer Academic Publishers),* pp. 1–35.

De Cuyper, C., Fromentin, J., Yocgo, R.E., De Keyser, A., Guillotin, B., Kunert, K., Boyer, F.D. and Goormachtig, S., 2015. From lateral root density to nodule number, the strigolactone analogue GR24 shapes the root architecture of Medicago truncatula. *Journal of Experimental Botany*, *66*(1), pp.137-146.

De Lange, J.H. and Boucher, C., 1990. Autecological studies on Audouinia capitata (Bruniaceae). I. Plant-derived smoke as a seed germination cue. *South African Journal of Botany*, *56*(6), pp.700-703.

De Saint Germain, A., Ligerot, Y., Dun, E.A., Pillot, J.P., Ross, J.J., Beveridge, C.A. and Rameau, C., 2013. Strigolactones stimulate internode elongation independently of gibberellins. *Plant Physiology, 163(2), pp.1012-1025.*

Delaux, P.M., Xie, X., Timme, R.E., Puech-Pages, V., Dunand, C., Lecompte, E., Delwiche, C.F., Yoneyama, K., Bécard, G. and Séjalon-Delmas, N., 2012. Origin of strigolactones in the green lineage. *New Phytologist*, *195*(4), pp.857-871.

Desnos, T., 2008. Root branching responses to phosphate and nitrate. *Current opinion in Plant Biology*, *11*(1), pp.82-87.

Ding, Z., Galván-Ampudia, C.S., Demarsy, E., Łangowski, Ł., Kleine-Vehn, J., Fan, Y., Morita, M.T., Tasaka, M., Fankhauser, C., Offringa, R. and Friml, J., 2011. Light-mediated polarization of the PIN3 auxin transporter for the phototropic response in Arabidopsis. *Nature Cell Biology*, *13*(4), pp.447-452.

Dixon, K.W., Merritt, D.J., Flematti, G.R. and Ghisalberti, E.L., 2009. Karrikinolide–a phytoreactive compound derived from smoke with applications in horticulture, ecological restoration and agriculture. *Acta Horticulturae*, *813*, pp.155-170.

Donaldson, L., 2020. Autofluorescence in plants. *Molecules*, *25*(10), p.2393.

Dos Santos Maraschin, F., Memelink, J. and Offringa, R., 2009. Auxin-induced, SCFTIR1-mediated poly-ubiquitination marks AUX/IAA proteins for degradation. *The Plant Journal*, *59*(1), pp.100-109.

Du, Y. and Scheres, B., 2018. Lateral root formation and the multiple roles of auxin. *Journal of Experimental Botany*, *69*(2), pp.155-167.

Dubrovsky, J.G., Sauer, M., Napsucialy-Mendivil, S., Ivanchenko, M.G., Friml, J., Shishkova, S., Celenza, J. and Benková, E., 2008. Auxin acts as a local morphogenetic trigger to specify lateral root founder cells. *Proceedings of the National Academy of Sciences*, *105*(25), pp.8790-8794.

Dun, E.A., de Saint Germain, A., Rameau, C. and Beveridge, C.A., 2012. Antagonistic action of strigolactone and cytokinin in bud outgrowth control. *Plant Physiology*, *158*(1), pp.487-498.

Fankhauser, C. and Christie, J.M., 2015. Plant phototropic growth. *Current Biology*, *25*(9), pp.R384-R389.

Feraru, E., Vosolsobě, S., Feraru, M.I., Petrášek, J. and Kleine-Vehn, J., 2012. Evolution and structural diversification of PILS putative auxin carriers in plants. *Frontiers in Plant Science*, *3*, p.227.

Flematti, G.R., Ghisalberti, E.L., Dixon, K.W. and Trengove, R.D., 2004. A compound from smoke that promotes seed germination. *Science*, *305*(5686), pp.977-977.

Flematti, G.R., Ghisalberti, E.L., Dixon, K.W. and Trengove, R.D., 2009. Identification of alkyl substituted 2 H-furo [2, 3-c] pyran-2-ones as germination stimulants present in smoke. *Journal of Agricultural and Food Chemistry*, *57*(20), pp.9475-9480.

Flematti, G.R., Goddard-Borger, E.D., Merritt, D.J., Ghisalberti, E.L., Dixon, K.W. and Trengove, R.D., 2007. Preparation of 2 H-furo [2, 3-c] pyran-2-one derivatives and evaluation of their germination-promoting activity. *Journal of Agricultural and Food Chemistry*, *55*(6), pp.2189-2194.

Foo, E., Bullier, E., Goussot, M., Foucher, F., Rameau, C. and Beveridge, C.A., 2005. The branching gene RAMOSUS1 mediates interactions among two novel signals and auxin in pea. *The Plant Cell*, *17*(2), pp.464-474.

Friml, J., Benková, E., Blilou, I., Wisniewska, J., Hamann, T., Ljung, K., Woody, S., Sandberg, G., Scheres, B., Jürgens, G. and Palme, K., 2002a. AtPIN4 mediates sink-driven auxin gradients and root patterning in Arabidopsis. *Cell*, *108*(5), pp.661-673.

Friml, J., Vieten, A., Sauer, M., Weijers, D., Schwarz, H., Hamann, T., Offringa, R. and Jürgens, G., 2003. Efflux-dependent auxin gradients establish the apical–basal axis of Arabidopsis. *Nature*, *426*(6963), pp.147-153.

Friml, J., Wiśniewska, J., Benková, E., Mendgen, K. and Palme, K., 2002b. Lateral relocation of auxin efflux regulator PIN3 mediates tropism in Arabidopsis. *Nature*, *415*(6873), pp.806-809.

Friml, J., Yang, X., Michniewicz, M., Weijers, D., Quint, A., Tietz, O., Benjamins, R., Ouwerkerk, P.B., Ljung, K., Sandberg, G. and Hooykaas, P.J., 2004. A PINOID-dependent binary switch in apical-basal PIN polar targeting directs auxin efflux. *Science*, *306*(5697), pp.862-865.

Galweiler, L., Guan, C., Muller, A., Wisman, E., Mendgen, K., Yephremov, A. and Palme, K., 1998. Regulation of polar auxin transport by AtPIN1 in Arabidopsis vascular tissue. *Science*, *282*(5397), pp.2226-2230.

Ganguly, A., Park, M., Kesawat, M.S. and Cho, H.T., 2014. Functional analysis of the hydrophilic loop in intracellular trafficking of Arabidopsis PIN-FORMED proteins. *The Plant Cell*, *26*(4), pp.1570-1585.

García-González, J., Lacek, J., Weckwerth, W. and Retzer, K., 2021. Exogenous carbon source supplementation counteracts root and hypocotyl growth limitations under increased cotyledon shading, with glucose and sucrose differentially modulating growth curves. *Plant Signaling & Behavior*, *16*(11), p.1969818.

Geisler, M., Blakeslee, J.J., Bouchard, R., Lee, O.R., Vincenzetti, V., Bandyopadhyay, A., Titapiwatanakun, B., Peer, W.A., Bailly, A., Richards, E.L. and Ejendal, K.F., 2005. Cellular efflux of auxin catalyzed by the Arabidopsis MDR/PGP transporter AtPGP1. *The Plant Journal*, *44*(2), pp.179-194.

Gommers CMM, Monte E. (2018). Seedling Establishment: A Dimmer Switch-Regulated Process between Dark and Light Signaling. *Plant Physiology*, 176, 1061-1074.

Gray, W.M., Kepinski, S., Rouse, D., Leyser, O. and Estelle, M., 2001. Auxin regulates SCFTIR1-dependent degradation of AUX/IAA proteins. *Nature*, *414*(6861), pp.271-276.

Guilfoyle, T.J. and Hagen, G., 2007. Auxin response factors. *Current Opinion in Plant Biology*, *10*(5), pp.453-460.

Guo, S., Xu, Y., Liu, H., Mao, Z., Zhang, C., Ma, Y., Zhang, Q., Meng, Z. and Chong, K., 2013. The interaction between OsMADS57 and OsTB1 modulates rice tillering via DWARF14. *Nature Communications*, *4*(1), pp.1-12.

Gutjahr, C., Gobbato, E., Choi, J., Riemann, M., Johnston, M.G., Summers, W., Carbonnel, S., Mansfield, C., Yang, S.Y., Nadal, M. and Acosta, I., 2015. Rice perception of symbiotic arbuscular mycorrhizal fungi requires the karrikin receptor complex. *Science*, *350*(6267), pp.1521-1524.

Halliday, K.J., Martínez-García, J.F. and Josse, E.M., 2009. Integration of light and auxin signaling. *Cold Spring Harbor perspectives in biology*, *1*(6), p.a001586.

Hamiaux, C., Drummond, R.S., Janssen, B.J., Ledger, S.E., Cooney, J.M., Newcomb, R.D. and Snowden, K.C., 2012. DAD2 is an α/β hydrolase likely to be involved in the perception of the plant branching hormone, strigolactone. *Current Biology*, *22*(21), pp.2032-2036.

Hayward, A., Stirnberg, P., Beveridge, C. and Leyser, O., 2009. Interactions between auxin and strigolactone in shoot branching control. *Plant Physiology*, *151*(1), pp.400-412.

He, W., Brumos, J., Li, H., Ji, Y., Ke, M., Gong, X., Zeng, Q., Li, W., Zhang, X., An, F. and Wen, X., 2011. A small-molecule screen identifies L-kynurenine as a

competitive inhibitor of TAA1/TAR activity in ethylene-directed auxin biosynthesis and root growth in Arabidopsis. *The Plant Cell*, *23*(11), pp.3944-3960.

Heller, R., Esnault, R., and Lance, C. 2004. Physiologie végétale, *Dunod, 6ème édition,* 65-67*.*

Honkanen, S. and Dolan, L., 2016. Growth regulation in tip-growing cells that develop on the epidermis. *Current opinion in plant biology*, *34*, pp.77-83.

Hopkins, W. G., 2003. Physiologie végétale*, De boeck, 2ème édition,* 310-311*.*

Jackson RG, Lim EK, Li Y, Kowalczyk M, Sandberg G, Hoggett J, Ashford DA, Bowles DJ. 2001. Identification and biochemical characterization of an Arabidopsis indole-3-acetic acid glucosyltransferase. *J Biol Chem*. 276(6):4350-6.

Jennifer J. Holland, Diana Roberts, Emmanuel Liscum, 2009. Understanding phototropism: from Darwin to today, *Journal of Experimental Botany,* Volume 60, Issue 7, , Pages 1969–1978*.*

Jensen, P.J., Hangarter, R.P. and Estelle, M., 1998. Auxin transport is required for hypocotyl elongation in light-grown but not dark-grown Arabidopsis. *Plant Physiology*, *116*(2), pp.455-462.

Jiang, L., Liu, X., Xiong, G., Liu, H., Chen, F., Wang, L., Meng, X., Liu, G., Yu, H., Yuan, Y. and Yi, W., 2013. DWARF 53 acts as a repressor of strigolactone signalling in rice. *Nature*, *504*(7480), pp.401-405.

Jiang, L., Matthys, C., Marquez-Garcia, B., De Cuyper, C., Smet, L., De Keyser, A., Boyer, F.D., Beeckman, T., Depuydt, S. and Goormachtig, S., 2016. Strigolactones spatially influence lateral root development through the cytokinin signaling network. *Journal of Experimental Botany*, *67*(1), pp.379-389.

Jones, A.R., Kramer, E.M., Knox, K., Swarup, R., Bennett, M.J., Lazarus, C.M., Leyser, H.M. and Grierson, C.S., 2009. Auxin transport through non-hair cells sustains root-hair development. *Nature Cell Biology*, *11*(1), pp.78-84.

Jonsson, K., Lathe, R.S., Kierzkowski, D., Routier-Kierzkowska, A.L., Hamant, O. and Bhalerao, R.P., 2021. Mechanochemical feedback mediates tissue bending required for seedling emergence. *Current Biology*, *31*(6), pp.1154-1164.

Kagiyama, M., Hirano, Y., Mori, T., Kim, S.Y., Kyozuka, J., Seto, Y., Yamaguchi, S. and Hakoshima, T., 2013. Structures of D 14 and D 14 L in the strigolactone and karrikin signaling pathways. *Genes to Cells*, *18*(2), pp.147-160.

Kapulnik, Y., Delaux, P.M., Resnick, N., Mayzlish-Gati, E., Wininger, S., Bhattacharya, C., Séjalon-Delmas, N., Combier, J.P., Bécard, G., Belausov, E. and Beeckman, T., 2011. Strigolactones affect lateral root formation and root-hair elongation in Arabidopsis. *Planta*, *233*(1), pp.209-216.

Kepinski, S. and Leyser, O., 2005. The Arabidopsis F-box protein TIR1 is an auxin receptor. *Nature*, *435*(7041), pp.446-451.

Khosla, A., Morffy, N., Li, Q., Faure, L., Chang, S.H., Yao, J., Zheng, J., Cai, M.L., Stanga, J., Flematti, G.R. and Waters, M.T., 2020. Structure–function analysis of SMAX1 reveals domains that mediate its karrikin-induced proteolysis and interaction with the receptor KAI2. *Plant Cell*, *32*(8), pp.2639-2659.

Kircher, S. and Schopfer, P., 2012. Photosynthetic sucrose acts as cotyledon-derived long-distance signal to control root growth during early seedling development in Arabidopsis. *Proceedings of the National Academy of Sciences*, *109*(28), pp.11217-11221.

Kleine-Vehn, J., Dhonukshe, P., Swarup, R., Bennett, M. and Friml, J., 2006. Subcellular trafficking of the Arabidopsis auxin influx carrier AUX1 uses a novel pathway distinct from PIN1. *The Plant Cell*, *18*(11), pp.3171-3181.

Kleine-Vehn, J., Ding, Z., Jones, A.R., Tasaka, M., Morita, M.T. and Friml, J., 2010. Gravity-induced PIN transcytosis for polarization of auxin fluxes in gravity-sensing root cells. *Proceedings of the National Academy of Sciences*, *107*(51), pp.22344-22349.

Kleine-Vehn, J., Łangowski, Ł., Wiśniewska, J., Dhonukshe, P., Brewer, P.B. and Friml, J., 2008. Cellular and molecular requirements for polar PIN targeting and transcytosis in plants. *Molecular Plant*, *1*(6), pp.1056-1066.

Kogl F, Haagen-Smits AJ. I. 1931. Mitteilung uber pflanzliche wachstumsstoffe. Uber die vhemie des euchsstoffs, *Proceedings Koninklijke Nederlandse Akademie van Wetenschappen*, vol. 34 (pg. 1411-1416)

Koltai, H., 2011. Strigolactones are regulators of root development. *New Phytologist*, *190*(3), pp.545-549.

Krouk, G., Lacombe, B., Bielach, A., Perrine-Walker, F., Malinska, K., Mounier, E., Hoyerova, K., Tillard, P., Leon, S., Ljung, K. and Zazimalova, E., 2010. Nitrate-regulated auxin transport by NRT1. 1 defines a mechanism for nutrient sensing in plants. *Developmental Cell*, *18*(6), pp.927-937.

Lakehal, A., Chaabouni, S., Cavel, E., Le Hir, R., Ranjan, A., Raneshan, Z., Novák, O., Păcurar, D.I., Perrone, I., Jobert, F. and Gutierrez, L., 2019. A molecular framework for the control of adventitious rooting by TIR1/AFB2-Aux/IAA-dependent auxin signaling in Arabidopsis. *Molecular plant*, *12*(11), pp.1499-1514.

Lavenus, J., Goh, T., Roberts, I., Guyomarc'h, S., Lucas, M., De Smet, I., Fukaki, H., Beeckman, T., Bennett, M. and Laplaze, L., 2013. Lateral root development in Arabidopsis: fifty shades of auxin. *Trends in Plant Science*, *18*(8), pp.450-458.

Laxmi, A., Pan, J., Morsy, M. and Chen, R., 2008. Light plays an essential role in intracellular distribution of auxin efflux carrier PIN2 in Arabidopsis thaliana. *PloS one*, *3*(1), p.e1510.

Lee I, Choi S, Lee S, Soh MS. 2019. KAI2-KL signaling intersects with light-signaling for photomorphogenesis. *Plant Signal Behaviour* 14, e1588660.

Lewis DR, Muday GK. (2009). Measurement of auxin transport in Arabidopsis thaliana. *Nature Protocols* 4, 437-51.

Leyser, O., 2018. Auxin signaling. *Plant Physiology*, *176*(1), pp.465-479.

Li L, Verstraeten I, Roosjen M, Takahashi K, Rodriguez L, Merrin J, Chen J, Shabala L, Smet W, Ren H, Vanneste S, Shabala S, De Rybel B, Weijers D, Kinoshita T, Gray WM, Friml J. (2021). Cell surface and intracellular auxin signalling for H(+) fluxes in root growth. *Nature* 599, 273-277

Li, W., Nguyen, K.H., Chu, H.D., Ha, C.V., Watanabe, Y., Osakabe, Y., Leyva-González, M.A., Sato, M., Toyooka, K., Voges, L. and Tanaka, M., 2017. The karrikin receptor KAI2 promotes drought resistance in Arabidopsis thaliana. *PLoS Genetics*, *13*(11), p.e1007076.

Liang, Y., Ward, S., Li, P., Bennett, T. and Leyser, O., 2016. SMAX1-LIKE7 signals from the nucleus to regulate shoot development in Arabidopsis via partially EAR motif-independent mechanisms. *The Plant Cell*, *28*(7), pp.1581-1601.

Lin W, Zhou X, Tang W, Takahashi K, Pan X, Dai J, Ren H, Zhu X, Pan S, Zheng H, Gray WM, Xu T, Kinoshita T, Yang Z. (2021). TMK-based cell-surface auxin signalling activates cell-wall acidification. *Nature,* 599, pp.278-282.

Liu, J., Cheng, X., Liu, P. and Sun, J., 2017. miR156-targeted SBP-box transcription factors interact with DWARF53 to regulate TEOSINTE BRANCHED1 and BARREN STALK1 expression in bread wheat. *Plant Physiology*, *174*(3), pp.1931-1948.

Ljung, K., 2013. Auxin metabolism and homeostasis during plant development. *Development*, *140*(5), pp.943-950.

Ljung, K., Bhalerao, R.P. and Sandberg, G., 2001. Sites and homeostatic control of auxin biosynthesis in Arabidopsis during vegetative growth. *The Plant Journal*, *28*(4), pp.465-474.

López-Ráez, J.A., Charnikhova, T., Gómez-Roldán, V., Matusova, R., Kohlen, W., De Vos, R., Verstappen, F., Puech-Pages, V., Bécard, G., Mulder, P. and Bouwmeester, H., 2008. Tomato strigolactones are derived from carotenoids and their biosynthesis is promoted by phosphate starvation. *New Phytologist*, *178*(4), pp.863-874.

Luschnig, C., Gaxiola, R.A., Grisafi, P. and Fink, G.R., 1998. EIR1, a root-specific protein involved in auxin transport, is required for gravitropism inArabidopsis thaliana. *Genes & Development*, *12*(14), pp.2175-2187.

Ma, H., Duan, J., Ke, J., He, Y., Gu, X., Xu, T.H., Yu, H., Wang, Y., Brunzelle, J.S., Jiang, Y. and Rothbart, S.B., 2017. A D53 repression motif induces oligomerization of TOPLESS corepressors and promotes assembly of a corepressor-nucleosome complex. *Science Advances*, *3*(6), p.e1601217.

MacGregor, D.R., Deak, K.I., Ingram, P.A. and Malamy, J.E., 2008. Root system architecture in Arabidopsis grown in culture is regulated by sucrose uptake in the aerial tissues. *The Plant Cell*, *20*(10), pp.2643-2660.

Machin, D.C., Hamon-Josse, M. and Bennett, T., 2020. Fellowship of the rings: a saga of strigolactones and other small signals. *New Phytologist*, *225*(2), pp.621-636.

Maloof, J.N., Borevitz, J.O., Dabi, T., Lutes, J., Nehring, R.B., Redfern, J.L., Trainer, G.T., Wilson, J.M., Asami, T., Berry, C.C. and Weigel, D., 2001. Natural variation in light sensitivity of Arabidopsis. *Nature Genetics*, *29*(4), pp.441-446.

Marhavý, P., Vanstraelen, M., De Rybel, B., Zhaojun, D., Bennett, M.J., Beeckman, T. and Benková, E., 2013. Auxin reflux between the endodermis and pericycle promotes lateral root initiation. *The EMBO Journal*, *32*(1), pp.149-158.

Martin-Arevalillo, R., Nanao, M.H., Larrieu, A., Vinos-Poyo, T., Mast, D., Galvan-Ampudia, C., Brunoud, G., Vernoux, T., Dumas, R. and Parcy, F., 2017. Structure of the Arabidopsis TOPLESS corepressor provides insight into the evolution of transcriptional repression. *Proceedings of the National Academy of Sciences*, *114*(30), pp.8107-8112.

Marzec, M. and Melzer, M., 2018. Regulation of root development and architecture by strigolactones under optimal and nutrient deficiency conditions. *International Journal of Molecular Sciences*, *19*(7), p.1887.

Marzec, M., Gruszka, D., Tylec, P. and Szarejko, I., 2016. Identification and functional analysis of the HvD14 gene involved in strigolactone signaling in Hordeum vulgare. *Physiologia Plantarum*, *158*(3), pp.341-355.

Mashiguchi, K., Tanaka, K., Sakai, T., Sugawara, S., Kawaide, H., Natsume, M., Hanada, A., Yaeno, T., Shirasu, K., Yao, H. and McSteen, P., 2011. The main auxin biosynthesis pathway in Arabidopsis. *Proceedings of the National Academy of Sciences*, *108*(45), pp.18512-18517.

Mayzlish-Gati, E., De-Cuyper, C., Goormachtig, S., Beeckman, T., Vuylsteke, M., Brewer, P.B., Beveridge, C.A., Yermiyahu, U., Kaplan, Y., Enzer, Y. and Wininger, S., 2012. Strigolactones are involved in root response to low phosphate conditions in Arabidopsis. *Plant Physiology*, *160*(3), pp.1329-1341.

Meng, Y., Varshney, K., Incze, N., Badics, E., Kamran, M., Davies, S.F., Oppermann, L.M., Magne, K., Dalmais, M., Bendahmane, A. and Sibout, R., 2021. KARRIKIN INSENSITIVE2 regulates leaf development, root system architecture and arbuscular-mycorrhizal symbiosis in Brachypodium distachyon. *The Plant Journal*, 109(6), pp.1559-1574.

Mishra, B.S., Singh, M., Aggrawal, P. and Laxmi, A., 2009. Glucose and auxin signaling interaction in controlling Arabidopsis thaliana seedlings root growth and development. *PloS one*, *4*(2), p.e4502.

Miura, K., Ikeda, M., Matsubara, A., Song, X.J., Ito, M., Asano, K., Matsuoka, M., Kitano, H. and Ashikari, M., 2010. OsSPL14 promotes panicle branching and higher grain productivity in rice. *Nature Genetics*, *42*(6), pp.545-549.

Mizuno, Y., Komatsu, A., Shimazaki, S., Naramoto, S., Inoue, K., Xie, X., Ishizaki, K., Kohchi, T. and Kyozuka, J., 2021. Major components of the KARRIKIN INSENSITIVE2-dependent signaling pathway are conserved in the liverwort Marchantia polymorpha. *The Plant Cell*, *33*(7), pp.2395-2411.

Moturu, T.R., Thula, S., Singh, R.K., Nodzyński, T., Vařeková, R.S., Friml, J. and Simon, S., 2018. Molecular evolution and diversification of the SMXL gene family. *Journal of Experimental Botany*, *69*(9), pp.2367-2378.

Mravec, J., Skůpa, P., Bailly, A., Hoyerová, K., Křeček, P., Bielach, A., Petrášek, J., Zhang, J., Gaykova, V., Stierhof, Y.D. and Dobrev, P.I., 2009. Subcellular homeostasis of phytohormone auxin is mediated by the ER-localized PIN5 transporter. *Nature*, *459*(7250), pp.1136-1140.

Nelson, D.C., Flematti, G.R., Riseborough, J.A., Ghisalberti, E.L., Dixon, K.W. and Smith, S.M., 2010. Karrikins enhance light responses during germination and seedling development in Arabidopsis thaliana. *Proceedings of the National Academy of Sciences*, *107*(15), pp.7095-7100.

Nelson, D.C., Riseborough, J.A., Flematti, G.R., Stevens, J., Ghisalberti, E.L., Dixon, K.W. and Smith, S.M., 2009. Karrikins discovered in smoke trigger Arabidopsis seed germination by a mechanism requiring gibberellic acid synthesis and light. *Plant Physiology*, 149(2), pp.863-873.

Nelson, D.C., Scaffidi, A., Dun, E.A., Waters, M.T., Flematti, G.R., Dixon, K.W., Beveridge, C.A., Ghisalberti, E.L. and Smith, S.M., 2011. F-box protein MAX2 has dual roles in karrikin and strigolactone signaling in Arabidopsis thaliana. Proceedings of the National Academy of Sciences, 108(21), pp.8897-8902.

Omelyanchuk, N.A., Kovrizhnykh, V.V., Oshchepkova, E.A., Pasternak, T., Palme, K. and Mironova, V.V., 2016. A detailed expression map of the PIN1 auxin transporter in Arabidopsis thaliana root. *BMC Plant Biology*, *16*(1), pp.1-12.

Pandya-Kumar, N., Shema, R., Kumar, M., Mayzlish-Gati, E., Levy, D., Zemach, H., Belausov, E., Wininger, S., Abu-Abied, M., Kapulnik, Y. and Koltai, H., 2014. Strigolactone analog GR 24 triggers changes in PIN 2 polarity, vesicle trafficking and actin filament architecture. *New Phytologist*, *202*(4), pp.1184-1196.

Park, J.Y., Kim, H.J. and Kim, J., 2002. Mutation in domain II of IAA1 confers diverse auxin-related phenotypes and represses auxin-activated expression of Aux/IAA genes in steroid regulator-inducible system. *The Plant Journal*, *32*(5), pp.669-683.

Peer, W.A., Cheng, Y. and Murphy, A.S., 2013. Evidence of oxidative attenuation of auxin signalling. *Journal of Experimental Botany*, *64*(9), pp.2629-2639.

Pěnčík, A., Simonovik, B., Petersson, S.V., Henyková, E., Simon, S., Greenham, K., Zhang, Y., Kowalczyk, M., Estelle, M., Zažímalová, E. and Novák, O., 2013. Regulation of auxin homeostasis and gradients in Arabidopsis roots through the formation of the indole-3-acetic acid catabolite 2-oxindole-3-acetic acid. *The Plant Cell*, 25(10), pp.3858-3870.

Péret, B., Clément, M., Nussaume, L. and Desnos, T., 2011. Root developmental adaptation to phosphate starvation: better safe than sorry. *Trends in Plant Science*, *16*(8), pp.442-450.

Péret, B., Middleton, A.M., French, A.P., Larrieu, A., Bishopp, A., Njo, M., Wells, D.M., Porco, S., Mellor, N., Band, L.R. and Casimiro, I., 2013. Sequential induction of auxin efflux and influx carriers regulates lateral root emergence. *Molecular systems biology*, *9*(1), p.699.

Péret, B., Swarup, K., Ferguson, A., Seth, M., Yang, Y., Dhondt, S., James, N., Casimiro, I., Perry, P., Syed, A. and Yang, H., 2012. AUX/LAX genes encode a family of auxin influx transporters that perform distinct functions during Arabidopsis development. *The Plant Cell*, *24*(7), pp.2874-2885.

Petrásek, J. and Friml, J., 2009. Auxin transport routes in plant development. *Development*, 136 (16): 2675–2688.

Petrásek, J., Mravec, J., Bouchard, R., Blakeslee, J.J., Abas, M., Seifertová, D., Wisniewska, J., Tadele, Z., Kubes, M., Covanová, M. and Dhonukshe, P., 2006. PIN proteins perform a rate-limiting function in cellular auxin efflux. *Science*, *312*(5775), pp.914-918.

Prigge, M.J., Greenham, K., Zhang, Y., Santner, A., Castillejo, C., Mutka, A.M., O'Malley, R.C., Ecker, J.R., Kunkel, B.N. and Estelle, M., 2016. The Arabidopsis auxin receptor F-box proteins AFB4 and AFB5 are required for response to the synthetic auxin picloram. G3: Genes, Genomes, Genetics, 6(5), pp.1383-1390.

Rameau, C., Goormachtig, S., Cardinale, F., Bennett, T. and Cubas, P., 2019. Strigolactones as plant hormones. In *Strigolactones-biology and applications* (pp. 47-87). Springer, Cham.

Rasmussen, A., Mason, M.G., De Cuyper, C., Brewer, P.B., Herold, S., Agusti, J., Geelen, D., Greb, T., Goormachtig, S., Beeckman, T. and Beveridge, C.A., 2012. Strigolactones suppress adventitious rooting in Arabidopsis and pea. *Plant Physiology*, *158*(4), pp.1976-1987.

Raven, J.A., 1975. Transport of indoleacetic acid in plant cells in relation to pH and electrical potential gradients, and its significance for polar IAA transport. *New Phytologist*, *74*(2), pp.163-172.

Retzer, K. and Weckwerth, W., 2021. The tor–auxin connection upstream of root hair growth. *Plants*, *10*(1), p.150.

Rouached, H., Arpat, A.B. and Poirier, Y., 2010. Regulation of phosphate starvation responses in plants: signaling players and cross-talks. *Molecular Plant*, *3*(2), pp.288-299.

Roy, R. and Bassham, D.C., 2014. Root growth movements: waving and skewing. *Plant Science*, *221*, pp.42-47.

Roycewicz, P. and Malamy, J.E., 2012. Dissecting the effects of nitrate, sucrose and osmotic potential on Arabidopsis root and shoot system growth in laboratory

assays. *Philosophical Transactions of the Royal Society B: Biological Sciences*, *367*(1595), pp.1489-1500.

Roychoudhry, S. and Kepinski, S., 2021. Auxin in Root Development. *Cold Spring Harbor Perspectives in Biology*, p.a039933.

Roychoudhry, S., Kieffer, M., Del Bianco, M., Liao, C.Y., Weijers, D. and Kepinski, S., 2017. The developmental and environmental regulation of gravitropic setpoint angle in Arabidopsis and bean. *Scientific Reports*, *7*(1), pp.1-12.

Ruyter-Spira, C., Kohlen, W., Charnikhova, T., van Zeijl, A., van Bezouwen, L., de Ruijter, N., Cardoso, C., Lopez-Raez, J.A., Matusova, R., Bours, R. and Verstappen, F., 2011. Physiological effects of the synthetic strigolactone analog GR24 on root system architecture in Arabidopsis: another belowground role for strigolactones?. *Plant Physiology*, *155*(2), pp.721-734.

Sairanen, I., Novák, O., Pěnčík, A., Ikeda, Y., Jones, B., Sandberg, G. and Ljung, K., 2012. Soluble carbohydrates regulate auxin biosynthesis via PIF proteins in Arabidopsis. *The Plant Cell*, *24*(12), pp.4907-4916.

Sami A, Riaz MW, Zhou X, Zhu Z, Zhou K. (2019). Alleviating dormancy in Brassica oleracea seeds using NO and KAR1 with ethylene biosynthetic pathway, ROS and antioxidant enzymes modifications. *BMC Plant Biology* 19, 577.

Sassi, M., Lu, Y., Zhang, Y., Wang, J., Dhonukshe, P., Blilou, I., Dai, M., Li, J., Gong, X., Jaillais, Y. and Yu, X., 2012. COP1 mediates the coordination of root and shoot growth by light through modulation of PIN1-and PIN2-dependent auxin transport in Arabidopsis. *Development*, *139*(18), pp.3402-3412.

Sauer, M. and Kleine-Vehn, J., 2019. PIN-FORMED and PIN-LIKES auxin transport facilitators. *Development*, *146*(15), p.dev168088.

Scaffidi, A., Waters, M.T., Ghisalberti, E.L., Dixon, K.W., Flematti, G.R. and Smith, S.M., 2013. Carlactone-independent seedling morphogenesis in Arabidopsis. *The Plant Journal*, *76*(1), pp.1-9.

Scaffidi, A., Waters, M.T., Sun, Y.K., Skelton, B.W., Dixon, K.W., Ghisalberti, E.L., Flematti, G.R. and Smith, S.M., 2014. Strigolactone hormones and their stereoisomers signal through two related receptor proteins to induce different physiological responses in Arabidopsis. *Plant Physiology*, *165*(3), pp.1221-1232.

Schöller, M., Sarkel, E., Kleine-Vehn, J. and Feraru, E., 2018. Growth rate normalization method to assess gravitropic root growth. In *Root Development* (pp. 199-208). Humana Press, New York, NY.

Schwartz, S.H., Qin, X. and Loewen, M.C., 2004. The biochemical characterization of two carotenoid cleavage enzymes from Arabidopsis indicates that a carotenoid-derived compound inhibits lateral branching. *Journal of Biological Chemistry*, *279*(45), pp.46940-46945.

Seale, M., Bennett, T. and Leyser, O., 2017. BRC1 expression regulates bud activation potential but is not necessary or sufficient for bud growth inhibition in Arabidopsis. *Development*, *144*(9), pp.1661-1673.

Sepulveda, C., Guzmán, M.A., Li, Q., Villaécija-Aguilar, J.A., Martinez, S.E., Kamran, M., Khosla, A., Liu, W., Gendron, J.M., Gutjahr, C. and Waters, M.T., 2022. KARRIKIN UP-REGULATED F-BOX 1 (KUF1) imposes negative feedback regulation of karrikin and KAI2 ligand metabolism in Arabidopsis thaliana. *Proceedings of the National Academy of Sciences*, *119*(11), p.e2112820119.

Seto, Y., Sado, A., Asami, K., Hanada, A., Umehara, M., Akiyama, K. and Yamaguchi, S., 2014. Carlactone is an endogenous biosynthetic precursor for strigolactones. *Proceedings of the National Academy of Sciences*, *111*(4), pp.1640-1645.

Shen, H., Zhu, L., Bu, Q.Y. and Huq, E., 2012. MAX2 affects multiple hormones to promote photomorphogenesis. *Molecular Plant*, *5*(3), pp.750-762.

Shinohara, N., Taylor, C. and Leyser, O., 2013. Strigolactone can promote or inhibit shoot branching by triggering rapid depletion of the auxin efflux protein PIN1 from the plasma membrane. *PLoS Biology*, *11*(1), p.e1001474.

Sieberer, T., Seifert, G.J., Hauser, M.T., Grisafi, P., Fink, G.R. and Luschnig, C., 2000. Post-transcriptional control of the Arabidopsis auxin efflux carrier EIR1 requires AXR1. *Current Biology*, *10*(24), pp.1595-1598.

Simon, S. and Petrášek, J., 2011. Why plants need more than one type of auxin. *Plant Science*, *180*(3), pp.454-460.

Smalle, J. and Vierstra, R.D., 2004. The ubiquitin 26S proteasome proteolytic pathway. *Annu. Rev. Plant Biol.*, *55*, pp.555-590.

Song, X., Lu, Z., Yu, H., Shao, G., Xiong, J., Meng, X., Jing, Y., Liu, G., Xiong, G., Duan, J. and Yao, X.F., 2017. IPA1 functions as a downstream transcription factor repressed by D53 in strigolactone signaling in rice. *Cell Research*, *27*(9), pp.1128-1141.

Sorin, C., Bussell, J.D., Camus, I., Ljung, K., Kowalczyk, M., Geiss, G., McKhann, H., Garcion, C., Vaucheret, H., Sandberg, G. and Bellini, C., 2005. Auxin and light control of adventitious rooting in Arabidopsis require ARGONAUTE1. *The Plant Cell*, *17*(5), pp.1343-1359.

Soundappan, I., Bennett, T., Morffy, N., Liang, Y., Stanga, J.P., Abbas, A., Leyser, O. and Nelson, D.C., 2015. SMAX1-LIKE/D53 family members enable distinct MAX2-dependent responses to strigolactones and karrikins in Arabidopsis. *The Plant Cell*, *27*(11), pp.3143-3159.

Stanga, J.P., Morffy, N. and Nelson, D.C., 2016. Functional redundancy in the control of seedling growth by the karrikin signaling pathway. *Planta*, *243*(6), pp.1397-1406.

Stanga, J.P., Smith, S.M., Briggs, W.R. and Nelson, D.C., 2013. SUPPRESSOR OF MORE AXILLARY GROWTH2 1 controls seed germination and seedling development in Arabidopsis. *Plant Physiology*, *163*(1), pp.318-330.

Staswick, P.E., Serban, B., Rowe, M., Tiryaki, I., Maldonado, M.T., Maldonado, M.C. and Suza, W., 2005. Characterization of an Arabidopsis enzyme family that conjugates amino acids to indole-3-acetic acid. *The Plant Cell*, *17*(2), pp.616-627.

Steffens, B. and Rasmussen, A., 2016. The physiology of adventitious roots. *Plant Physiology*, *170*(2), pp.603-617.

Stepanova, A.N., Yun, J., Robles, L.M., Novak, O., He, W., Guo, H., Ljung, K. and Alonso, J.M., 2011. The Arabidopsis YUCCA1 flavin monooxygenase functions in the indole-3-pyruvic acid branch of auxin biosynthesis. *The Plant Cell*, *23*(11), pp.3961-3973.

Stirnberg, P., Furner, I.J. and Ottoline Leyser, H.M., 2007. MAX2 participates in an SCF complex which acts locally at the node to suppress shoot branching. *The Plant Journal*, *50*(1), pp.80-94.

Strader, L.C. and Bartel, B., 2008. A new path to auxin. *Nature Chemical Biology*, *4*(6), pp.337-339.

Sun, H., Tao, J., Hou, M., Huang, S., Chen, S., Liang, Z., Xie, T., Wei, Y., Xie, X., Yoneyama, K. and Xu, G., 2015. A strigolactone signal is required for adventitious root formation in rice. *Annals of Botany*, *115*(7), pp.1155-1162.

Sun, H., Tao, J., Liu, S., Huang, S., Chen, S., Xie, X., Yoneyama, K., Zhang, Y. and Xu, G., 2014. Strigolactones are involved in phosphate-and nitrate-deficiency-induced root development and auxin transport in rice. *Journal of Experimental Botany*, *65*(22), pp.6735-6746.

Sun, K., Chen, Y., Wagerle, T., Linnstaedt, D., Currie, M., Chmura, P., Song, Y. and Xu, M., 2008. Synthesis of butenolides as seed germination stimulants. *Tetrahedron Letters*, *49*(18), pp.2922-2925.

Sun, X.D. and Ni, M., 2011. HYPOSENSITIVE TO LIGHT, an alpha/beta fold protein, acts downstream of ELONGATED HYPOCOTYL 5 to regulate seedling de-etiolation. *Molecular Plant*, *4*(1), pp.116-126.

Swarbreck, S.M., Guerringue, Y., Matthus, E., Jamieson, F.J. and Davies, J.M., 2019. Impairment in karrikin but not strigolactone sensing enhances root skewing in Arabidopsis thaliana. *The Plant Journal*, *98*(4), pp.607-621.

Swarbreck, S.M., Mohammad-Sidik, A. and Davies, J.M., 2020. Common components of the strigolactone and karrikin signaling pathways suppress root branching in Arabidopsis. *Plant Physiology*, *184*(1), pp.18-22.

Swarup, R., Friml, J., Marchant, A., Ljung, K., Sandberg, G., Palme, K. and Bennett, M., 2001. Localization of the auxin permease AUX1 suggests two functionally distinct hormone transport pathways operate in the Arabidopsis root apex. *Genes & Development*, *15*(20), pp.2648-2653.

Symons GM, Reid JB. (2003). Hormone levels and response during de-etiolation in pea. *Planta* 216, 422-31.

Szemenyei, H., Hannon, M. and Long, J.A., 2008. TOPLESS mediates auxin-dependent transcriptional repression during Arabidopsis embryogenesis. *Science*, *319*(5868), pp.1384-1386.

Tan, X., Calderon-Villalobos, L.I.A., Sharon, M., Zheng, C., Robinson, C.V., Estelle, M. and Zheng, N., 2007. Mechanism of auxin perception by the TIR1 ubiquitin ligase. *Nature*, *446*(7136), pp.640-645.

Thussagunpanit, J., Nagai, Y., Nagae, M., Mashiguchi, K., Mitsuda, N., Ohme-Takagi, M., Nakano, T., Nakamura, H. and Asami, T., 2017. Involvement of STH7 in light-adapted development in Arabidopsis thaliana promoted by both strigolactone and karrikin. *Bioscience, Biotechnology, and Biochemistry*, *81*(2), pp.292-301.

Tiwari, S.B., Hagen, G. and Guilfoyle, T.J., 2004. Aux/IAA proteins contain a potent transcriptional repression domain. *The Plant Cell*, *16*(2), pp.533-543.

Toh, S., Holbrook-Smith, D., Stogios, P.J., Onopriyenko, O., Lumba, S., Tsuchiya, Y., Savchenko, A. and McCourt, P., 2015. Structure-function analysis identifies highly sensitive strigolactone receptors in Striga. *Science*, *350*(6257), pp.203-207.

Ulmasov, T., Murfett, J., Hagen, G. and Guilfoyle, T.J., 1997. Aux/IAA proteins repress expression of reporter genes containing natural and highly active synthetic auxin response elements. *The Plant Cell*, *9*(11), pp.1963-1971.

Umehara, M., Hanada, A., Yoshida, S., Akiyama, K., Arite, T., Takeda-Kamiya, N., Magome, H., Kamiya, Y., Shirasu, K., Yoneyama, K. and Kyozuka, J., 2008. Inhibition of shoot branching by new terpenoid plant hormones. *Nature*, *455*(7210), pp.195-200.

van Gelderen, K., Kang, C. and Pierik, R., 2018. Light signaling, root development, and plasticity. *Plant Physiology*, *176*(2), pp.1049-1060.

Van Rongen, M., Bennett, T., Ticchiarelli, F. and Leyser, O., 2019. Connective auxin transport contributes to strigolactone-mediated shoot branching control independent of the transcription factor BRC1. *PLoS Genetics*, *15*(3), p.e1008023.

Végh, A., Incze, N., Fábián, A., Huo, H., Bradford, K.J., Balázs, E. and Soós, V., 2017. Comprehensive analysis of DWARF14-LIKE2 (DLK2) reveals its functional divergence from strigolactone-related paralogs. *Frontiers in Plant Science*, *8*, p.1641.

Vermeer, J.E., von Wangenheim, D., Barberon, M., Lee, Y., Stelzer, E.H., Maizel, A. and Geldner, N., 2014. A spatial accommodation by neighboring cells is required for organ initiation in Arabidopsis. *Science*, *343*(6167), pp.178-183.

Viaene, T., Delwiche, C.F., Rensing, S.A. and Friml, J., 2013. Origin and evolution of PIN auxin transporters in the green lineage. *Trends in Plant Science*, *18*(1), pp.5-10.

Villalobos, L.I.A.C., Lee, S., De Oliveira, C., Ivetac, A., Brandt, W., Armitage, L., Sheard, L.B., Tan, X., Parry, G., Mao, H. and Zheng, N., 2012. A combinatorial TIR1/AFB–Aux/IAA co-receptor system for differential sensing of auxin. *Nature Chemical Biology*, 8(5), pp.477-485.

Villaecija-Aguilar JA, Hamon-Josse M, Carbonnel S, Kretschmar A, Schmidt C, Dawid C, Bennett T, Gutjahr C. (2019). SMAX1/SMXL2 regulate root and root hair development downstream of KAI2-mediated signalling in Arabidopsis. *PLoS Genetics* 15, e1008327

Villaécija-Aguilar JA, Struk S, Goormachtig S, Gutjahr C (2021b) Bioassays for the effect of strigolactones and other small molecules on root and root hair development. Methods in Molecular Biology 2309: 129-142. In: Prandi C, Cardinale F (eds.) Strigolactones: Methods and Protocols. Springer Nature, Switzerland.

Villaécija-Aguilar, J.A., Körösy, C., Maisch, L., Hamon-Josse, M., Petrich, A., Magosch, S., Chapman, P., Bennett, T. and Gutjahr, C., 2022. KAI2 promotes Arabidopsis root hair elongation at low external phosphate by controlling local accumulation of AUX1 and PIN2. *Current Biology*, *32*(1), pp.228-236.

Walker, CH., Siu-Ting, K., Taylor, A., O'Connell, MJ., Bennett, T., (2019). Strigolactone synthesis is ancestral in land plants, but canonical strigolactone signalling is a flowering plant innovation. *BMC Biology* 17, 70.

Wallner, E.S., López-Salmerón, V. and Greb, T., 2016. Strigolactone versus gibberellin signaling: reemerging concepts?. *Planta*, *243*(6), pp.1339-1350.

Wallner, E.S., López-Salmerón, V., Belevich, I., Poschet, G., Jung, I., Grünwald, K., Sevilem, I., Jokitalo, E., Hell, R., Helariutta, Y. and Agustí, J., 2017. Strigolactone-and karrikin-independent SMXL proteins are central regulators of phloem formation. *Current Biology*, *27*(8), pp.1241-1247.

Wang L, Wang B, Yu H, Guo H, Lin T, Kou L, Wang A, Shao N, Ma H, Xiong G, Li X, Yang J, Chu J, Li J. (2020a). Transcriptional regulation of strigolactone signalling in Arabidopsis. *Nature* 583, 277-281.

Wang L, Xu Q, Yu H, Ma H, Li X, Yang J, Chu J, Xie Q, Wang Y, Smith SM, Li J, Xiong G, Wang B. (2020b). Strigolactone and Karrikin Signaling Pathways Elicit Ubiquitination and Proteolysis of SMXL2 to Regulate Hypocotyl Elongation in Arabidopsis. Plant Cell 32, 2251-2270.

Wang, L., Wang, B., Jiang, L., Liu, X., Li, X., Lu, Z., Meng, X., Wang, Y., Smith, S.M. and Li, J., 2015. Strigolactone signaling in Arabidopsis regulates shoot development by targeting D53-like SMXL repressor proteins for ubiquitination and degradation. *The Plant Cell*, *27*(11), pp.3128-3142.

Wang, L., Waters, M.T. and Smith, S.M., 2018. Karrikin-KAI2 signalling provides Arabidopsis seeds with tolerance to abiotic stress and inhibits germination under

conditions unfavourable to seedling establishment. *New Phytologist*, *219*(2), pp.605-618.

Waters, M.T. and Smith, S.M., 2013. KAI2-and MAX2-mediated responses to karrikins and strigolactones are largely independent of HY5 in Arabidopsis seedlings. *Molecular Plant*, *6*(1), pp.63-75.

Waters, M.T., Nelson, D.C., Scaffidi, A., Flematti, G.R., Sun, Y.K., Dixon, K.W. and Smith, S.M., 2012. Specialisation within the DWARF14 protein family confers distinct responses to karrikins and strigolactones in Arabidopsis. *Development*, *139*(7), pp.1285-1295.

Waters, M.T., Scaffidi, A., Flematti, G. and Smith, S.M., 2015a. Substrate-induced degradation of the α/β-fold hydrolase KARRIKIN INSENSITIVE2 requires a functional catalytic triad but is independent of MAX2. *Molecular Plant*, *8*(5), pp.814-817.

Waters, M.T., Scaffidi, A., Moulin, S.L., Sun, Y.K., Flematti, G.R. and Smith, S.M., 2015b. A Selaginella moellendorffii ortholog of KARRIKIN INSENSITIVE2 functions in Arabidopsis development but cannot mediate responses to karrikins or strigolactones. *The Plant Cell*, *27*(7), pp.1925-1944.

Went FW. Wuchsstoff und Wachstum*,* 1928. *Receuil des Travaux Botaniques Neerlandais,* vol. 25 (pg. 1-116).

Wilson A, Pickett B, Turner J, Estelle M. (1990). A dominant mutation in Arabidopsis confers resistance to auxin, ethylene and abscisic acid. *Molecular and General Genetics* 222, 377–383.

Wisniewska, J., Xu, J., Seifertová, D., Brewer, P.B., Ruzicka, K., Blilou, I., Rouquié, D., Benková, E., Scheres, B. and Friml, J., 2006. Polar PIN localization directs auxin flow in plants. *Science*, *312*(5775), pp.883-883.

Won C, Shen X, Mashiguchi K, Zheng Z, Dai X, Cheng Y, Kasahara H, Kamiya Y, Chory J, Zhao Y (2011) Conversion of tryptophan to indole-3-acetic acid by TRYPTOPHAN AMINOTRANSFERASES OF ARABIDOPSIS and YUCCAs in Arabidopsis. Proc Natl Acad Sci USA 108: 18518–18523

Woodward, A.W. and Bartel, B., 2005. Auxin: regulation, action, and interaction. *Annals of Botany*, *95*(5), pp.707-735.

Xu J, Scheres B., 2005. Dissection of Arabidopsis ADP-RIBOSYLATION FACTOR 1 function in epidermal cell polarity. *Plant Cell* 17, 525-536.

Xu, M., Zhu, L., Shou, H. and Wu, P., 2005. A PIN1 family gene, OsPIN1, involved in auxin-dependent adventitious root emergence and tillering in rice. *Plant and Cell Physiology*, *46*(10), pp.1674-1681.

Yang, H. and Murphy, A.S., 2009. Functional expression and characterization of Arabidopsis ABCB, AUX 1 and PIN auxin transporters in Schizosaccharomyces pombe. *The Plant Journal*, *59*(1), pp.179-191.

Yang, X., Lee, S., So, J.H., Dharmasiri, S., Dharmasiri, N., Ge, L., Jensen, C., Hangarter, R., Hobbie, L. and Estelle, M., 2004. The IAA1 protein is encoded by AXR5 and is a substrate of SCFTIR1. *The Plant Journal*, *40*(5), pp.772-782.

Yang, Y., Hammes, U.Z., Taylor, C.G., Schachtman, D.P. and Nielsen, E., 2006. High-affinity auxin transport by the AUX1 influx carrier protein. *Current Biology*, *16*(11), pp.1123-1127.

Yao, R., Ming, Z., Yan, L., Li, S., Wang, F., Ma, S., Yu, C., Yang, M., Chen, L., Chen, L. and Li, Y., 2016. DWARF14 is a non-canonical hormone receptor for strigolactone. *Nature*, *536*(7617), pp.469-473.

Yao, R., Wang, L., Li, Y., Chen, L., Li, S., Du, X., Wang, B., Yan, J., Li, J. and Xie, D., 2018. Rice DWARF14 acts as an unconventional hormone receptor for strigolactone. *Journal of Experimental Botany*, *69*(9), pp.2355-2365.

Yoneyama, K., Xie, X., Kisugi, T., Nomura, T. and Yoneyama, K., 2013. Nitrogen and phosphorus fertilization negatively affects strigolactone production and exudation in sorghum. *Planta*, *238*(5), pp.885-894.

Yoneyama, K., Xie, X., Kusumoto, D., Sekimoto, H., Sugimoto, Y., Takeuchi, Y. and Yoneyama, K., 2007. Nitrogen deficiency as well as phosphorus deficiency in sorghum promotes the production and exudation of 5-deoxystrigol, the host recognition signal for arbuscular mycorrhizal fungi and root parasites. *Planta*, *227*(1), pp.125-132.

Yoneyama, K., Xie, X., Nomura, T. and Yoneyama, K., 2016. Extraction and measurement of strigolactones in sorghum roots. *Bio-protocol*, *6*(6), pp.e1763-e1763.

Yoneyama, K., Xie, X., Sekimoto, H., Takeuchi, Y., Ogasawara, S., Akiyama, K., Hayashi, H. and Yoneyama, K., 2008. Strigolactones, host recognition signals for root parasitic plants and arbuscular mycorrhizal fungi, from Fabaceae plants. *New Phytologist*, *179*(2), pp.484-494.

Yoneyama, K., Xie, X., Yoneyama, K., Kisugi, T., Nomura, T., Nakatani, Y., Akiyama, K. and McErlean, C.S., 2018. Which are the major players, canonical or non-canonical strigolactones?. *Journal of Experimental Botany*, *69*(9), pp.2231-2239.

Yoshida, S., Kameoka, H., Tempo, M., Akiyama, K., Umehara, M., Yamaguchi, S., Hayashi, H., Kyozuka, J. and Shirasu, K., 2012. The D3 F-box protein is a key component in host strigolactone responses essential for arbuscular mycorrhizal symbiosis. *New Phytologist*, *196*(4), pp.1208-1216.

Žádníková, P., Petrášek, J., Marhavý, P., Raz, V., Vandenbussche, F., Ding, Z., Schwarzerová, K., Morita, M.T., Tasaka, M., Hejátko, J. and Van Der Straeten, D., 2010. Role of PIN-mediated auxin efflux in apical hook development of Arabidopsis thaliana. *Development*, *137*(4), pp.607-617.

Zhang, J., Mazur, E., Balla, J., Gallei, M., Kalousek, P., Medveďová, Z., Li, Y., Wang, Y., Prát, T., Vasileva, M. and Reinöhl, V., 2020. Strigolactones inhibit

auxin feedback on PIN-dependent auxin transport canalization. *Nature Communications*, *11*(1), pp.1-10.

Zhang Y., Li C., Zhang J., Wang J, Yang J., Lv Y., Yang N., Liu J, Wang X., Palfalvi G., Wang G., Zheng L., 2017. Dissection of HY5/HYH expression in Arabidopsis reveals a root-autonomous HY5-mediated photomorphogenic pathway. *PLoS One* 12, e0180449

Zhang, Y., He, P., Ma, X., Yang, Z., Pang, C., Yu, J., Wang, G., Friml, J. and Xiao, G., 2019. Auxin-mediated statolith production for root gravitropism. *New Phytologist*, *224*(2), pp.761-774.

Zhao, H. and Bao, Y., 2021. PIF4: Integrator of light and temperature cues in plant growth. *Plant Science*, *313*, p.111086.

Zhao, L.H., Zhou, X.E., Wu, Z.S., Yi, W., Xu, Y., Li, S., Xu, T.H., Liu, Y., Chen, R.Z., Kovach, A. and Kang, Y., 2013. Crystal structures of two phytohormone signal-transducing α/β hydrolases: karrikin-signaling KAI2 and strigolactone-signaling DWARF14. *Cell Research*, *23*(3), pp.436-439.

Zhao, L.H., Zhou, X.E., Yi, W., Wu, Z., Liu, Y., Kang, Y., Hou, L., De Waal, P.W., Li, S., Jiang, Y. and Scaffidi, A., 2015. Destabilization of strigolactone receptor DWARF14 by binding of ligand and E3-ligase signaling effector DWARF3. *Cell Research*, *25*(11), pp.1219-1236.

Zhao, Y., 2012. Auxin biosynthesis: a simple two-step pathway converts tryptophan to indole-3-acetic acid in plants. *Molecular Plant*, *5*(2), pp.334-338.

Zhao, Y., Christensen, S.K., Fankhauser, C., Cashman, J.R., Cohen, J.D., Weigel, D. and Chory, J., 2001. A role for flavin monooxygenase-like enzymes in auxin biosynthesis. *Science*, *291*(5502), pp.306-309.

Zhou, F., Lin, Q., Zhu, L., Ren, Y., Zhou, K., Shabek, N., Wu, F., Mao, H., Dong, W., Gan, L. and Ma, W., 2013. D14–SCFD3-dependent degradation of D53 regulates strigolactone signalling. *Nature*, *504*(7480), pp.406-410.